Neurogenesis in the Zebrafish Hindbrain

by David Lyons

Submitted to the University of London in 2003 in partial fulfilment

of the requirements for the award of

PhD

University College London

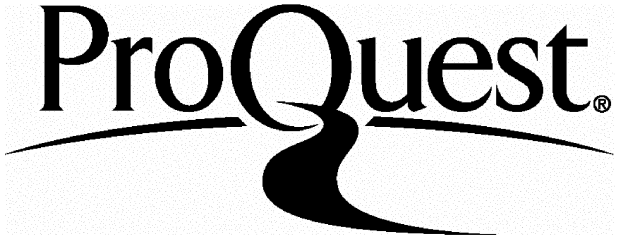

Abstract

This thesis examines neurogenesis in the zebrafish hindbrain. The behaviour of neural progenitors in the intact vertebrate brain is poorly understood, chiefly because of the inaccessibility and poor optical qualities inherent in many model systems. To overcome these problems I have established the zebrafish hindbrain as a suitable system in which to study the dynamic behaviour of the progenitor cells that generate the neurons and glia of the brain. The morphology, behaviour and molecular characteristics of hindbrain progenitors are described and a rigorous quantification of neurogenesis is provided. The main focus of the thesis centres on the mode of division that neural progenitors undergo during neurogenesis. This has been established by following the progeny of single progenitors, labelled with a fluorescent dye, through multiple rounds of division in the living embryo. The development of such clones was often monitored in a transgenic embryo that expresses GFP in post mitotic neurons. This approach allowed individual cells to be followed through to their terminal mitosis and neurons to be phenotyped in the living animal and for lineage trees to be reconstructed. I have found that the vast majority of neurons are born following a division that generates two neurons and that asymmetric divisions that generate a neuron and a progenitor cell are comparatively rare. Furthermore I find that no progenitor behaves in the manner of a classic stem cell i.e. by undergoing repeated rounds of asymmetric division and find also that the plane of the progenitor cell's division relative to the ventricular zone does not correlate with the fate of daughter cells. In characterising the zebrafish neurogenic mutant, *mindbomb* I find, in contrast to published data, that non-neuronal cells exist throughout its development and that mature oligodendrocytes can be generated by mechanisms that do not involve Notch Delta mediated lateral inhibition. I propose a model that the progenitors that give rise to oligodendrocytes in the mutant were never competent to produce neurons and therefore that neuronal and glial lineages must diverge relatively early in development.

Acknowledgments

I have feared writing this part of the thesis more so than any other, due to the huge pressure to be funny and original. Therefore let me start off by listing everyone who has helped me in getting this far in the chronological order that they did so. Parents for creating, feeding, nappy changing, schooling and more feeding, teachers for teaching, friends and relatives for something or other, police for punishing (thanks guys) and parents again for paying (for bail).

Anyway, fate (incidentally a major topic of discussion in this thesis) took its course and I ended up at U.C.L. to do an undergraduate degree in Neuroscience and after two years of sweating blood I came to work in the lab of a fine fellow called Jonathan Clarke to do a summer project and then my final year undergraduate project. Clearly a moment of insanity came over the normally clear thinking Dr. Clarke and he offered me the opportunity to do a PhD in his lab. After consulting with my life coach I decided to embark upon this endeavour, which has finally led to the completion of this here thesis. Jon must be thanked and commended for putting up with my incessant ramblings through the years. At one point it clearly all became too much for him and I was sent to exile in Germany for three months to Janni Nusslein-Volhard's lab where I was force fed crisp German beer by the Tübingen massive as they came to be known. Back at U.C.L. innumerable people have made my passage through this PhD all the more memorable. Adders, Manuel and Philip have provided eating competitions, unrivalled tales of debauchery and an astounding gullibility to entertain me through the years. The Martin lab have provided many instances of gambling madness including the infamous moustache growing competition as well as good drinking time. The Wilson lab has also provided a few drunken hoolies (a horrible theme is developing I fear) and the odd game of football to maintain a façade of health and John Scholes and Tom Hawkins have been great since our collective decision to stop drinking (okay, maybe not),

Last and certainly not least to all the gang outside of academic life, especially to Dom, I'd like to say something.....because I haven't done for so long because of writing this thesis.

Table of contents

Chapter 3

Live imaging of progenitor cell behaviour and characterisation of zebrafish radial glia

Chapter 4

Quantification of neurogenesis in the zebrafish hindbrain

Chapter 5

In vivo analysis of cell lineage in the zebrafish hindbrain through multiple rounds of division

Chapter 6

Novel characterisation of the zebrafish neurogenic mutant *mindbomb*

Chapter 7

List of Figures, Graphs and Tables

List of supplementary movies

These movies are all on a CD that accompanies this thesis. A file describing the details of each individual movie is also included on the CD.

Chapter 3: Live imaging of progenitor cell behaviour and characterisation of zebrafish radial glia

Movie 3.1. Cell behaviour during neurulation.

Movie 3.2. Some cells round up to divide at a distance from the future midline region before the midline seam has formed.

Movie 3.3. All cells round up to divide at the midline seam once it has formed.

Movie 3.4. Cell behaviour around the time of the midline division.

Movie 3.5. Behaviour of elongated progenitor cells during the neural rod to neural tube stage of development.

Chapter 4: Quantification of neurogenesis in the zebrafish hindbrain

Movie 4.1. Expansion of the HuC-GFP +ve population between 24 and 36hpf.

Chapter 5: In vivo analysis of cell lineage in the zebrafish hindbrain through multiple rounds of division

Movie 5.1. Dextran labelled cells divide within the plane of the ventricular zone.

Movie 5.2. Bodipy 505/515 labelled cells divide within the plane of the ventricular zone.

Chapter 1

General Introduction

The central nervous system (CNS) of the vertebrate is one of the most complex structures known to man with an incredible number and diversity of cells and an even more complex set of connections between them. Understanding the mechanisms that generate the correct number and type of cell in the CNS is a major goal of developmental biology. The aim of this thesis is to characterise neurogenesis throughout the early development of a vertebrate embryo. Neurogenesis is the process of generating neurons. Neurons are produced by mitotically active progenitor cells, which are the predominant cell type in the early vertebrate neural plate and neural tube. There is an astounding lack of concrete data describing how individual progenitors behave and contribute to the mature brain and surprising confusion about the morphology of progenitor cells during neurogenesis. I will address these issues in detail and provide a rigorous quantification of neurogenesis throughout embryonic development. Finally I will present novel phenotypic characterisation of the first neurogenic mutant isolated by forward genetics in a vertebrate, the zebrafish mutant, *mindbomb*.

The early neuroepithelium

Progenitor cells in the early neuroepithelium have a characteristic morphology. In the neural plate they have a cuboidal shape. As the neural plate undergoes morphogenetic movements, neurulation, to form the neural tube the apico-basal thickness of the neuroepithelium increases dramatically. When the neural tube has formed neuroepithelial cells retain contact with both apical and basal faces of the epithelium and hence adopt an elongate morphology (Figure 1.1 A+B). In a transverse section cut through the neural tube the position of progenitor nuclei vary in distance between the apical and basal surfaces giving rise to a stratified appearance. This is why the early neuroepithelium is often referred to as a pseudostratified epithelium.

F.C. Sauer identified this property of the early neuroepithelium in pig and chick embryos in 1935. He also correlated the position of the progenitor's nucleus along the apico-basal axis with the stage of the cell cycle that the cell was in. Sauer noted that the size of the nucleus varied with its distance from the apical surface (Figure 1.1 C). He saw that nuclei further from the apical surface were bigger and postulated that the nuclear material was

replicated away from the apical surfaces (Sauer, 1935 a, b; 1936, 1937). Later studies showed that immediately after administration of ^{3}H-Thymidine, which is incorporated into cells only during DNA synthesis, labelled cells were only seen in the basal half of the neuroepithelium. By looking at various intervals after ^{3}H-Thymidine administration the labelled nuclei were seen to have moved towards the apical surface to divide (Sidman et al 1959; Fujita, 1962). Many studies in various systems have confirmed that cells undergoing mitosis congregate at the apical surface (e.g. Seymour and Berry, 1975; Nagele and Lee, 1979; Provis et al., 1985; Alvarez-Buylla et al., 1998; Murciano et al., 2002; Das et al., 2003). The process of progenitor nuclear movement between the apical surface and the basal surface of the neuroepithelium is called interkinetic nuclear migration. Once the neural tube has formed the apical surface is more commonly referred to as the ventricular surface.

Once the neural tube has formed, a number of progenitors begin to undergo neurogenic divisions i.e. divisions that generate one or two post-mitotic neurons. Newborn neurons migrate away from the ventricular surface to differentiate (see review by Nadarajah and Parnavelas, 2002). As significant numbers of neurons are generated a distinct cellular organization becomes apparent in the neuroepithelium. In the spinal cord and hindbrain this arrangement is very simple. The region nearest to the ventricle contains the cell bodies of progenitor cells and is called the ventricular zone. Cells that have left the cell cycle and are migrating to their final position are called neuroblasts and they occupy an area called the intermediate zone. Once post mitotic neurons have reached their destination they differentiate and the region containing neuronal cell bodies is called the mantle zone. The region of the neuroepithelium that is largely composed of axonal tracts is called the marginal zone and lies at the very basal surface of the neuroepithelium, which is now called the pial surface. As the embryo develops the size of the mantle zone and marginal zone increases dramatically (Thors et al., 1982). The ventricular zone (VZ) maintains a fairly constant size until the end of embryogenesis when the majority of neurons are generated. The size of the VZ then decreases markedly.

Progenitor cells and Radial Glia

As the mantle and marginal zones become prominent, information regarding the precise nature and morphology of progenitor cells becomes unclear. Debate over the composition of the neuroepithelium at these stages has gone on for over a century and only now is the issue approaching elucidation (Bentivoglio and Mazzarello, 1999). One cell type that has featured throughout this lengthy debate and which is receiving renewed attention is the radial glial cell. Long radial processes that stretched throughout the thickness of the neuroepithelium were first detected in the embryonic spinal cord by Camillo Golgi using the technique that now bears his name (Golgi, 1886) and a similar observation was made by Giuseppe Magini whilst using the Golgi technique to look at developing mammalian forebrain tissue (Magini, 1888). Indeed the term "radial cells" is thought to have been coined by Magini. Magini not only described the appearance of these cells beautifully but also noted the presence of neurons in close apposition to these radial cells an observation that was to re-emerge accompanied by a new theory nearly 100 years later. Santiago Ramon y Cajal also had an opinion on these cells. Cajal became obsessed with the idea of using the Golgi technique to investigate the structure of the nervous system. In 1888 Cajal started working on embryonic tissue and is quoted as saying "Since the full grown forest turns out to be impenetrable and indefinable, why not revert to the study of the young wood in the nursery stage as we might say," (Ramon y Cajal, 1996). While Cajal confirmed Magini's description of radial cell morphology he was apparently unable to identify cell nuclei associating with them along their extent (Ramon y Cajal, 1889; 1890; 1906, 1911). Cajal's dismissal of the radial cells as uninteresting may explain why it took so long for their significance to resurface.

The radial cell, of course, did resurface and with a vengeance. Some molecular characteristics of immature astrocytes, such as the presence of the intermediate filament protein vimentin were also found in radial cells suggesting a potential lineage relationship between the radial cells and astrocytes (Voigt et al., 1989). Astrocytes are one of two predominant types of glial cell found in the higher vertebrate brain. This lineage relationship was confirmed by a tracing study where radial glia were labelled with DiI via their endfeet at the pial surface. When specimens were examined later the labelled cells had generated astrocytes (Voigt, 1989).

Given these findings it was somehow assumed that a distinct type of progenitor cell must be involved in generating neurons (see Figure 1.2A). The concept of the radial cell as a

putative neural progenitor faced an uphill struggle when a new function was proposed for the cell. Using a combination of Golgi impregnation and EM reconstruction it was claimed that new-born neurons 'embraced' radial cells as they migrated away from the ventricular zone and that the neurons used the radial glia as a scaffold for migration (Rakic, 1971a; 1971b; 1972). It was intuitive that these scaffold like cells would not divide since it was assumed that this would involve loss of the radial process and doing this would neglect their support function. Rakic also introduced the term radial glia following the finding that radial cells expressed the astrocyte marker glial fibrillary acidic protein (GFAP) (Eng et al., 1971; Levitt and Rakic, 1980). The introduction of this term probably did not help the radial cell's cause to be considered as a neural progenitor.

Analysis of cell markers has shown that whilst radial glia share many molecular characteristics with astrocytes they also express markers common to early progenitor cells as well. Ironically, the same authors that showed that radial cells had glial characteristics by virtue of their GFAP expression showed soon after that GFAP +ve cells were still capable of dividing (Levitt et al., 1981). More recently, it has been verified that radial glia are capable of dividing (e.g. Noctor et al., 2001: Figure 1.2 C) and many labs have looked extensively at expression profiles of progenitor cells with a radial glial morphology throughout development especially in the mammalian cortex. It has been shown that almost all neural progenitors contain radial glial markers throughout neurogenesis. Whilst the majority of progenitors express the radial cell marker RC2 (a Nestin antigen) throughout neurogenesis, progenitors are heterogeneous in their co-expression of two other radial glial markers, GLAST and BLBP (Hartfuss et al., 2001). The correlation between these molecularly distinct populations of progenitors and cell morphology or behaviour remains to be resolved. However it is now becoming generally accepted that radial glia generate significant numbers of neurons (e.g. Malatesta et al., 2000; Noctor et al., 2001; Heins et al., 2002).

It is shocking to find that there is still controversy over the morphology of progenitor cells and radial glia throughout development. One model proposes that prior to the onset of neurogenesis all progenitor cells have contact with both apical and basal surfaces of the neuroepithelium and that when neurogenesis begins, it is only the radial glia that keep an attachment to the ventricular and pial surfaces whilst other progenitors have their processes restricted within the ventricular zone (Figure 1.2A). One study describes a marker, 2G12, and a GAP-43 antigen, which is expressed in mitotically active cells with

radial glial like processes. In the spinal cord it seems that these radial processes terminate within the VZ and don't enter the ventral horn, which contains neuronal cell bodies (Brittis et al., 1995; Figure 1.2 B). However there is no reason to believe that expression of this marker is a reliable readout of cell shape. A study published during the course of this thesis in fact provides evidence that when single cells in the rodent cortex are filled with a fluorescent dye there is only one morphologically distinct progenitor cell present in the VZ at any one time and that it always maintains contact with both the ventricular and pial surfaces. The study also shows that the electrophysiological properties of radial glia and progenitors are also identical throughout development (Noctor et al., 2002; Figure 1.2D). Such findings have motivated some to suggest that radial glia should be re-named again with the glia part replaced simply by cell (Parnavelas and Nadarajah, 2001).

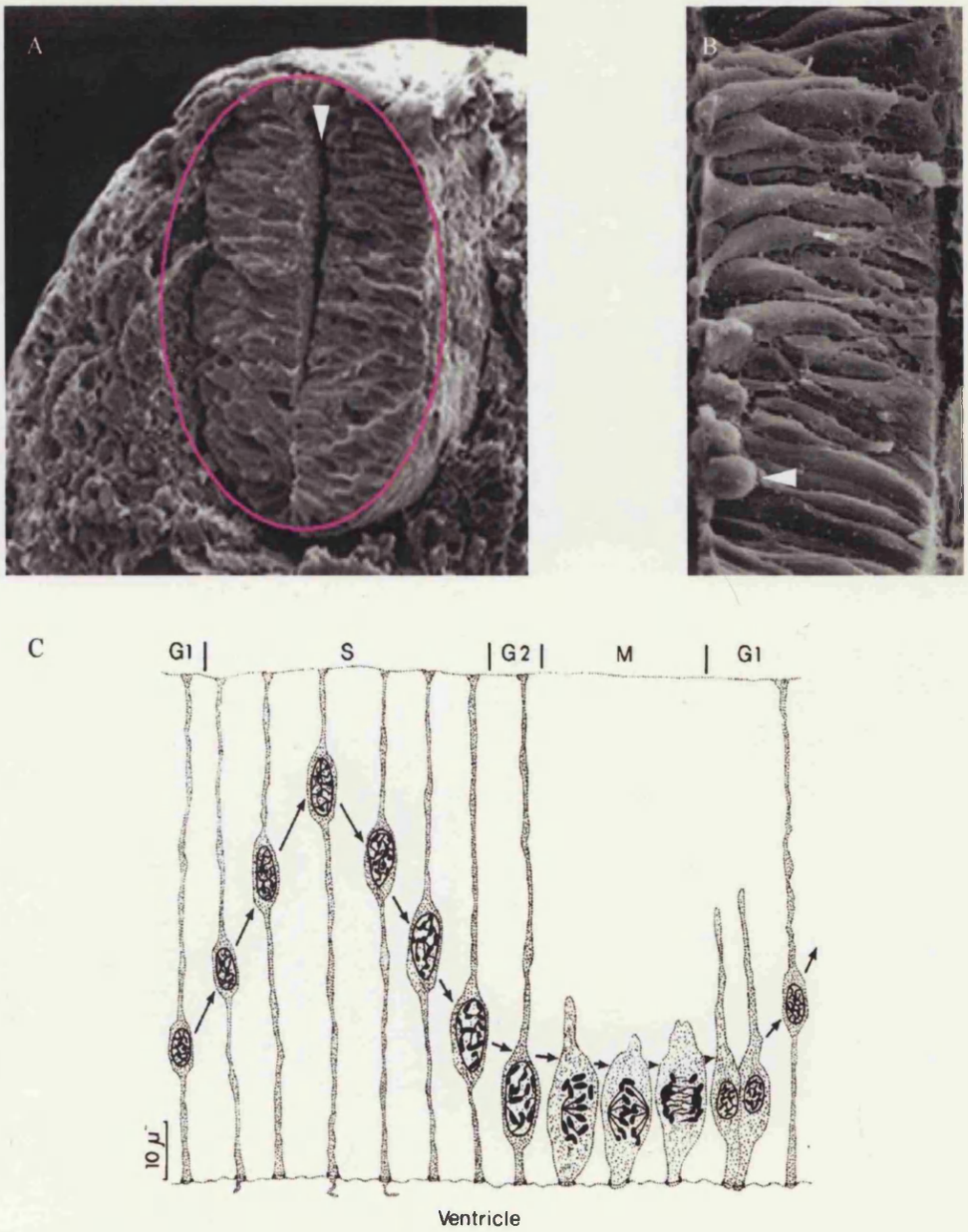

Figure 1.1. Behaviour in the early neuroepithelium.
A shows a scanning electron microscope image of a section through the mouse neural tube. The outline of the neural tube is highlighted by the purple ellipse and the arrowhead points to the ventricle that has just formed.
B shows a higher magnification image of another scanning electron micrograph of the neural tube. Only one side of the neural tube is shown. Cells are clearly elongate and polarised between the two faces of the epithelium, the apical or ventricular surface on the left and the basal or pial surface on the right. The arrowhead points to a cell that has rounded up at the ventricular surface. This indicates that this cell was about to undergo mitosis.
C shows a diagram based on the work of FC Sauer that described the behaviour of neuroepithelial cells during the cell cycle. The stages of the cell cycle are indicated at the top of the figure. Note that the nucleus gets bigger as it moves towards the apical surface (top of image) indicating that DNA synthesis, which takes place during S phase of the cell cycle occurs when the nucleus is far away from the ventricle. The nucleus comes to the ventricular surface to undergo mitosis and divide.

Figure 1.2. Nature of radial glial progenitor cells.

A is a cartoon representing two models of progenitor cell morphology throughout neurogenesis. The cartoon on the left shows the elongate neuroepithelial cells that lie in the ventricular zone before the onset of neurogenesis. The two cartoons on the right show the alternative models of progenitor cell morphology once neurons (blue) have been generated. The top cartoon suggests that at one time two morphologically distinct cells can exist within the ventricular zone, a so called neuroepithelial cell that has its processes restricted within the ventricular zone and a radial glial cell that stretches right throughout the neuroepithelium.The lower cartoon suggests that only one morphologically distinct cell exists in the ventricular zone and that this cell stretches throughout the neuroepithelium.

B, taken from Brittis et al., 1997, supports the model suggested in the top cartoon in A and shows cells with elongate processes (arrowhead) expressing a GAP-43 antigen in the ventricular zone that do not extend a process through the entire thickness of the neuroepithelium (up to arrow) and terminate within the ventricular zone.

C, taken from Noctor et al., 2001, shows that cells with a radial glial morphology in the mammalian cortex can incorporate BrdU (arrowheads) and are thus capable of dividing. The extent of the ventricular zone is indicated on the right and is the region where the bulk of the BrdU +ve cells are found. The process of this radial glial cell extends right throughout the neuroepithelium through the cortical plate (CP) that contains post mitotic neurons.

D, taken from Noctor et al., 2002 shows that cells labelled in the ventricualr zone (VZ) always extend a radial process throughout the thickness of the neuroepithelium to the pial surface (P) despite the age of the animal (indicated at the top right of each panel) and that the cell bodies of radial glia are always within the VZ. This data and that illustrated in C support the model of progenitor cell morphology shown in the lower cartoon in A.

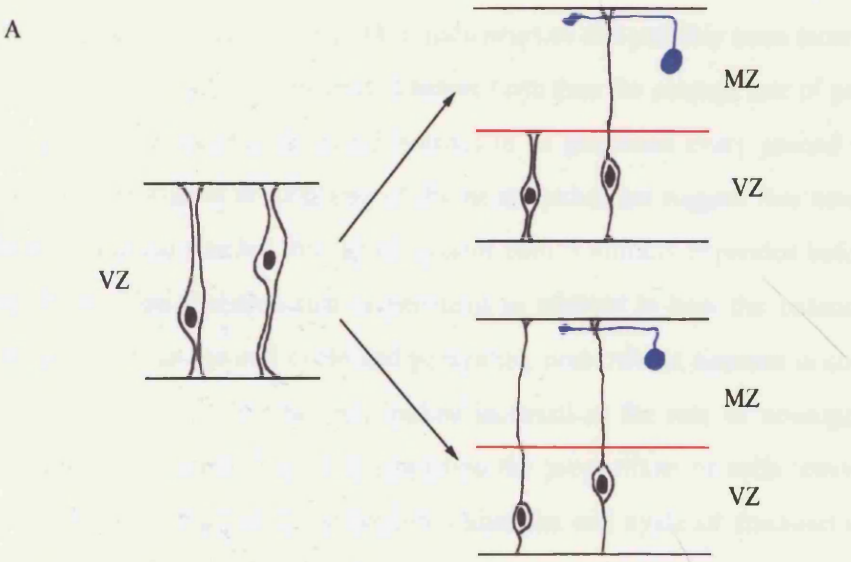
A
VZ
MZ
VZ
MZ
VZ

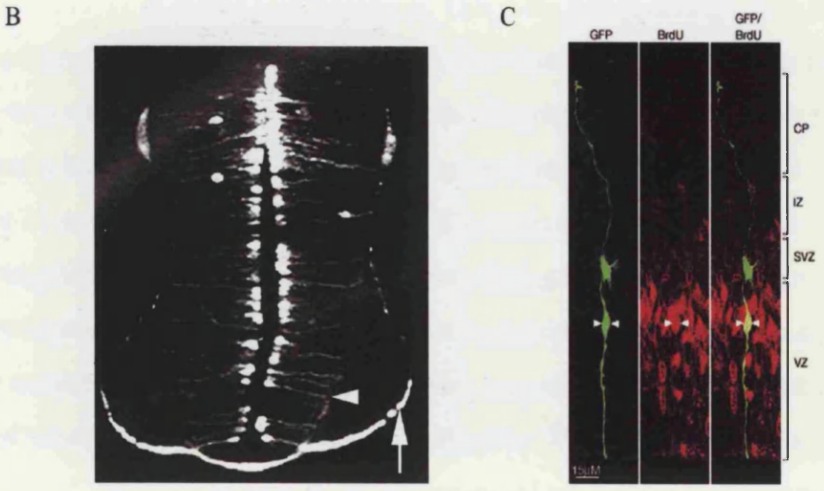
B
C
GFP
BrdU
GFP/
BrdU
CP
IZ
SVZ
VZ
15μM

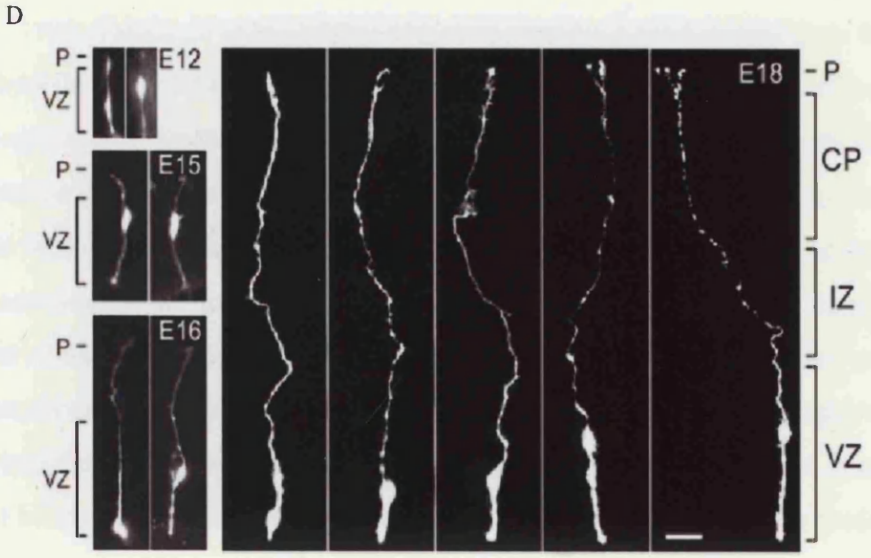
D
P
VZ
E12
P
E15
VZ
P
E16
VZ
E18
P
CP
IZ
VZ

Dynamics of neurogenesis

The human brain contains roughly 100 billion neurons and possibly even more glial cells. If the majority of neurons are generated before birth then the average rate of neurogenesis in humans requires several thousand neurons to be generated every second throughout pregnancy. Histological descriptions of the neuroepithelium suggest that neurons aren't produced at a linear rate but that the progenitor pool is initially expanded before neurons are produced. One question that is pertinent to address is how the balance between maintaining cells in the cell cycle and generating post-mitotic neurons is co-ordinated. Work in Verne Caviness's lab has looked in detail at the rate of neurogenesis over embryogenesis in rodents and has quantified the proportions of cells leaving the cell cycle (Q fraction) and those that remain within the cell cycle (P fraction) at different times during neurogenesis. The observations were made over an 11 cell cycle period between E11-17 of mouse embryogenesis. This is the period during which the majority of cortical layer II-VI neurons are produced. The fraction of cells leaving the ventricular zone was very small for the first few rounds of division in the ventricular zone and only reached a half in the course of the 8^{th} cell cycle. It increases further to 0.8 during the 10^{th} of the 11 cycles (Takahashi et al., 1996). The basic conclusion is simple and intuitively pleasing. Neurons are produced at a slow rate during the first days of neurogenesis whilst the ventricular zone population of progenitors multiplies. Once neurons are produced in large numbers the ventricular zone maintains a constant size until toward the end of the period when almost all cells leave the cell cycle. The authors further suggest that this principle of cortical histogenesis will be conserved across mammalian species (Caviness et al., 1995; Takahashi et al., 1996). This data provides a solid ground from which one can hypothesise on the behaviour of progenitor cells, specifically on division modes. Throughout this thesis I will describe three basic modes of progenitor cell division, a progenitor pair division, where both daughter cells divide again, a neuron pair division where both daughters leave the cell cycle and differentiate as neurons and an asymmetric division where one daughter cell remains in the cell cycle and one differentiates. The model of mouse cortical expansion suggests that during early phases there are largely progenitor pair divisions and during the latest stages predominantly neuron pair divisions. The intermediate period, where the Q and P fractions are changing most dramatically, could be accounted in a variety of ways. For instance there might well be a predominance of asymmetric divisions during the period or simply a co-ordination of the balance

between the progenitor pair and neuron pair divisions or indeed a combination of all three modes of division. Understanding how progenitors behave with respect to their division mode during neurogenesis is a major aim of this thesis.

Cellular basis of neurogenesis in vertebrates

Lineage studies during vertebrate neurogenesis

It is not a novel aim to try and understand the behaviour of vertebrate neural progenitors but success in the field has been limited and data often contradictory. There are several reasons for this, one simply being the sheer complexity of the systems being studied, in terms of their size, inaccessibility and poor optical qualities and another reason being the limited number of technical approaches available to address such issues. Until recently the techniques used were primarily retroviral tracing in rodents and chicks and fluorescent dye tracing in amphibians, chicks and to a lesser extent zebrafish. Figure 1.3 shows one of the fundamental differences between retro-viral tracing and fluorescent dye tracing i.e. the ability to recognise whether a single cell has been labelled or not.

One of the central questions that lineage tracing studies have tried to address is what the nature of a progenitor cell's potential is. Do progenitor cells in the early neuroepithelium have the potential to generate neurons and glia of any type, i.e. are they multipotent, or is their developmental potential restricted from an early stage, e.g. such that they can only produce neurons or a specific sub-class of neurons? A point that is worth making now is to note the difference between analysis of a cell's potential and a cell's fate. Although the more interesting question is perhaps the one of developmental potential, cell tracing by itself can only provide information about cell fate i.e. what a cell becomes. A cell's potential is defined as what it could become, for instance if placed in a different environment.

Initial retro-viral lineage tracing studies in rodent cortex implied that neuronal clones were largely comprised of only pyramidal neurons or only non-pyramidal neurons (Parnavelas et al., 1991) and when extended further showed that clones were comprised of only astrocytes, only oligodendrocytes and again clones with only pyramidal or only non-pyramidal neurons (Luskin et al., 1993). This data provided evidence that the early ventricular zone might be a mosaic of fate-restricted progenitors. Unfortunately these studies are riddled with confounding factors. A major problem with retro-viral tracing is

that labelling of progenitor cells is carried out blind as the retro-viral solution is administered into the brain ventricle from where it infects cells and it is technically impossible using current technology to target single cells in mammalian tissue for viral infection. The dose is titred such that only a single progenitor should be infected in any one area of the ventricular zone, hence clusters of cells seen later in development are assumed to be clonally related although this cannot always be directly demonstrated. Furthermore clones are only analysed at a single time-point and in the two studies mentioned above analysis was made when the animals were adults. Indeed when a similar analysis was carried out and clones were analysed three weeks after birth as opposed to in the adult, clones of mixed neuronal phenotype were found. The conclusions made were that either cells switched phenotype during the intervening period or that selective cell death eliminated neurons of one of the two subclasses (Parnavelas et al., 1995). Neither of these possibilities can be addressed directly using single time-point lineage analysis.

A number of lineage studies have also shown that the assumption that cells clustered together are likely to be derived from a common progenitor is dangerous. In a clonal analysis in the ferret cortex, Reid et al, 1997, followed progenitors tagged with an amphotropic retroviral library encoding alkaline phosphatase and determined sibling relationships unambiguously by PCR at the end of the analysis. The findings revealed that cells clustered together were not necessarily clonally related and that clonally related cells spread over considerable distances in the cortex (Reid et al., 1997). Numerous other studies have also documented extensive tangential migration of neurons throughout the rodent cortex (O' Rourke et al., 1995; 1997). Tangential migration is that which occurs at a tangent to the orientation of cells in the neuroepithelium. Migration along the ventricular to pial axis is called radial migration and was though to have been the predominant mode of neuronal migration following early work on neurons associating with radial glia (Rakic, 1971a; b; 1972) and later time-lapse imaging (O'Rourke et al., 1992). Other lineage tracing studies have documented non-radial migration of clonally related cells for up to 500 μm within the ventricular zone (Walsh and Cepko, 1993). These arguments whilst alarming for basic retroviral lineage tracing do not necessarily mean that the studies that concluded that the early neuroepithelium is a mosaic of fate restricted cells are wrong. Similar findings, that early progenitors have a restricted fate have been reported using fluorescent dye fate mapping. In this case single cells can be unambiguously labelled. Lumsden et al., 1994, showed that clones derived from

individual early progenitors usually contained neurons of only one of several potential phenotypic classes.

In a retro viral study of gliogenesis evidence was provided for the restricted nature of glial progenitor cells. If cells were infected with a retrovirus postnatally then clones contained no neurons. Clones were only composed of either exclusively astrocytes or exclusively oligodendrocytes, with the number of astrocyte clones being in the majority. If the retrovirus was administered 14 days after birth then only oligodendrocyte containing clones were reported (Parnavelas, 1999). This data suggests a temporal order in the generation of neurons, astrocytes and oligodendrocytes respectively through development.

Data that individual neural progenitors are multipotent also exists. Retroviral tracing of post-natal rat retina has shown that clones can comprise several different types of neurons or indeed neurons and glia (Turner and Cepko, 1987). These differences may well reflect a difference in neurogenesis between the retina and the rest of the CNS or differences in the dispersion of cells within the retina. An elegant dye labelling fate map examined the issue of progenitor potential in the early frog retina. The results again showed that individual progenitors could give rise to different cell types and concluded similarly that cells of the early retinal neuroepithelium are multipotent (Wetts and Fraser, 1988). Fluorescent dye tracing was performed in the neural plate of the axolotl embryo to address a similar question. Due to uncharacterised neuronal subtypes the study was restricted to the level of neuronal versus glial fate. The authors report that the majority of their clones (83%) contained a mixture of neurons and glia (Soula et al., 1993). They phenotyped their glial cells by expression of the marker GFAP. Despite their referring to these cells as astroglia, by virtue of their GFAP expression, it is now clear that the antibody that recognises astrocytic GFAP in mammals recognises an additional epitope in lower vertebrates (Dahl et al., 1985). Therefore it cannot be assumed that these cells are indeed true astrocytes.

One of the many curiosities of retroviral lineage tracing studies is the absence of radial glia in the clones described. It is possible that in most studies the animals are only ever examined at a time when radial glia have generated or differentiated into astrocytes but it is also possible that the reporters used to visualise cells are not capable of revealing very

thin radial processes. One study addressed the issue of radial glial lineage in the chick optic tectum. It was found that clones that contained radial glia often also contained neurons and or astrocytes. Interestingly clones only ever seemed to have one radial glial cell. Production of radial glia was said to continue beyond the main period of neurogenesis but that the population decreased dramatically around birth when the numbers of astrocytes increased. This is interesting and the authors provide evidence that radial glia transform into astrocytes at a one to one ratio (Gray and Sanes, 1992). If clones with radial glia contain many neurons and each astrocyte derives from a single radial glial cell then one would expect to see clones with many neurons and one astrocyte in other lineage analysis. It also suggests that the large clones of astrocytes described in other studies (Price and Thurlow, 1988; Parnavelas, 1999) must derive from a separate progenitor. However the relative number of neurons to glia varies between brain regions and species and this simple fact may explain the discrepancy between these studies.

Another aspect that could drastically affect the interpretation of lineage data is the influence of cell death on clone size and composition. Work in Josh Sanes' lab addressed the question of whether spinal cord motor neuron cell death was specific to individual lineages or whether it occurred independently of the ancestry of the neurons. They found that motor neurons and other neurons and glia were clonally related, suggesting that they were derived from multi-potential progenitors and observed that cell death was not correlated with cell lineage but occurred as an independent process affecting individual neurons within lineages stochastically (Leber et al., 1990). The question of what the overall influence of cell death is on individual lineages will remain difficult to address until clones can be unambiguously followed throughout their development and not at a single time-point as has historically been the case.

Division mode during neurogenesis

In addition to addressing the question of progenitor potency a number of lineage tracing studies have sought to describe the division mode that progenitor cells undergo during neurogenesis. The evidence that individual progenitors could give rise to clones with different types of neuron and neurons plus glia implied that asymmetric divisions played a role in their lineage. Mione et al., 1997, tried to assess the relative contribution of asymmetric and neuron pair divisions during corticogenesis by using a combination a retroviral lineage tracing and BrdU labelling. Clonally related cells with similar amounts

of BrdU, quantified immunochemically, were thought to have been born at the same time, hence as a result of a neuron pair division. Clonally related cells with different levels of BrdU was taken as evidence that the cells were born at a different time in the lineage and hence via an asymmetric division. The levels of BrdU are quantified by the percentage of nuclear area that is BrdU +ve. For clusters of cells arranged horizontal to the VZ most cells within clones had equal and small amounts of BrdU in their nucleus. In contrast, clusters which were oriented radial to the ventricular zone often contained one cell with considerably more BrdU than its siblings suggesting that it divided earlier in the lineage via an asymmetric division (Mione et al., 1997). The conclusions made were simply that both asymmetric and neuron pair divisions operate during neurogenesis. A study in the ferret cortex also suggested that at least some neurons arise following an asymmetric division. This was concluded following the observation that there were relatively equal numbers of isolated single neuron clones and clones with many more cells at the end of their analysis. Since a retrovirus only labels one of the two daughters of the infected cell the idea was that a stereotypic asymmetric division might generate one neuron and a progenitor that divided many more times (Reid et al., 1997). A more recent lineage tracing study provided additional evidence for the existence of asymmetric divisions during neurogenesis. Mouse cortical cells were labelled following an in utero infection by a retro virus encoding Green Fluorescent Protein (GFP) at E 15. When animals were sacrificed just 24 hours after infection single cells were commonly found labelled and were often single radial glial like cells. Infected radial glia were shown to be mitotically active by double labelling with BrdU. By leaving the animals to develop for increasing periods after infection the cell number in clones was seen to increase, the interesting point being that often a single radial glial cell was seen alongside a number of neurons (Figure 1.3B). The hypothesis was that the radial glial cell was generating these neurons and doing so by repeated rounds of asymmetric divisions, although this was not directly demonstrated (see Figure 1.5 C). When clones were analysed just 48 hours after initial infection almost exactly half were single neurons and half radial glia. As described for the previous study, since only one daughter inherits the retro virus from the infected cell these proportions indicate a potential prevalence of asymmetric divisions during this period (Noctor et al., 2001).

A recent study (Cai et al., 2002) has attempted to compare experimental data with mathematical models to predict what division modes progenitor cells undergo during

neurogenesis. A retroviral analysis was performed in the mouse cortex over four periods from E11-13, E11-14, E11-15 and E12-15. The number of cells that remained in the proliferating ventricular zone at the end of each interval was counted for each infection. The average number that remained at the end of each of the four intervals was calculated. These numbers were compared to those predicted by three mathematical models of progenitor behaviour based on different combinations of division mode. Model 1 allowed probabilistic combinations of progenitor pair, neuron pair and asymmetric divisions to operate throughout the period of neurogenesis. It was assumed that the decision to re-enter the cell cycle (P fate) or exit the cell cycle (Q fate) was made independently in daughter cells after mitosis. The relative proportion of each division mode was given by $P^2 + 2PQ + Q^2=1$ where P^2 was a progenitor pair, 2PQ an asymmetric and Q^2 a neuron pair division. The P and Q fractions for the population were know from previous work (Takahashi et al., 1996) and for instance when the P fraction is 0.7 it predicts P^2 $(0.7)^2$ 49% progenitor pair divisions, 2PQ 2(0.7)(0.3) 42% asymmetric divisions and Q^2 (0.3)2 or 9% neuron pair divisions. Over a certain period these probabilities of division mode predict an average number of cells that would remain in the cell cycle. This number could then be compared with the number determined experimentally. Model 2 forbade the co-existence of progenitor pair divisions and neuron pair divisions at any one time and was based on an initial combination of asymmetric and progenitor pair divisions followed by a later combination of asymmetric and neuron pair divisions. In model 3 a balance between progenitor pair divisions and neuron pair divisions throughout was used to account for the known Q and P fractions and no asymmetric divisions were permitted. When the numbers calculated from the retroviral analysis were compared to those predicted by each of the models model 1 correlated best with the observed experimental data implying that all three modes of division are likely to operate throughout neurogenesis (Cai et al., 2002).

Time-lapse analysis of vertebrate neural progenitors

There is little more pleasing to a developmental biologist than to be able to watch an embryo develop unperturbed. This goal is only now becoming a reality for studies of vertebrate systems and a wealth of data is sure to emerge soon. One brave study carried out before the recent explosion of imaging techniques attempted to follow cells by time-lapse microscopy in living brain tissue. The authors labelled progenitor cells in slices of

ferret cortex with DiI and monitored cell divisions by time-lapse microscopy. They attempted to correlate the symmetry of cell division and daughter cell fate with the orientation that the progenitor cell divided in relative to the ventricular surface. They showed that if a cell divided within the plane of the VZ an equal amount of a putative cell fate determinant, Notch-1, was inherited by both daughter cells. If cells divided such that one daughter was deposited out of the plane of the ventricular zone then unequal amounts of Notch-1 were inherited by daughter cells with more Notch-1 being inherited by the basal daughter cell after mitosis. The authors claimed that cells dividing within the plane of the VZ remained as progenitors and that the cell which divided out of the plane and inherited Notch-1 preferentially became a post-mitotic neuron (Chenn and McConnell, 1995). However there was no direct evidence that daughter cells adopted either of these alternative fates. The cells were not followed for a sufficiently long time to observe further division of the apical daughter cell or the acquisition of a definite neuronal phenotype in the putative basal neuronal cell. There was no molecular analysis to back up the claims about the fate of daughter cells either. What the authors did report however was that following a division out of the plane of the ventricular zone the basal daughter migrated further towards the pial surface than its sister cell whereas in divisions within the ventricular zone daughter cells did not separate as far from one another (Chenn and McConnell, 1995). It should also be noted that the divisions oriented in this way were only 18% of the total (Chenn and McConnell, 1995). No mention was made of the possibility of neuron pair divisions.

A more recent study, published just before completion of this thesis, readdressed this question using an almost identical approach. Rat retinae were infected with a retrovirus that encoded GFP and explanted retinae were imaged by time-lapse microscopy for up to 5 days (Figure 1.4 A). This was done using newborn rat tissue and most cells analysed only divided once in the analysis as the main period of retinal proliferation had finished. The authors managed to determine the division orientation of 49 progenitor cells and found that 58% divided within the plane of the ventricular zone and 34% divided so separate daughters perpendicular to the plane of the ventricular surface. The authors were able to follow 12 daughter pairs from a horizontal division and 11 daughter cells from a vertical division. Interestingly they found that sister cells of 11/12 pairs following a horizontal division adopted similar fates as judged by their morphology and position in the retina whilst sister cells in 9/11 of the pairs followed after a vertical division adopted

different fates again judged solely by morphology. The authors claim that the daughters of horizontal divisions become photoreceptors although this is only based on the size of the nucleus and was not confirmed by molecular analysis. The authors are more cautious about what phenotype the sister cells of vertical divisions adopt and only confirmed the phenotype in one case where they found that one cell became an interneuron and one a photoreceptor, although again this analysis was made on the comparison of nuclear size only (Cayouette and Raff, 2003). These observations are interesting and certainly are an advance on the earlier work on the ferret cortex but this study also highlights the difficulty that remains in analysing neural progenitor behaviour in highly complex mammalian systems. In order to get this time-lapse system to be viable the whole retina had to be cultured and to analyse the orientation of progenitor cells the retina had to be folded in half in the culture dish. The study had to be carried out at a relatively late stage of development due to the inaccessibility and fragility of the tissue at earlier stages of development. Developmental processes occur much slower in a culture system which means that imaging must be carried out for a considerably longer time than would be natural in an intact animal and it is difficult to keep whole tissues alive and stable for a long time in a culture system. The complexity of the system is also a limiting factor and the authors of this latest paper comment on the difficulty of finding the pairs of cells that they were monitoring after the tissue has been fixed (Cayouette and Raff, 2003). The relatively low numbers of observations made in the time-lapse analysis further highlights the complexity of the system.

Nonetheless several other studies have recently been published that have sought to follow cells by time-lapse microscopy in culture in complex mammalian tissues. In one case radial glia were labelled with DiI in the E14 mouse cortex and something very unexpected was reported. By following the labelled cells through their mitosis by time-lapse microscopy it was seen that the elongated radial fibre remained attached to the pial surface throughout mitosis and that it was inherited by one daughter cell only. In cases where an asymmetric division was documented the putative neuron inherited this radial process and the cell that was proposed to divide again extended a new process towards the pial surface (Miyata et al., 2001; Figure 1.4B). Unfortunately out of 89 divisions followed in this way no daughter cell was seen to divide again. In fact the criteria for phenotyping a cell as neuronal was also poor. In 65% of cases a cell was phenotyped as neuronal if it separated from its sister by >20μm, in a tissue 250μm thick. In the

remainder (35%) of the cases one daughter migrated completely out of the ventricular zone but only 10 such cells were phenotyped molecularly as neuronal (Miyata et al., 2001). This is weak evidence for a paper that states that all neurogenic divisions during this period are asymmetric. Interestingly, they noted only 5/89 divisions that divided out of the plane of the VZ, which is interesting in that there is certainly a reported asymmetry in terms of fibre inheritance in the 84 other divisions. This suggests that there is no correlation between division out of the plane of the ventricular zone and the symmetry of division as defined in this study.

Another recent study observed radial glial like neural progenitors by time-lapse microscopy in slice cultures. The time-lapse analysis again could not be followed for long enough to establish sister cell fate. However, again it did seem that during mitosis that the radial cell process remained intact during the division although the time intervals between frames may have been of a significant enough delay to allow a retraction and re-growth of the process to have been missed (Noctor et al., 2001). The authors of this study suggest that the process is inherited by the progenitor cell and not the neuron after mitosis in contrast to the previous study. However, it is slightly curious that in the figure that documents this time-lapse data the time-point that may have shed most light on the issue of the basal process behaviour has been cut in half and filled in in black (Figure 1.4C).

Further evidence that the orientation of division may alter with the onset of neurogenesis and that the basal process may remain intact during mitosis comes from an in vivo time-lapse study in the zebrafish retina. No mitoses were seen to separate daughters along the apico-basal axis. Instead there is a shift in division orientation between the radial axis to the circumferential axis of the retina at a time that correlates with the onset of neurogenesis. Interestingly this shift in division is delayed in both sonic you (shh) and lakritz (ath 5) mutants where there are defects in retinal ganglion cell differentiation and generation (Das et al., 2003). The dynamics of the radial process are also observed. This data comes from two sources. The first hint that the dividing cells may keep a radial process attached to the basal surface of the neuroepithelium came from time-lapse studies of retinae labelled with the vital dye Bodipy Ceramide that labels the interstitium and membranes of zebrafish live tissue. It was shown that a long process like structure extended from a profile of a cell undergoing mitosis (Das et al., 2003). The second approach used to study the basal process was a time-lapse analysis of progenitors labelled mosaically by injection of GAP-GFP a membrane associated GFP. In this case labelled

cell profiles did seem to indicate that the basal process was not fully retracted during division but it was impossible to identify an attachment of this process to the pial surface. The fate of daughter cells observed exhibiting this behaviour was not followed in detail (Das et al., 2003).

In vitro time-lapse analysis

Studies have been carried out in vitro looking at cell types produced by vertebrate neural progenitor cells. In one notable case progenitors isolated from E10.5 mouse cortex were plated at single cell density and monitored by time-lapse video microscopy for up to three weeks. Sixty-nine clones were analysed in detail and generated between two and ten cells the majority of which expanded by symmetric divisions (see Figure 1.5 A). Nineteen clones contained at least one asymmetric division in their lineage tree. One characteristic asymmetric division generated one daughter that divided only once more to generate two neurons. The other daughter of this asymmetric division typically divided more than once again (Qian et al., 1998; Figure 1.5B). It must be pointed out that this asymmetric division is one that generates two different progenitor cells. This asymmetric division in fact is similar to the division of the Drosophila neural progenitor the neuroblast that produces another neuroblast and a daughter that only divides once more usually to produce two neurons. This study illustrated also that progenitors seem to undergo very stereotyped patterns of division in vitro before giving rise to differentiated progeny, highlighting the possibility that stereotyped lineages may exist in vivo (Qian et al., 1998). Work from the same lab has shown that an individual multi-potential progenitor can produce neurons and glia in a temporal order reminiscent of their development in vivo (Qian et al., 2000). There are two ways in which this could take place. In the first model the early divisions in a lineage produce predominantly neurons and later progenitors become restricted to generating glia. Alternatively, early divisions could produce progenitors restricted to generating either neurons or glia and the temporal control of neuron and glial production could be determined by these restricted progenitors independently. Analysing clones by time-lapse microscopy over a period of seven days showed behaviour consistent with the first model (Qian et al., 2000). The results demonstrated that in mixed clones the behaviour of a multi-potential progenitor cell changed over time during the transition from neuron to glial production. It should be noted that these multi-potential progenitors were a minority and that 80-90% of plated

progenitor cells generated purely neuronal clones. It is also worthy of note that no single division resulted in one neuron and one glial cell. This is in contrast to the Drosophila where the NB1-1A lineage produces ganglion mother cells that divide asymmetrically to give one neuron and one glial cell (Udolph et al., 1993) Work yet again from the Temple lab has more recently reported progenitor neuron pairs following an asymmetric division (Shen et al., 2002) and these will be discussed below in relation to molecular mechanisms in neurogenesis.

Stereotyped invertebrate neural lineage

Whilst the behaviour of cells in generating the vertebrate nervous system is far from clear the same is thankfully not the case for invertebrates. Every division that gives rise to the 302 neurons of the nematode worm C elegans has been carefully traced and the lineage is invariant between animals (Sulston et al, 1983). In fact in more complex systems such as the fruit fly Drosophila Melanogaster the formation of the nervous system is also remarkably stereotyped (e.g. Doe and Technau, 1993; Brewster and Bodmer, 1996; Bossing et al., 1996; Schmid et al., 1999). Indeed much of what we know about the actual mechanisms of neurogenesis and cell fate specification has stemmed from work pioneered in these two model organisms. The Drosophila CNS forms in a very different way to that of the vertebrate. The progenitor cells that give rise to the nervous system delaminate from a ventral ectodermal sheet. These cells are known as neuroblasts. About 30 neuroblasts delaminate in each hemi-segment. They do so at precise but asynchronous intervals throughout development. The remaining cells in the ectoderm go on to produce the epidermis. Molecular markers are available to identify individual neuroblasts uniquely (e.g. Doe 1992). Following delamination each neuroblast undergoes a very stereotyped programme of division so much so that the entire lineage of many neuroblasts can be predicted. The neuroblast division is asymmetric and generates a new neuroblast and a smaller cell called a ganglion mother cell (GMC). The ganglion mother cell usually divides once more to generate two postmitotic neurons. This mode of division is repeated a set number of times until the correct number of neurons are present (see Figure 1.5 D). The molecular mechanisms that control invertebrate neurogenesis and asymmetric divisions will be discussed in a later section.

Progenitor restriction through time

The cerebral cortex is eventually comprised of six laminae between the apical and basal surfaces of the neuroepithelium. These laminae are composed of different types of neurons and can easily be identified down the light microscope. The birth order of these neurons is counterintuitive in mammals in terms of the position that they eventually adopt. Late born neurons migrate past earlier born neurons in a so called inside out manner. This behaviour would suggest that the time of a neuron's birth might influence its laminar fate. To test if this reflected a restriction of late progenitors McConnell and Kaznowski, 1991, labelled embryonic progenitors in S phase with ^{3}H thymidine and transplanted them into older host brains. Cells transplanted into the older brains immediately after labelling, i.e. whilst still in S-phase, migrated to the laminae 2 and 3, appropriate for the time of the hosts' development. This showed that the environment played a role in determining the fate of the daughter neurons of these progenitors. However if progenitors were left to develop for just 4 hours before transplantation, when they were predicted to be in late S-phase or G2, then the daughter neurons occupied deep layer 6, appropriate for the donor's younger stage of development. The conclusion was that although the environment played a role in determining daughter cell fate there was a restricted time window in which this could take place and beyond which the progenitor had become restricted to generating neurons of a specific fate (McConnell and Kaznowski, 1991). Another study looked at the restriction of progenitors that generate the last cortical neurons that migrate through the entire cortex to layer one. When these progenitors were transplanted to younger cortices that were making deep layer neurons the environment could not regulate the fate of the donor cells progeny at all, irrespective of when in the cell cycle they were transplanted. Late progenitors were committed to generating layer one neurons (Frantz and McConnell, 1996). This suggests that progenitors become more fate restricted as development proceeds.

There is also evidence from studies in the retina that progenitor cell fate becomes restricted over time. There is a distinct temporal order in the generation of post-mitotic cells in the retina. Retinal ganglion cells are the first to be born, followed by horizontal cells, amacrine cells and cones. Rods, bipolar cells and Muller glia are the last to be generated. When young retinal progenitors are cultured alongside older retinal cells the young progenitors are inhibited from producing ganglion cells. However, if the old retinal culture is devoid of ganglion cells then the younger progenitors can generate ganglion

cells again (Waid and McLoon, 1998). This suggests that the retinal ganglion cells produce a signal that inhibits the production of more retinal ganglion cells. A similar finding has also been reported with respect to the generation of amacrine cells. When progenitors that normally generate amacrine cells are cultured with older tissue that include an abundance of amacrine cells then their ability to produce new amacrine cells is compromised (Belliveau and Cepko, 1999). Interestingly the sensitivity to inhibition by this feedback signal was dependent on the stage of the cell cycle that the progenitor cell was in, as progenitors entering mitosis were blind to the inhibition (Belliveau and Cepko, 1999). The molecular identity of these inhibitory signals from the ganglion cell or amacrine cell remain unknown but a candidate in mediating a similar feedback strategy in the mouse olfactory epithelium has recently been isolated, the growth and differentiation factor 11 (GDF11). Olfactory receptor neurons feedback on progenitors to inhibit neurogenesis (Mumm et al., 1996). Progenitors and neurons of the olfactory epithelium both express GDF11 and its receptor. GDF11 can inhibit neurogenesis in culture and mice lacking GDF11 have more neurons and more progenitors than wild type. Conversely mice lacking an inhibitor of GDF11, follistatin, have reduced neurogenesis (Wu et al., 2003). These studies highlight the importance of the environment in restricting the subsequent fate of progenitor cells.

However, it is clear that progenitors differ intrinsically at any one time also. Although there is a general order in the generation of the post-mitotic repertoire of the retina there is some overlap in the production of different cell types at any one time. Molecular differences between progenitors can predict the post-mitotic progeny that they will generate. A subset of retinal progenitors express the VC1.1 epitope at a time when amacrine cells, horizontal cells and cones are being generated and other progenitors do not. By selectively labelling the VC1.1+ve progenitors and following their fate they were seen to generate only amacrine cells or horizontal cells whilst VC1.1 –ve progenitors generated cones showing that molecular differences between progenitors correlates with the fate of their daughter cells (Alexiades and Cepko, 1997).

It is clear that a combination of environmental influences combined with the intrinsic properties of a progenitor determine the fate of its progeny.

Recent evidence from the Drosophila has shown the temporal order of a neuron's birth within the neuroblast cell lineage determines its identity. Neuroblasts delaminate from the

ventral ectoderm asynchronously through development, which means that a neuron born following three rounds of division in one neuroblast lineage may be born before the first born neuron in another lineage. Despite this there is a remarkably stereotyped programme of transcription factor expression for each of the first four rounds of division in any neuroblast lineage, irrespective of the specific identity of the neuroblast itself. Furthermore these transcription factors are both necessary and sufficient to specify the identity of neurons produced. For instance hunchback is always expressed during the first division of a neuroblast lineage and also in the ganglion mother cell that generates the two first born neurons (Isshiki et al., 2001). Beautiful genetic experiments have shown that removal of hunchback for instance will remove first born neuronal phenotype at the expense of second born phenotype and conversely that forced expression of hunchback will give rise to repeated rounds of divisions that produce first born neuronal phenotypes. Similar results can be obtained by disturbing the expression of krupple, pdm and castor, the factors that determine the second, third and fourth order neuronal phenotypes respectively (Isshiki et al., 2001).

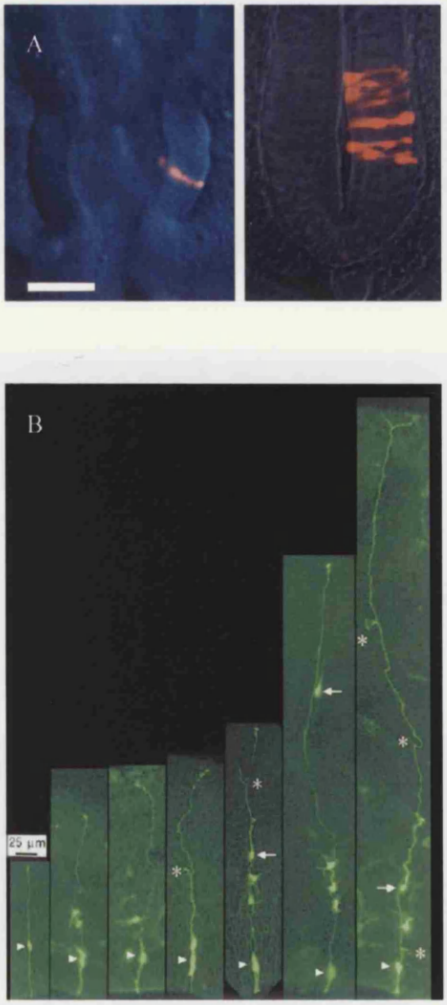

Figure 1.3. Lineage analysis in the vertebrate neuroepithelium.
This figure shows images taken from two lineage studies and highlights a difference between lineage studies followed by fluorescent dye injection and retro-viral infection.
A, taken from Lumsden et al., 1994 shows one of the main advantages of lineage tracing using fluorescent dyes i.e. the ability to verify that a single cell has been labelled at the time of injection (left panel). A section through a resultant clone at the time of final analysis is also shown.
B, taken from Noctor et al., 2001 in fact shows cells from seven different specimens. A serious disadvantage of retro-viral lineage studies is the fact that labelled cells can only be examined at a single time-point after the animal has been sacrificed. The authors in this case are performing an intellectual time-lapse in this figure as the seven images are taken from seven different specimens that were left to develop for increasing periods of time following retro-viral infection at an equivalent start point. The number of cells increases with the length of time that the embryo is left to develop following infection but only one cell that stretches throughout the neuroepithelium is ever seen. The conclusion drawn from these observations is that these radial cells are the progenitors and that the neurons observed in association with them are born following repeated rounds of asymmetric division of the radial cell although this can never be shown directly using this approach.

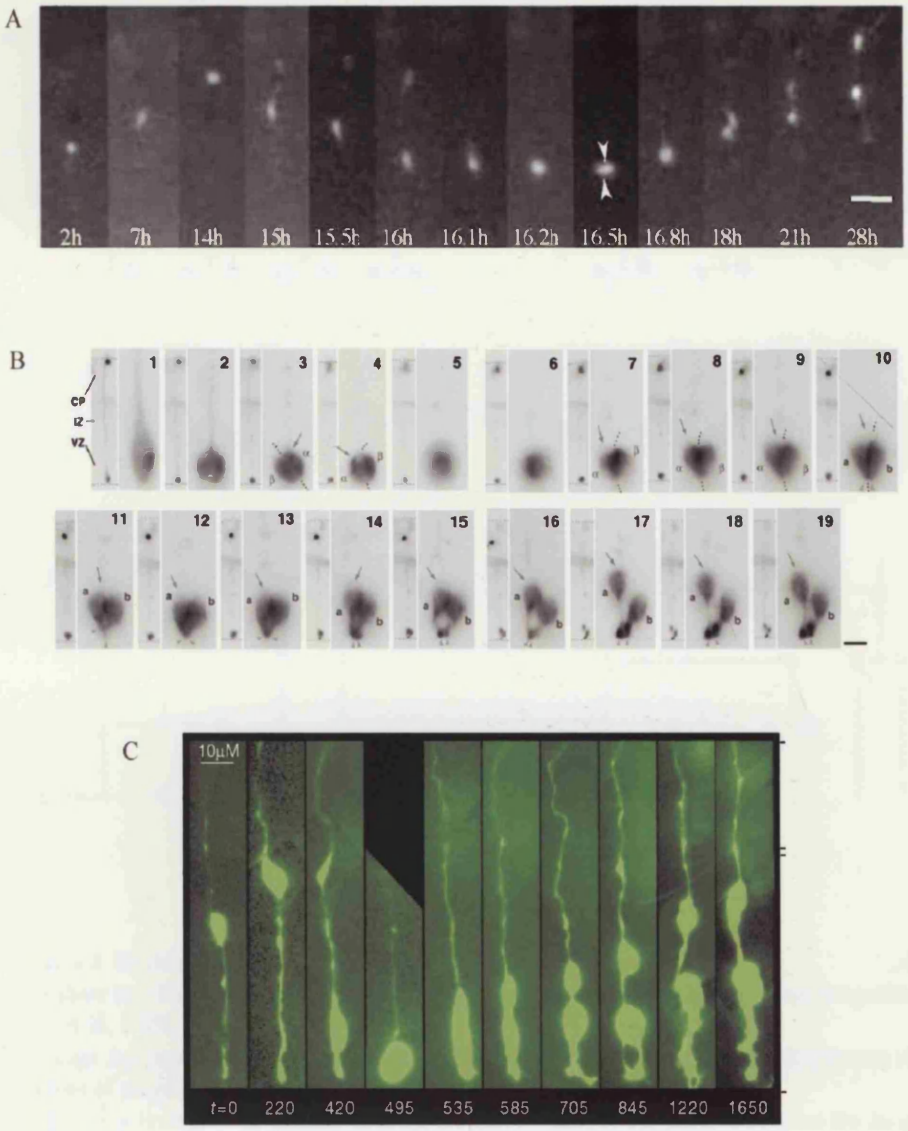

Figure1.4. Time-lapse analysis of vertebrate progenitor cells.
This figure shows three time-lapse sequences taken from papers published during the course of this thesis. All three sequences come from mammalian tissue that was imaged in culture.
A is a sequence from Cayouette and Raff, 2003 that shows a progenitor cell undergoing interkinetic nuclear migration and dividing at the ventricular surface with daughter separating in the plane of the VZ.
B is a timelapse sequence from Miyata et al, 2001 that shows that a process is maintained at the basal pial surface during cytokinesis. A low power view showing the whole cell and a higher power view showing the cell behaviour at the ventricular surface is shown for each timepoint.
C is a sequence from Noctor et al., 2001 showing a radial glial like progenitor divide. Again it appears as though a process is maintained at the basal pial surface during cytokinesis although it is not clear why some of the image at 495 mins is missing.

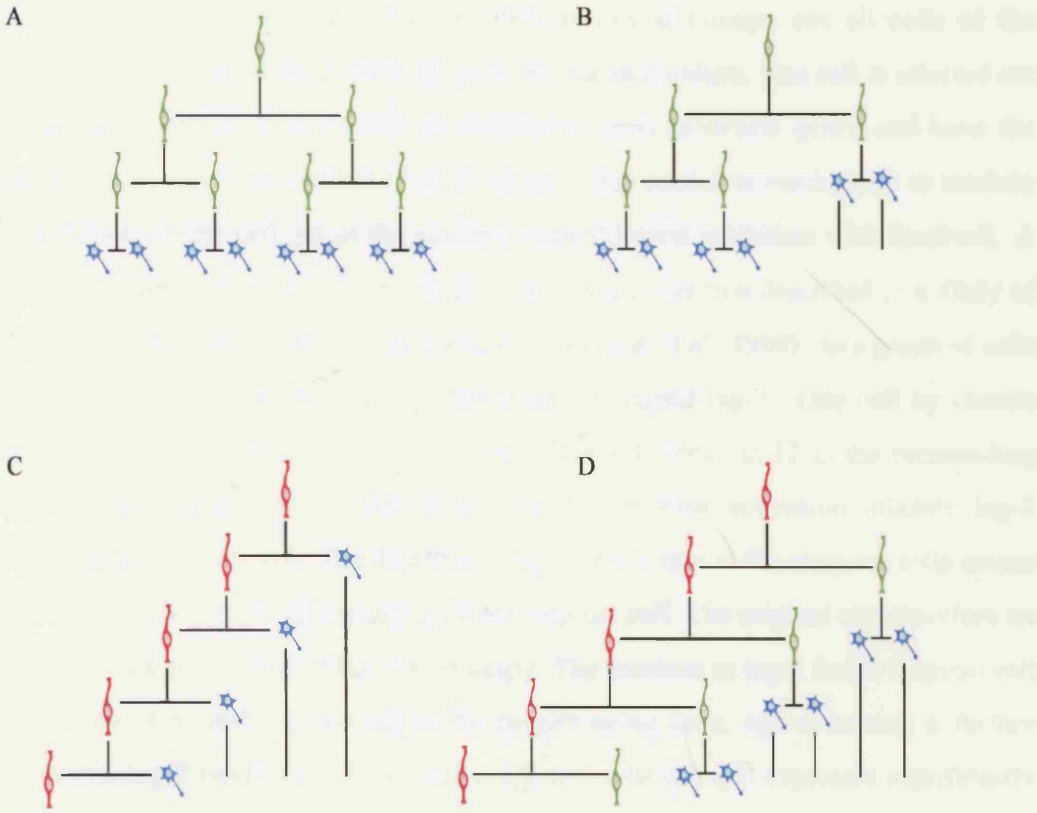

Figure 1.5. Models of progenitor cell division during neurogenesis.
A+B show two lineages observed in an in vitro time-lapse study of isolated cortical progenitor cells (Qian et al, 1998).
In lineage A progenitors divide symmetrically according to the authors, as they all generate similar numbers of progenitors or neurons.
In contrast in lineage B the authors describe the first division as asymmetric because the daughter cells differ in the number of divisions they subsequently undergo. It must be noted that all divisions in these two lineages generate either two progenitors or two neurons.
C shows a hypothetical stem cell like model of neurogenesis where each progenitor divides asymmetrically to generate a neuron and a progenitor. This model was supported indirectly by clonal analysis in the mouse cortex where radial glial cells were proposed to divide in this manner. This model is attractive as if progenitors continued to divide in this fashion a link between embryonic and adult neurogenesis could be easily explained. There is very little direct data to date to support such a model however.
D. A modified version of this stem cell like model is known to exist during Drosophila neurogenesis where the neuroblast (red) repeatedly divides asymmetrically. However this asymmetric division typically produces another neuroblast and a restricted progenitor called a ganglion mother cell that typically divides once more to generate two neurons. It is not known if this mode of division is generally that adopted by the progenitors of adult neurons in the fly.

Genetics of neurogenesis

As mentioned in the section about invertebrate neural lineage, not all cells of the Drosophila ventral ectoderm delaminate and become neuroblasts. One cell is selected out of a group of cluster of cells that all initially express proneural genes and have the potential to become a neuroblast (Figure 1.6 A). One candidate mechanism to mediate the selection of one cell out of the cluster is called lateral inhibition with feedback. A molecular pathway that could underlie this mechanism was first described in a study of cell fate specification in the C Elegans gonad (Wilkinson et al., 1994). In a group of cells each cell expresses both the lin-12 receptor and its ligand lag-2. One cell by chance expresses higher levels of lag-2 at one time. This activates llin-12 in the surrounding cells at higher than constitutive levels. Lin-12 receptor activation inhibits lag-2 production in the same cell. The decrease in lag-2 production in the recipient cells means there is a decrease in lin-12 signalling on the original cell. The original cell therefore no longer inhibits production of lag-2 as strongly. The increase in lag-2 in the original cell further activates lin-12 signalling in the neighbouring cells, again causing a further decrease in lag-2 production. This cycle continues until one cell expresses significantly higher levels of lag-2 than its neighbours and it is this cell that is selected from its neighbours (Wilkinson et al., 1994).

Evidence that a lateral inhibition with feedback pathway exists in the Drosophila during neurogenesis is strong. When a neuroblast delaminates from the ventral ectoderm it does so out of a cluster of cells each of which had the potential to do so. Initially all cells in the cluster, called a proneural cluster express proneural genes. Eventually the levels of proneural genes in one cell become elevated and reduced in the neighbours and it is the one with elevated levels of proneural genes that delaminates. One pathway dissected from studies on the sensory organ precursor in the PNS shows that activation of the lin-12 homologue Notch induces expression of the enhancer of split complex which together with another repressor, groucho, downregulate bHLH proneural genes of the achaete scute class. The achaete scute genes code for activator bHLH proteins that promote expression of the lag-2 homologue, delta. The result of notch activation is a reduction of delta expression through reduction of the achaete scute genes (Heitzler et al., 1996). This explains very nicely how the levels of proneural genes can be regulated and how one cell can eventually express very high levels of proneural genes whilst its neighbours do not. Genes of the Notch Delta pathway are called neurogenic genes due to the fact that

mutations in them had previously been seen to give rise to excess numbers of neuroblasts delaminating from the ventral ectoderm (Lehman et al., 1983; Hartenstein et al, 1992).

Members of proneural gene families such as the achaete scute and atonal families have been isolated in vertebrates either on the basis of sequence similarity to Drosophila by RT-PCR or by yeast 2 hybrid screens. This has allowed the classification of vertebrate bHLH subfamilies based on conservation within the bHLH domain. Achaete scute and atonal families have been defined as well as additional families with some similarity to atonal such as the neurogenin, neuro D and olig families (see review by Bertrand et al., 2002).

Neurogenin was one of the first vertebrate proneural genes shown to act in an analogous way to the Drosophila proneural genes. Neurogenin is expressed in the Xenopus spinal cord in three bilateral longitudinal stripes that predict where the first neurons are generated. Overexpression of neurogenin induces ectopic neurogenesis. Neurogenin expression induces Delta expression and activated notch expression reduces neurogenin expression showing that it exists in the Notch-Delta pathway in a similar way to invertebrate proneural genes (Ma et al., 1996). Further evidence that neurogenin acts as a proneural gene has come from similar overexpression studies in zebrafish where overexpression of neurogenin induces ectopic neurons (Blader et al., 1997) and mouse knockout experiments where subsets of neurons are lost (e.g. Ma et al., 1999). It is now becoming clear that there is a degree of redundancy between the plethora of proneural genes isolated in vertebrates with respect to neurogenesis and also that individual proneural genes may influence the development of distinct subclasses of neuron (e.g. Gowan et al., 2001). The details of these interactions are beyond the scope of this introduction but reviews are available (Bertrand et al., 2002).

In the zebrafish mutant Deadly Seven, which is a mutation in the Notch 1 gene (Holley et al., 2002) there are numerous Mauthner neurons instead of the one that is normally found bilaterally in rhombomere 4. The Mauthner neuron is one of the first neurons in the zebrafish to be born, undergoing its terminal mitosis towards the end of gastrulation (Mendelson, 1986). The ectopic neurons in deadly seven are located in the same position as the wild type neuron and have a similar morphology and axonal projection. By birthdating the Mauthner neuron in wild type and mutant embryos it was seen that all of

the ectopic neurons were born at the same time (Gray et al., 2001). This suggests that a notch delta dependent mechanism normally operates in the neural plate to select which cell out of a cluster becomes the Mauthner neuron.

These studies show that proneural domains regulated by delta notch signalling play a role in vertebrate neurogenesis but do not necessarily tell us how this is temporally regulated. Are all cells of the neural plate competent to express proneural genes and differentiate as neurons or are there regions where neurogenesis is not permitted (Figure 1.6 B). When delta RNA was injected into Xenopus embryos in one cell at the two-cell stage there was a complete abolition of neurons on the injected side of the neural plate. The idea was that with every cell expressing delta there was global inhibition and no cell could differentiate. However if a truncated form of delta was injected the opposite phenotype was observed, nearly every cell differentiated as a neuron, as there was no notch mediated signalling to inhibit neurogenesis (Chitnis et al., 1995). When essentially the same kind of experiment was carried out in the chick retina a similar result was obtained, groups of progenitors exposed to delta did not differentiate whilst groups exposed to a dominant negative form of delta almost all differentiated (Henrique et al., 1997). When Notch was interfered with in the chick retina by expressing antisense notch or constitutively active notch largely consistent results were obtained. Antisense Notch gave rise to an excess of retinal ganglion cell differentiation and constitutively active notch to a deficit (Austin et al., 1995). However 30% of progenitors did not differentiate with the antisense notch suggesting that perhaps not all retinal progenitors have the potential to generate ganglion cells. How the domains of proneural gene expression are set up sheds some potential light on the restriction of early progenitors in the normal environment. The gli superfamily member Zic 2 is expressed in complementary domains between the proneural gene expression domains. Zic 2 inhibits neurogenesis and recognises Gli binding sites. Gli proteins are widely expressed in the neural plate and induce neurogenesis. An interaction between Gli and Zic genes is a likely candidate to specify the patterns of early proneural domains and early neurogenesis (Brewster et al., 1998).

These experiments help to define the concepts of progenitor cell potential and progenitor cell competence. A progenitor's potential defines what a cell could become or generate when placed in a foreign environment. By exposing groups of cells to dominant negative Delta and seeing that they all differentiate into neurons one can say that early progenitors all have the potential to generate primary neurons.

The concept of a progenitor's competence is defined as "the ability of a cell to respond to a cue or set of cues to produce a defined outcome," within the normal tissue environment of the cell's development (Livesey and Cepko, 2001). This can be highlighted by the case of the cells that express Zic 2 in the neural plate. During early stages they are not competent to generate neurons. However a cell's competence state is temporally regulated and thus when the same cells later lose expression of Zic2 they will likely become competent to generate neurons.

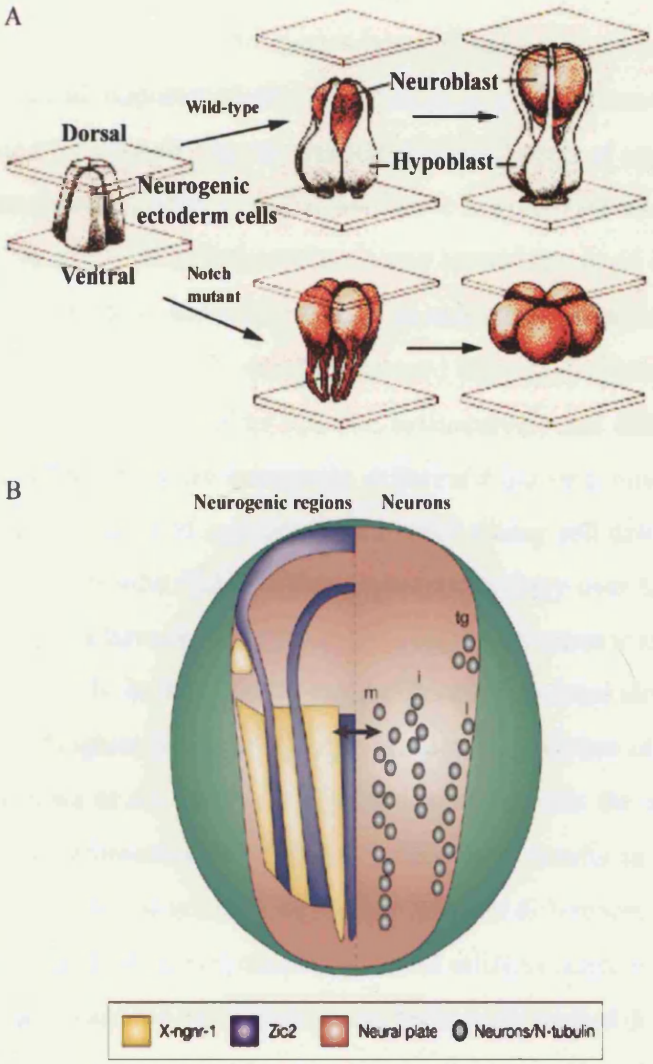

Figure 1.6. Neurogenesis and proneural domains.
A shows how a neuroblast delaminates from a cluster of ectodermal cells in Drosophila. Clusters of cells at a particular space and time express a set of genes (proneural genes) that makes them competent to become neuroblasts, neural progenitor cells. In the wild-type however only one cell out of a cluster becomes neuronal and the other cells of the cluster become hypoblasts. In Notch pathway mutants however, all cells in the cluster become neuroblasts becasue the mechanism that mediates the competition between the alternative fates is defective. Image adapted from source on the Virtual library of Developmental Biology (http://zygote.swarthmore.edu).
B shows a schematic cartoon of the early vertebrate neural plate (Red). On the left side of the cartoon three yellow stripes run along what is the anterior posterior axis of the embryo and they represent domains of cells that express proneural genes and are thus thought to be competent to differentiate into neurons. On the right we see the position of the early born differentiated neurons and they correspond in position to the domains of initial proneural gene espression but are fewer in number than those that expressed the proneural genes. They are thought to differentiate following a similar Notch pathway dependent selection process as regulates Drosophila neuroblast delamination. On the left side of the neural plate cartoon we see the expression of another gene (purple) in between the proneural domains . Differentiated neurons are excluded from this region and this gene is thought to be an anti-neurogenic factor that renders cells incompetent to differentiate as neurons. Image taken from a review by Diez del Corral and Storey, 2001.

Genetics of asymmetric division

The division mode of Drosophila neuroblasts and sensory organ precursor cells highlights the fundamental importance that the mechanism of asymmetric division plays in invertebrate neurogenesis. Genetic dissection of the process of asymmetric division in the invertebrate nervous system over the last decade has provided an absolute wealth of data. A detailed summary of this information is way beyond the scope of this thesis but several comprehensive reviews are available (e.g. Lu et al., 2000a; Jan and Jan, 1998). There are two obvious ways in which sister cells could become different. One way is that the environment influences daughter cell fate independently and differently and the other is that the daughter cells are inherently different following mitosis. The study of the asymmetric inheritance of cell fate determinants during cell division has probably been one of the most fruitful fields of developmental biology over the last decade. To date three mechanisms have been shown to mediate the asymmetric inheritance of molecules between sister cells. In the first case molecules can be directed along actin microfilaments into a single daughter cell in as in the asymmetric localisation of Ash1 RNA in budding yeast (Takizawa et al., 1997). The second mechanism is the association of different mRNAs with centrosomes in different cells, which results in their being distributed asymmetrically into daughter cells. In fact inherent differences in the centrosomes are thought to mediate the differential attraction of mRNAs (Lambert and Nagy, 2002). The third mechanism and the one that is almost exclusively studied during neurogenesis is the localisation of determinants to one pole of a dividing cell such that they are inherited asymmetrically. The two most well studied cell fate determination factors are prospero and numb and come from work carried out in Drosophila. Prospero is a transcription factor that is expressed initially in the neuroblast but is then required in the GMC for GMC gene expression and to repress NB genes. In prospero mutants some GMC genes are not activated and some NB genes are not repressed (Doe et al., 1991; Vaessin et al., 1991; Chu Lagraff et al., 1991; Matsuzaki et al., 1992; Hassan et al, 1997). During NB mitosis the prospero protein moves to the basal cortex of the cell and is inherited asymmetrically in the basal daughter cell i.e. the GMC where it enters the nucleus to alter gene function (Hirata et al., 1995; Knoblich et al., 1995; Spana and Doe, 1995; Broadus et al., 1998).

Numb is also found at the basal cortex of the neuroblast during mitosis and is asymmetrically inherited in the GMC (Knoblich et al., 1995). However, the clearest role

of Numb in determining cell fate is in the Sensory Organ Precursors (SOP) and in the MP2 neural lineage. In the SOP numb becomes asymmetrically localised and is inherited by the IIb cell. In numb mutants both cells adopt the fate of the other daughter of the SOP division, the IIa cell, and when numb is overexpressed both cells adopt the IIb fate (Uemura et al., 1989; Rhyu et al., 1994). This suggests that the levels of numb in this system determine the cell's fate.

The MP2 lineage in the Drosophila is well characterised. The MP2 cell delaminates from the ectoderm and looks morphologically similar to a neuroblast. The main difference is that it divides only once to produce two neurons dMP2 and vMP2. Numb specifies the dMP2 cell fate as Numb -/- embryos have two vMP2 neurons. Numb is asymmetrically partitioned into dMP2 during the MP2 mitosis. A Notch or Delta single mutant however gives the opposite phenotype, giving rise to two dMP2 neurons. The double mutants of either notch or delta and numb also give two dMP2 neurons. This suggests that numb is not necessary for dMP2 fate but that it inhibits the delta notch mediated vMP2 fate. The interesting point is that the Delta ligand is not expressed in the MP2 lineage but is expressed in the surrounding tissue. If the MP2 neurons are isolated in culture, away from delta notch signalling then two dMP2 cells are produced whereas if they are cultured in the presence of the surrounding tissue then the normal lineage is observed (Spana and Doe, 1996). This is a nice example of the interaction between the intrinsic properties of a cell and the environment in regulating asymmetric sister cell fate.

How cell fate determinants actually become localised during cell division is another hot topic of investigation. Mutations in several molecules disrupts the localisation of prospero e.g. miranda and staufen (Shen et al., 1997; 1998) and numb e.g. partner of numb (Lu et al., 1998) but these molecules themselves are also localised in characteristic crescents during mitosis. The protein Inscutable is expressed asymmetrically in neuroblasts and its asymmetric localisation precedes that of the other asymmetrically localised molecules. When Inscutable is mutated none of the cell fate determinants are asymmetrically localised within cells any more and furthermore the orientation of spindles during mitosis is also severely disrupted (Kraut et al., 1996). For a more in depth review of this huge field see an excellent review by Lu et al., 2000a.

Homologues of asymmetric division genes in vertebrates

Considerable effort has been placed into finding vertebrate homologues of the genes responsible for asymmetric division. The factor that has received the most attention in the vertebrate is numb. Numb protein is widely expressed in the rodent CNS but has been found to localise asymmetrically in dividing cells in the late ventricular zone of the rat retina (Cayouette et al., 2001). Asymmetric inheritance of numb between daughter cells was demonstrated in a dissociated culture system of cells isolated from the rat retina. The asymmetric distribution of numb in retinal progenitors was observed at the end of neurogenesis and when seen at the greatest incidence was only in 21% of progenitors (Cayouette et al., 2001). Another recent study (Shen et al., 2002) has tried to correlate cell behaviour and asymmetry of numb expression in vertebrate cells. Isolated cortical progenitor cells at E10 and E13 were plated a single cell density and left to develop for 24hrs. Pairs of cells that arose from a cell division were then analysed. For both timepoints 31% of the pairs of cells were asymmetric with respect to numb expression. By examining cell pairs just 10 minutes after division even higher levels of asymmetric expression of numb was observed suggesting that it did indeed arise as a result of asymmetric inheritance following the cell's division. To correlate the asymmetry of numb expression with asymmetric cell fate the authors looked at pairs of cells where one cell expressed β tubulin III and one cell not. These were considered as progenitor/neuron pairs but comprised only 16% of the total. The authors claim that in 81% of progenitor/neuron pairs numb was asymmetrically expressed but not consistently in either the progenitor or neuron. The other pairs that express numb asymmetrically are neuron-neuron sisters, which account for 19% of the total and this was shown to correlate with an asymmetry in neuronal morphology between the neurons (Shen et al., 2002). This data suggests that numb's function is simply to make daughter cells different but not direct the fate of the cell as has also been shown to be the case from work in invertebrates. The vertebrate numb story took an interesting twist recently with the publication of a paper in which a numblike null mutant was crossed with a conditional knockout of numb restricted to the nervous system. The phenotype is like that of a neurogenic mutant with an early over-production of neurons at the expense of nearly all progenitors implicating that numb and numblike play a role in maintaining cells as progenitors (Petersen et al., 2002). How this might work is obscure considering that numblike expression found primarily in differentiated neurons (Zhong et al., 1997). Furthermore the potential

relationship between this mutant phenotype and asymmetric division has not yet been explored largely because of the lack of information with respect to division mode during vertebrate neurogenesis

Quiescent progenitors and late neurogenesis

The neuroblasts that generate the adult Drosophila brain arrest their development after embryogenesis and remain quiescent until the larva has hatched. Cells then re-enter the cell cycle and renew neurogenesis (Truman and Bate, 1988). There are a number of mutants that affect this process. In the anachronism (ana) mutant quiescent cells re-enter the cell cycle, in S-phase, too early. The ana gene was found to be a novel protein that was expressed in glia surrounding the quiescent neuroblast showing that glia exert an influence in negatively regulating proliferation (Ebens et al., 1993). Quiescent neuroblasts in Trol (terribly reduced optic lobes) mutants fail to re-enter the cell cycle (Datta et al., 1992; Datta, 1995). Trol is the Drosophila Perlecan, a large multidomain heparan sulfate proteoglycan which is normally found in the extracellular matrix, suggesting a possible function for the ECM in signalling mechanisms to control proliferation (Voigt et al., 2002).

The relationship between embryonic neurogenesis and adult neurogenesis is very poorly understood in vertebrate systems. It is not known if progenitors enter states of quiescence and arise later in adulthood as in Drosophila but a possible candidate to bridge the divide between embryonic and adult proliferation are neural stem cells.

Neural stem cells

A textbook definition of a stem cell is that it is a multi-potential cell capable of repopulating a tissue with a regenerative capacity to self renew. If the stem cell has a self-renewal capacity in line with the ability to produce differentiated progeny then the basis of its cell division mode must be asymmetric in that it must divide to produce a differentiated cell and a progenitor cell. Cells isolated from distinct areas of adult vertebrate brain have exhibited properties of neural stem cells in culture. These cells have been isolated from many regions of the adult CNS and can produce neurons and glia in culture (Reynolds and Weiss, 1992; Weiss et al., 1996). Furthermore, cells in some areas of the adult brain including the hippocampus, have been shown to remain mitotically active and to generate new neurons under normal conditions. The most likely

in vivo source of neural stem cells in the mammalian forebrain is the sub ventricular zone SVZ, a layer of proliferating cells that lines the lateral walls of the lateral ventricle. The SVZ is comprised of a number of cell types (Doetsch et al., 1997; Garcia-Verdugo et al., 1998) and is separated from the lateral ventricle by an epithelial layer of ependymal cells. In fact one study has shown that DiI labelled ependymal cells were seen to divide and generate cells later found in the SVZ and that these labelled cells of the subventricular zone divided further to generate neurons. This led to the suggestion that cells of the ependymal layer were in fact the true source of stem cells (Johansson et al., 1999). However, in contrast, it was shown that after long survival times after incorporation of 3H thymidine, which is incorporated into progenitors during S phase, only SVZ astrocytes were still cycling showing that these cells had a greater capacity to self renew, one of the requirements of a true stem cell. These SVZ astrocytes could additionally produce many differentiated cell types in neurosphere cultures showing their multipotentiality, another requirement of true stem cells (Doetsch et al., 1999). More recently a molecule has been isolated that is expressed by a small subset of these SVZ astrocytes and that seems to selectively mark stem cells within this population. When cells expressing this marker, a carbohydrate called Lewis X (LeX), are purified by FACS sorting they exhibit stem cell behaviour in vitro (Capela and Temple, 2002). Crucially ependymal cells do not express LeX and when purified do not exhibit stem cell behaviour confirming a subset of SVZ astrocytes as the source of stem cells (Capela and Temple, 2002).

The potential therapeutic benefits that could result from understanding the fundamental biology of neural stem cells cannot be overstated. The field has consequently exploded over the last decade. A pub med search for neural stem cells pulled up 2050 hits at the time of writing, 1800 of which were published in the last 10 years.

A direct demonstration of stem cell like behaviour during embryonic neurogenesis has not been shown. One idea is that adult neural stem cells are lineally descended from embryonic progenitor cells but there is currently no direct evidence of such a relationship between these cell types in a vertebrate system (see review by Temple, 2001). It would be interesting to know whether such stem cell like progenitors exist from the beginning of neurogenesis or if they emerge as a specialised cell type once the majority of embryonic neurons are generated. In fact, distinguishing between these possibilities and investigating if embryonic progenitors behaved in the manner expected of a classic stem

cell i.e. by undergoing repeated rounds of asymmetric division or not was a major focus of this thesis.

Summary

Despite an absolute wealth of data there are still many unanswered questions in the field of vertebrate neurogenesis. Some of the most glaring gaps in our knowledge of vertebrate neurogenesis relates to descriptions of very basic cell behaviour. The zebrafish is ideally suited to the analysis of dynamic cell behaviour due to its fantastic transparency and the relative simplicity of its nervous system. In this thesis I have tried exploit these qualities to establish a system in which many unanswered questions in the field of neurogenesis that I have highlighted in this general introduction can be addressed. I will analyse progenitor morphology throughout neurogenesis, explore the relationship between radial glia and neural progenitors and analyse the dynamic behaviour of progenitor cells. I will present a quantitative account of neurogenesis and in the main part of the thesis will try to fill the lacuna in the field that relates to our understanding of the modes of division that progenitor cells undergo during neurogenesis. In so doing I will also explore the possibility that the orientation of progenitor cell division correlates with the fate of daughter cells. Finally I present novel phenotypic characterisation of the neurogenic mutant mindbomb in an attempt to gain more understanding of the nature of progenitor cells during vertebrate neurogenesis.

Chapter 2

General Methods

A number of procedures listed below were used repeatedly throughout different aspects of this project. I will describe these in detail here and refer to this chapter where relevant throughout the thesis. Methods specific to individual chapters will be dealt with therein.

1. General embryo care
2. Antibody labelling
3. BrdU labelling and visualisation
4. Biotin visualisation
5. Iontophoresis
6. Bodipy labelling
7. Imaging
8. Image analysis

1. General embryo care

Embryos were staged according to Kimmel et al., 1995 and cared for according to standard protocols described in the "Zebrafish Book" (Westerfield, 1995). Embryos were grown at 28.5°C. Development could be accelerated by incubation at 33°C and slowed down by incubation at 22°C as detailed in Kimmel et al., 1995. In almost all cases embryos were grown in embryo medium (Westerfield, 1995) and occasionally in system water from the zebrafish facility to which a small amount of methylene blue was added to offset infection. 0.003% w/v Phenylthiocarbamide (PTU, Sigma) was added to the embryo medium at 24 hpf to prevent pigment formation in the embryos. This has no reported additional adverse effects on the early embryogenesis of the zebrafish. Wild type embryos were generally provided by communal stocks of fish. I also used and looked after two transgenic lines, the Islet-1 GFP line (Higashijima et al., 2000) and the HuC-GFP line (Park et al., 2000b). These lines were outcrossed at regular intervals to maintain stocks and ensure health of consecutive generations. Embryos were anaesthetised according to the zebrafish book (Westerfield, 1995) using tricaine (3-amino benzoic acid ethylester, Sigma).

2. Antibody labelling

A standard antibody labelling protocol was used for all antibodies apart from anti-BrdU, described in the next section. All washes and incubations were done with the embryos in a plastic universal tube placed on its side and agitated gently.

1. Embryos should be fixed in 2% Trichloroacetic acid (TCA, Sigma) for 3 hours at room temperature if older than 36 hpf.

They should be fixed in 4% Paraformaldehyde (PFA, Sigma) in PBS (Phosphate Buffered Solution) overnight at 4˚C if younger.

2. Wash 3 x 5 minutes in PBTr (PBS + 1% Triton X-100(Sigma))

3. Permeabilise embryos if older than 36 hpf. Prechill trypsin solution on ice (0.25% trypsin (Sigma) in PBS).

Incubate the embryos in this solution on ice for 5-10 minutes. Older embryos may need longer time and time of incubation also depends on sensitivity of the antibody.

Each batch of trypsin can be different so titration is often necessary upon first use.

4. Wash 5 x 5 minutes in PBTr.

5. Wash in 5% normal goat serum (Sigma) in PBTr for 1 hour at room temperature.

6. Incubate embryos in primary antibody + 1% goat serum in PBTr overnight at 4°C.

The concentration of primary antibody depends on the individual antibody.

7. Wash 4-5 x 20 minutes with PBTr.

8. Block endogenous peroxidase.

This step depends on the secondary antibody used and is never necessary when using fluorescence conjugated antibodies

Wash 1 x 5 minutes in 50% methanol/PBS

Wash 1 x 10 minutes in 100% methanol

Incubate in methanol/peroxide for 10 minutes at room temperature, (1ml methanol/ 50µl 6% H_2O_2).

Wash 5 minutes 50% methanol/PBS.

9. Wash 5 minutes in PBTr.

10. Incubate in secondary antibody + 1% normal goat serum in PBTr overnight at 4˚C or for 4 hours at room temperature.

11. Wash for 6-8 x 15 minutes in PBTr.

If using fluorescent secondary this is the end of the procedure.

12. If developing embryos with Diaminobenzoic acid (DAB (Sigma)) then prepare a dilute potassium permanganate solution and keep to one side in case of spillages of DAB.
13. Develop embryos in DAB (1 tablet (10mg) per 12ml PBS).
Incubate embryos in this for 10 minutes.
14. Start reaction by adding 1-2µl 6% H_2O_2 per 3 ml of DAB solution.
Monitor reaction under dissecting microscope. Can take from 30 seconds to 20 minutes.
15. End reaction by transferring embryos back to PBS.
Pour DAB waste into potassium permanganate solution to oxidise the DAB.
Refix embryos in 4% PFA for 20 minutes.
Store in either PBS or 30% glycerol (Sigma) until imaging.

3. BrdU pulse labelling and visualisation

BrdU pulse labelling protocol
BrdU is made up at a working concentration of 1-2mg/ml in embryo medium with 15% dimethyl sulfoxide (DMSO, Sigma).
Take embryos through washes of 5% DMSO and 10% DMSO until they equilibrate before placing them in the final solution. Care must be taken when moving from embryo medium into solutions containing DMSO as the currents created by the solutions mixing can move the embryos around violently.
Place embryos in the petri dish with the solution containing BrdU and place dish on ice for 20minutes.
Wash embryos back into embryo medium until fixation or further manipulation.

Detection of the BrdU signal
1. Fix in 4% Paraformaldehyde (PFA) for at least 24h at 4°C
2. Wash in PBS
3. Dehydrate embryos through a methanol series into 100% MeOH for at least 1hr at –20°C. Embryos can be stored like this for several weeks.
4. Rehydrate embryos through PBS/MeOH series back into PBS.
5. Wash in PBS 2 x 5 minutes.
6. Permeabilise embryos in 10 µg/ml proteinase K (Roche) for 20-40 minutes if older than 10 hpf.

7. Rinse in 2 mg/ml Glycine (Sigma)/ PBS 2-3 times.

8. Rinse in PBS 3-4 times.

9. Re-fix in 4%PFA for 30-60 minutes.

10. Rinse in H_2O 3-4 times.

11. Incubate in 2N HCL for 1hr (8.6ml stock/50ml dH20) at room temperature. It is important to make this 2N solution up fresh each time.

12. Wash in PBTr 3-4 x 5 minutes

13. Block in 2% normal goat serum in PBTr for 1 hr at room temperature

14. Incubate in primary antibody (anti-BrdU, 1-200, Sigma) at least over night at 4°C.

15. Wash in PBTr 6-8 x 15minutes

16. Incubate in secondary antibody overnight.

17. Wash off secondary antibody by 6-8 x 15 minutes PBTr. If revealing secondary antibody using DAB then follow antibody labelling protocol from step 12.

18. Refix for about 24 hrs prior to dissection.

4. Biotin visualisation

1. Fix embryos overnight in 4% PFA at 4°C if younger than 36hpf or 2% TCA at room temperature if older than 36hpf.

2. Wash into PBS.

3. Wash into 100% Methanol for at least 1 hour –20°C.

4. Optional. Block endogenous peroxidase.

Wash 10 minutes in 100% methanol at room temperature.

Incubate in methanol/peroxide for 10 minutes at room temperature, (50µl 6% H_2O_2/1ml methanol).

Wash 5 minutes 50% methanol/PBS.

5. Wash 5 minutes in PBT.

6. Permeabilise in 0.2% trypsin (Sigma) if older than 36hpf.

7. Refix in 4%PFA for 30 minutes if permeabilised

8. Wash 3 x 40 minutes in PBTr

9. Block in 10% normal goat serum in PBTr for 40 minutes.

If using a fluorescent avidin compound go to number 15.

10. Incubate in reaction solution 10 µl sol A and 10 µl sol B per 1 ml PBTr and 1% serum

Solution A and B come from the ABC kit (Vector laboratories).

11. Wash 3 x 40 minutes in PBTr.

12. Develop in 0.5mg/ml DAB.

13. Add 1 µl of 6% H2O2 after 2 minutes.

14. Wash out Dab 3-4 times with PBS (skip 15+16)

15. Add 1/200 dilution of Texas Red Avidin (Zymed) compound to a solution of PBTr with 2% serum.

Incubate overnight at 4°C.

16. Wash out with PBTr until background is suitably low.

17. Re-fix in 4%PFA before dissection.

5. Iontophoresis

Single cells were labelled with dextrans at a variety of stages depending on the experiment to be carried out. The protocol for preparing embryos for single cell labelling at different stages varied slightly.

Single cells were labelled at 3-4hpf to generate large clones of cells by the time of the appearance of the neural plate, 9hpf.

To label individual cells at 3-4hpf embryos were placed on a glass slide with a reservoir containing embryo medium. The walls of the reservoir were built out of hpoxyresin and were about 3-4mm high, 20mm long and 15mm wide. Three to four embryos could be placed in this reservoir and labelled in one session. At this stage of development there is no peridermal layer covering the cells of the blastula and so the embryos do not require anything in addition to the embryo medium to prevent their movement during cell labelling. About 20-30 embryos per hour could be labelled using this method.

Single cells of the neural plate were labelled between 9 and 11hpf. However, there is a tough periderm covering the neural plate at his stage. To facilitate passage of the microelectrode through this periderm embryos were incubated briefly in a solution of 5mg/ml Pronase (Sigma) in embryo medium for 30 seconds to 1 minute. This had no visible morphological effect on the specimen but allowed the electrode to pass through the periderm with greater ease. Embryos were quickly washed 3-4 times in embryo medium after pronase treatment before labelling. The tough nature of the periderm also meant that embryos had to be kept still in the reservoir during iontophoresis. To ensure that movement of the electrode would not move the whole embryo they were mounted

against a drop of 3% methyl cellulose (Sigma). The reservoir was then flooded with embryo medium when the embryo was stably attached to the drop of methyl cellulose.
Single cell labelling was more difficult at this stage and 5-10 embryos could be labelled in 1 hour.
Occasionally single cells were labelled at later stages of development up to 48hpf. At these stages there is still a tough skin covering the whole embryo. Embryos are incubated in 5mg/ml pronase for 2 minutes to make passage of the electrode through the skin easier.
To label cells at this stage embryos are mounted in 1.5% agarose in the labelling reservoir and the reservoir is flooded with embryo medium. The agarose is then cut out above the region where the cell is to be labelled, as the microelectrode does not pass through the agarose easily. Following cell labelling the remainder of the agarose is carefully cut out from around the embryo and it is returned to the embryo medium.

Microelectrodes

The other parameter that changes depending on the stage at which cells are labelled is the size of the microelectrode tip. Generally cells get smaller with age during zebrafish embryogenesis and hence the tip of the microelectrode used to label cells has to be made sharper as the embryo gets older.
Microelectrodes were made from 1.2mm diameter, thin walled aluminosilicate glass with an internal filament (A-M Systems, Everett, WA) using a Flaming/Brown micropipette puller (Model P-87, Sutter Instruments, Novarto, CA).
The tip of the microelectrode can be analysed under a x 40 objective lens on a compound microscope and should have a constant fine taper.
The microelectrode is backfilled with a tiny amount of dextran. This moves by capillary action to the tip of the microelectrode. The microelectrode is then backfilled with an electrolyte (1M Potassium Chloride) and placed on the microelectrode holder.

Hardware

To carry out reliable cell labelling by iontophoresis several pieces of hardware are indispensable.
The Clarke lab uses a fixed stage microscope for cell labelling. This is one that focuses on the specimen by moving the objective lens up and down as opposed to moving the stage that holds the specimen. This is to avoid moving the specimen too much. This microscope has a fluorescent attachment and an extra long working distance x 20 dry

lens. This is necessary to allow sufficient space for the microelectrode to fit between the lens and the specimen.

The microscope is placed on an antivibration table (Newport). This is very important as movement of the specimen and microelectrode has to be kept to an absolute minimum during iontophoresis as the tip of the microelectrode actually penetrates the membrane of the cell being labelled and adverse movement could easily and irrevocably damage the cell.

The microelectrode holder was controlled by a high resolution micromanipulator that had a hydraulically driven fine axial drive that moved along the axis of the microelectrode.

To generate the current that ultimately drives the dye out of the microelectrode an amplifier and a current injection facility (Neurolog system, Digitimer Ltd.) is used.

For iontophoresis to work the resistance of a electrolyte loaded microelectrode should be on the order of 50 to 150 megaohms.

Iontophoresis

1. Place the labelling reservoir on the microscope stage.
2. Move microelectrode into place by adjusting the micromanipulator and find the microelectrode under the objective lens. Lower the microelectrode down into the embryo medium solution.
3. Place the reference earth electrode into the reservoir and make sure it contacts embryo medium so that the electrical circuit can be complete.
4. Turn on amplifier. One can add an oscilloscope to the circuit to measure resistance as the tip of the microelectrode penetrates the plasma membrane of a cell. However, I never did this, as it is possible to target single cells by eye in the zebrafish.
5. Move the microelectrode tip near the embryo and pick a single cell to try and hit and carefully advance the tip of the electrode towards the cell.
6. Once the tip of the microelectrode is upon a cell membrane it can be made to pass through the cell membrane by pressing the negative capacitance button on the amplifier. The makes the tip of the electrode vibrate which has the consequence of pushing the electrode into the cell and at the same time squirting out dye from the electrode's tip. Most of this dye should remain within the cytoplasm unless the cell has been damaged by the movements of the electrode in the tissue. If there is excess movement of the electrode

in the tissue then the integrity of neighbouring cells may be compromised and upon dye release several cells may be labelled.

7. Check cells under epifluorescence 10-15 minutes after labelling to ensure that only a single cell has been labelled and also that the cell is healthy.

8. Once a cell has been labelled gently reverse the microelectrode tip away from the cell and out of the embryo. The longer the period of time that the electrode remains in the embryo the more likely it is to clog up with cell debris.

9. After cells have been labelled return specimens to embryo medium until they need to be fixed or imaged.

Dextrans

During the course of this thesis I tried a variety of different dextrans with varying degrees of success.

The first dextran I used was a 3000 MW tetramethylrhodamine lysine fixable dextran (Molecular Probes, D-3308). This had previously been used with some success in fate mapping studies carried out in the chick embryo (e.g. Lumsden et al., 1994; Clarke et al., 1998). However, I found that this compound was quite phototoxic to zebrafish cells.

I then used a non-fixable 3000 MW tetramethylrhodamine dextran (Molecular Probes, D-3307). This seemed less phototoxic to cells but fluorescence was not observable in fixed tissue. Therefore this dextran had to be used in conjunction with a 10000 MW biotinylated dextran that was lysine fixable (Molecular Probes, D-1956). The biotinylated dextran could then be visualised in fixed tissue (see section 4, above). This combination worked well on epifluorescent microscopes but was not optimal for use on the confocal microscopes due to the properties of the fluorophore, tetramethylrhodamine, which is optimally excited at 543nm whereas the krypton laser on our Leica confocal microscopes excites at 568nm. I tried additional dextrans in the hope that they would be more suited to use on the confocal microscope. I tried both a fluoroscein conjugated 3000 MW lysine fixable dextran (Molecular probes, D 3306) and an Oregon Green conjugated 3000 MW lysine fixable dextran (Molecular Probes, D-7171) and found that both gave better resolution on the confocal microscope but were not as clear under epifluorescence. I also found that the fluoroscein conjugated dextran was quite phototoxic.

As I wanted to carry out may single cell labelling in a transgenic fish that expressed GFP in its neurons I wanted a dye that fluoresced red and that could be used on the confocal microscope. In an attempt to find this I used the Alexa Fluor 568 conjugated 10000 MW

fixable dextran (Molecular Probes, D-22912) but did not find it suitable due to very weak fluorescence under epifluorescent illumination.

The combination of the non fixable 3000 MW tetramethylrhodamine dextran (Molecular Probes, D-3307) and the 10000MW biotinylated dextran that was lysine fixable (Molecular Probes, D-1956) was therefore used for the vast majority of analyses presented in this thesis. These were made up in distilled water at a concentration of 4% and 10% w/v respectively and combined at a 1:1 ratio to give a final concentration of 2% w/v and 5% w/v for the two dyes respectively.

Further details about iontophoresis are available in Clarke, 1999.

6. Bodipy labelling

Bodipy dyes are a collection of fluorophores that span the visual spectrum. The basic fluorophore is non polar, electrically neutral and its simple structure means that conjugates to other molecules can be of a relatively low molecular weight and hence quite permeant in living tissue.

I used three Bodipy dyes during the course of this thesis, Bodipy 505/515 (Molecular probes, D-3921), Bodipy FL C5-ceramide (Molecular Probes, D-3521) and Bodipy TR-ceramide (Molecular Probes, D-7540).

Bodipy 505/515 is a simple fluorophore that permeates cell membranes and binds to yolk platelets in the cell cytoplasm of zebrafish embryos (Mark Cooper, pers. comm.). This means that the fluorophore stains the cytoplasm selectively when imaged on the confocal microscope gives a contrast between the stained cytoplasm and unstained nuclei and interstitial space.

Bodipy FL C5-ceramide and Bodipy TR ceramide are conjugations of the respective Bodipy fluorophores with a ceramide molecule. Ceramides are lipid second messengers and both Bodipy conjugates in the zebrafish permeate through the cell membrane and bind to a mobile lipid binding protein in the tissue's interstitium (Mark Cooper, pers. comm.). The result of this is that the interstitium between all cells is eventually labelled by diffusion of the molecule and thus the outlines of cells in a tissue can be seen.

All Bodipy dyes were made up in 100% DMSO at a concentration of 100 μM and can be stored at –20°C.

Embryos are labelled in their chorions from the one cell stage at a final concentration of 5μM of the Bodipy dyes in embryo medium. Embryos are washed 2-3 times in embryo

medium before being imaged. Bodipy dyes are not fixable and hence can only be used on live tissue.

7. Imaging

In almost all cases where live embryos were imaged by time-lapse microscopy or at a single time-point during lineage analysis they were mounted in 1.5% low melting point agarose (Sigma) and anaesthetised in tricaine (Sigma). Single embryos were picked up in a fire polished glass Pasteur pipette and plunged into a glass Bijou containing the melted agarose. The embryo was almost immediately pulled back into the pipette and the solution of agarose containing the embryo was placed on a 22 mm x 22 mm glass coverslip. The area of the embryo to be imaged was pushed closest to the face of the coverslip and the embryo was oriented quickly as the agarose sets in 5-10 seconds. Mounting the embryo in this way was advantageous as it minimised the distance between the coverslip and the embryo. A reservoir whose walls were made of silicone grease was made on a glass microscope slide according to the dimensions of the coverslip and filled with embryo medium containing tricaine. The coverslip was then placed on the slide with the agarose and embryo going into the reservoir. In some cases time-lapse analysis was carried out on single embryos for over 12 hours. In these cases the procedure for preparing the embryos was almost identical but a small piece of agarose was typically cut out around the tail of the embryo to allow it to undergo relatively normal morphogenesis. The remainder of the agarose allowed the embryo to be kept still.

Fixed tissue was also prepared for imaging. Many antibody labelled specimens were visualised by fluorescent secondary antibodies. Typically these were viewed as either hindbrain wholemounts where the hindbrain was dissected using fine forceps and surgical blades (John Weiss) or as transverse sections. Transverse sections were hand cut using a surgical blade and were cut at the level of rhombomeres 3 to 6 of the hindbrain. All antibody and fluorescent avidin labelled specimens were mounted on glass slides with coverslips in 30% Glycerol/PBS and slides were sealed with unwanted nail varnish, donated by my girlfriend. Fixed tissue that was visualised by non-fluorescent substrates was mounted in the same way but was typically mounted in 70% glycerol/PBS.

Specimens were imaged on a variety of microscopes. During the initial period of this thesis dextran labelled cells were imaged on a Nikon compound microscope with an epifluorescent attachment using x20 and x 40 dry lenses and images were captured by Biovision 2.2 (Improvision) using a cooled ccd (charge coupled device) camera (Photonic Sciences).

Later on in the course of my studies specimens were imaged on a Zeiss Axioplan 2 using x20, x40 and x63 water immersion lenses and images were captured by Openlab (Improvision) using a Hamamatsu Orca ER digital camera. This microscope had an automated specimen stage that allowed three-dimensional stacks of images to be collected.

Confocal microscopy was carried out on a variety of Leica confocal microscopes and images were initially acquired by Leica software and saved as single TIF files for export to other software. Maximum intensity projections were made on the Leica software but no other processing was carried out using this software.

Time-lapse microscopy was carried out on all of the aforementioned microscopes. The confocal microscope that was used for time-lapse imaging had a fixed stage where the position of the objective lens was varied to acquire information in the third dimension, to minimise movement of the embryo over long periods of time.

8. Image analysis

During the initial period of my study almost all data was analysed using NIH image.

This programme allowed analysis of single time-point two-dimensional images and importantly three-dimensional stacks of images acquired on the confocal microscope. Its features included the ability to rotate 3-D images through 360° in any axis and make maximum intensity projections of stacks of images. NIH image could also present simple time-lapse data where information was acquired in a single focal plane on a confocal microscope or a standard compound microscope.

Macros were written with the help of Antonio Jacinto for NIH image to deal with 4-D data sets. The data that was manipulated in this way was saved as a single TIF file on Leica confocal software that contained many individual images. Macros were written that would convert this single file into its constitutive time-points that contained n number of z sections. Additional macros were written that could perform a maximum intensity

projection on the information from the stack of information and recreate a time-lapse movie of this. Additionally macros were written that would create a maximum intensity projection of individual time-points from a variety of orientations and recreate time-lapse movies of this information. Other macros were written to create time-lapse movies from single z-planes within TIF files that contained 4-D information.

During the course of this thesis we acquired Openlab software (Improvision) and this was used to capture images from the Zeiss Axioplan 2. A visual programming language called the Automator that was part of the Openlab software was used to create macros that allowed collection of 3-D and 4-D stacks of information in multiple channels.

Images seen through a microscope contain information from the focal plane of interest plus out-of-focus information from other focal planes. I found that when stacks of z-sections acquired from the Axioplan 2 were projected as one image using a maximum intensity projection that a misleading image was occasionally created. One could tell this was so both from scrolling through individual sections in a stack as well as inspecting samples down the microscope. To overcome the problem of out of focus information the Openlab software has a feature called volume deconvolution to remove the out-of-focus information. Deconvolution is a mathematical technique that calculates the out-of-focus information from other images in a 3-D stack of images by calculating the "point spread function" of the fluorescence source. The deconvolution algorithm calculates the likely source of fluorescence seen in consecutive sections and subtracts the information in certain sections that it calculates originates from sources in different sections. This method is very memory intensive and I found that single 3-D stacks could take up to 1 hour to process fully. To do this I also found it necessary to have 1GB of RAM on our Macintosh G4 of which 800MB was assigned to Openlab. However this technique made it easier to create 2-D images that more faithfully represented the information that could be seen by eye.

The lab also acquired a 3-D/ 4-D data analysis software called Volocity (Improvision). Stacks of raw data acquired on the Leica confocal microscope could be imported directly into this software and the software included programmes to sort the raw data by different channels and/or different time-points. This programme created virtual orthogonal sections

from raw data and also could recreate 3-D volumes with which the user can interact, rotating the volume through all orientations. A vast array of measurement in three dimensions could be made using this software. This software was indispensable for measuring tissue volume in my quantitative analysis (see chapter 4) and in gaining a 3-D understanding of many data sets.

Adobe Photoshop 5-6 and Adobe Illustrator 8 were used to enhance individual images throughout.

Chapter 3

Live imaging of progenitor cell behaviour and characterisation of zebrafish radial glia

Introduction

The aim of this chapter is to establish the zebrafish hindbrain as a suitable system for live imaging and the study of vertebrate neurogenesis. There are a handful of previous descriptive studies of the zebrafish neuroepithelium that serve as background for this study. The zebrafish undergoes morphogenetic movements akin to secondary neurulation that occurs in the caudal spinal cord of amniotes, whereby cells of the neural plate converge on the dorsal midline to form a dense neural keel and eventually a neural rod (Schmitz et al., 1993; Figure 3.1A). The lumen of the neural tube forms later, by cavitation of the neural rod (Schmitz et al., 1993). One feature of zebrafish neurulation is that when neural plate cells reach the dorsal midline they often divide and deposit a daughter cell on either side of the midline. This division is called the midline division and is generally the first division that neuroepithelial cells undergo (Kimmel et al., 1994). Nearly ninety percent of single cells labelled by fluorescent tracers in the early neural plate generate daughters that are separated across the midline in this way during neurulation (Papan and Campos-Ortega, 1994).

Despite undergoing neurulation in this way similarities to primary neurulation in higher vertebrates have also been reported. During primary neurulation the lateral edges of the neural plate fold towards the embryonic midline where they meet one another, thus forming the neural tube. Cells of the lateral neural plate end up in the dorsal neural tube and those of the medial neural plate in the ventral neural tube. Cells labelled with a fluorescent tracer in the zebrafish lateral neural plate also tend to end up in the dorsal neural tube and those labelled in the medial neural plate in the ventral neural tube (Papan and Campos Ortega, 1994) (Figure 3.1A) suggesting some level of similarity between zebrafish neurulation and that of higher vertebrates. Previous reports also suggested that cells of the zebrafish neural plate and neural keel were polarised and maintained an attachment to the apical and basal surfaces during neurulation (Schmitz et al., 1993; Figure 3.1A), which is also the case during neurulation in higher vertebrates. This polarised epithelial structure of the neural plate is different in fact to that in the Xenopus embryo where the cells of the neural plate do not maintain contact with both the apical

and basal surfaces of the epithelium. The Xenopus neural plate is a bilayered structure (Hartenstein, 1989; Figure 3.1B). The dynamic behaviour of cells during zebrafish neurulation has not been reported and I wanted to see if cells did indeed maintain a polarised morphology and contact between the apical and basal surfaces of the epithelium, as it was difficult to imagine how such strictly polarised cells could form a neural keel.

Previous studies have shown that it is possible to observe cell division in the living zebrafish embryo during neurulation and early neurogenesis by analysing cells either labelled with fluorescent dye or unlabelled cells by differential interference contrast, (DIC), (Kimmel et al., 1994; Concha and Adams, 1998). These studies followed the behaviour of progenitor cells during gastrulation and neurulation and showed that the first cell division in the neural plate is often the midline division where the plane of mitosis separates daughter cells along the medio-lateral axis (Kimmel et al., 1994; Concha and Adams, 1998). The orientation of the subsequent division changes and tends to separate daughters along the anterior-posterior axis or the dorso-ventral axis of the neural rod (Concha and Adams, 1998). I wanted to analyse cell division orientation in the zebrafish hindbrain and analyse how this related to the putative apical and basal surfaces during neurulation. I was interested in finding if a midline division could really occur in the presence of a distinct epithelial surface as the conclusion from previous work would suggest (Schmitz et al., 1993; Papan and Campos-Ortega, 1994; Kimmel et al., 1994; Concha and Adams, 1998). Such a division would presumably have to break the integrity of the epithelial surface to deposit a cell on either side of the midline.

Recent data has raised the possibility that zebrafish neural progenitors maintain a process oriented along the apico-basal axis of the neuroepithelium during cytokinesis (Das et al., 2003). This study followed cells of the retina in vivo, that had been labelled mosaically with a membrane bound GFP, by time-lapse microscopy. I wanted to see if I could observe a similar phenomenon in my system. I also wanted to study the behaviour of progenitor cells in other stages of the cell cycle and specifically to look at the process of interkinetic nuclear migration that has been described in many systems. Despite there being evidence that cells generally undergo DNA synthesis away from the ventricular zone and undergo mitosis at the ventricular surface very little information exists about the

actual behaviour of cells undergoing this process or what the significance of the process is.

Despite over a century of investigation there is still confusion over the distinction between neuroepithelial progenitor cells and radial glia in vertebrates. One model holds that these cell types are morphologically different (e.g. Brittis et al., 1995; Figure 1.2 B) and can co-exist within the neuroepithelium whereas recent evidence suggests that radial glia and progenitor cells are one and the same (Noctor et al., 2002). A descriptive report of the anatomy of the zebrafish hindbrain described a structure that may be composed of zebrafish radial glia, the glial curtain (Trevarrow et al, 1990). This structure was labelled by antibodies generated against zebrafish brain proteins and consisted of bundles of fibres that were oriented in a radial fashion between the ventricular and pial surfaces of the hindbrain. GFAP expression was also seen in the glial curtain in the hindbrain (Marcus and Easter, 1995). This marker was previously reported to exist in primate radial glia (Levitt and Rakic, 1980) and this strengthened the possibility that the cells of the glial curtain may be analogous to radial glia in other vertebrate systems. DiI tracing has shown that the cell bodies of glial curtain radial fibres are near the ventricle and that individual fibres condense into bundles as they pass through the neuroepithelium from the ventricular to the pial surfaces (Marcus and Easter, 1995). The position of the cell body within the ventricular zone further suggested a radial glial cell identity. I wished to investigate if in fact the cells of this structure were radial glial like and importantly to establish if they had mitotic activity as has been reported for radial glia in higher vertebrates (e.g. Noctor et al., 2001). I also wanted to know if there was another morphologically distinct type of progenitor that existed at the same time as putative radial glial cells in the zebrafish hindbrain.

The extent of proliferation in the zebrafish neuroepithelium throughout and beyond embryonic stages of development has been primarily addressed in the laboratory of Mario Wullimann. A proliferating cell nuclear antigen (PCNA) study was carried out on zebrafish embryos and larvae on days 1-5 of development. All brain areas were examined and unsurprisingly most cells expressed PCNA on day 1 of development. At 48hpf the number of PCNA expressing cells in the hindbrain was shown to be dramatically reduced and when present were located near the ventricle in the ventral neural tube. It was also

mentioned that those in the dorsal ventricular zone later become restricted to the rhombic lip. By day 3 proliferation in the hindbrain becomes "greatly diminished" and is more tightly located to the ventral domain and the rhombic lip (Wullimann and Knipp, 2000). However the half-life of PCNA is 20h long, which means that PCNA will invariably be detected in post-mitotic cells. This may lead to overestimating the number of progenitor cells at any particular time. Given the relatively fast development of the zebrafish embryo this may give a misleading idea of the location of progenitors during neurogenesis. I wanted to re-address this issue to examine what the extent of proliferation is towards the end of embryogenesis and to compare the development of the proliferative ventricular zone with the neuronal mantle zone.

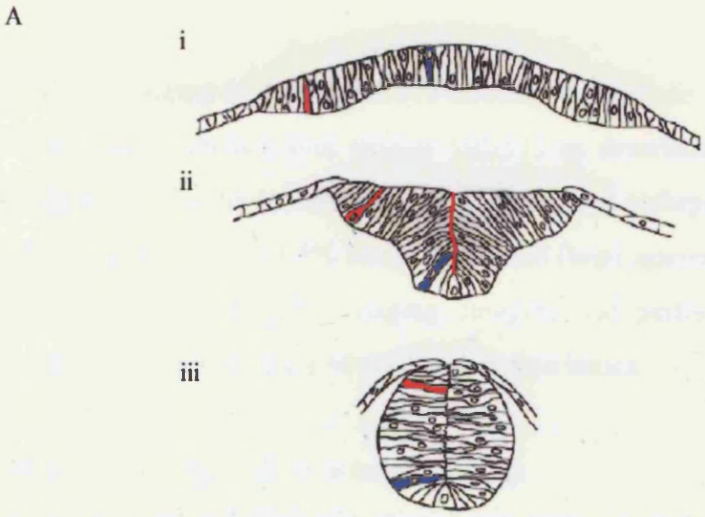

Figure 3.1 A. A proposed model of zebrafish neurulation. Cells of the zebrafish neural plate (i) move towards the midline to form a neural keel (ii). Once all cells have reached the dorsal midline a neural rod (iii) is formed. The neural tube forms later by cavitation of the neural rod. Cells of the lateral neural plate (red) end up in the dorsal neural rod and cells of the medial neural plate (blue) in the ventral neural rod. (Schmitz et al., 1993; Papan and Campos-Ortega, 1994). Note also that a distinct seam (red line) was proposed to exist at the midline region during the neural keel stage.

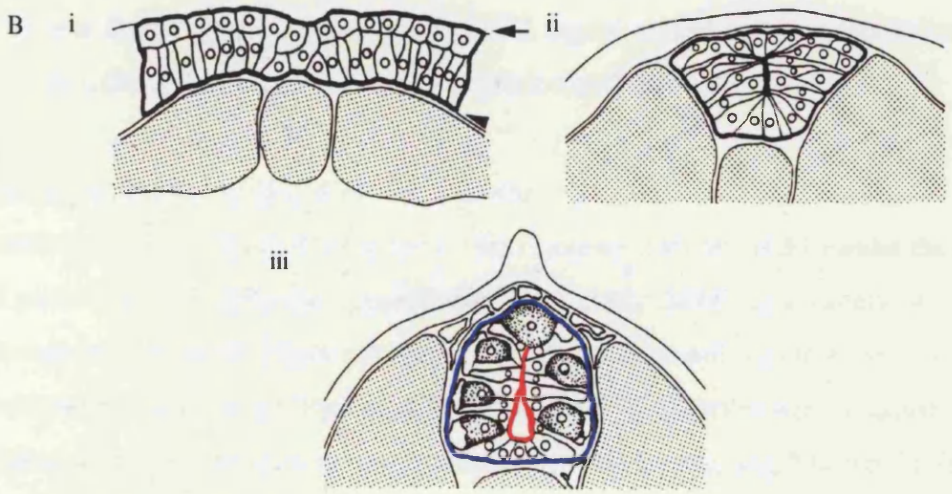

Figure 3.1 B. Neurulation in the Xenopus neural plate.
i-iii show cells in the Xenopus neural plate, neural keel and neural tube respectively, adapted from Hartenstein (1989).
i shows that the Xenopus neural plate is a bilayered structure and that the cells of each layer do not stretch between the apical (arrow) and basal (arrowhead) surfaces of the plate.
iii shows that by the neural tube stage that progenitor cells (white cells) do stretch between the ventricular (red) surface and the pial (blue) surface. Primary neurons are also shown as the darker cells.

Methods

Time-lapse imaging of Bodipy 505-515 labelled embryos

Embryos were labelled with Bodipy 505/515 as described in chapter 2 to stain the cytoplasm of all cells in the living embryo. Stained embryos were washed in embryo medium and mounted in 1.5% low melting point (lmp) agarose (Sigma) and anaesthetised using Tricaine (Sigma) for imaging. Imaging was performed on a Leica confocal microscope using x 20 and x 40 water immersion lenses.

Time-lapse imaging of dextran labelled clones

Single cells were labelled with fluorescent dextran by iontophoresis at the 3-4hpf as described in chapter 2 to generate large clones of labelled cells by 9hpf that were selected for time-lapse imaging. Embryos were grown in embryo medium until required for imaging and then mounted in 1.5% lmp agarose. Imaging was performed on a Nikon optiphot microscope using x 20 or x 40 dry lenses or on a Zeiss Axioplan 2 using x 20 or x 40 water immersion lenses. Images were acquired using a cooled CCD camera (Photonic Sciences) or a Hamamatsu Orca ER digital camera and was data collected on Biovision (Improvision) or Openlab (Improvision) software respectively.

Time-lapse imaging of HuC-GFP +ve embryos

I used a transgenic line that expressed Green Fluorescent Protein (GFP) under the control of part of the HuC promoter, generated by Park et al., 2000b, in a variety of analyses throughout this thesis. These transgenic animals produce embryos that express GFP in their post-mitotic neurons (Park et al., 2000b; chapter 4). Embryos were mounted in 1.5% lmp agarose and anaesthetised in Tricaine as normal for imaging (chapter 2). Imaging was performed on a Leica confocal microscope using x 40 water immersion lenses.

BrdU labelling

BrdU was administered to embryos by pulse labelling as described in chapter 2. Embryos were grown up for differing periods of time (indicated throughout) before being fixed in 4% paraformaldehyde and processed as described in chapter 2.

Antibody staining

Antibody staining was carried out as described in chapter 2. The following primary antibodies were used anti zrf-1 (Trevarrow et al., 1990), anti GFAP (Nona et al., 1989), anti pH-3 (Juan et al., 1998), anti BrdU (Sigma), anti GFP (Upstate Biotech) and anti acetylated tubulin (Sigma).

α-tubulin Gal4UAS-GFP DNA labelling

α-tubulin Gal4UAS-GFP DNA (Koster and Fraser, 2001) was injected into the cytoplasm at the one cell stage at a concentration of 20ng/ul to generate embryos with a mosaically labelled nervous system. The GFP eventually translated by this construct was excluded from the nucleus, which facilitated detailed imaging of cell process morphology.

Results

Throughout this chapter references are made to a number of supplementary movies, which may aid the reader in appreciating the dynamic behaviour of the processes described in each section.

Cells of the neural plate do not maintain contact with the faces of a neuroepithelium during zebrafish neurulation

To address whether cells maintain a contact between apical and basal surfaces during neurulation I imaged cells using the vital dye Bodipy 505/515 as optical transverse sections through the hindbrain by time-lapse microscopy. This dye selectively stains the cytoplasm of all cells and so the interstitial space between cells and the nucleus are negatively stained and stand out in contrast to the stained cytoplasm. Using this method I saw that the neural plate was 3-6 cell layers deep and that many individual cells clearly did not stretch all the way between the apical and basal surfaces (Figure 3.2 A+B and Supplementary movie 3.1). This could not be unequivocally stated for each cell but I never saw any cell that stretched all the way between the inside and outside of the neuroepithelium at the neural plate stage. This suggests that cells of the zebrafish neural plate are not arranged as a simple epithelium as had previously been thought (Schmitz et al., 1993).

To address if a distinct apical surface was always visible during neurulation I analysed the same time-lapse data of Bodipy 505/515 labelled specimens as described above. Previous reports had suggested that a very defined seam along the dorsal to ventral midline of the neural keel exists at this stage of development (Figure 3.1 A). My data showed, in contrast, that cells were intercalated in the region of the prospective midline during the neural keel stage (Figure 3.2 C+D, Figure 3.3 A+B and Supplementary movie 3.1) and that a clear demarcation between the left and right side of the animal did not form until the neural rod stage when the midline seam became obvious (Figure 3.2 E+F, Figure 3.3 C+D and Supplementary movie 3.1). This suggested that cells of the neural keel were not attached to an apical and basal surface because it appeared that there was no distinct apical surface in the future midline region of the neural keel for them to attach to.

To analyse if the morphological appearance of the midline seam corresponded with a change in mitotic behaviour I performed time-lapse analyses of Bodipy 505/515 labelled specimens between the neural keel and neural tube stages of development. Cells rarely divided during the neural plate stage but began to do so from about 13hpf during the neural keel stage of development. A distinct midline seam was not apparent until the neural rod was fully formed by about 15-16hpf. Between 13hpf and 16hpf when cells did round up to divide 37% (130/351) of them did so at a distance of at least one cell body away from the future midline or a putative apical surface of the tissue (Figure 3.3 A+B, Supplementary movie 3.2). However once the midline seam was visible from 16hpf almost all cells (98% (356/364)) divided absolutely adjacent to it (Figure 3.3 C+D, Supplementary movie 3.3).

To examine the dynamics of individual neuroepithelial cells during neurulation single cells were labelled with fluorescent dextran at 3-4hpf. This gave rise to large clones of cells by 9hpf, when the neural plate was just visible. These large clones typically consisted of many cells scattered throughout the embryo. Many embryos labelled in this way were examined until a specimen was found that contained cells that were likely to contribute to the hindbrain neuroepithelium. The selection of such embryos was facilitated by previous fate maps of the zebrafish embryo (Woo and Fraser, 1995). Time-lapse imaging was then carried out on suitable specimens. The embryos were mounted dorsal up so that labelled cells could be viewed in the horizontal plane of the neural plate. As single cells reached the future midline region they often became stretched along the medio-lateral axis relative to the anterior-posterior axis (Figure 3.4 A+B). When cells became elongated in this way it seemed that part of the cell's cytoplasm extended beyond the future midline before the cell rounded up to divide (Figure 3.5 A-C). However the position of the nucleus in such cells was difficult to demonstrate and the significance of this behaviour was not analysed further.

This elongated shape was often transitory as cells frequently rounded up to divide when they were near the midline (Figure 3.4 C+D). Within 30 minutes after division daughter cells adopted a very elongate morphology along the medio-lateral axis (Figure 3.4 E+F and Supplementary movie 3.4).

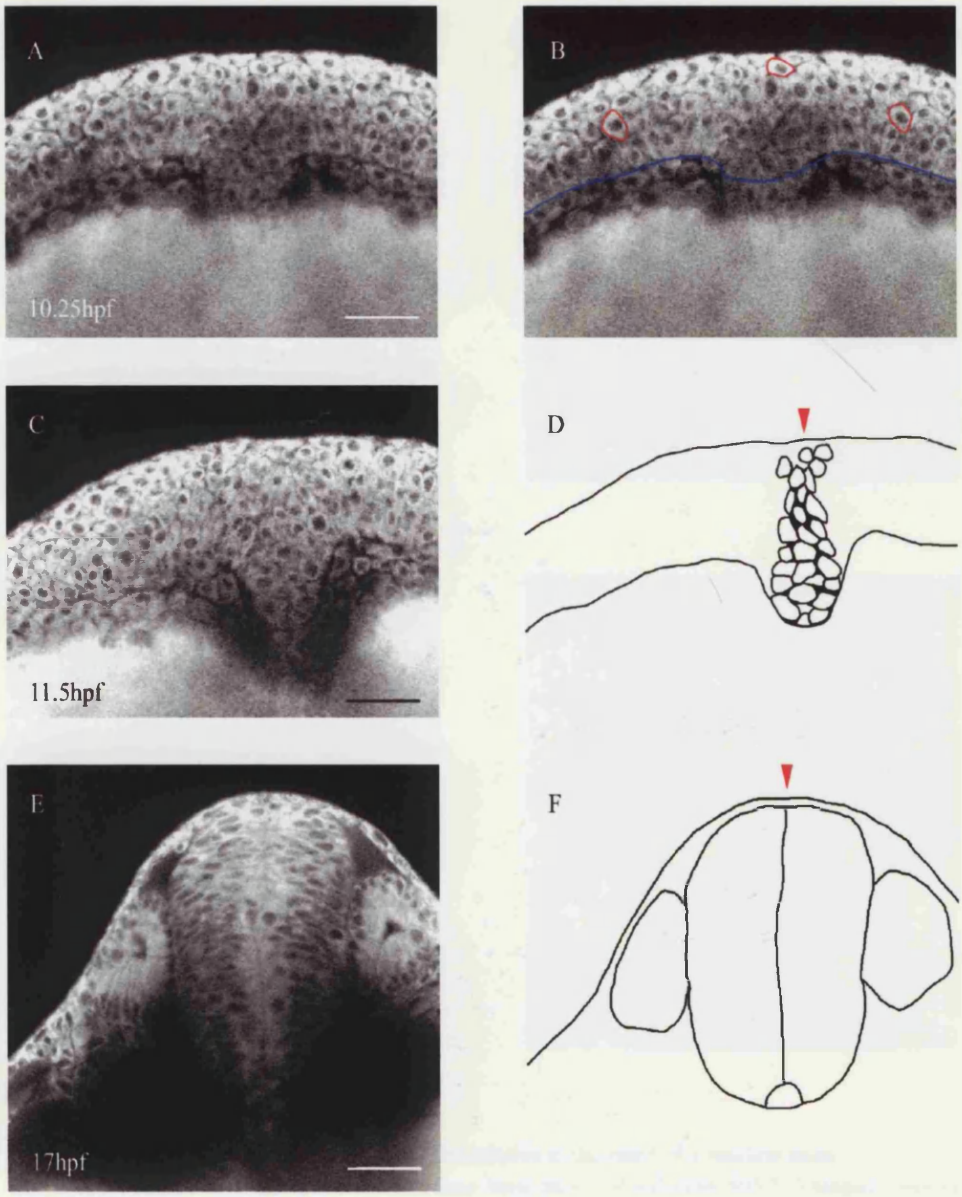

Figure 3.2. Neurulation in the zebrafish hindbrain.
A+B show a transverse section through a living hindbrain labelled with Bodipy 505/515. This labels the cytoplasm leaving the space between cells and the nucleus unstained. The images show the neural plate at 10.25hpf and it can be seen that it is a multilayered structure and that cells do not contact both the apical (outside of embryo) and basal surfaces. The basal surface is indicated by the blue line in B. Cells that clearly do not contact both faces of the tissue are surrounded by a red line in B.
C shows a transverse section through the hindbrain neural keel at 11.5hpf. The embryo has been stained with Bodipy 505/515 as described for A.
D is a schematic drawing showing the outline of the neuroepithelium of section C and also the outline of cells in the midline region of section C. It is clear that there is no distinct midline seam running from dorsal to ventral (direction indicated by arrowhead) at this stage.
E shows a transverse section of the neural rod at 17hpf. Embryo has been stained as in A, B and C.
F is a schematic representation of the section shown in E. It is clear that by this stage there is a distinct midline seam running (arrowhead) along the D-V axis of the neuroepithelium.
All scale bars = 50 μm.
See also supplementary movie 3.1.

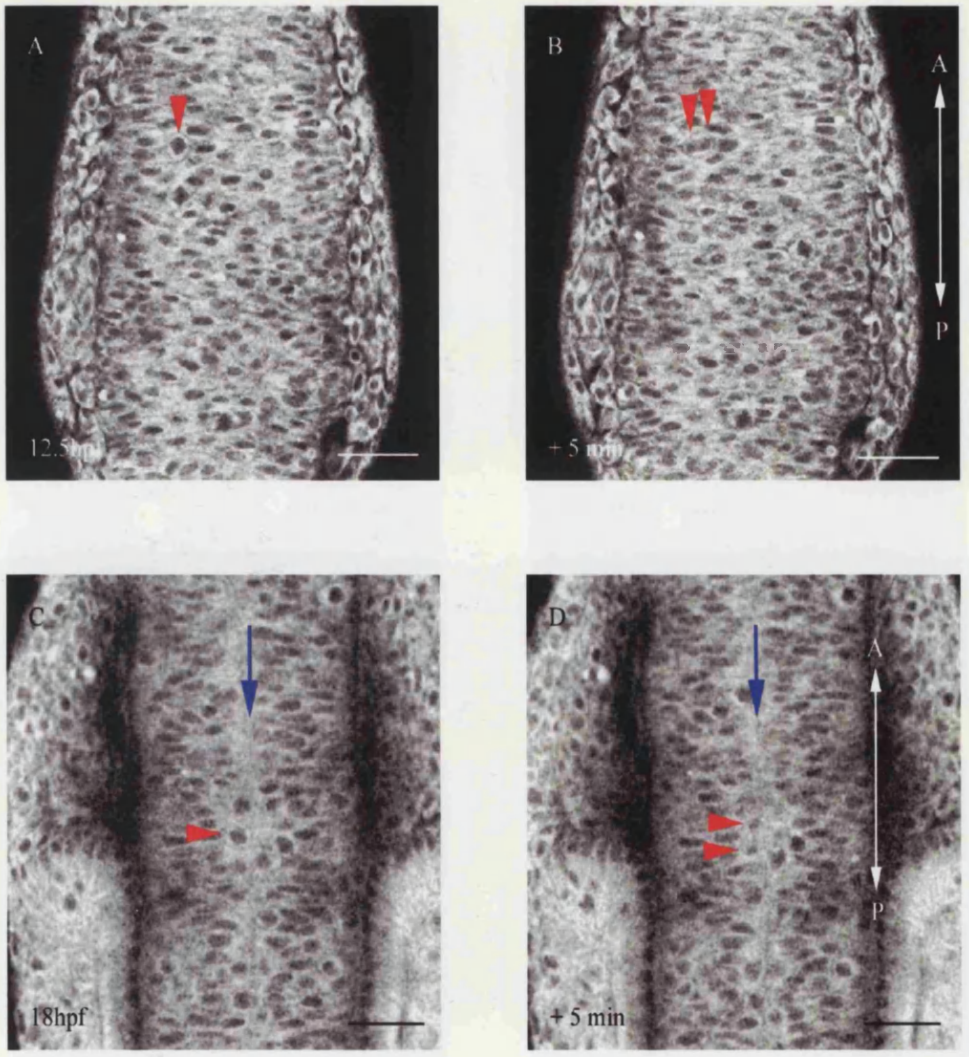

Figure 3.3. Localisation of dividing cell bodies relative to the onset of a midline seam.
A + B show consecutive time points from a time-lapse movie of a Bodipy 505/515 stained embryo during the neural keel to neural rod transition. There is no midline seam or epithelial face in the future midline of the tissue. A cell can be seen to undergo cytokinesis (arrowheads) at a distance from the future midline. Direction of the anterior-posterior axis is indicated in B by white arrowed line. A=anterior. P=Posterior. See also supplementary movie 3.2.
C + D show consecutive frames from a similar movie at the neural rod to neural tube transition. A distinct midline seam is now visible running (blue arrow). Red arrowheads point to cells undergoing cytokinesis between consecutive frames. Cells undergo cytokinesis adjacnet to the midline seam once it has formed. Direction of the anterior-posterior axis is indicated in D by white arrowed line. A=anterior. P=Posterior. See also supplementary movie 3.3.
All scale bars = 50 µm.

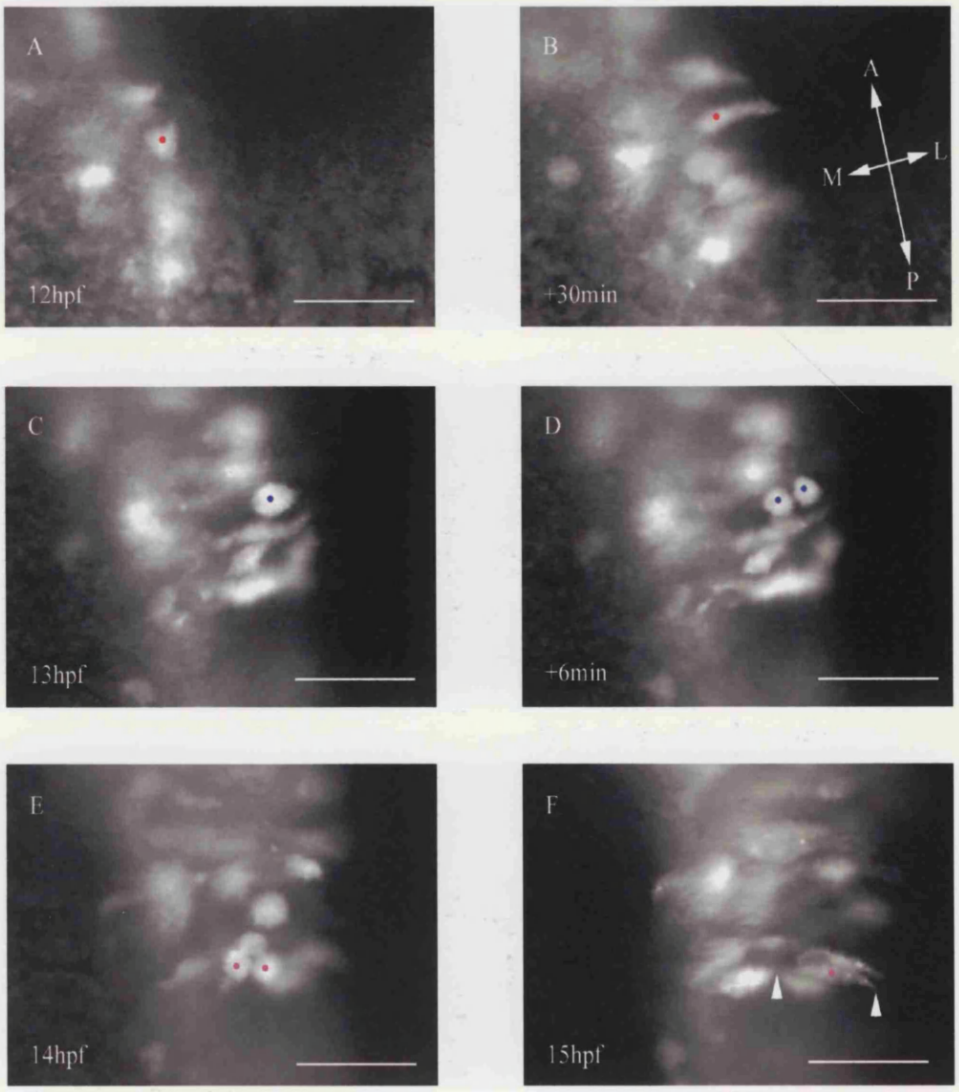

Figure 3.4. Behaviour of individual cells during neurulation.
All images taken from a single time-lapse movie of dextran labelled cells beahving during neurulation. All views are horizontal sections with anterior to the top. The direction of the anterior-posterior and medio-lateral axes are indicated in B by the arrowed lines. A= anterior. P= posterior. M= medial. L= lateral.
A+B show a single cell (red spot) that changes shape and elongates dramatically as it approaches the are of the future midline of the tissue.
C+D show a cell (blue spot) that had elongated upon reaching the future midline region. This cell rounds back up to undergo division, separating daughter cells across the future midline.
E+F show two cells that have just undergone cytokinesis. After division these cells adopt an elongate shape oriented along the mediolateral axis. The cell stretches throughout the limit of one side of the neuroepithelium as indicated by the arrowheads. The cell on the left side of the midline cannot be followed as it has slipped out of the plane of focus.
All scale bars = 50μm.
See also supplementary movie 3.4.

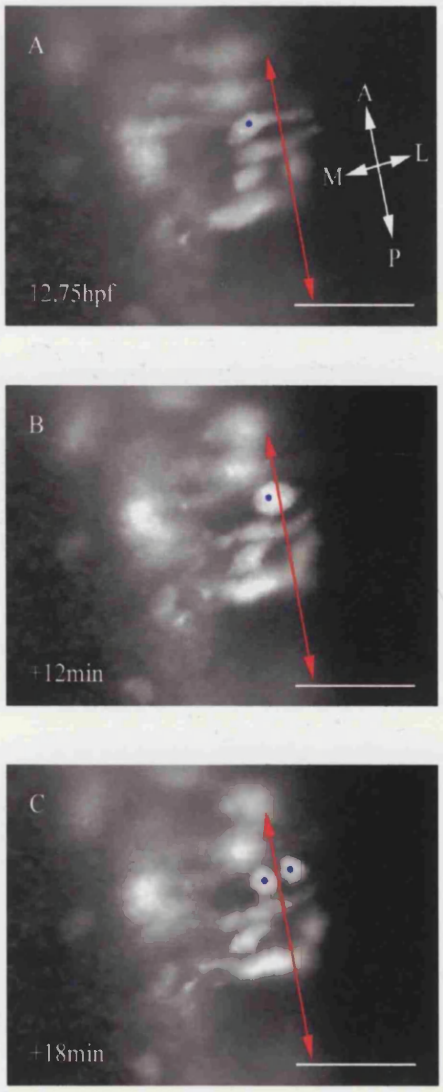

Figure 3.5. Progenitor cells stretch across the future midline before the midline division.
A-C show images from a time-lapse movie of dextran labelled cells. All images are horizontal views looking down on the hindbrain. The anterior-posterior and medio-lateral axes are indicated by the white arrowed lines in A. A=Anterior. P= posterior. M=medial. L=lateral.
A shows a cell (blue spot) that has reached the region of the future midline as indicated by the red line. It is clear that the cell has stretched across the future midline although the position of the nucleus cannot be determined.
B shows that the same cell rounds up to divide almost exactly where the future midline will lie.
C shows that after division daughter cells lie on either side of the midline. See also supplementary movie 3.4.

Neuroepithelial cell behaviour after the midline seam has formed is more analogous to that in higher vertebrate systems

The behaviour of neuroepithelial cells during neural rod and neural tube stages was also monitored by time-lapse imaging of large dextran labelled clones and Bodipy 505/515 labelled specimens.

The orientation of division was compared before and after the appearance of a distinct midline seam by time-lapse analyses of Bodipy 505/515 labelled specimens to see if the appearance of the midline seam corresponded with the disappearance of the midline division. 82% (744/907) of divisions prior to the appearance of the midline seam generated daughters that separated across the midline whereas only 3% (16/459) did so after the appearance of the midline seam. This suggested that the presence of the midline seam inhibited the midline division.

Once the neural rod formed, all neuroepithelial cells adopted a very elongate morphology and stretched from the midline seam to the lateral edge of the neuroepithelium (Figure 3.6 A). Nuclei were positioned at all levels along the medio-lateral axis (Figure 3.3 C+D). The neuroepithelium can be described as pseudostratified at this stage and resembles that of higher vertebrates more closely than during early fish neurulation.

Elongated neuroepithelial cells rounded up and divided exclusively at the midline seam in the neural rod and at the ventricular surface once the neural tube formed (Figure 3.4 C+D and Figure 3.6). The behaviour of these cells could be monitored by time-lapse microscopy (Figure 3.6, Supplementary movie 3.5). Large clones of dextran labelled cells were imaged with embryos mounted dorsal up. A trailing piece of dye filled cytoplasm was observed in cells rounding up to divided up until 5 minutes before cytokinesis (Figure 3.6 B, Supplementary movie 3.5) but I saw no evidence for a trailing dye filled process that maintained contact with the basal pial surface during cytokinesis (Figure 3.6 C) (n=30). However, in 33% (10/30) of divisions monitored in this way I saw a tiny spot of dye at the basal surface that initially seemed part of a progenitor cell and that stayed at the pial surface whilst the cell underwent cytokinesis. In these 10 cases one daughter cell sent a process back to the basal surface that seemed to recapture and encapsulate this spot of dye (Figure 3.6 D-F, Supplementary movie 3.5). This suggests that it is possible that cells do indeed maintain a process attached to the basal surface during cytokinesis but that it is not visible in my system for technical reasons. Cells could send a cytoplasmic process back to the pial surface within 30 minutes of undergoing cytokinesis (Figure 3.6

E-F, Supplementary movie 3.5). At this stage the average length between the ventricular and pial surfaces is about 50μm meaning that the cell re-grows back to the pial surface at the rate of about 100μm/h or1.66μm/min.

These results show that it is possible to monitor the division of neural progenitors in the living intact embryo using this system.

Morphology of neuroepithelial cells and radial glia throughout neurogenesis

To analyse the relationship between neuroepithelial and radial cell morphology I analysed dextran labelled cells and cells labelled with α tubulin Gal-4 VP16 GFP. This construct is injected into embryos at the one cell stage and gives rise to a mosaic of labelled and unlabelled cells later in development. The GFP encoded by this construct is excluded from the nucleus giving excellent cellular resolution and detail of fine processes.

Dextran labelled cells were seen that stretched between the ventricular surface and the pial surface from neural rod stages up until 48hpf (Figure 3.6 and 3.7 A+C). The ventricular-pial thickness of the neural tube increases as development proceeds. By 48 hpf has expanded to a thickness of 120μm. The cytoplasmic processes between the ventricular and pial surfaces become thinner during this period and the progenitor cells adopt a morphology that resembles that of radial glia by about 30hpf. These cells have a very distinct endfoot at the ventricular and pial surfaces, a very thin radial process and a cell body that remains close to the ventricular surface (Figure 3.7 C). No dextran labelled cell was ever seen that was attached to the ventricular surface without also being attached to the pial surface apart from when undergoing mitosis. This suggests that there is no cell type that has its processes restricted within the ventricular zone as had previously been postulated (Brittis et al., 1995).

To confirm this, embryos injected with α tubulin Gal-4 VP16 GFP at the 1 cell stage were analysed at 24, 36 and 48hpf to determine cell morphology. Cells that contacted the ventricular and pial surfaces and had a cell body in between were seen that were similar to dextran labelled cells (Figure 3.7 B+D). At 36 and 48hpf the cell body was always closer to the ventricular surface than to the pial surface and thus these cells had a distinct radial glial like morphology. I saw no morphological evidence of any α tubulin Gal-4 VP16 GFP labelled cell that was restricted to the ventricular zone. This suggests that a differentiation between elongate neuroepithelial cells and radial glia cannot be made on

morphological grounds alone and it is my opinion that neuroepithelial cells simply change their morphology subtly through time and hence almost morph into cells that are referred to as radial glia. This theory is strongly supported by observations of progenitor cell morphology in the rodent cortex that were published during the course of this thesis that suggest similarly that neuroepithelial cells morph into radial glia (Noctor et al., 2002).

A distinct mantle zone is obvious in the zebrafish hindbrain

HuC-GFP +ve embryos were used to characterise the development of the mantle zone. The GFP in these embryos is expressed in differentiated neurons and their processes meaning that the both the mantle zone and marginal zone of the neuroepithelium are labelled (Figure 3.8). Transverse sections were cut through the hindbrain at the level of rhombomeres 3-6 at 12-hour intervals. By 36 hours a distinct mantle zone had formed (Figure 3.8 A). Neurons were clustered together away from the ventricular zone in ventro-lateral domains of the tissue. This mantle zone had expanded dramatically by 48 hours and was 10-12 cell diameters deep. By 72 hours the mantle zone seemed to encapsulate almost the entire neuroepithelium and was now 14-16 cell diameters deep leaving only 1-2 cell layers of non-neuronal cells at the ventricular surface (Figure 3.8 B-D).

To assess the relative number of neuronal and non-neuronal cells at 48hpf, α-tubulin labelled cells were analysed and counted using morphological criteria alone.

Neurons were phenotyped by one or more of the following criteria, round cell body, no attachment to the ventricular surface and presence of an axon. Non-neuronal cells were phenotyped as such if they had an elongate cell body and a process attached to both the ventricular and pial surfaces (e.g. Figure 3.7 A-D). Using these criteria it was found that the neuroepithelium comprised 91% neurons (233/246 n=10) at 48hpf. The remainder had a radial glial cell morphology.

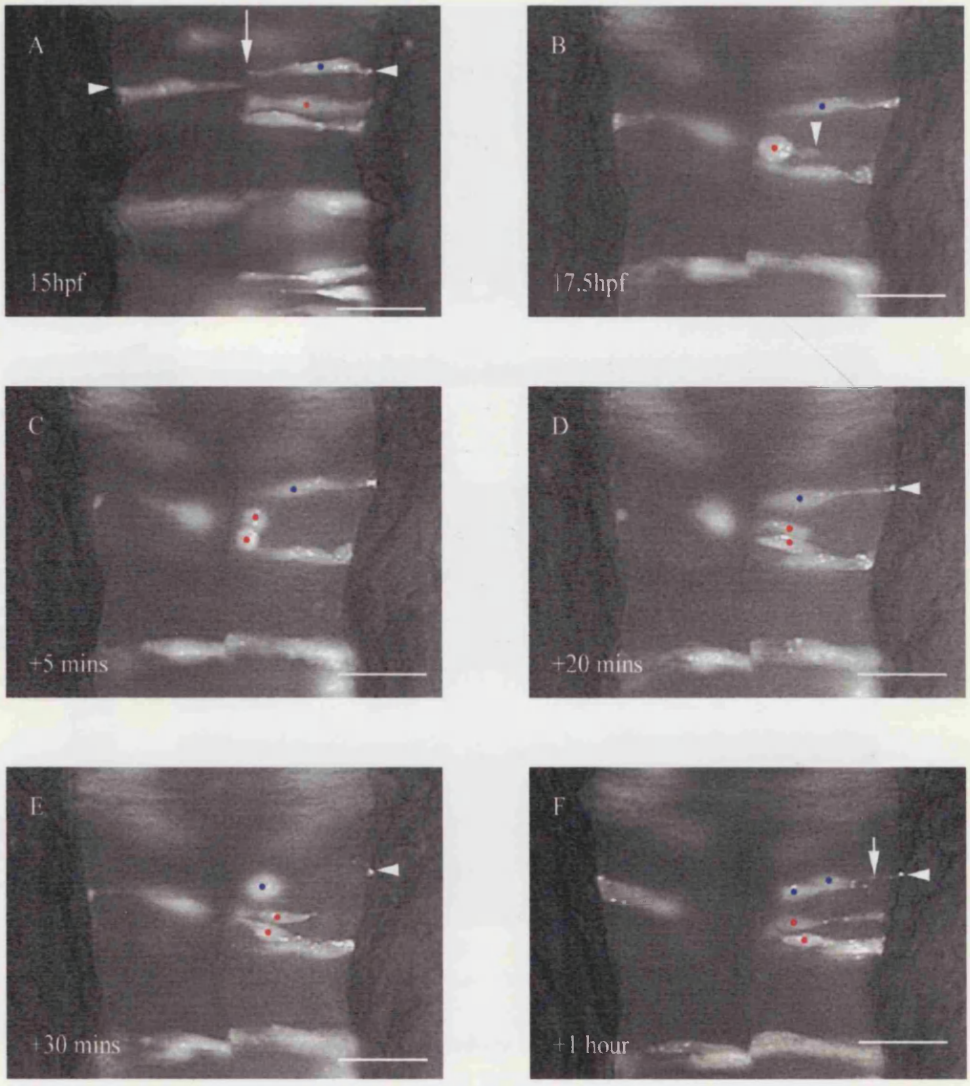

Figure 3.6. Neuroepithelial cell behaviour during the neural rod stage.
A-F are stills from a time-lapse movie looking at a large clone of dextran labelled cells.
All images are horizontal sections with anterior to the top. The midline seam is indicated by an arrow in A. See also supplementary movie 3.5.
A shows that neuroepithelial cells of the neural rod are elongate and stretch between the midline seam (arrow) and the edge of the epithelium (arrowheads). Two cells are marked, one with a blue spot and one with a red spot. These cells and their progeny are followed throughout the time-lapse sequence.
B shows that the red cell is rounding up its cytoplasm at the ventricular surface in preparation to divide. A trailing piece of cytoplasm can still be seen (arrowhead).
C shows that five minutes later the red cell has undergone cytokinesis and there is no sign of any trailing cytoplasm oriented along the apico-basal axis.
D shows the blue cell has a concentrated piece of dye in its endfoot at the pial surface (arrowhead).
E shows that 10 minutes later the blue cell has rounded up to divide and that the concentrated piece of dye remains at the pial surface. No process can be seen adjoining the main part of the cell and the piece of dye at the pial surface at this resolution.
F shows that one of the progeny of the blue cell's division has extended a process (arrow) and reconnected to the dye spot (arrowhead) at the pial surface.
All scale bars = 50μm.

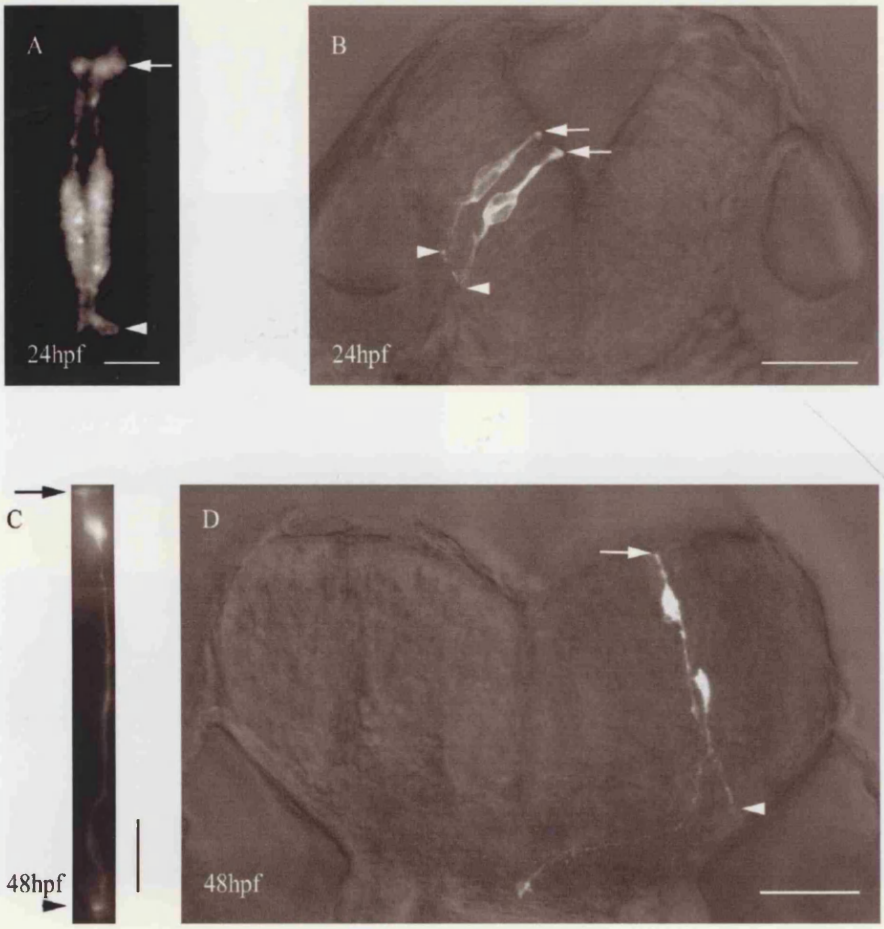

Figure 3.7. Neuroepithelial/ Radial cell morphology in the hindbrain.
A shows two dextran labelled cells at 24hpf that stretch between the ventricular surface (arrow) and the pial surface (arrowhead). Scale bar = 20μm.
B shows cells expressing α tubulin GFP at 24 hpf in a transverse section cut through the hindbrain at the level of rhomobmere 5. Four radial cells stretch processes between the ventricular surface (arrows) and the pial surface (arrowheads). Scale bar = 50μm.
C shows a single cell that has been injected with dextran at 48hpf that stretches from the ventricular surface (arrow) to the pial surface (arrowhead). The cell body is closer to the ventricular surface at this stage and is within the ventricular zone. Scale bar = 20μm.
D shows cells expressing α tubulin GFP at 48hpf in a transverse section cut through the hindbrain at the level of rhomobmere 5. A cell can be seen that stretches a process between the ventricular surface (arrow) and the pial surface (arrowhead). A neuron with an axon and a growth cone near the ventral midline is also shown. Scale bar = 50μm.

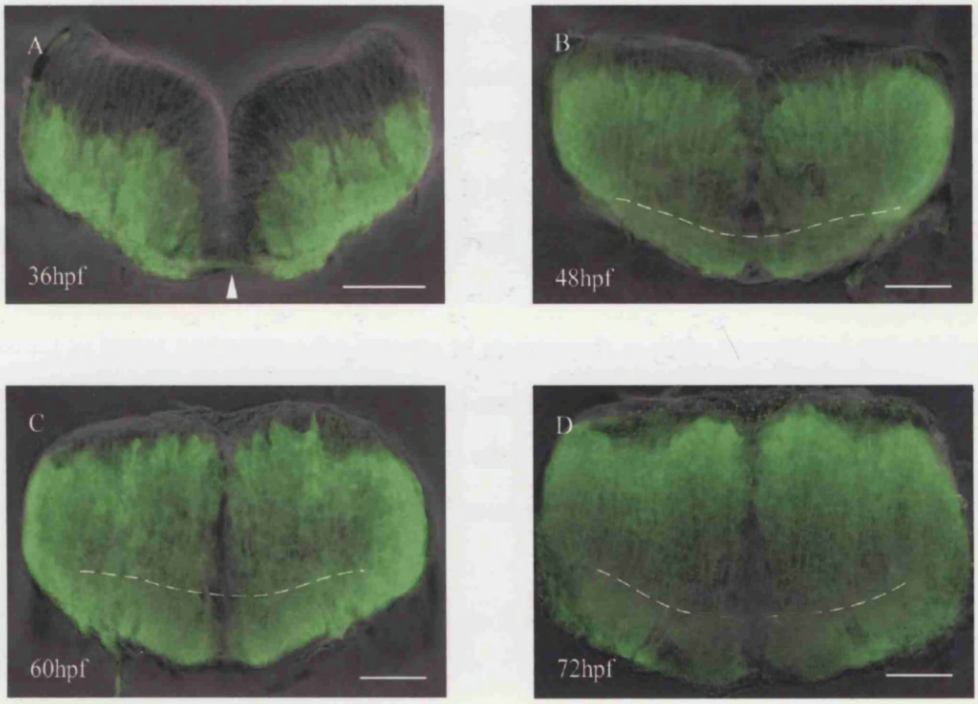

Figure 3.8. Expansion of the HuC-GFP +ve mantle zone.
A-D show transverse views of the hindbrain at the level of rhombomeres 4-5. HuC-GFP +ve cells are green and the non-neural venticular zone is seen as non fluorescent regions. By 36hpf (A) there is a distinct T shaped ventricular zone. Dorsal to the top in all images. Cell processes also contain GFP and are obvious by 36hpf (arrowhead). The boudary between the mantle zone of neuronal cell bodies and the marginal zone of axonal processes is indicated by a white dashed line in B, C and D with cell bodies lying above the line and the processes below. Scale bars = 50μm.

Inter-kinetic nuclear migration takes place throughout neurogenesis and is restricted within the ventricular zone

Time-lapse analysis of dextran labelled cells showed that the position of the nucleus changed over time and moved from a region near to the pial surface to the ventricular surface when the cell was going to divide (Supplementary movie 3.5). However there was no direct evidence from this data that nuclei seen further from the ventricular surface were synthesising DNA. Furthermore it was not clear if the process of interkinetic nuclear migration continued at later stages of development when a distinct mantle zone has formed or when the ventricular zone begins to get much smaller. Furthermore it was not clear to what extent progenitor cell nuclei could move in the neuroepithelium.

In order to better understand the process of interkinetic nuclear migration I pulse labelled HuC-GFP +ve embryos with BrdU at 24 and 36h and left the embryos to develop for intervals of 1, 3, 5, 7, 9, 13, 17 and 21h after which time the embryos were fixed and double stained for BrdU and HuC-GFP immunoreactivity.

The first and most striking observation was that BrdU labelled nuclei did not move into the mantle zone without co expressing GFP (Figure 3.9). The conclusion from this is that if progenitors undergo interkinetic nuclear migration then that this movement is restricted to the ventricular zone.

To examine if the BrdU +ve population did undergo interkinetic nuclear migration the distance from the ventricular surface to the centre of BrdU +ve nuclei was measured for many individual cells in the ventricular zone in individual specimens and the average distance was calculated. The distance from the ventricular surface to the edge of the mantle zone was measured through each of the BrdU +ve nuclei that were included in the previous measurement. Again the average length between the ventricular surface and the mantle zone was calculated for each individual specimen. The average distance of BrdU +ve nuclei from the ventricular surface was divided by the average length of the ventricular zone to give a relative index of how far the BrdU +ve population was away from the ventricular surface in a given embryo at a particular time relative to the size of the ventricular zone.

Embryos fixed just 1hr after pulse labelling at 24hpf had their nuclei (n=21) furthest from the ventricular surface. The BrdU labelled population of nuclei (n=52) moved relatively closer to the ventricular surface when left to develop for a 5-hour period after pulse

labelling. Over the next 4-hour period the movement of the nuclear population (n=47) was back away from the ventricular surface. This showed that the population does undergo interkinetic nuclear migration in the zebrafish hindbrain (Graph 3.1) and indirectly suggests that the cell cycle at this time is on the order of 9 hours long at 24hpf. The same analysis was made on embryos pulse labelled at 36 hpf. The movement of the population of nuclei between those analysed 1 hour (n=20) after pulse labelling and those 5 hours (n=28) after pulse labelling was towards the ventricular surface again showing that the process still takes place at this stage of development. However, the relative movement of the population after this point was difficult to ascertain as the size of the ventricular zone had decreased to just 2-3 cell layers deep such that cells moving to the ventricular zone to divide were essentially swapping positions with those not at the ventricular surface and hence the population did not seem to move at all,

The ventricular zone expresses molecular characteristics of radial glia

I wanted to know if the cells I had observed with radial morphology in my dextran and α tubulin analysis were the radial glia that formed the glial curtain or if the glial curtain was a more specialised structure. In order to examine the glial curtain I stained embryos with the tools that were used to identify this structure initially i.e. antibodies against zebrafish radial cell (zrf) 1 and against Glial Fibrillary Acidic protein (GFAP). I found that the outline of radial cell bodies could be recognised when both anti zrf-1 and anti GFAP were revealed by fluorescent secondary antibodies (Figure 3.10 A+B). Furthermore it was apparent that most cells in the ventricular zone were zrf-1 and GFAP +ve (Figure 3.10 A+B). As these cell bodies were in the ventricular zone it became obvious to ask if these glial markers were co-expressed with mitotic markers. A large number of cells co-expressed zrf-1 and pH-3 indicating that these glial cells had molecular characteristics of progenitors (Figure 3.10 B-E).

In order to be sure that the zrf-1/ GFAP +ve cells were largely in the ventricular zone I double stained HuC-GFP +ve embryos with anti zrf-1 and anti GFP. The GFP in these embryos is expressed in post-mitotic neurons and thus demarcates the mantle zone. The zrf-1 +ve population was seen to exist in largely complimentary domains to the HuC-GFP +ve neuronal population (Figure 3.10 F). This suggested that the cells stained by these glial markers made up the bulk of the non-neuronal ventricular zone.

The glial curtain may also contain neuronal processes

Horizontal sections of anti GFAP labelled specimens showed clearly that these cells contributed to the glial curtain as described by Trevarrow et al., 1990 (Figure 3.11 A+B) but it was not certain if the glial curtain was only comprised of these cells. I observed that acetylated tubulin reactivity could also be detected in cell processes that corresponded in position to the glial curtain (Figure 3.11 C+D). This marker is more traditionally used to visualise axonal tracts in zebrafish although acetylated tubulin is expressed at some level in all cells. This raised the possibility that either the glial curtain also contains fibres belonging to radially projecting neurons or that radial glial like cells express acetylated tubulin. I found that there are indeed neurons that extend processes radially (Figure 3.11 E) but did not investigate if these neurons also express glial markers transiently after their birth and or acetylated tubulin. Further characterisation of the glial curtain was pursued by another student in the Clarke lab.

Proliferative zones are vastly reduced and very localised by 48hpf

BrdU pulse labelling was carried out to analyse the domains of proliferation during late neurogenesis. Embryos were pulse labelled with BrdU at 36 and 48 hpf and fixed 15 minutes later. BrdU +ve nuclei were seen in the 36hpf specimen in the entire ventricular zone (Figure 3.12A). By this time BrdU +ve cells were only located 3-5 cell diameters away from the edge of the ventricle in a characteristic T shape (Figure 3.12B). The number of BrdU+ve nuclei was vastly reduced by 48hpf (Figure 3.12C). Almost all dividing cells in the dorsal ventricular zone seemed to be at the rhombic lip (Figure 3.12 D). There were still a large number of BrdU+ve nuclei in the ventro-medial domain at 48hpf (Figure 3.12D). These results show that the number of cells still in the cell cycle is vastly reduced by 48hpf. The localisation of cell bodies within the ventricular zone may denote the restricted position of progenitors or a difference in the cell cycle length between progenitors in the rhombic lip and the more medial part of the dorsal ventricular zone.

The ventro-medial domain of BrdU +ve nuclei corresponds in position to the region where oligodendrocytes arise in the zebrafish hindbrain later in development (Brösamle and Halpern, 2002). A few cells in this domain seem to lie outside the ventricular zone (Figure 3.12 B) and could correspond to oligodendrocyte progenitors that divide as they migrate away from the VZ.

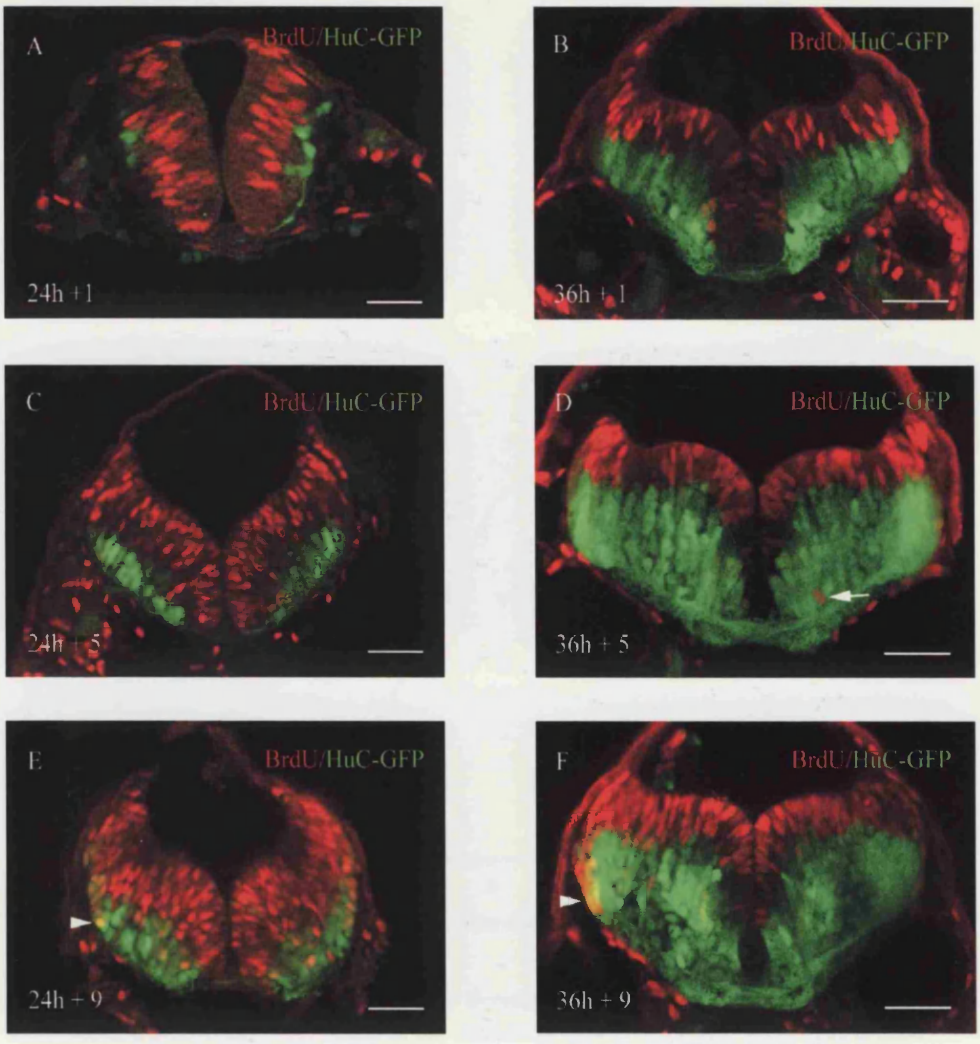

Figure 3.9. Domains of interkinetic nuclear migration. Embryos are pulse labelled with BrdU and left to grow for increasing intervals of time. All images are single transverse confocal sections through the hindbrain at the level of rhombomeres 4-5.

A, C + E show embryos pulsed at 24 hpf and left to grow for 1, 5 and 9 hours respectively. BrdU+ve nuclei almost never enter the green mantle zone unless they appear yellow (arrowhead) indicating that they express HuC-GFP and have differentiated. All scale bars = 50µm.

B, D and F show embryos pulsed at 36 hpf and left to grow for 1, 5 and 9 hours. BrdU+ve nuclei do not enter the green mantle zone unless the also appear yellow (arrowhead) indicating that they express HuC-GFP and have differentiated. A single exception to the rule is shown in D (arrow). This could be an oligodendrocyte progenitor, which are known to divide whilst migrating to the white matter. All scale bars = 50µm.

G

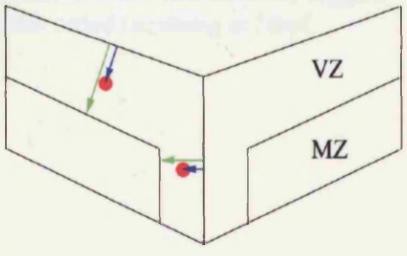

G shows a schematic diagram of a transverse section and explains how measurements were made in this study. The distance from the ventricular surface to the centre of BrdU +ve nuclei (blue arrows to red spots) was measured as was the distance from the ventricular surface to the edge of the mantle zone (green arrows) through each BrdU +ve nucleus examined. This was done for many cells in a section and the average distance of all BrdU +ve nuclei in this population from the ventricular surface was divided by the average depth of the ventricular surface (average of all green arrows) to get an index of how far the BrdU+ve population was from the ventricular surface relative to size of the VZ.

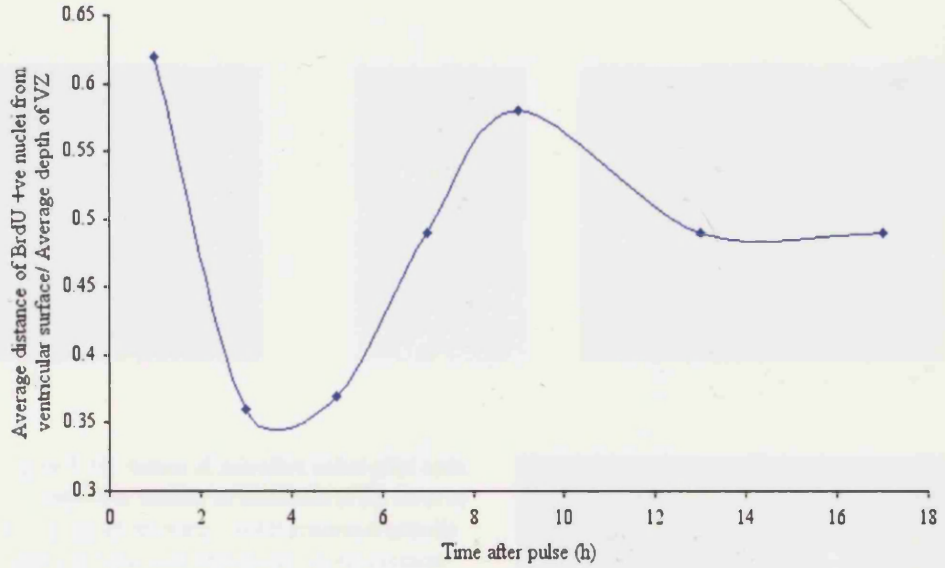

Graph 3.1. Interkinetic nuclear migration. The distance of nuclei from the ventricular surface was measured as a proportion of the length of the ventricular zone for a population of cells at each timepoint. This graph represents the net movement of the population of BrdU +ve clls pulse labelled at 24 hpf relative to the ventricular surface over the next seventeen hours. This indirectly suggests that the cell cycle is of the order of 8-10 hours long during this period i.e. startng at 24hpf.

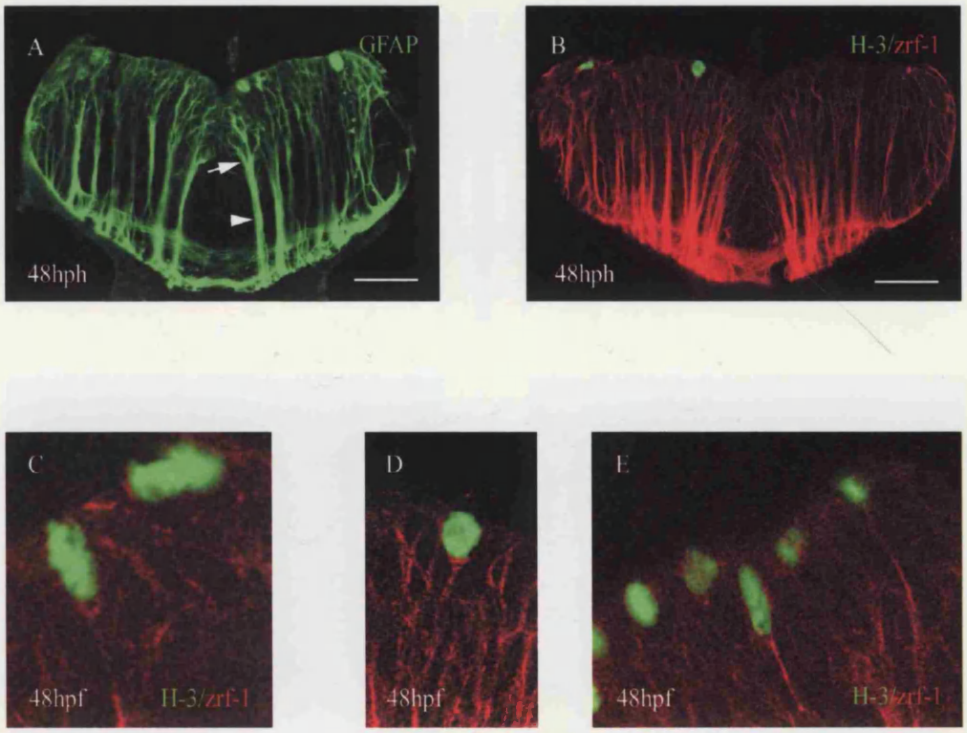

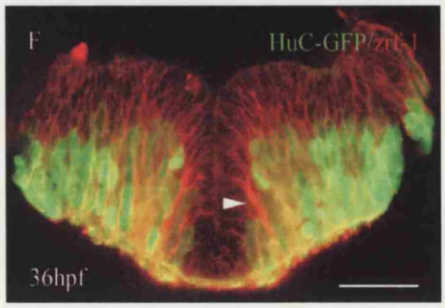

Figure 3.10. Nature of zebrafish radial glial cells.
A. Transverse section of hindbrain at the level of r4-5 at 48hpf showing GFAP immunoreactivity. Dorsal is to the top. The dorsal region contains widespread labelling that covers the majority of the ventricular zone. GFAP +ve fibres funnel (arrow) into bundles (arrowhead) that are radially oriented along the ventricular to pial axis. It was only the brightly stained fibre bundles (e.g. arrowhead) that were recognised in the initial characterisation of the glial curtain.
B. Transverse section through the hindbrain at the level of r4-5 at 48hpf showing zrf-1 immunoreactivity (red) and H-3 reactivity (green).
C-E Higher magnification views of cells in the ventricular zone that co-express zrf-1 and H3. All images are transverse views of the VZ with dorsal to the top. The zrf-1 outlines the cell bodies of cells in the ventricular zone whereas the H-3 stain is restricted to the nucleus.
F is a transverse view of the hindbrain at 36hpf. Dorsal is to the top. The widespread labelling of the ventricular zone by zrf-1 (red) is obvious at this stage and outlines the cell bodies within the VZ. This widespread labelling again becomes funneled into bundles of radially oriented fibre tracts (e.g. arrowhead) that run through the HuC-GFP +ve (green) mantle zone.
All scale bars = 50μm.

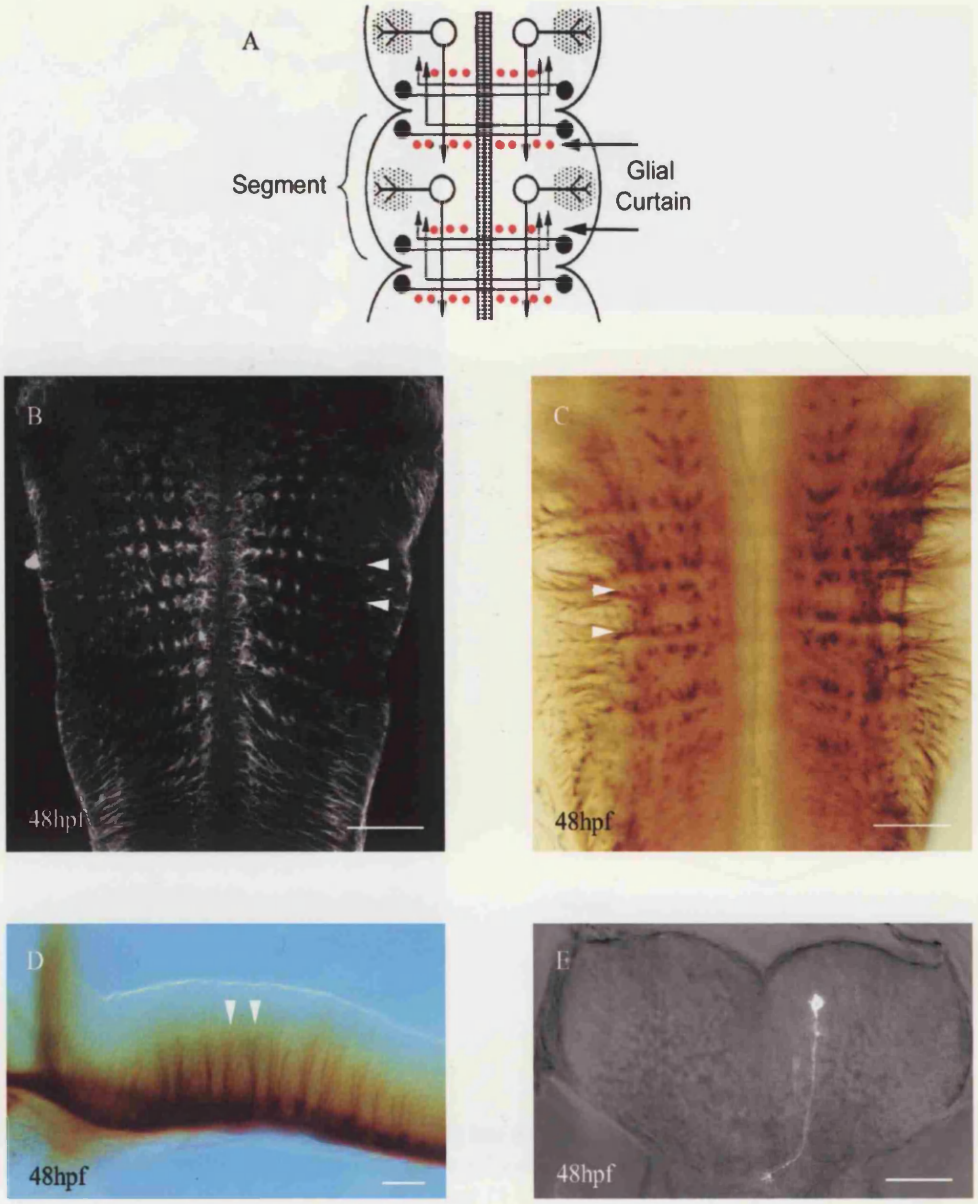

Figure 3.11. The glial curtain may contain neuronal processes.
A, taken from Trevarrow et al., 1990, shows the arrangement of the glial curtain at 48hpf in a hindbrain segment. Bundles of fibres run through the plane of the cartoon and are coloured in red. Two rows of radially oriented fibres exist in each segment.
B shows a horizontal view of the hindbrain at 48hpf labelled with anti GFAP. The glial curtain arrangement of radial fibres described by Trevarrow et al., 1990, can be seen in this view. The two rows of fibres per segment are indicated by the two arrowheads.
C shows a similar view to B but is a specimen labelled with anti acetylated tubulin. Again the two rows of radial fibres per segment are visible and are indicated by the two arrowheads.
D shows a parasaggital view of an anti acetylated tubulin labelled embryo showing the radial arrangement of the glial curtain. Again the two rows of radial fibres per segment are visible and are indicated by the two arrowheads. Dorsal is to the top and anterior to the left.
E shows an α tubulin GFP labelled cell in a transverse section of the hindbrain at 48hpf that projects a process radially into the white matter. It has a growth cone on the end suggesting that it is a neuron.
All scale bars = 50μm.

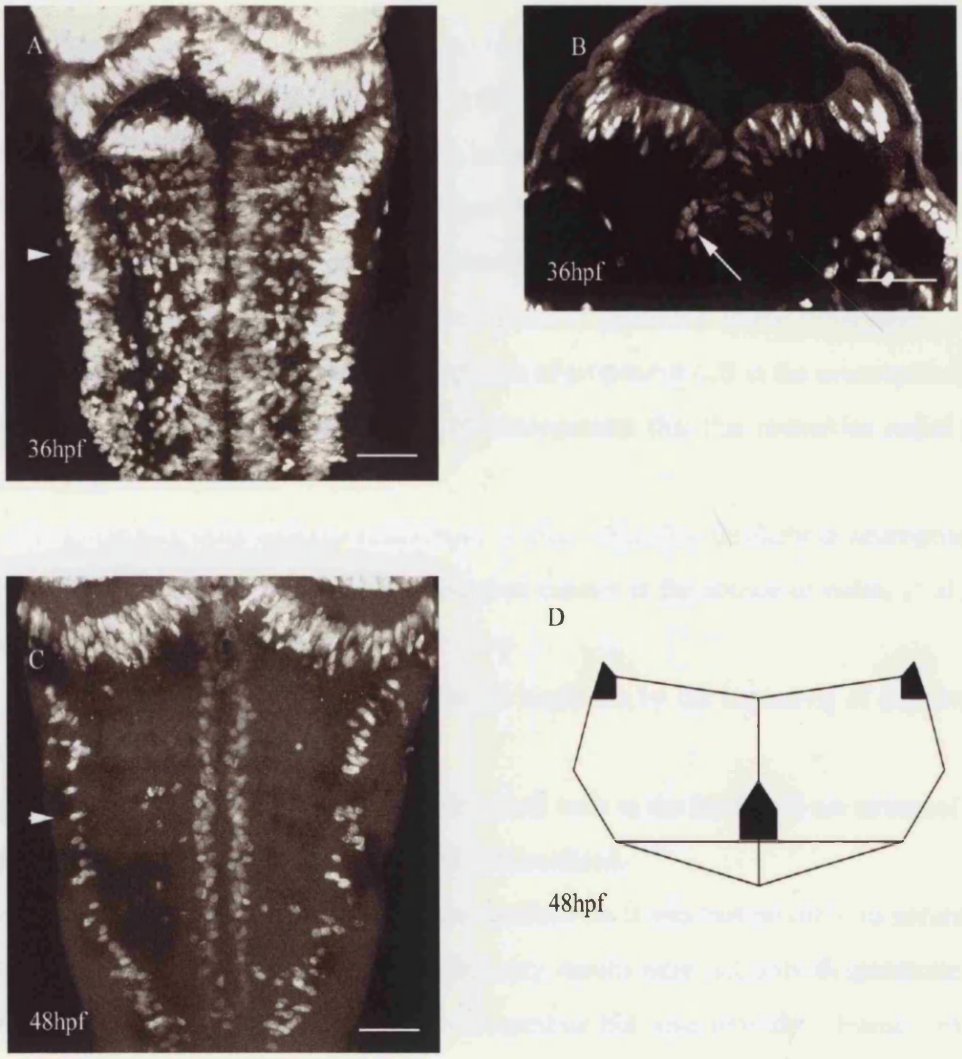

Figure 3.12. Localisation of progenitors during late embryogenesis.
A is a maximum intensity projection of a stack of horizontal confocal sections of a specimen that was pulse labelled with BrdU at 36hpf and fixed 15 minutes later. The ventricular zone contains a wide distribution of BrdU +ve nuclei.
B is a single confocal transverse section cut at roughly the region indicated by the arrowhead in A. This show a distinct T shaped arrangement of the ventricular zone at this stage with the entire dorsal surface covered with BrdU +ve nuclei and also a domain in the ventral midline region. The arrow points to a group of cells that seem to lie outside the ventricular zone and may be oligodendrocyte progenitors that are known to divide whilst migrating towards the white matter.
C is a maximum intensity projection of a stack of horizontal confocal sections of a specimen that was pulse labelled with BrdU at 48hpf and fixed 15 minutes later. Now the location of BrdU +ve nuclei is very restriced and they are seen primarily on the rhombic lip or near the midline.
D is a schematic transverse section through the hindbrain at 48hpf at a region that would correspond to a section cut at the level indicated by the arrowhead in C. The regions filled in in black show the location of most BrdU +ve nuclei at this stage i.e. at the rhombic lip and in the ventral midline region.
All scale bars = 50μm.

Discussion

In this chapter I have tried to establish that the zebrafish hindbrain is a suitable model in which to study the behaviour of cells in an intact embryo during vertebrate neurogenesis. In so doing I have addressed a number of specific questions and found that:

-The zebrafish neural plate is not a pseudostratified epithelium but that it is multilayered.

-Some neuroepithelial cells may not retract their basal processes during cytokinesis.

-There is only one morphologically distinct type of progenitor cell in the neuroepithelium at any one time and that at later stages of neurogenesis that this resembles radial glia described in other systems.

-Neural progenitor cells undergo interkinetic nuclear migration throughout neurogenesis.

-The structure previously described as the glial curtain is the source of radial glial like progenitors in the hindbrain.

-A distinct mantle zone exists in the zebrafish hindbrain by the beginning of day two of development.

-By the end of day two of development almost all cells in the hindbrain are neuronal and that progenitor domains are vastly reduced and localised.

As such a wide range of topics have been touched on it was not possible to scrutinize each completely but I hope that the preliminary results here not only demonstrate the suitability of the system for studying neurogenesis but also provide a framework on which more detailed work can be built in the future.

Neural plate to neural keel

The structure of the neural plate that I have described in this chapter is different to that of published data. It was thought that the cells of the zebrafish neural plate were polarised and maintained contact with both the apical and basal surfaces throughout neurulation (Schmitz et al., 1993). My data shows that cells do not maintain contact with both the apical and basal surfaces of the neuroepithelium during neurulation and my time-lapse analysis shows that very complex cell and tissue movements take place during zebrafish neurulation, the analysis of which was beyond the scope of this thesis. These cell movements contrast the simple folding mechanism that is thought to underlie primary neurulation in higher vertebrates and that would have been predicted to mediate neurulation in the zebrafish according to the model of the neuroepithelium proposed by

Schmitz et al., 1993. The analysis of cell movements during neurulation will be an interesting topic for future study in the zebrafish where there are a number of mutants that do not undergo neurulation correctly e.g. the N-Cadherin mutant parachute (Lele et al., 2002)

Cells of the early zebrafish neural plate seem to resemble those in the Xenopus neural plate to some degree. The neural plate of Xenopus is a bilayered structure and cells do not stretch between the apical and basal surface until the neural tube has formed (Hartenstein, 1989 and Figure 3.1B). An additional correlation has been observed in Xenopus, that the deeper, basal, cells of the neural plate give rise to early born primary neurons after one cell division whereas more superficial, apical, cells give rise to secondary neurons later in development after further rounds of division (Hartenstein, 1989). Whether there are any such differences in cell fate between the cells at different depths in the zebrafish neural plate is obviously unknown.

Early neural tube behaviour

In my analysis once progenitor cells become polarised and elongate they seemed to retract their basal cell process during cytokinesis. However, in some cases a spot of dye could be seen at the pial surface during cytokinesis that was associated with the same cell prior to mitosis. It is likely that there is a process connecting the endfoot to the cytoplasm undergoing division that is invisible in my system and this would agree with recent data that has shown that cells in the mammalian cortex and zebrafish retina keep basal process extended during cytokinesis (Miyata et al., 2001; Das et al., 2003). There is a difference in the details of this process between these two studies. In the cortical study it appears that not only is the basal process maintained during division but that there is a clear endfoot at the pial surface (Miyata et al., 2001). However in the zebrafish retina study there in no indication that an endfoot is maintained at the pial surface but a very fine process extended along the apico- basal axis can be seen during cytokinesis. There are a number of reasons why these results may differ from mine. In my time-lapse analysis the time-intervals were typically of the order of 3-5 minutes. A trailing process oriented along the apico-basal axis could be observed just 5 minutes before cytokinesis but was not seen during cytokinesis. In the retinal study the time interval between frames of movies that document this behaviour is 10-15 minutes (Das et al., 2003). However my observation of a spot of dye, possibly in the pial endfoot of cells during division indicates

that it may be a matter of the resolution of my system that means that I cannot see an intermediate process between the endfoot and the cytoplasm that is dividing. The study in the cerebral cortex analysed DiI labelled cells which is a lipophilic dye that remains in the membrane and the study in the zebrafish retina followed cells that expressed a membrane bound GFP. My study followed cells labelled with dextran, which is of course restricted to the cytoplasm. If prior to mitosis the bulk of cytoplasm is moved towards the ventricular surface for division it is possible that most dextran is also moved with this, as it is a relatively large molecule. It is conceivable that a process that remains attached to the pial surface may not contain a large volume of cytoplasm and hence would not be visible by illuminating dextran molecules. However, the process will still be surrounded by a membrane, meaning that molecules trapped in the membrane may still be visible, as seems to be the case in the cortical study and the zebrafish retinal study. Another recent paper has made a comment on a process being maintained at the basal surface during cytokinesis. In this case a cytoplasmic GFP was used and the cells being studied were imaged in an explanted rat retina. The authors claim that in only 19% of cases did they see such a basal process being maintained during division (Cayouette and Raff, 2003). This low incidence may correlate with the fact that they also used a cytoplasmic tracer as I did in my analysis. Furthermore my study was carried out on a compound microscope and at relatively low resolution using a dry x 20 objective lens. The study in the zebrafish retina (Das et al., 2003) on the other hand was carried out using a multiphoton microscope and a x63 objective lens making it possible that finer processes could be observed using this system.

Interkinetic nuclear migration

The process of interkinetic nuclear migration (iknm) was first documented nearly 70 years ago (Sauer, 1935a; b; 1936; 1937) but its importance at stages of development when a distinct mantle zone exists is unclear. I have shown that interkinetic nuclear migration does continue during late neurogenesis and found also that the position of BrdU +ve nuclei never invades the mantle zone. The fact that the nucleus never moves through the mantle zone region might seem intuitive but it is unclear how this could be mediated. How does the nucleus know where the boundary between the ventricular zone and mantle zone is when it is migrating inside a progenitor cell which itself extends through both regions. The nucleus makes no direct contact with the surface of neurons or

other progenitor cells. One possible explanation is that whilst some markers are expressed throughout the length of the progenitor cell others restrict their expression in accordance with the growth of the mantle zone. The Gap43 antigen 2G12 was excluded from the grey matter whilst expressed in radial fibres (Brittis et al., 1995). Although this was taken as evidence that the cell terminated its process before the mantle zone there was no direct evidence of this which means it is possible that it was only it expression within the cell that was restricted from the mantle zone. This kind of asymmetry along the extent of the progenitor cell may form some part of a network that communicates the limits of a progenitor's nuclear migration.

There is no definitive theory as to why neural progenitor nuclei undergo this movement. One study has suggested that movement towards the apical or ventricular surface brings cells into a state where they are competent to express genes of the neurogenic pathway e.g. Notch1, Delta1 and neurogenin 2. Movement in and or out of a region where cells are competent to express these factors in theory limits the potential of progenitor cells to differentiate (Murciano et al., 2002). It is clear that neurogenic genes are primarily expressed in the ventricular zone but this data is usually based on analysis of mRNA and not of the proteins. It is not clear whether expression of Notch or Delta proteins correlates with the movement of the nucleus and main cytoplasm or whether these proteins can be expressed and signal from endfeet or radial processes. In the zebrafish system at late stages of neurogenesis I have shown that iknm still does occur but that nuclei are restricted in their movement within the VZ. This restriction of movement could mean that cells become more restricted to a domain of neurogenic gene expression and thus it is possible that a mechanism that regulates the process and extent of iknm could determine the rate of neurogenesis in the embryo. Sadly very little is known about iknm and it is currently not a topic of intense study in the field.

Radial glia as progenitors

During the duration of this thesis many papers were published that were directly related to some of the results presented in this chapter. The majority of these studies focussed on analysis of the rodent cortex. The main conclusions to emerge are that so called radial glia play a major role as neural progenitors (Hartfuss et al., 2001; Noctor et al., 2001; Heins et al., 2002) and that there is no evidence for a morphologically distinct type of neural progenitor at times when radial glia exist (Noctor et al., 2002). The observations I

have made in the zebrafish hindbrain correspond remarkably with the findings for mammalian cortical progenitors, which is interesting given the evolutionary difference between species and between the two brain areas.

I have provided evidence that the majority of late progenitors express characteristics of radial glia. It is possible that within this population there are a variety of distinct progenitors that may be specified to generate cells of different fates or that have different cell cycle characteristics. The molecular differences that underlie the diverse characteristics between different populations of progenitors are likely to be very complex. Some labs have looked at the expression of a host of molecular markers in the embryo and have shown that neural progenitors are indeed a heterogeneous population (Hartfuss et al., 2001) but such studies are limited to the analysis of a few markers at a time and don't necessarily deal with markers that fundamentally determine the behaviour of the progenitor cell. Other labs have scaled up analysis of the molecular differences between progenitors by using microarrays of cDNA from different cell types and cells at different stages. This type of analysis will vastly expand our understanding of a cell's molecular repertoire and should also allow quantification of expression profiles for genes of interest as well. Connie Cepko's lab has initiated such a screen to analyse retinal progenitors and has specifically looked at the difference in expression profile between progenitor cells and newborn neurons. Initial results showed nearly 800 genes differentially expressed between the two cell types about half of which are known genes (Cepko, pers. comm.). A similar screen was recently published where hundreds of genes were isolated that were transcribed in olfactory progenitors but not in mature olfactory sensory neurons (Tietjen et al., 2003).

Although it may be some time before the rewards of such large-scale approaches will be realised it seems an inherently more logical approach to understanding the complexity of such a vast problem.

Mature glia in zebrafish

At the end of embryogenesis it appears as though the vast majority of cells in the neuroepithelium are neurons but there are a number of non-neuronal cells. These are most likely to be a mixture of radial glial cells, oligodendrocyte progenitors, mature oligodendrocytes and perhaps the zebrafish equivalent of astrocytes. Gliogenesis in higher vertebrates takes place primarily in post-embryonic stages (Parnavelas, 1999) and

given the dearth of mature glia at the end of my analysis of the neuroepithelium the same must also be the case in the zebrafish. The question is what kind of glia might be expected to emerge in post-embryonic stages. One cell type that is certain to exist are oligodendrocytes because CNS axons are myelinated in zebrafish and this starts at approximately 4-5 days post fertilization (Brösamle and Halpern, 2002; Hawkins pers comm.). In fact the Myelin Basic Protein (MBP) is first detected in a small number of cells in the ventro-medial region of the hindbrain (Brösamle and Halpern, 2002). This corresponds to the ventromedial domain of proliferation I have observed at similar stages of development although the fact that they are one and the same cell type needs to be shown directly. Over the next week of development the number of MBP +ve cells increases dramatically and they are seen to migrate into the white matter corresponding to the onset of myelination.

The existence of astrocytes, the other main glial type of the mammalian brain, in zebrafish is much more contentious. One Japanese lab has generated a monoclonal antibody, A-22, which is said to recognise "star shaped cells with long processes," which the authors have called astrocytes. All A-22 cells are also GFAP +ve but there are many GFAP +ve cells that are not A-22 +ve. The vast majority of A-22 +ve cells are found in the grey matter and many are said to contact small veins, a trait of astrocytes in higher vertebrates (Kawai et al., 2001). Despite these claims there is very little visual evidence in the paper to back them up apart from the interpretative drawing of rows of stars kindly provided by the authors. The existence of astrocytes in other lower vertebrate systems is also controversial, almost always relying on expression of GFAP (e.g. Maier and Miller, 1995). A studied has been carried out comparing the nature of GFAP in different species. In the majority of mammalian vertebrates, anti GFAP antibodies recognised a single protein whereas in fish and in frogs two distinct epitopes are recognised by the antibody. In fact the molecular weight of the GFAP recognised by antibodies varies between higher mammalian systems and lower vertebrates such as fish and frogs (Dahl et al., 1985; Holder et al., 1990). Others have found little direct evidence for the existence of stellate astrocytes in Xenopus despite searching extensively (Hollis Cline, pers comm.). A more plausible substitute for the astrocyte in lower vertebrates is the mature radial glia. The existence and diversity of these cells has been demonstrated in the axolotl system. Morphologically distinct radial glia were identified that corresponded with distinct regions of the spinal cord. One common characteristic was the position of the cell body

within the grey matter and the vast elaboration of branched fibres in the white matter (Holder et al., 1990). Others have suggested that the functions of higher vertebrate astrocytes are fulfilled by cells with a radial morphology in the Xenopus (Miller and Liuzzi, 1986).

It will be interesting to see if mature radial glia also exist in the zebrafish system and attempts to uncover the fate of radial glia beyond embryonic stages are ongoing in the Clarke lab.

Chapter 4

Quantification of neurogenesis in the zebrafish hindbrain

Introduction

There are no quantitative analyses of neurogenesis in the zebrafish embryo. One of the main motivations for carrying out such an analysis was to determine if the data I would acquire in my lineage analysis would correlate well with quantification of neurogenesis in a large population. The quantitative analysis would also be helpful in knowing over what period of development a lineage analysis should be carried out.

It struck me that a correlation between lineage analysis and population expansion is rarely provided in other systems and that providing such would not only potentially strengthen observations made in lineage studies but would also help predict what range of behaviour should be expected in a lineage study. This analysis would also provide information about a number of other unanswered questions in the system like, what the relative contribution of primary neurogenesis is in the zebrafish hindbrain and how the proliferative ventricular zone develops during neurogenesis.

In the spinal cord of fish and amphibians a set of early born neurons are generated. Their production is referred to as primary neurogenesis. In the spinal cord neural plate three longitudinal rows of primary neurons are visible either side of the embryonic midline, primary sensory neurons, called Rohon Beard neurons, primary interneurons and primary motor neurons (e.g. Chitnis et al., 1995; 1996; Beattie et al., 1997; Itoh et al., 2003). In the Xenopus the birthdate of these neurons is distinct from later differentiating neurons with most of the primary neurons stemming from a single mitosis in the neural plate that occurs soon after gastrulation (Hartenstein, 1989). In zebrafish there is also a distinct temporal and molecular separation in the generation of primary and secondary motorneurons. Secondary motorneurons depend on signals from the floor plate and notochord to differentiate, as is the case for motor neurons in higher vertebrates. Primary motor neurons on the other hand do not require the presence of either of these tissues for their specification but only on sonic hedgehog signalling from axial mesoderm during gastrulation (Beattie et al., 1997). A recent study has claimed that there are differences between the superficial and deep layers of the Xenopus neural plate ectoderm that control the differentiation of primary neurons (Chalmers et al., 2002). I have shown in Chapter 3 that the zebrafish neural plate is a multilayered structure and that its cells do not maintain

contact with an apical and basal surface throughout neurulation but there is as yet no evidence to suggest whether or not the depth of cells within the neural plate correlates with primary neurogenesis. Previous studies have shown that some reticulospinal neurons in the zebrafish hindbrain are born soon after gastrulation (Mendelson, 1986). I wished to know if these early born primary neurons were a minority or a large proportion of the whole hindbrain neuronal population. My quantification analysis would answer this question directly.

In addition to documenting the dynamics of neurogenesis I wanted to characterise the development of the complementary non-neuronal population in the hindbrain and was particularly keen to see how the progenitor population developed in relation to the neuronal population. I also wanted to examine how many progenitors were retained to generate mature glia or were kept for potential further development in post-embryonic stages.

Another reason for quantifying the dynamics of neurogenesis is that it would serve as a standard against which mutants could be compared in the future. This seemed to me to be a feature of phenotypic analysis often ignored in genetic studies.

The zebrafish hindbrain provided an ideal system in which to perform cell quantification. Determining cell number accurately in a three dimensional tissue is problematic due to several factors. Cell size and cell density are often heterogeneous in a tissue. It is often necessary to fix the tissue for sectioning prior to counting cells. This introduces problems of tissue shrinkage due to the fixation and imperfections that arise as a result of physical sectioning of a tissue. It is also necessary to differentiate between cell types in the same tissue, which might involve additional confounding factors such as antibody staining.
I bypassed several of these problems using my system. The data is collected from the living organism by confocal microscopy and isn't subject to any artefacts of fixation, physical sectioning or other processing. Cells are phenotyped using a combination of transgenic embryos and fluorescent vital dyes that have no observable adverse effects on the development of the specimen. The compartmental nature of rhombomeric segments means that very few cells present in a segment at neural plate stages leave the rhombomere during the course of embryogenesis (Fraser et al., 1990; Birgbauer and

Fraser, 1994). This allowed me to use rhombomeres as a stable unit in which to count cells throughout embryogenesis.

Methods

Unbiased stereology

The problem of determining cell number in a 3D tissue in an unbiased fashion was so contentious that journals started reviewing their policy regarding data that included cell counts. The Journal of Comparative Neurology was one of the first to take measures towards tightening up on the quality of such quantitative data. They requested that authors and referees adhered to the policy that "stereologically based unbiased estimates are always preferable for establishing absolute counts or densities of structures in tissue sections" (Saper, 1996). I have used the unbiased stereological method called the "disector" in my investigation. This method was published under the pseudonym D C Sterio (anagram of disector) in 1984. The principle is very simple. One needs a set of serial sections such as can be acquired using the confocal microscope, although physical sections are often used. The sections must transect (cut) each unit that is to be counted at least once (Figure 4.1A). Therefore the step size between consecutive sections must be smaller than the smallest object that has to be counted. If a section transects a cell profile it is counted as long as the same cell was not seen in the previous section, therefore each cell is only counted the first time it is encountered (Figure 4.1 B). The previous section to the one in which cells are being counted is called the lookup section (Figure 4.2). Instead of counting every cell in a tissue using this method one determines the number of cells in a sample volume of the tissue and uses this value to estimate the real number. How this extrapolation is made is explained below. When determining the number of units in a sample volume an unbiased counting frame is used. The frame has a square of known area bounded by two acceptance lines and two forbidden lines (Figure 4.1C and Figure 4.2). Any cell profile that fits entirely within the area of the counting frame can be counted as well as any cell that is cut by an acceptance line even if the majority of the cell's area lies outside the acceptance line. In accordance with its name, any cell that is cut at any point by a forbidden line cannot be included in the count.

The counting frame can be used to count cells in the third dimension. The area outlined by the counting frame is examined in consecutive sections with cells being counted in one section with the previous section acting as a lookup section. As was described above cells are only counted the first time they are seen and now only if they obey the rules of

the counting frame as well (Figure 4.2). Cells are counted in this way for all consecutive sections through the tissue.

The actual area outlined by the counting frame can either be physically measured or is known due to the properties of the objective lens and the dimensions and number of sections through the tissue being counted from are also known. This means that you can now calculate how many cells exist in that defined volume. Several such sample volumes are made for an individual specimen or tissue. This is done, as there may be differences in cell density between different areas of the tissue making it important to sample from many areas of the tissue. To estimate the number of cells present in the whole tissue you have to measure the total volume of the tissue.

The Cavalieri method is often used to measure tissue volume and its principles are very simple. Due to the variable cross sectional area in different sections through the depth of the tissue it is not accurate to measure the cross sectional area in any one section and multiply it by the entire depth of the tissue. Instead, one measures the cross sectional area of the tissue at equal intervals throughout the tissue. One multiplies the individual areas at each of these intervals by the distances between consecutive points where these areas are measured and then adds all of these sub-volumes together to find the total volume of the tissue (Cavalieri, 1665; Figure 4.3). I used a software package called Volocity (Improvision) to make these calculations. This programme is designed for studying three dimensional data sets and allows the user to easily measure three dimensional volumes and cross sectional areas as are necessary to implement the Cavalieri method. Once the total volume of a tissue has been established, total cell number is established by multiplying the number counted in the sample volumes by the factor by which the real volume is greater than the sample volumes.

Embryo preparation for cell counting

Embryos were incubated from the one cell stage in their chorions in 5μM Bodipy 505/515 or in 5μM Texas Red Bodipy Ceramide in embryo medium. Bodipy 505/515 exclusively labels the cytoplasm and so nuclei can easily be seen as they are not stained and Texas red Bodipy Ceramide labels the cell membrane and interstitial spaces between cells, which means that the outline of individual cells can be deciphered. Wild type embryos were stained with Bodipy 505/515 to see all cells and HuC-GFP +ve embryos

were stained with the Texas Red Bodipy Ceramide to allow co-incident detection of the neurons and non-neuronal cells (Figure 4.2 and Figure 4.4).

Embryos were also put into 0.003% PhenylThioCarbamide (PTU) in embryo medium at 24hpf to prevent pigment formation. Stained embryos were dechorionated and rinsed 3-4 times in embryo medium before being imaged. Imaging was performed on a Leica confocal microscope using x40 or x63 water immersion lenses. Intervals between z planes varied between 2-4μm. The smaller z steps were used as the embryos grew older as cell size decreased accordingly. The total number of cells was counted from stacks of confocal images collected from wild-type embryos stained with Bodipy 505/515 and from HuC-GFP +ve embryos stained with Texas Red Bodipy Ceramide. The number of neurons was determined by subtracting the number of non HuC-GFP +ve cells in specimens counterstained with TR Bodipy ceramide from the total number of cells counted in the same specimen.

Determining onset of HuC-GFP expression

To determine when HuC-GFP expression could be visualised relative to neuronal birth embryos were pulse labelled with BrdU at 24 and 36hpf and left to develop for either 1, 3, 5, 7 or 9 hours. BrdU is incorporated into nuclei during DNA synthesis in S-phase of the cell cycle. By leaving these specimen to grow for increasing time intervals the labelled nuclei will exit S-phase and move through the consecutive stages of the cell cycle. For instance the first cells to leave S-phase will likely be the first cells to enter mitosis. By determining how long it takes for cells labelled in S-phase by BrdU to co-express markers of mitosis one can determine the duration between the end of S-phase and mitosis. Embryos were double immunostained for the presence of BrdU and phosphorylated Histone H-3, which marks cells in mitosis. The same rationale was used to determine the length of time between the end of S-phase and the onset of HuC-GFP expression. Embryos were left to grow for increasing time intervals and double stained for the presence of BrdU and GFP in HuC-GFP +ve embryos. When the minimum time between the end of S-phase and mitosis is subtracted from the minimum time between the end of S-phase and GFP onset then you get the minimum time between mitosis and the onset of GFP expression.

Time-Lapse analysis of HuC-GFP +ve embryos

Embryos were mounted in 1.5% agarose anaesthetised using tricaine and imaged on a Leica confocal using water immersion lenses as described in the General methods.

Acridine orange

The vital dye acridine orange (acridinium chloride hemi- (zinc chloride), Sigma) was used to detect apoptotic corpses in live embryos. Embryos were incubated in a solution of acridine orange at 5μg/ml in embryo medium for 30 minutes and washed in embryo medium several times before imaging. Imaging of the live embryo was performed immediately after on a Leica confocal microscope using x 20 and x 40 water immersion lenses.

Neuronal birthdating

HuC GFP +ve or Islet-1-GFP (Higashijima et al., 2000) +ve embryos were placed in a solution of 2mg/ml BrdU in embryo medium with 2% DMSO at 28.5°C from a succession of defined starting points and left to develop in BrdU until a defined end point. The duration of the shortest incubation in BrdU was of a sufficient length that all cells in the cell cycle at the beginning of the incubation had sufficient time to enter S-phase and thus incorporate BrdU. A neuron's birthday was determined as follows. If a GFP +ve neuron was labelled with BrdU at the end of the study then it was still in the cell cycle at the time when the embryo was placed in BrdU. If a GFP +ve neuron did not incorporate BrdU during the entire incubation time then it had left the cell cycle before the embryo was first incubated in BrdU. Birthdating was carried out on the HuC-GFP population of neurons at 24hpf and on the Islet-1 GFP population of neurons at 30hpf. Embryos were placed in BrdU from 10, 12, 14 and 16hpf until 24hpf to examine the HuC-GFP population and from 9, 10, 11, 12, 13, 14, 15, 16, 17 and 18hpf until 30hpf to examine the islet-1 GFP population. The proportion of neurons at the end points, 24hpf for the HuC-GFP and 30hpf for the Islet-1 GFP, which had left the cell cycle at the initial time of incubation was calculated for each time-point.

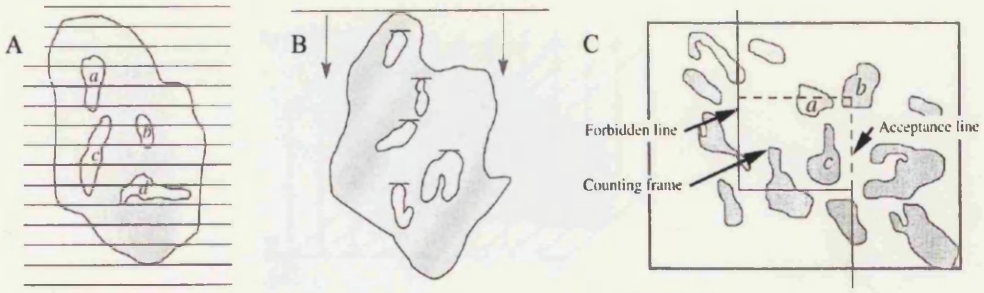

Figure 4.1. The disector principle (Sterio, 1984).
A. Each object to be counted must be intersected by at least one section.
B. Each object is only counted the first time it is cut by a section.
C. The counting frame is a square of known area bounded by acceptance lines (dashed lines) and forbidden lines (full lines). Any cell that falls enitely within the counting frame can be counted (c) as can cells that are cut by the acceptane line (a+b). Cells that are cut by the forbidden lines can not be counted.
All images adapted from Howard and Reed, 1998.

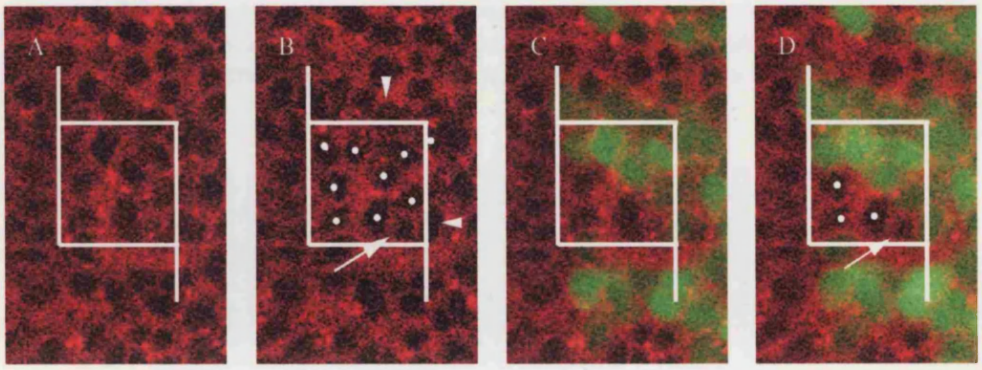

Figure 4.2. Disector principle counting protocol in action.
These are single confocal sections taken in an area of the living hindbrain that is to be counted from. C and D are the same sections as A and B respectively but also show the HuC-GFP +ve neurons. The outline of all cells is shown in red by Texas red Bodipy ceramide and the neurons in green are the HuC-GFP +ve neurons. Counting cells from a volume composed of sections like Aand B give rise to a count of total cell number in that volume and those from volumes containing sections like C and D to a count of non-neuronal number. The number of neurons is calculated by subtracting the number of non-neurons from the total number of cells.
A counting frame as described in Figure 4.1 C is shown in each image. A and C act as lookup sections and B and D as counting sections. Cells are marked with a white spot in the counting section if their profile was seen in the lookup section. Only unmarked cells are counted and only if they obey the rules of the counting frame i.e. if they reside entirely within the frame or touch the acceptance lines. Unmarked cells (arrow) are not counted if they cross the forbidden line. Therefore there are two new cells in the counting section B (arrowheads).
The same counting method was carrid out on sections like C and D but all green cells were ignored. Thus an estimate of non-neuronal number can be made. In section D there are no new non-neuronal cells as they have all been seen in the lookup section (white dots) or are touching the forbidden line (arrow).

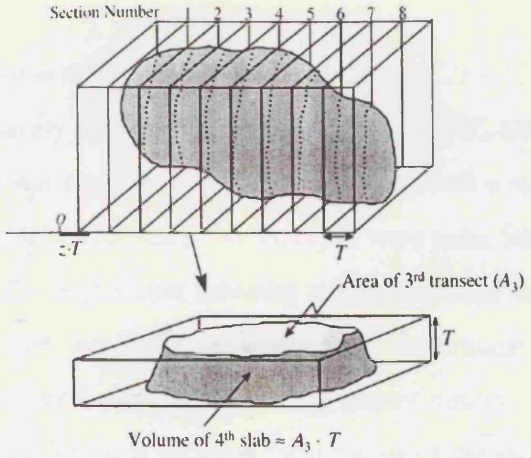

Figure 4.3. Cavalieri method of volume estimation.
The cross sectional area through a tissue is not always uniform and therefore it is inaccurate to measure the cross sectional area at one point in the tissue and multiply this by the depth of the tissue to estimate the volume. Alternatively the volume is divided up into several sub volumes. The cross sectional area in each of these is measured by the depth of the sub volume and the sub-volumes are added together to calculate the total volume. Image taken from Howard and Reed, 1998.

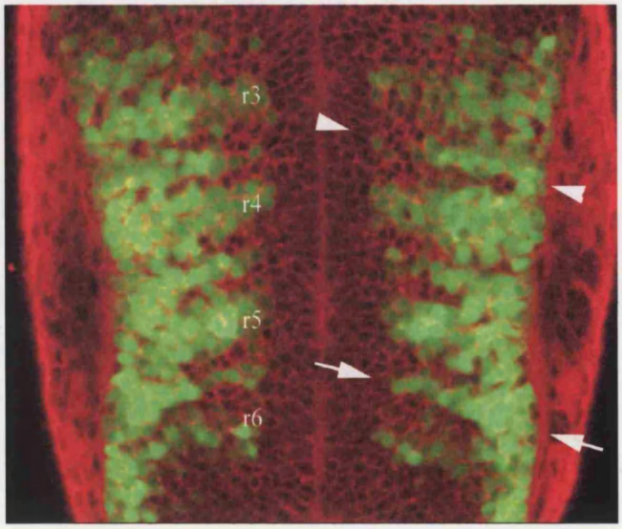

Figure 4.4. HuC-GFP +ve embryo stained with TR Bodipy Ceramide.
Single horizontal confocal section through the living hindbrain at 36hpf. Neurons that express HuC-GFP can be seen in green and the outline of all cell bodies is highlighted by the vital dye Texas red Bodipy ceramide. Stacks of similar confocal sections were used for cell quantification. Cells were counted in rhombomeres 4 and 5. The domain of rhombomeres 4 and 5 is shown with arrowheads pointing to the r3/r4 boundary and arrows to the r5/r6 boundary both of which can be recognised because of the stereotyped arrangement of the HuC-GFP +ve neurons.

Results

HuC-GFP is expressed in neurons soon after their birth

Neurons were exclusively phenotyped by expression of HuC-GFP during the counting analysis. Therefore it was imperative that HuC-GFP was both a reliable and early marker of neuronal differentiation. HuC-GFP +ve embryos were pulse labelled with BrdU at 24, 36 and 48hpf, fixed 10 minutes after labelling and analysed for co-expression with GFP. HuC-GFP +ve cells were not BrdU +ve under these conditions. This shows that HuC-GFP +ve cells do not enter S-phase and that they are post-mitotic.

Time-lapse movies were made at multiple focal planes of the HuC-GFP +ve population between 24 and 36hpf at intervals of five minutes. HuC-GFP +ve cells were never seen to undergo cell division during this period (Supplementary movie 4.1). This further suggests that HuC-GFP +ve cells are post-mitotic.

Neurons recognisable by morphology e.g. Mauthner's neuron or behaviour, or the caudally migrating facial motor neuron pool were all labelled by HuC-GFP. Furthermore neurons such as the dorsal commissural neurons that are recognised by the zn-5 antibody co-localised with HuC-GFP, as did all axonal tracts recognised by anti-acetylated tubulin. These results suggest that all neurons express HuC-GFP.

I determined the time between S-phase and mitosis by determining the shortest interval between incorporation of BrdU, which marks cells in S-phase and co-expression of pH-3, which marks cells in mitosis. The shortest period of time before co-localisation of BrdU and pH-3 was observed was 3 hours. I also measured the shortest time between S-phase and onset of HuC-GFP expression by determining how long it took for co-expression of cells labelled in S-phase with BrdU and GFP. This was found to be 7 hours (Figure 4.5 and 4.6). By combining these two pieces of data I found that a duration of 4 hours took place between mitosis and HuC-GFP expression. This was true at both 24hpf (Figure 4.5) and 36hpf (Figure 4.6). This shows that GFP can be visualised in neurons only 4 hours after their birth and establishes HuC-GFP as a reliable early marker of neuronal differentiation.

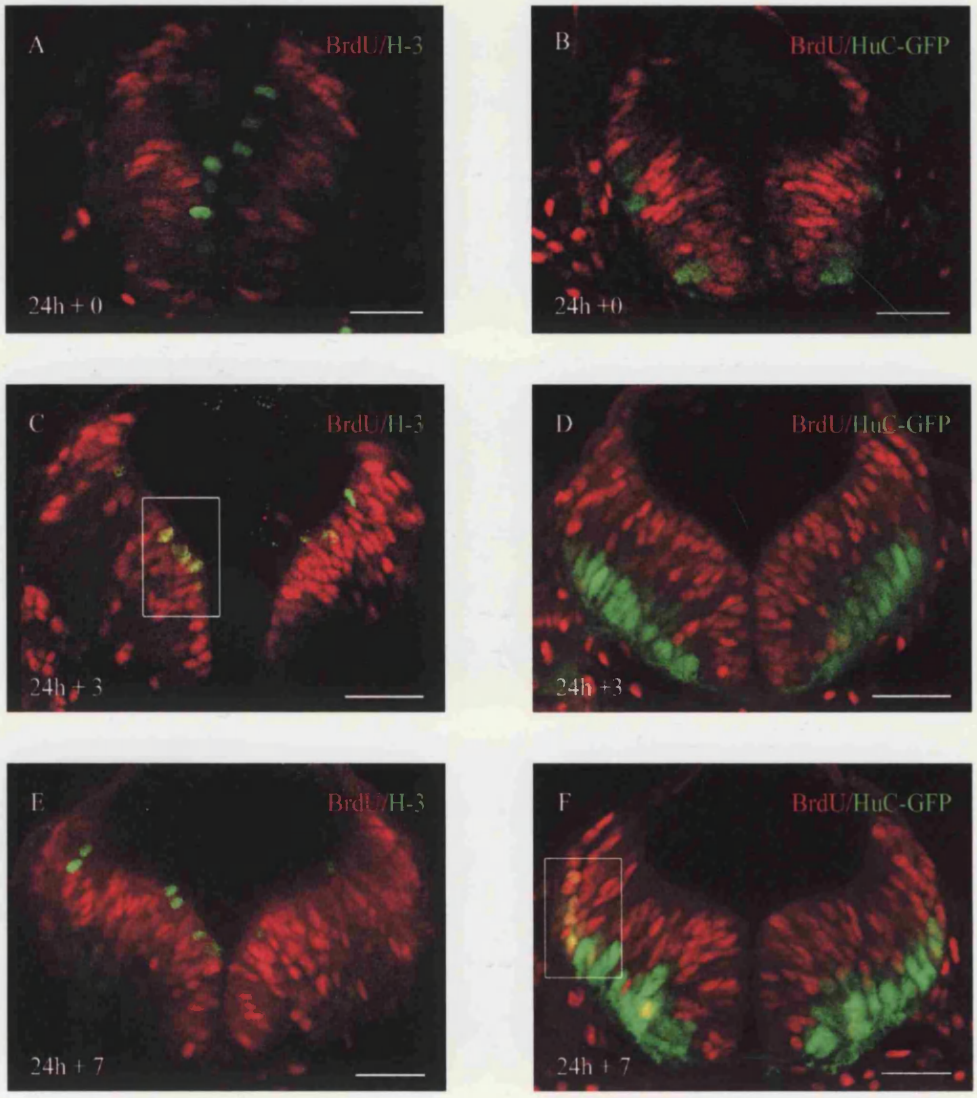

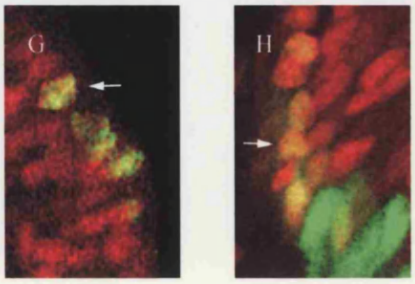

Figure 4.5. HuC-GFP expression is seen 4 hours after mitosis I.
A, C, E and G are single confocal sections that show BrdU in red and H-3 in green.
Embryos have been pulse labelled with BrdU and left to develop for 0h (A), 3h (C+G) and 7h (E).
G is a magnified image of the area outlined by the box in C and shows a yellow cell (arrow) that has been labelled with BrdU (red) and that now expresses H-3 (green). No colocalisation of BrdU and H-3 was before this time-point. This shows that mitosis occurs 3 hours after the end of S-phase.
B, D, F and H are also single confocal sections and show BrdU in red and HuC-GFP in green.
Embryos have been left to develop for 0h (B), 3h (D+H) and 7h (F). H shows a magnified image of the box outlined in F and shows yellow cells (e.g. arrow) that have been labelled with BrdU (red) and that now express HuC-GFP (green). The first cells to co-express seem located to the lateral rhombic lip area magnified in H. No co-localisation was seen at other time-points prior to this. This shows that HuC-GFP expression is first detectable in neurons 7 hours after the end of S-phase and four hours after mitosis.
All scale bars = 50 µm

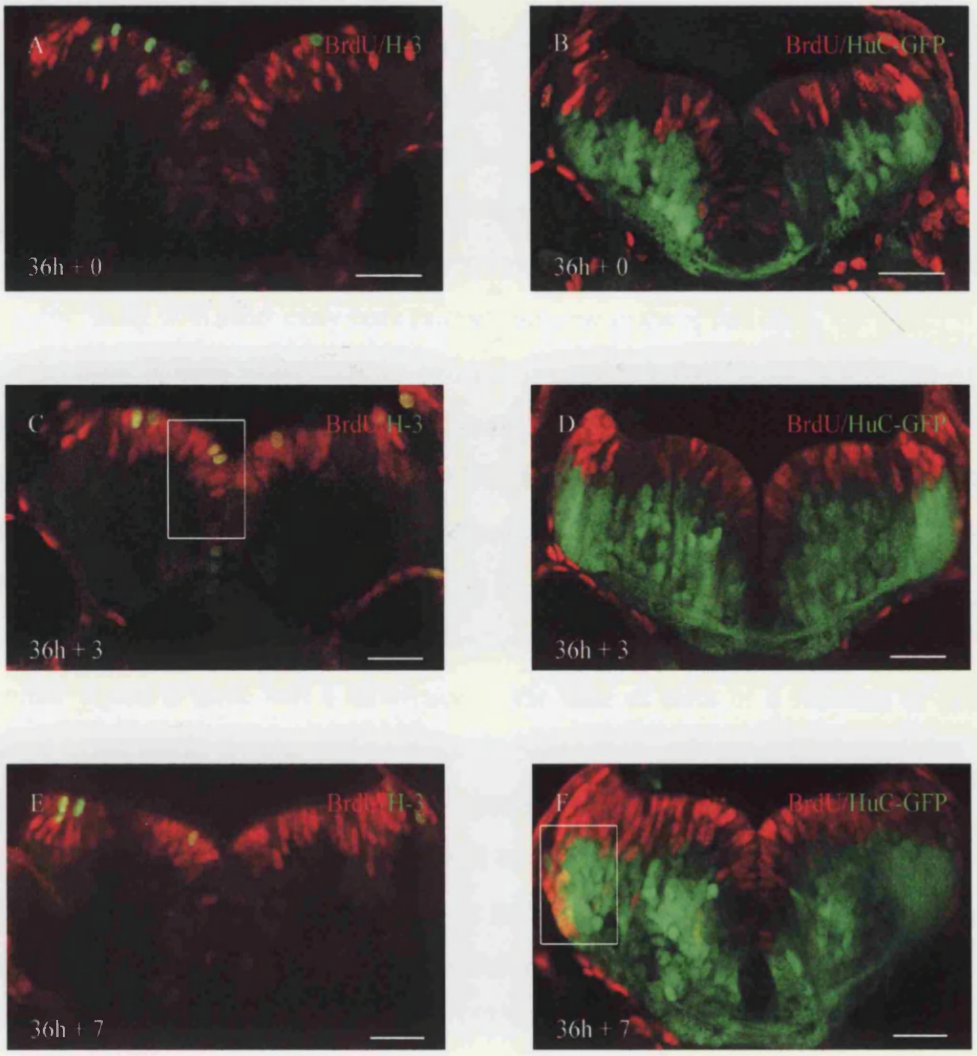

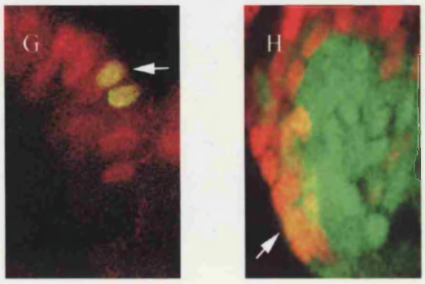

Figure 4.6. HuC-GFP expression is seen 4 hours after mitosis II.
A, C, E and G are single confocal section that show BrdU in red and H-3 in green.
Embryos have been pulse labelled with BrdU and left to develop for 0h (A), 3h (C+G) and 7h (E).
G is a magnified image of the area outlined by the box in C and shows yellow cells (e.g. arrow) that have been labelled with BrdU (red) and that now express H-3 (green). No colocalisation of BrdU and H-3 was before this time-point. This shows that mitosis occurs 3 hours after the end of S-phase.
B, D, F and H are also single confocal sections and show BrdU in red and HuC-GFP in green.
Embryos have been left to develop for 0h (B), 3h (D+H) and 7h (F). H shows a magnified image of the box outlined in F and shows yellow cells (e.g. arrow) that have been labelled with BrdU (red) and that now express HuC-GFP (green). The first cells to co-express seem located to the lateral rhombic lip area magnified in H. No co-localisation was seen at other time-points prior to this. This shows that HuC-GFP expression is first detected in neurons 7 hours after the end of S phase and jence four hours after mitosis.
All scale bars = 50 µm.

Few neurons are born before 15 hpf

Birthdating analysis of the reticulospinal neurons in the zebrafish hindbrain has shown that many of them arise early in development (Mendelson, 1986; Gray et al., 2001). The average birthdate for the Mauthner neuron for instance is about 10hpf, which is just at the end of gastrulation and very soon after the neural plate is visible (Gray et al., 2001). The reticulospinal neurons form one of the first functional networks in the developing animal communicating with other early born primary neurons in the spinal cord.

To determine if early born primary neurons represent a significant proportion of the entire neuronal population in the hindbrain I performed a birthdating study on the population of HuC-GFP neurons found at 24hpf (Figure 4.7). Less than 5% (4/85, n=2) of neurons examined at 24hours were post-mitotic by 12hours, with 10% (10/98, n=2) post-mitotic at 14hours and 17% (18/107, n=2) at 16 hours. Therefore the vast majority of neurons that express HuC-GFP at 24hpf are born between 16 and 24 hours (Graph 4.1).

In order to see if there was a difference in the time of birth of a subclass of neuron relative to the whole population I performed a birthdating analysis on the Islet-1 GFP +ve subclass of motor neurons. Islet-1 +ve neurons are among the first to be seen in the spinal cord. In the Islet-1 GFP line only a subset of Islet-1 +ve neurons in the zebrafish, the cranial motor neurons of the hindbrain. In my birthdating analysis of this population I found that by 15hpf 32% (20/63, n=3) of the total population seen at 30hpf had left the cell cycle and that this increased to 57% (47/83, n=3) by 18hpf (Graph 4.2). This shows that this Islet-1 GFP +ve population of neurons can differentiate early relative to the whole population.

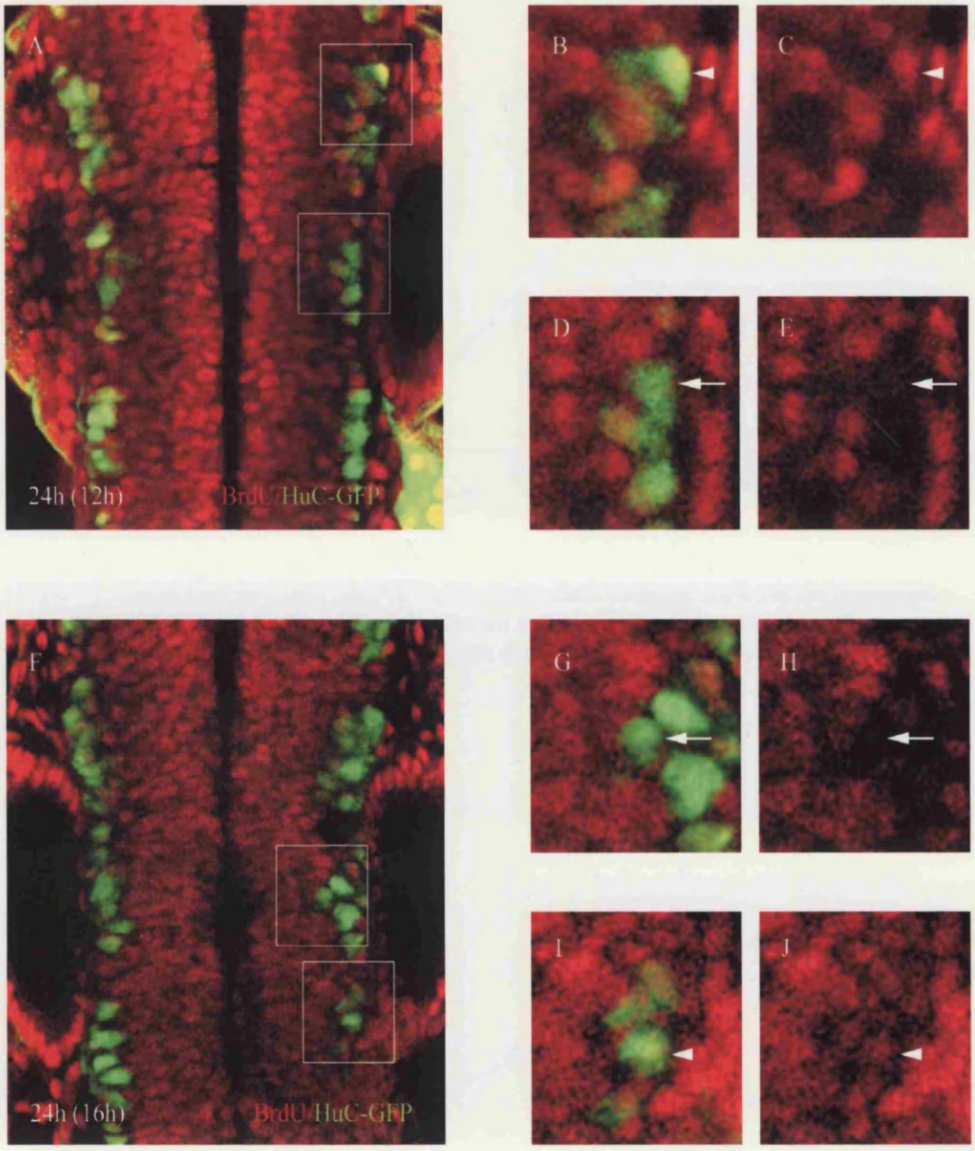

Figure 4.7. Birthdating the HuC-GFP population at 24hpf.
A-E show images of a specimen that was incubated in BrdU from 12 hpf until 24hpf.
F-J show images of a specimen that was incubated in BrdU from 16hpf until 24hpf.
BrdU is red in all images and the HuC-GFP is green and all images are single horizontal confocal sections through the hindbrain with anterior to the top.
Neurons that were born before the initial time of incubation do not incorporate BrdU (arrows) between the initial time of incubation and 24hpf .
Neurons that were born between the initial time of BrdU incubation and 24hpf do incorporate BrdU (arrowheads).
B+C correspond to the top box outlined in A. C is the same images as B without the green channel.
D+E correspond to the bottom box outlined in A. E is the same image as D without the green channel.
G+H correspond to the top box outlined in F. H is the same images as G without the green channel.
I+J correspond to the bottom box outlined in F. J is the same image as I without the green channel.

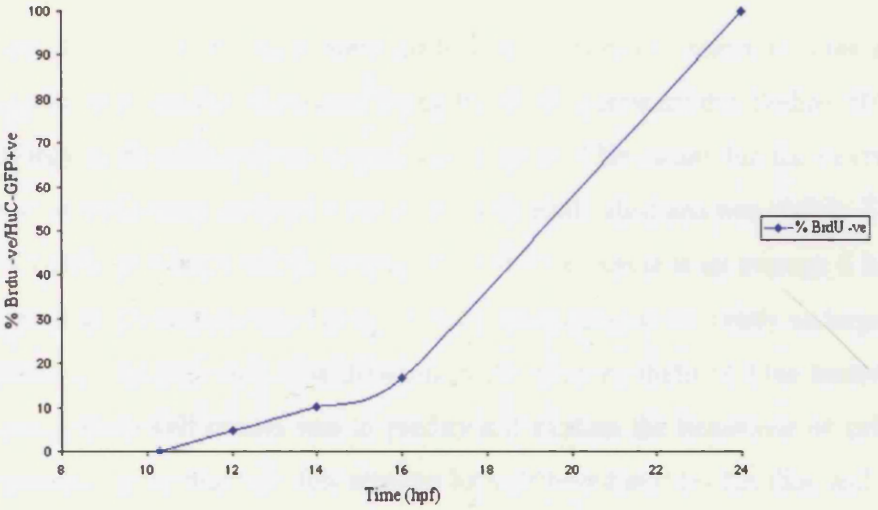

Graph 4.1. Birthdating the 24hpf HuC-GFP population. Each timepoint indicates the proportion of the total HuC-GFP +ve cells at 24hpf that did not incorporate BrdU between the indicated time point and 24hpf. This gives the proportion of cells that had left the cell cycle up to the indicated time point.

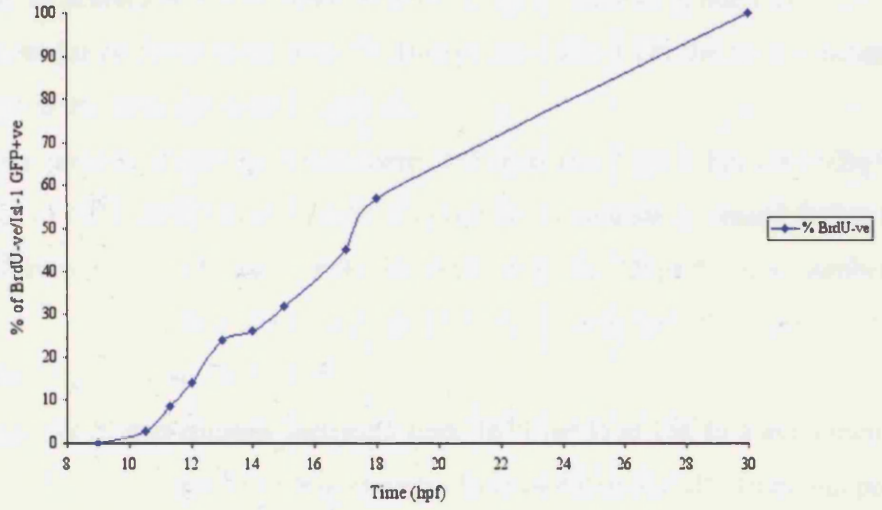

Graph 4.2. Birthdating the 30hpf Islet 1-GFP population. Each timepoint indicates the proportion of the total Islet 1-GFP +ve cells at 30hpf that did not incorporate BrdU between the indicated time point and 30hpf. This gives the proportion of cells that had left the cell cycle up to the indicated time point.

Cell counting

The first stage at which counts were made was at 15hpf (12 somites). This stage was appropriate for a number of reasons. Using the vital fluorescent dye Bodipy 505/515 the morphology of rhombomere boundaries was obvious. This meant that the morphological unit from which counts were to be made had been established and was visible. The neural plate is visible at 9 hours and the length of the first cell cycle is on average 6 hours long (Kimmel et al., 1994) meaning that by 15 hours most cells have recently undergone or are just about to undergo their first division in the neuroepithelium. One motivation for performing these cell counts was to predict and explain the behaviour of cells during neurogenesis. Given that very few neurons have differentiated by this time and that most cells have just undergone one division in the neuroepithelium the population at 15 hours has probably doubled in number since the neural plate formed. Starting the cell counts at this stage was also appropriate as I quantified my lineage analysis from the period following the first division in the neuroepithelium i.e. from 15hpf. Counts were performed at 15, 24, 36, 48, 60 and 72hpf in rhombomeres 4+5. Total cells were counted from stacks of confocal images collected from wild-type embryos stained with Bodipy 505/515 and from HuC-GFP +ve embryos stained with Texas Red Bodipy Ceramide. The number of neurons was determined by subtracting the number of non HuC-GFP +ve cells in specimens counterstained with TR Bodipy ceramide from the total number of cells counted in the same specimen (Figure 4.2).

The total number of cells in rhombomeres 4+5 increased from 15hpf until 60hpf from an average of 1639 (n=3) to 6183 (n=5). The number of neurons increased during the same period from 20 (n=5) to 5607 (n=4). However, from 60-72hpf the total number of cells decreased by 312 from 6183 (n=5) to 5871 (n=3) although the number of neurons increased by 101 from 5607-5708.

The number of non-neurons increased from 1639 (n=3) at 15h to a maximum of 2887 (n=3) at 36h. This number of non-neurons decreased dramatically from this point on to only 163 cells by 72h (n=3) as the relative number of neurons increased.

These initial counts are referred to throughout this thesis as the basic counts and are depicted in Graphs 4.3 + 4.4. The standard deviation was calculated for each data point and was very small (Graphs 4.3) showing that the variation between specimens was relatively minimal and that the unbiased counting method was very reproducible from specimen to specimen.

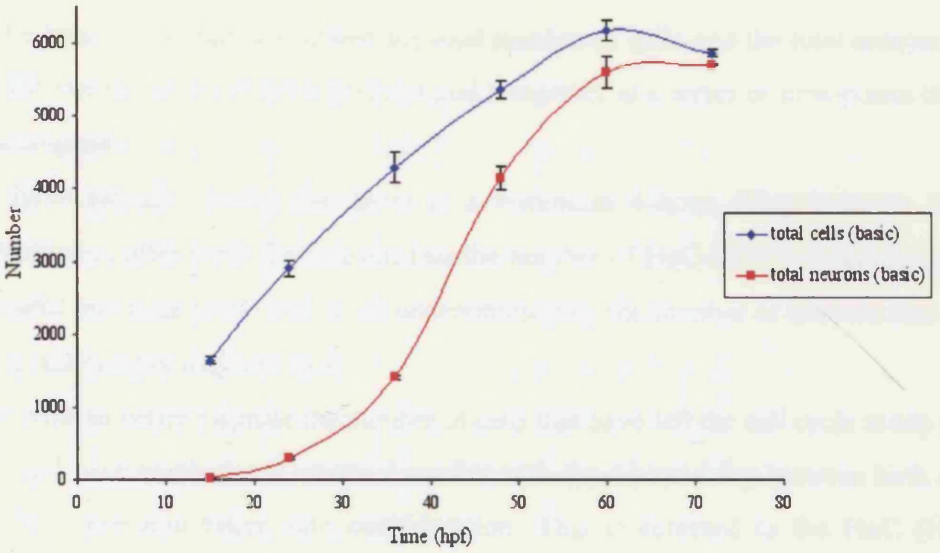

Graph 4.3. Total cell number and neuron number I.
Average total cell number (Blue) and average total HuC-GFP +ve neurons (Red) throughout the first three days of embryogenesis. The error bars show the standard deviation above and below the average.

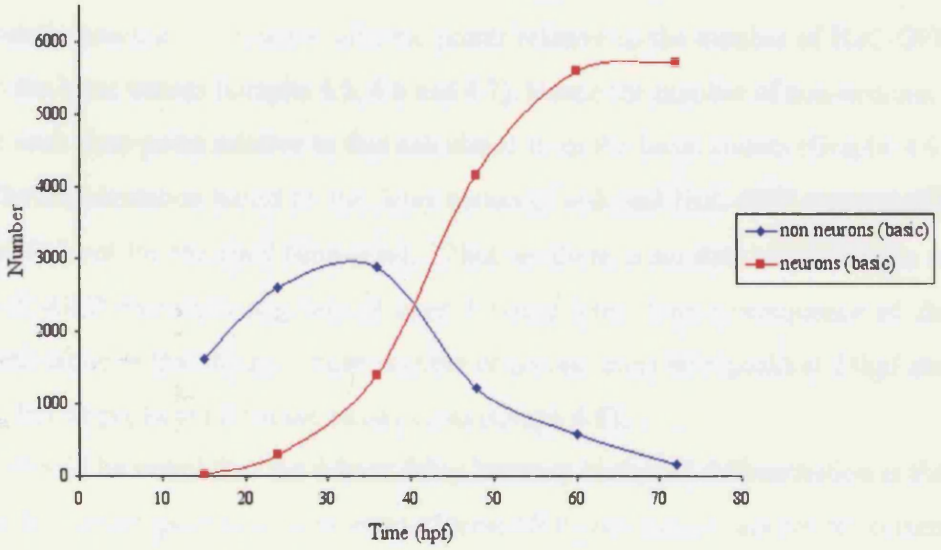

Graph 4.4. Non-neuronal and neuronal number I.
Average total HuC-GFP +ve neurons (Red) and average total non-neurons (Blue) throughout the first three days of embryogenesis. The total non-neuronal number was calculated by subtracting the number of HuC-GFP +ve neurons from the average total number of cells (shown in blue in Graph 4.3)

Refinements of basic cell counts

The basic cell counts calculated the total number of cells and the total number of HuC-GFP +ve neurons in rhombomeres 4 and 5 together at a series of time-points throughout neurogenesis.

I have already shown that there is a minimum 4-hour delay between HuC-GFP expression after birth. This means that the number of HuC-GFP +ve neurons in my cell counts any time-point will be an underestimate of the number of neurons that have left the cell cycle at that time-point.

In order to better estimate the number of cells that have left the cell cycle at any one time-point I have recalculated neuronal number with the 4 hour delay between birth and HuC-GFP expression taken into consideration. This is referred to the HuC (Hu) delay throughout this thesis. The number of post mitotic neurons at a certain time-point now corresponds to the number of HuC-GFP +ve cells predicted to exist four hours after this time-point as these HuC-GFP +ve cells would all have left the cell cycle at least 4 hours previously. The consequence of this refinement is that the calculated number of post-mitotic neurons increases at all time-points relative to the number of HuC-GFP neurons in the basic counts (Graphs 4.5, 4.6 and 4.7). Hence the number of non-neurons decreases at each time-point relative to that calculated from the basic counts (Graphs 4.6 and 4.8). The re-calculation based on the delay between birth and HuC-GFP expression cannot be carried out for the final time-point, 72hpf, as there is no data to predict the number of HuC-GFP +ve cells that would exist 4 hours later. One consequence of this Hu re-calculation is that the maximum number of non-neurons now peaks at 24hpf instead of at 36 hpf as predicted from the basic counts (Graph 4.8).

It should be noted that the 4-hour delay between birth and differentiation is the quickest time in which post-mitotic neurons express GFP and it is not known for certain whether all neurons express GFP after this duration. If some neurons do not express GFP for a lot longer than 4 hours after their birth then my re-calculations could underestimate the number of post-mitotic neurons at each time-point.

Rates of neurogenesis

I have calculated the rates of neurogenesis over different periods of development based on the basic counts and the refined count taking in the delay between birth and differentiation into consideration and these calculations are shown in table 4.1. This data

is presented as the number of neurons produced per hour in both rhombomeres 4 and 5 over each period between consecutive time-points where quantification was carried out. The rate of neurogenesis was highest between 36 and 48hpf whether the data was taken from the basic counts or from the re-calculations that took the Hu delay into consideration. Again, using data from either quantification method, I saw that the rate of neurogenesis slows down considerably during the third day of embryogenesis and that overall generation of neurons occurred at less than 10 neurons per hour between 60 and 72hpf. This may well reflect the fact that the majority of embryonic neurons have been produced by 72hpf. This data only pertains to the region from which cell counts were made i.e. rhombomeres 4 and 5 and the time-course of neurogenesis is likely to vary between distinct brain areas.

Cell death

One factor that could confound an attempt to accurately quantify the rates of neurogenesis in this system is a considerable amount of cell death. Previous studies have shown that there is very little cell death in the developing wild type zebrafish brain (Cole and Ross, 2001; Furutani-Seiki et al., 1996; Abdelilah et al., 1996). To confirm these findings I estimated cell death by analysing acridine orange incorporation in rhombomeres 4 and 5 throughout the period during which the counting analysis was carried out and found an average of 15 dead cells at 15hpf (n=3), 14 at 24hpf (n=2), 12 at 36hpf (n=2) and only 3 at 48hpf (n=2) and basically none at 72hpf. If clearance of corpses takes an average of 2 hours (Cole and Ross, 2001) then the predicted number of cells undergoing apoptosis between 24 and 36 hpf is less than 2% (84/4294) of the total cell number and only 1.3% (72/5367) of the total cells for the period between 36 and 48 hours. I never detected apoptosis by analysing time-lapse movies of HuC-GFP +ve embryos (Supplementary movie 4.1) or Bodipy 505/515 stained embryos between 15 and 36hpf. These results confirm previous work and suggest that cell death plays a minor role in hindbrain development at these stages and should not effect an accurate interpretation of cell quantification dramatically.

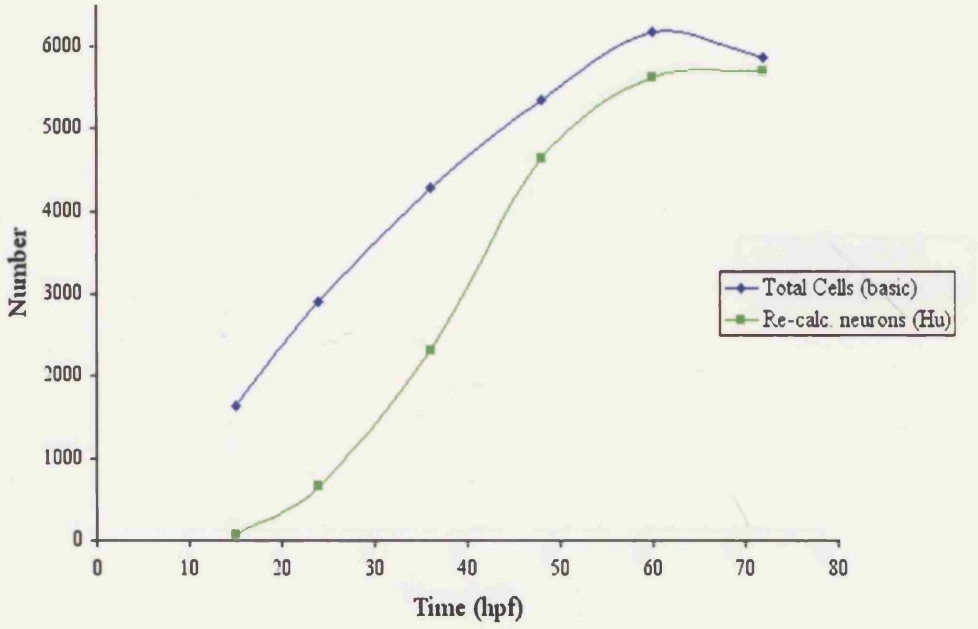

Graph 4.5. Total cell number and re-calculated neuron number.
Average total cell number (Blue) and total neuron number (green) re-calculated taking both limits set by the consecutive time point and the delay between birth and HuC-GFP expression into consideration (Hu).

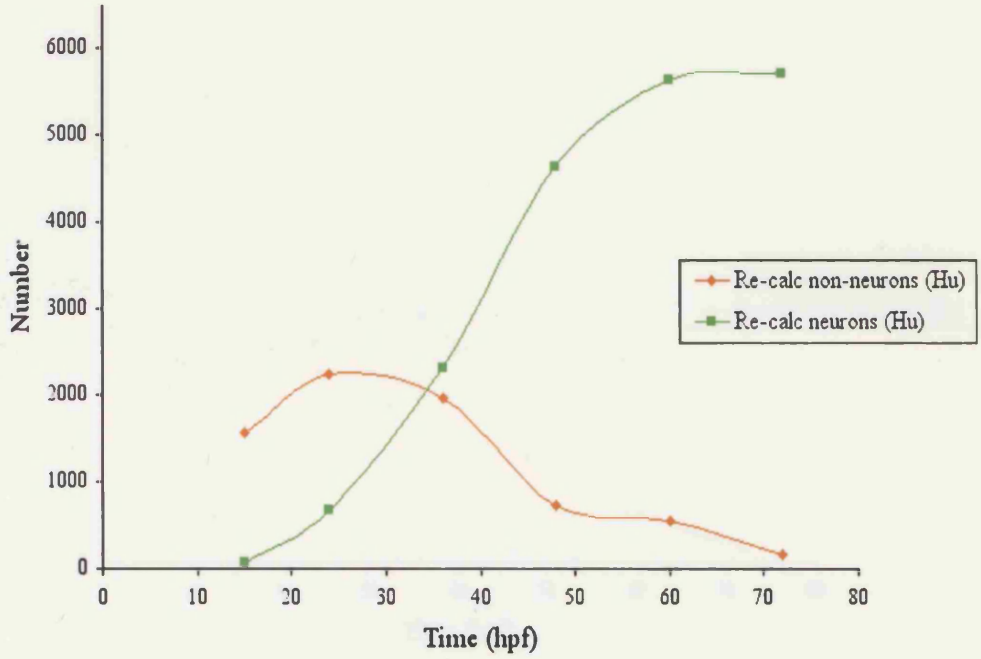

Graph 4.6. Re-calculated non-neuronal and neuronal numbr (Hu).
Total non-neural cell number (orange) and total neuron number (green) both of which have been re-calculated taking the limits set the delay between birth and HuC-GFP expression taken into consideration. The non neuronal number was calculated by taking the recalculated neuron number (Hu) from the total cell number of the basic counts.

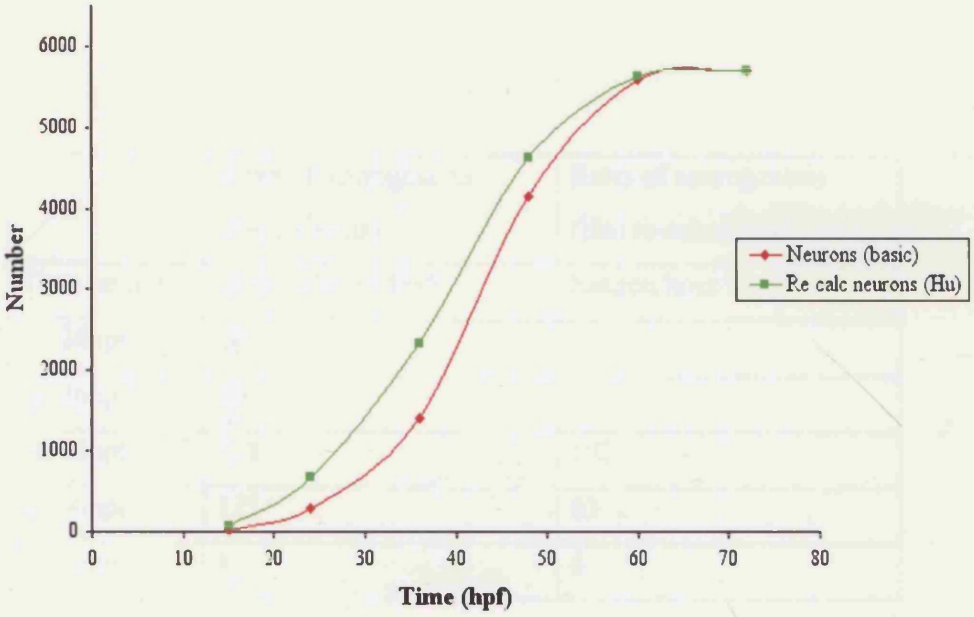

Graph 4.7. Comparison of neuron number between basic counts and recalculations.
Total neuron number as calculated by the basic counts (red), re-calculation based on the delay between birth and HuC-GFP expression (green).

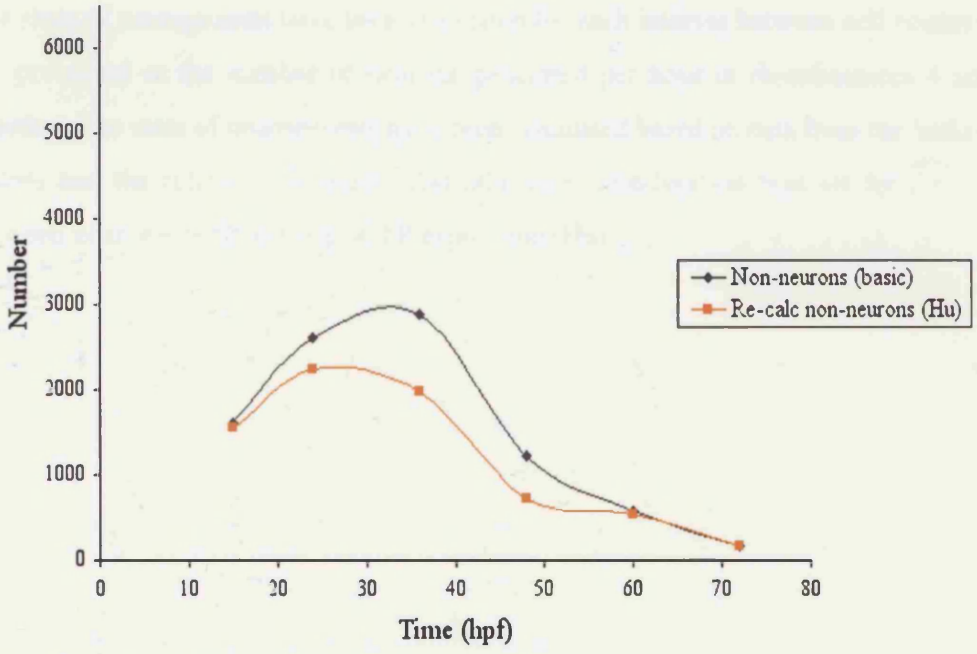

Graph 4.8. Comparison of basic and recalculated non-neuron number.
Total non-neuronal number as calculated by the basic counts (black) and re-calculation based on the delay between birth and HuC-GFP expression (oramge).

	Rates of neurogenesis (basic counts)	Rates of neurogenesis (Hu) re-calculation
Time period	Neuron/hour/r4+r5	Neuron/hour/r4+r5
15-24hpf	19	65
24-36hpf	92	137
36-48hpf	228	192
48-60hpf	121	83
60-72hpf	8	6

Table 4.1. Rates of neurogenesis.

The rates of neurogenesis have been calculated for each interval between cell counts and are presented as the number of neurons generated per hour in rhombomeres 4 and 5 together. The rates of neurogenesis have been calculated based on data from the basic cell counts and the refined cell counts that take into consideration bias set by the delay between neuronal birth and HuC-GFP expression (Hu).

Discussion

I have documented the number of differentiated neurons and the number of non-neuronal cells for two whole rhombomeres over the course of the first 3 days of zebrafish embryogenesis. I have found that by the end of these three days each rhombomere examined has produced nearly 3000 neurons and only has about 100 non-neurons retained for later development. I have found that a relatively small proportion of neurons leave the cell cycle and differentiate during neurulation when primary neurogenesis takes place. Only about 5% (300/5708) of the total neuronal population seen at the end of day 3 have differentiated by 24hpf as analysed by HuC-GFP expression. This shows that the relative number of primary neurons is low in the zebrafish hindbrain. By measuring the overall rates of neurogenesis I have seen that there is a steady increase in neurogenesis until it reaches a maximum rate between 36 and 48hpf. The production of neurons decreases dramatically after this period and the overall progression of neurogenesis through the first three days of zebrafish development resembles a model of the entirety of mouse neurogenesis where the rate of neurogenesis starts off slowly and increases until the progenitor pool is depleted by which time the vast majority of neurons have been produced and after which time the rate of neurogenesis drops dramatically (Takahashi et al., 1996).

Predictions for cell behaviour

A major reason for carrying out this study was to be confident that the data acquired in a lineage study would reflect the behaviour of the population as a whole. The counting data in turn makes predictions for how this lineage data should turn out. I have documented the fact that very few neurons are born in the early neural plate stage of development. Therefore by labelling cells in the neural plate I should expect that most progenitors will divide at least once, the prediction being that the majority would do so as a midline division as has been shown in previous studies (Kimmel et al., 1994; Papan and Campos-Ortega, 1994). My quantification shows that the peak in non-neuronal number occurs at about 24hpf. The total number of cells almost doubles between 15 and 24hpf but a distinct set of neurons has now formed and comprises about 10% (300/2904) of the whole population. The prediction therefore is that most divisions during this period between 15 and 24hpf will have produced at least one progenitor due to the overwhelming majority

of non-neuronal cells at 24hpf. It is difficult to speculate on the division mode that might generate the neurons seen at 24hpf as they could easily be accounted for by either terminal divisions producing pairs of neurons or asymmetric divisions that produce a neuron and a progenitor. My refined counts predict that there are just over 2000 non-neuronal, putative progenitors, at 24 hours. These cells go on to generate about 3000 new cells by the end of the study i.e. at the end of day 3. However at the end of the study there are nearly 5000 new neurons in addition to those seen at 24hpf. The fact that 3000 new cells are generated by 2000 potential progenitors predicts that each of the 2000 progenitors should on average divide at least once over this period. This would generate 2000 new cells. Some cells would have to divide twice to generate the 1000 extra cells seen. The counting also predicts that the vast majority of these divisions have to generate two neurons as there are less than 200 non-neurons left at the end of the study.

The cell counts can be used to predict how development would proceed if asymmetric division accounted for the majority of neurons generated over this period. Throughout this thesis I define an asymmetric division as one that generates a neuron and a progenitor. If one round of asymmetric division takes place after 24hpf then the 2000 non-neuronal cells that my data suggest exist would generate 2000 new cells, 2000 cells would remain non-neuronal and 2000 would differentiate into neurons. My quantification shows that this would leave 1000 new cells to be generated but also 3000 differentiated neurons to be generated. If the 2000 non-neuronal cells that remained following the first asymmetric division divided again this would generate 2000 new cells, irrespective of their phenotype. This would lead to 1000 more cells than my analysis shows exist at the end of day three of development. Incidentally, if this division were also asymmetric it would have generated 2000 more neurons and 2000 more non-neurons. This would give a final total of 4000 neurons instead of 5000 and 2000 non-neurons instead of about 200.
This shows that asymmetric division is unlikely to generate the majority of neurons in this system but doesn't preclude asymmetric divisions per se. The largest number of asymmetric divisions that could take place to explain my cell counts over this period can also be predicted. If 1000 of the original 2000 non-neuronal cells divide asymmetrically they would directly generate 1000 non-neuronal cells and 1000 neurons. In addition if the other 1000 non-neuronal cells generate terminal neuron pairs this gives 2000 neurons. After this first round of division there are 2000 extra cells and 3000 newly differentiated

neurons with 1000 cells still capable of dividing. If these 1000 cells divided to produce terminal neuron pairs they would generate 1000 new cells and 2000 neurons. These two consecutive rounds of division would in total generate 3000 new cells and 5000 new neurons which is almost exactly the number required according to the cell counts. In total 1000/3000 divisions were asymmetric in this model. Thus 1/3 of cells could maximally divide asymmetrically during this period and that they ought to do so before the final round of cell division. It will be interesting to see if these predictions are borne out the actual division modes as revealed in the lineage analysis (Chapter 5).

Are neurons committed to their fate at birth?

I found that HuC-GFP can be expressed in newborn neurons just 4 hours after their birth. However it is not clear whether all newborn neurons express HuC-GFP over a similar time frame. There are a number of ways in which this information could be acquired. One way would be to calculate the number of cells that are post-mitotic at a certain time-point and find out how long it takes before you can see that number of cells expressing HuC-GFP. This would require heroic quantitative birthdating studies to find exactly how many cells are post mitotic at one time and a very in depth quantification of the HuC-GFP +ve population over small time intervals. However, this would ultimately give rise to a prediction of how long it takes on average for all post mitotic neurons to express HuC-GFP after their birth. This would show whether all neurons express HuC-GFP over a stereotyped and short 4 hour delay or if the neurons that expressed HuC-GFP quickly were distinct from others that exhibited a longer delay between their birth and HuC-GFP expression. I noticed in my analysis when I calculated the minimum time between birth and HuC-GFP expression that the first neurons to co-express BrdU and GFP i.e. after a 9 hour delay were usually in the lateral rhombic lip region (Figure 4.5 + 4.6). This may indicate that neurons born in this region express HuC-GFP and differentiate more quickly after birth than neurons born in other regions or it may simply mean that more neurons are generated in this region throughout development relative to other areas of the neuroepithelium.

The question of how variable the delay between birth and HuC-GFP expression is is very important with respect to the differentiation of sister cells following terminal mitosis. My quantification predicts that many neurons will be produced by divisions that generate two neurons. If both of these neurons express HuC-GFP over a similar timeframe this may

reflect the synchrony of their differentiation programme and may indicate an important role for cell lineage in determining the immediate fate of daughter cells. However, if there is a distinct difference in the delay between sister neurons' birth and their onset of HuC-GFP expression this would show an asymmetry in their differentiation that may implicate a role of the environment in determining cell fate immediately after terminal mitosis. Determining what the relationship between birth and differentiation is for neurons will thus be an important issue to address in the future.

What limits cell number in the developing brain?

The number of cells in the early ventricular zone and cell cycle length during neurogenesis could both theoretically set limits on the eventual composition of the nervous system. I have shown that the total number of cells at the end of embryogenesis has increased by a factor of about 3-4 from the population present at 15hpf. The number of cell divisions could limit this multiplication factor. If only 3 rounds of division were permitted during this period then the maximal factor by which the cell number could increase in the tissue is 2^3 (8). Mouse neurogenesis proceeds over an estimated 11 cell cycles (Takahashi et al., 1995), giving each progenitor the potential to make 2^{11} (2048) cells and hence the brain the capacity to generate 2048 times the number of cells in the original VZ. If neurogenesis in the human proceeds throughout pregnancy for even 200 days and if the cell cycle length was 24h then a single progenitor could make 2^{200} neurons during this period. This is more neurons than there are atoms in the universe. It is unlikely that the original ventricular zone is multiplied by this factor. In the mouse the original progenitor population is only multiplied 140 times over the course of neurogenesis (Takahashi et al., 1997) In the human forebrain the cell number increases by a factor of only 4.3 between weeks 13 and 20 of gestation and only by a further factor of 2.9 by birth to a total of about 40 billion (Samuelsen et al., 2003). This shows that there is little correlation between the possible number of cells that can theoretically be generated by progenitor cells and the number that actually are. Although the human brain eventually comprises maybe 100 billion cells, generating this huge number is not a logistical problem. Clearly the number of cell cycles or the size of the early ventricular zone at any one time cannot inherently limit future proliferation to a great extent.

It is primarily the mode of division that the individual progenitor cell undergoes that must determine the eventual cell number, whether this is driven by intrinsic properties of the progenitor cell or signals from the environment. The only way to control a cell's proliferative capacity is to remove it from the cell cycle, either temporarily by inducing a state of quiescence or permanently by generating post-mitotic progeny. There is indirect evidence from the studies of the period of neurogenesis in mouse that suggest that the progenitor pool must be expanded by proliferative progenitor pair divisions and that neurogenesis must end with a flurry of terminal neuron pair divisions (Takahashi et al., 1996). What division modes predominate in between these stages is unknown. Given the highly exponential nature of repeated progenitor pair divisions the simplest way to regulate neuronal number would be to have a predominance of asymmetric divisions in mid neurogenesis stages. In this case a cell that cycled 200 times would not cause the destruction of the universe but would merely generate 200 neurons. There is some indirect evidence to support this model of repeated rounds of asymmetric divisions in vertebrate forebrain (Noctor et al., 2001) and in the next chapter I will focus on exactly what modes of progenitor division operate during zebrafish hindbrain neurogenesis.

Why does the total cell number decrease between 60 and 72hpf?

The total cell number between 60 hpf and 72 hpf decreases by about 300. During this same period the number of neurons increases, but only by 100. The most simple explanation for the reduction in overall cell number during this period is that it is due to cell death. Previous studies have shown, however, that there is remarkably little cell death taking place during this period in the hindbrain (Cole and Ross, 2001; Furutani-Seiki et al., 1996; Abdelilah et al., 1996) and I have also found also very little evidence that cell death was elevated during this period. However quantification of cell death is notoriously difficult to measure equivocally and thus remains a possible explanation of this reduction in cell number.

Another possible explanation for the apparent reduction in cell number at 72 hpf results from the fact that it is difficult to recognise rhombomere boundaries from the pattern of HuC-GFP +ve neurons at 72hpf. This makes it more difficult to be certain about measuring the exact volume of segments at this stage. A slight inaccuracy in volume estimation would easily account for what is only a 5% change in cell number.

An additional reason why there might be a reduction in cell number during this period could result from neurons moving out of the rhombomeres being counted from. There is evidence from the chick embryo that the rhombomeric compartmental restriction of neurons breaks down as neurons congregate into longitudinally oriented nuclei (Marin and Puelles, 1995; Wingate and Lumsden, 1996). If this is also the case in the zebrafish then some neurons may migrate out of the r4-5 territory between 60-72 hours. This may account for the reduction in cell number.

Zebrafish metamorphosis

One area of vertebrate neurogenesis research that is largely ignored is the period between the end of embryogenesis and adulthood. It is absolutely clear there is a huge difference in size between a 3 day old zebrafish and an adult zebrafish. However, what is less clear is how much of this size difference relates to cell growth or continued proliferation, especially in the case of the brain. There is no direct comparison that I know of that quantifies neuron and glial number between these stages. I have shown that only a tiny minority of cells exist at the end of embryogenesis that would be capable of acting as progenitors later in life but have argued that this number is not necessarily a limiting factor due to the potentially exponential nature of cell proliferation. The observation of very few potential progenitors in a tissue at any one time can therefore be misleading and it is still possible that the adult hindbrain contains vastly more neurons and glia than are present at the end of my analysis. It is also entirely plausible that the primary difference in brain size is due to the elaboration and growth of cells present early on in life.

The zebrafish undergoes a dramatic increase in its size from about three weeks of development and may reflect a response to a hormonal stimulus (Dave Raible, pers. comm.). Evidence that this is due to renewed proliferation and indeed renewed neurogenesis exists for at least one area of the PNS. Analysis of the dorsal root ganglion (DRG) in zebrafish shows that at 14 days of development the ganglion contains only 10-15 neurons whereas by 28 days it contains well over 100 neurons. This increase was shown to follow a burst of renewed proliferation (An et al., 2002). Whether neurogenesis takes place around this time in other brain areas is unknown but would be interesting to study in the future. This would be especially interesting in the context of neural stem cells and the possibility of providing a link between embryonic and adult neurogenesis in a vertebrate system.

A quantitative analysis of cell number in the adult hindbrain might be a suitable preliminary project for anyone who thinks they are hard enough!

Chapter 5

In vivo analysis of cell lineage in the zebrafish hindbrain through multiple rounds of division

Introduction

The aim of this chapter is to characterise the modes of division that neural progenitors undergo during neurogenesis.

Progenitor behaviour is well understood in invertebrates and it is clear that during neurogenesis in these systems asymmetric cell division is a fundamental mechanism for generating cell diversity. In invertebrates asymmetric division is often based on the unequal partitioning of cytoplasmic determinants during division (reviewed by Lu et al., 2000a) and this relies on mechanisms that co-ordinate the plane of progenitor division with the sub-cellular localisation of fate determinants. In Drosophila the neuroblast division is clearly asymmetric in that cytoplasmic determinants are inherited asymmetrically by daughter cells and daughter cells have different fates (Hirata et al., 1995). However the neuroblast division generates two progenitors. Not only is there evidence from work in Drosophila that a division that produces two progenitors is clearly asymmetric but there is also evidence that divisions that generate two neurons can be asymmetric as in the case of the MP2 division (e.g. Bossing et al., 1996).

In vertebrate studies it has been common practice to refer to divisions that produce either two neurons or two progenitors as symmetric divisions irrespective of the exact identities of the neurons or progenitors (e.g. Mione et al., 1997; Cai et al., 2002) and an asymmetric division is typically defined as one that generates a progenitor and a neuron (e.g. Mione et al., 1997; Noctor et al., 2001; Cai et al., 2002).

For the purposes of this thesis I will describe a division that generates two neurons a neuron pair division and a division that generates two progenitors a progenitor pair division and not as symmetric divisions. I will describe a division that generates a neuron and a progenitor as an asymmetric division.

Despite the confusion over terminology it is clear that a mixture of progenitor pair, neuron pair and asymmetric divisions operate during vertebrate neurogenesis (e.g. Gray and Sanes, 1992; Mione et al., 1997; Reid et al., 1997; Noctor et al., 2001; Cai et al., 2002). However, there is still controversy about what the relative contribution of each division mode is during neurogenesis. Furthermore there is precious little data with respect to the behaviour of progenitor cells through multiple rounds of division during

neurogenesis. Indeed the only direct observations of such have come from time-lapse analysis of dissociated cortical progenitor cells maintained in culture, where some progenitors were seen to divide in stereotypical lineages (Qian et al., 1998; 2000). The relevance of this type of behaviour to normal development in the embryo is difficult to assess.

It is for these reasons that I sought to follow the fate of neural progenitors over several rounds of division in an intact embryo. I have already shown that the zebrafish hindbrain is a good system in which to perform live imaging and have documented the dynamics of neurogenesis within the hindbrain. This has allowed me to restrict my lineage analysis to a period over which the majority of embryonic neurons are generated. My quantitative analysis has also predicted the average number of neurons that a single progenitor should generate during neurogenesis, which will serve as a standard against which the accuracy and representative nature of my lineage analysis can be tested.

Clonal analysis has in fact already been carried out in the zebrafish, in the spinal cord. The goal of one particular study was similar to mine in that it set out to address the modes of division that underlie neurogenesis. Single cell injections were made into the neural plate at 10.5hpf. Embryos were allowed to develop until 3.5 days or 2 weeks post fertilization. Results showed that clones in the neural plate were heterogeneous with respect to cell number, varying in composition between 1 and 21 cells at 3.5 days post fertilization. The clonal analysis predicted that the factor by which cell number increased in the spinal cord between 10.5hpf and 3.5 days is 6.5 and that this increased only very slightly by 20 days post fertilisation to an overall factor of 8.7. Further calculations based on the clonal data presented predicted that 25% of spinal cord cells are post-mitotic before the end of neurulation (Papan and Campos-Ortega, 1999). To address the issue of the mode of progenitor division during neurogenesis BrdU pulse labelling was carried out in conjunction with the clonal analysis. Single cell injections were made at the 10.5 hpf and BrdU was administered from 30hpf until the embryos were processed at 38hpf. The authors report three classes of clone. In the simplest case all of the cells of the clone were BrdU positive and hence mitotically active at 30hpf when it was administered. This was observed in 4/20 cases. In the next case the opposite was true and no cell in the clone incorporated BrdU when a the drug was administered at 30hpf, which the authors took to mean that all cells were post-mitotic even though this implies knowledge of the cell cycle length, which was not reported. If the duration between the end of one S-phase and the

beginning of another was more than 8 hours long for any cell in the clone then it would not necessarily incorporate BrdU even though it was still in the cell cycle. Nonetheless this class of clone was only observed in 2/20 cases (Papan and Campos-Ortrega, 1997).
The final and most common class of clone comprised a mixture of cells that took up BrdU between 30 and 38 hpf and cells that didn't. The authors write that, "the lineages of these clones comprised cells which had originated from asymmetric mitoses" (Papan and Campos-Ortrega, 1997). The authors in this case define an asymmetric division as I do for the purposes of this thesis i.e. a division that generates a progenitor and a neuron. One figure used to highlight the incidence of this asymmetric division shows a clone of four cells, two cells are BrdU positive and thought to be progenitors, due to their position and two cells are BrdU negative and thought to be neurons, again due to their position (Figure 5.1 A). The authors make an assumption that the two divisions that gave rise to these four cells took place before 30 hpf i.e. before the time that the embryo was incubated in BrdU otherwise all four cells including the two neurons would have incorporated BrdU. They conclude that the two BrdU +ve cells have re-entered the cell cycle thus showing that the previous divisions were asymmetric in that they generated a neuron and a progenitor each. Unfortunately there are a number of problems with this initial assumption. It is clear that the two BrdU +ve cells underwent S-phase at some point between 30 and 38hpf but there is absolutely no evidence that both cell divisions occurred before 30hpf. If one progenitor left S-phase before 30 hpf and underwent a division that generated a pair of neurons then these cells would not incorporate BrdU. If the other progenitor divided and generated two progenitors that progressed through to S phase between 30 and 38hpf then these would incorporate BrdU. This scenario would explain the raw data (Figure 5.1B) just as easily as the author's own interpretation and shows that asymmetric divisions did not necessarily underlie the clones analysed in this study.

It is clear, despite efforts in many systems using a variety of techniques, that the nature of progenitor cell fate during neurogenesis is unclear. It seems obvious that the easiest way to address this problem is to find a system in which it is feasible to monitor progenitor behaviour at multiple time-points throughout development in the intact embryo. The aim of this chapter therefore is simply to do that. I have shown that it is possible to image neural progenitor behaviour in the intact zebrafish embryo and have shown further that the process of neurogenesis in the hindbrain reaches a peak during the first two days of

development and that it slows down dramatically thereafter. For this reason I have sought to follow the fate of individual progenitors during this period of development, to monitor clones at regular intervals throughout their development and to marry this data with information about the length of the cell cycle.

In addition to documenting the mode of division that generates the majority of hindbrain neurons I have also sought to analyse whether there is any correlation between the plane of mitosis and asymmetric divisions that generate a progenitor and a neuron. Pioneering experiments that followed neural progenitors in the ferret cortex suggested that cells that divided within the plane of the ventricular zone adopted similar fates and those that divided out of the plane of the ventricular zone adopted different fates i.e. that one cell became a neuron and one a progenitor (Chenn and McConnell, 1995). However the fate of sister cells was not followed for a sufficient duration of time or phenotyped with adequate cell markers to establish their identity unequivocally. Since this original study the correlation between the plane of mitosis and daughter cell fate has been a hot topic of investigation but conflicting reports have been published (e.g. Cayouette et al., 2001; Silva et al., 2002; Das et al., 2003). Very few studies have been able to follow cells for a sufficiently long time to establish cell identity but a recent report indicates that there may be a correlation between the plane of division and daughter cell fate in the post-natal rat retina (Cayouette and Raff, 2003). In this case cells that divided within the plane of the ventricular zone tended to generate similarly fated cells, usually generating rods in this system. In contrast, cells that divided out of the plane of the ventricular zone generated progeny with different fates e.g. a rod and an interneuron (Cayouette and Raff, 2003). In this analysis daughter cells rarely ever divided again. This is because of two things; the analysis was carried out in a postnatal system where the majority of cells have already been generated and also because it was carried out in a culture system where developmental processes were slowed down dramatically (Cayouette and Raff, 2003). It is interesting to note that the correlation in this system is not between the plane of division and an asymmetric division as defined in this thesis but between the plane of division and the fate of two post-mitotic cells. It is tempting to marry the findings of this recent investigation with those of the initial Chenn and McConnell story and suggest that the plane of division might be a determining factor throughout development in that it could make cells different, whether in terms of making a neuron and a progenitor or

different types of post mitotic neurons, but it has been reported by the same group that in the rat retinal system that cells dividing out of the plane of the ventricular zone are most prominent at post natal stages and even then only comprise 21% of the total dividing cells (Cayouette et al., 2001). This suggests that either there are very few asymmetric divisions during early neurogenesis or that there is a difference in the correlation between plane of division and cell fate between neurogenesis in the ferret cortex and rat retina.
I have attempted to address this problem in zebrafish where I was confident of being able to address any potential correlation between the plane of division during the main period of neurogenesis and asymmetric cell fate as defined by divisions that generate a neuron and a progenitor by comparing my lineage data with a large-scale analysis of division orientation.

My previous chapters have suggested that by the end of day two of development the majority of cells in the hindbrain are neurons and that the other cells that exist are likely to belong to a set of progenitors with characteristics of radial glial or a population of oligodendrocyte progenitors, both of which are very localised by 48 hpf (Chapter 3). How these non-neuronal populations that exist at the end of neurogenesis arise is another question of interest. They could be specified early in development and undergo a distinct pattern of division during development or arise stochastically and independently of their lineage. A study that describes the behaviour of isolated cortical progenitor cells in culture by time-lapse microscopy suggests that glial progenitors do not diverge from early progenitor cell lineages and undergo independent programmes of division but rather emerge from lineages that have generated neurons in previous generations (Qian et al., 2000). It was also noted in these cultures that most progenitors generated neuron only clones and that less than 10% of neural progenitors went on to generate a cell that gave rise to glia (Qian et al., 2000). The predictions of my quantitative analysis are similar and suggest that most progenitors would generate clones consisting of neurons only but it was impossible to predict if the non-neuronal populations would arise independently or descend from a multipotential progenitor as was shown in the aforementioned in vitro study. I intended to investigate this question also by means of the lineage analysis.

Methods

Iontophoresis

Iontophoresis was carried out as described in the General methods (Chapter 2). Single cells were labelled with a mixture of a non-fixable 3000 MW tetramethylrhodamine dextran and a lysine fixable 10000 MW biotinylated dextran (Molecular Probes) at the neural plate stage, between 9 and 11hpf. At this stage the periderm is quite tough and embryos were pre-treated in 5mg/ml Pronase (Sigma) in embryo medium for one minute to facilitate the electrode passing through the skin. The skin was never visibly damaged and no adverse effects were ever noted in subsequent development. Embryos were placed against a drop of 2% methyl cellulose (Sigma) to prevent them from moving during iontophoresis. Specimens were examined to ensure that only one healthy cell was labelled 10-15 minutes after injection before being returned to embryo medium to develop.

Imaging

Specimens were imaged every 8-12 hours up until either 48hpf or 72 hpf (Figure 5.2). Embryos were placed in 1.5% low melting point agarose in embryo medium with 0.03% tricaine to prevent movement and were viewed from dorsal and or lateral aspects. Embryos were cut out of the agarose after imaging with a surgical blade and returned to embryo medium until they were imaged next. Imaging was performed on a Nikon Optiphot microscope using x 20 and x 40 dry lenses or on a Zeiss Axioplan 2 using x 20, x 40 and x 63 water immersion lenses. Fixed specimens were also imaged on a Leica confocal microscope using x 20, x 40 and x 63 water immersion lenses.

Detection of biotinylated dextran and GFP

Cells belonging to clones analysed throughout the lineage study were detected in fixed embryos by revealing the biotinylated dextran that was initially co-injected with the fluorescent dextran. Embryos were fixed in 4% PFA at 48hpf or 72hpf. Biotinylated dextran was visualised by staining the embryos with Texas red Avidin (Vector Laboratories; see General methods). The GFP signal was usually stable after fixation for two weeks and so did not always require processing to be detected. Otherwise the signal was detected by immunochemistry using an anti-GFP antibody (see General methods).

Time-lapse analysis

Time-lapse analysis of Bodipy 505/515 stained embryos was carried out on a Leica confocal microscope using x 20, x 40 and x 63 water immersion lenses as described in the General Methods.

Generation of large clones of dextran labelled cells and their imaging by time-lapse microscopy on the Nikon Optiphot microscope and the Zeiss Axioplan 2 was carried out as described in the General Methods.

Cell cycle calculation

BrdU was administered to embryos at 36 hpf to HuC-GFP +ve embryos by pulse labelling as described in the General methods. Additional BrdU pulses were administered to embryos to at intervals to generate a series of embryos that were pulse labelled at 36hpf, 36hpf +38hpf, 36hpf + 40hpf, 36hpf +39hpf +42hpf and 36hpf +40hpf +44hpf.

Specimens were fixed 15 minutes after their last pulse of BrdU.

Specimens were processed to detect the presence of BrdU and GFP by immunochemistry as described in the General methods.

These specimens were imaged by confocal microscopy using x 40 water immersion lenses.

This series of specimens made it possible to detect how long after the initial pulse of BrdU it took before all of the cells that would enter S-Phase incorporated BrdU. This could be judged by a saturation of BrdU +ve cells in the ventricular zone. The extent of the ventricular zone could be determined as these experiments were carried out in HuC-GFP +ve embryos. The time it took for all of the cells that would express BrdU to do so gave an estimate of the length of time between the end of one S phase and the beginning of another.

To calculate the proportion of the cell cycle occupied by S-phase the number of cells in S-phase was divided by the number of cells in the cell cycle at 36hpf. The number of cells in S-phase was determined by counting the number of BrdU +ve cells in fixed specimens after pulse labelling at 36hpf. The optical dissector method was used to do this. The total number of cells in the cell cycle at 36hpf was calculated from data acquired in the quantitative analysis (Chapter 4). By combining the information on the duration between the end of one S-Phase and the beginning of another and the

information about the proportion of the cell cycle occupied by S-Phase the length of the cell cycle could be estimated.

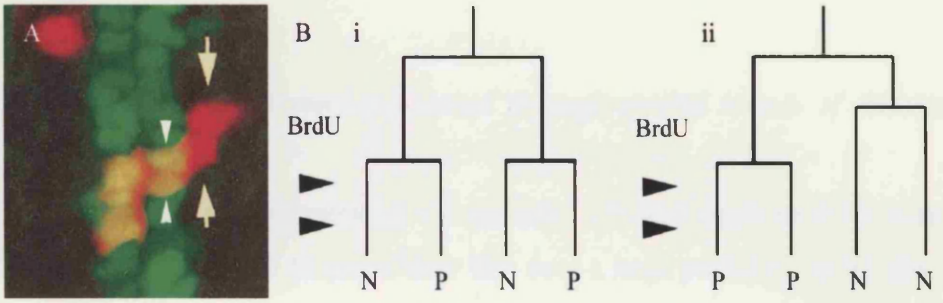

Figure 5.1. Interpretation of a previous zebrafish lineage study.
A. Image taken from Papan and Campos-Ortega, 1997. Red cells are dextran labelled cells and green cells are BrdU +ve cells. Arrows point to two putative neurons that are not BrdU +ve. Two other yellow cells on the right side of the midline (arrowheads) are part of the same clone.
B. Interpretation of figure A.
i.The authors assume both mitoses take place before BrdU administration (arrowheads) and consequently that the divisions are asymmetric and generate a neuron (N) and a progenitor (P).
ii. The data can also be explained if one neuron pair division takes place before the time of Brdu administration and a progenitor pair division takes place during the time of exposure to BrdU or indeed if the last S-phase took place before these times.

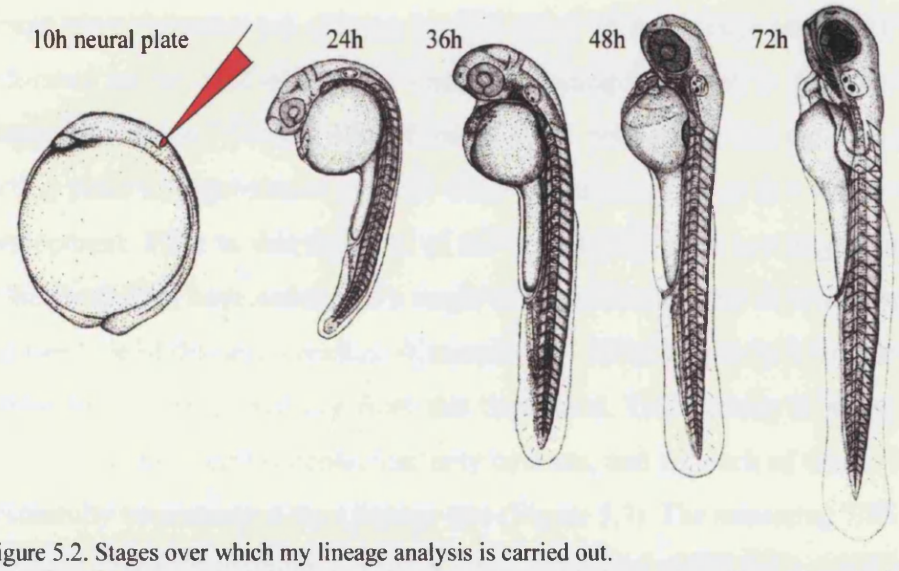

Figure 5.2. Stages over which my lineage analysis is carried out.
A single cell is injected with fluorescent dextran at the neural plate stage and imaged at regular intervals up to either 48hpf or 72hpf. The staging series shows the overall development of the embryo during the time over which the lineage study was carried out. By 72hpf the embryo has hatched out of its chorion, can swim and is just about to start feeding by itself.

Results

Individual progenitors can be followed through several rounds of division to their terminal mitosis

In order to analyse the generation of neurons, I labelled single neural progenitors with fluorescent dextran and followed their fate over a large period of embryogenesis. Cells were labelled between 9hpf and 11 hpf during the neural plate stage. I tried to target many different areas along the mediolateral axis of the neural plate but injections were restricted along the anterior-posterior (A-P) axis to those regions fated to generate rhombomeres 3-7. This A-P position could be predicted following previous fate maps of the zebrafish neural plate (Woo and Fraser, 1995). Each labelled progenitor was checked at the time of injection to ensure that only one cell was labelled and then re-observed every 8-12 hours until the embryo was 48 to 72 hours old (Figure 5.2). The 8-12 hour interval is sufficient for only one round of division (see below and Figure 5.11). The descendents of labelled progenitors could be followed for several rounds of division and lineage trees reconstructed (Figure 5.3-5.7). Most of the lineage analyses (54/86) were performed in the HuC-GFP line, thus eliminating the need to phenotype cells by morphology alone. For the sake of simplicity I present the lineage tree data from a starting point of approximately 15hpf when the hindbrain is at the neural rod stage of development. Prior to this the cells of the neural plate have converged on the dorsal midline and most have undergone a single midline division that deposits one progenitor on either side of the neural midline (Kimmel et al 1994; Chapter 3). I have monitored the development of 86 progenitors from this time-point. The majority of these progenitors (79/86) resulted in clones containing only neurons, and for each of these clones I have successfully reconstructed their lineage tree (Figure 5.7). The remaining 7/86 progenitors generated clones containing a mixture of neurons and radial cells at the end of their analysis. I will describe the analyses of these two classes of clones separately.

Development of neuron-only clones

From the 79 neuron-only clones I have monitored the ancestry of 222 neurons. Early in clonal expansion cells have a typical elongate progenitor morphology, which allowed their phenotype to be easily determined (e.g. Figure 5.3 B, 5.4 A). At later time-points post-mitotic neurons are generated. This lineage analysis relied heavily on my being able

to accurately phenotype neurons that were generated in the clones observed. I had the great advantage of being able to carry out the lineage study in HuC-GFP +ve embryos that express GFP in newborn neurons soon after their birth. This allowed me to phenotype dextran labelled neurons in vivo unequivocally. It was possible to phenotype neurons in vivo using the Zeiss Axioplan 2 microscope, as the tetra methyl rhodamine signal did not bleed into the GFP channel. Cells co-expressing HuC-GFP and dextran could be easily recognised by looking down the microscope and switching between Rhodamine and GFP filter sets (e.g. Figure 5.3 D). In addition neurons co-expressing HuC-GFP and dextran were analysed on the confocal microscope after fixation where possible (e.g. Figure 5.3 G, 5.4 F). Furthermore, neurons could be phenotyped by their morphology. Their cell bodies tended to lie further away from the ventricular surface and they lost their cytoplasmic contact with the ventricular surface and extended axons (Figure 5.3, 5.4, 5.5 and 5.6).

The range of lineage trees that were characterised in their entirety is shown in Figure 5.7. The reconstructed trees for neuron-only clones fall into two clear categories. Most trees, 68%, (46/68) are composed only of a combination of progenitor pair and neuron pair divisions, while in the remainder, 32% (22/68) one or two asymmetric divisions are seen. When present, the asymmetric divisions were usually the first division of the lineage (19/22) and usually occurred one cell cycle before a terminal neuron pair division that generated a three neuron sub-clone motif (19/22) (Figure 5.5). None of the fully reconstructed lineage trees contained a progenitor that followed a classic stem-cell mode of division, i.e. one that self-renews and generates a differentiated cell type at each division. The clones were evenly distributed in the mantle layer of the hindbrain (Figure 5.8) suggesting that I sampled progenitors from many regions of the ventricular zone as intended.

Most neurons are generated from terminal neuron pair divisions

Of the 222 neurons observed, the large majority, 84%, (186/222) are born from neuron pair divisions and only 11% (25/222) of neurons are born from asymmetric divisions. The remaining 5% (11/222) neurons differentiated directly from the original progenitor without division. I observed 118 neurogenic divisions, i.e. divisions generating at least one neuron and find that only 21% (25/118) of neurogenic divisions are asymmetric. In

fact, of all progenitor divisions reconstructed, 83% (118/143) generated either two mitotically active progenitor cells or two neurons. Thus only 17% (25/143) of all progenitor divisions were asymmetric as defined by cell fate.

I have documented the relative proportion of neuron pair, progenitor pair and asymmetric divisions for two consecutive rounds of division (Table 5.1). Table 5.1 clearly shows a dramatic change in the relative number of neuron pair and progenitor pair divisions over the two periods. The proportion of neuron pair divisions more than doubles from 40% to 86% of the total divisions between the two rounds of division and the proportion of progenitor pair divisions drops massively from 32% to 5% of the total over the same period. The proportion of asymmetric divisions also drops between the two periods from 28% to 9% of the total. Table 5.2 shows the relative proportion of cells that leave the cell cycle following the same two rounds of division. Just over half (54%) of cells of leave the cell cycle after the first round of division whereas 90% do so following the second round of division.

Most asymmetric divisions occur within the plane of the ventricular zone

Previous studies have suggested that the plane of mitosis within the ventricular zone is correlated with the fate of the daughter cells, such that progenitors that divide within the plane of the VZ generate two further progenitors, whereas mitoses that occur perpendicular to the VZ produce an asymmetric division that generates one neuron and one progenitor (Chenn and McConnell, 1995). In order to assess this possibility in the zebrafish hindbrain I carried out a large-scale analysis of mitotic orientation. I analysed time-lapse data of progenitors labelled with fluorescent dextran (Figure 5.9 A, C +E, Supplementary movie 5.1). Also using the vital dye Bodipy 505/515 and time-lapse microscopy I was able to visualize cells as they round up in the ventricular zone and divide (Figure 5.9 B, D+F, Supplementary movie 5.2). I concentrated on the period between 18-30hpf because my lineage analysis demonstrated that 28% (19/68) of divisions in this specific period are asymmetric (Table 5.1). However only 2% (12/557) of progenitor divisions were perpendicular to the plane of the ventricular zone i.e. divided apico-basally, during this period. This suggests that in this system there is no correlation between cells dividing out of the plane of the ventricular zone and asymmetric divisions that generate a neuron and a progenitor.

A small minority of clones still contain progenitors at 48hpf

Less than 10% of progenitors generated clones that retained putative progenitors at 48hpf. Seven of the 86 clones fixed at 48hpf contained a mixture of neurons and cells with a radial glial morphology. These radial cells had cell bodies within 1 to 3 cell diameters of the ventricular surface and they did not express GFP in the HuC-GFP embryos (Figure 5.10 A). They often had processes that contacted the ventricular surface and they possessed a single thin process that stretched down towards the pial surface (Figure 5.10 A+B). At least some of these radial cells will be mitotically active progenitors as described in Chapter 3, Figure 3.10. Most of these clones (4/7) were composed of two radial cells and two neurons, one clone had two radial cells and three neurons, one had three radial cells and one neuron and the final clone had four radial cells and two neurons. Unfortunately I was not able to follow the fate of individual cells throughout the development of these clones and therefore cannot be sure of the symmetry of the divisions that generated these neurons and radial cells. However, the two most likely lineage trees for the four clones containing two neurons and two radial cells are shown in Figure 5.10 C. I never saw a clone that contained a single radial cell in addition to several neurons as described in previous studies (Gray and Sanes, 1992; Noctor et al., 2001). Furthermore I never saw a clone that consisted only of radial cells suggesting that their lineage does not diverge very early on in development.

The cell cycle at 36hpf is about 14hours long

In order to be certain that alternative division modes couldn't operate between the time intervals of my observations I needed to calculate the length of the cell cycle. If the cell cycle was considerably shorter than the time intervals between my observations then a progression from two cells to four neurons could be explained by three rounds of division as easily as by two rounds of division, where the first and second round of division were both asymmetric and produced one neuron and one progenitor each and the third round produced two neurons. If this were possible then the interpretation of my results would potentially be incorrect.

Calculation of the cell cycle relied in part on information from the cell counts. The likely number of non-neuronal cells that can exist at 36h is 1973 taking into consideration the delay to HuC GFP expression (Chapter 4, Graphs 4.6 + 4.8 (orange line)). There are an

average of 839 BrdU +ve cells in S-phase at 36hpf (n=5). By combining these two pieces of data I calculated that the likely proportion of the cell cycle occupied by S phase is 839/1973 (42.5%) at 36hpf. I calculated by cumulative BrdU labelling (Figure 5.11) that the duration between the end of one S-phase and the beginning of the next is about 6 hours which means that the minimum cell cycle length at this stage is (100/42.5) x 6 = 14 hours long.

Figure 5.3. Development of two clones, one on either side of the hindbrain.

A shows a single cell immediately after injection at 9hpf.

B shows two elongated neuroepithelial cells one on either side of the embryonic midline (arrowhead) at 15hpf. This is a horizontal section with anterior to the top. These cells have been generated following the midline division that separates daughter cells across the embryonic midline. The description of all clones analysed in my lineage study starts following the first division in the neuroepithelium, which is almost always the midline division. This means that an individual specimen could provide information about two clones, one on either side of the embryonic midline. Cells did not move across the midline after the neural tube had formed meaning that the clones could be considered as separate once the midline division had taken place. Scale bar = 50μm.

C is also a horizontal section through the hindbrain at 24hpf with anterior to the top. The neural tube has now formed along the embryonic midline (arrowhead). The clone on the left side of the midline now contains two cells indicating that the progenitor on the left side of the midline in B has undergone a division. There are also two cells in the clone on the right hand side of the midline, indicating that the progenitor seen on the right hand side of the midline in B has also divided. Scale bar = 20μm.

D is a lateral view of the clone on the left hand side of the midline at 36hpf. Anterior is to the left and the direction of the dorso-ventral (D-V) axis is indicated by the arrowed line . There are still two cells in this clone, both of which have now moved into the HuC-GFP +ve mantle zone (green). Both dextran labelled cells now appear orange/ yellow indicating that they are co-expressing GFP and are therefore neurons.
Scale bar = 20μm.

E is a projection of a stack of images of the clone on the right hand side of the midline at 36hpf, collected and deconvolved on Openlab (Improvision). The embryo was imaged on its side and therefore anterior is to the right and the direction of the dorso-ventral (D-V) axis is indicated by the arrowed line. Four cells can be seen, indicating that the two progenitors seen at 24hpf have both divided once more. These four cells have a complicated morphology, which makes their identity difficult to establish. These cells were not HuC-GFP +ve at 36hpf. Scale bar = 20μm.

F is a projection of a stack of images through both clones at 48hpf. The embryo was fixed at 48hpf and the dextran labelled cells were revealed by staining the embryo with Texas Red avidin that bound to the biotinylated dextran that was injected with the fluorescent dextran. The fixed embryo was dissected and the region of the hindbrain that included the two clones was isolated. This tissue was then viewed as a transverse section on the confocal microscope. Therefore dorsal is to the top. The position of the midline is indicated by the arrowhead. There are still two cells in the clone on the right hand side of the midline and these have axons further verifying their neuronal phenotype.
There are still the same four cells in the clone on the right hand side of the midline as were seen at 36hpf. These cells also now have a neuronal morphology and extend axons.
Scale bar = 50μm.

G is a confocal projection through the two clones in the same view as F, but now the dextran labelled cells are shown in red and the mantle zone of HuC-GFP +ve cells in green. All of the cells in the two clones co-express HuC-GFP verifying their neuronal identity. Arrowhead indicates position of the midline. Scale bar = 50μm.

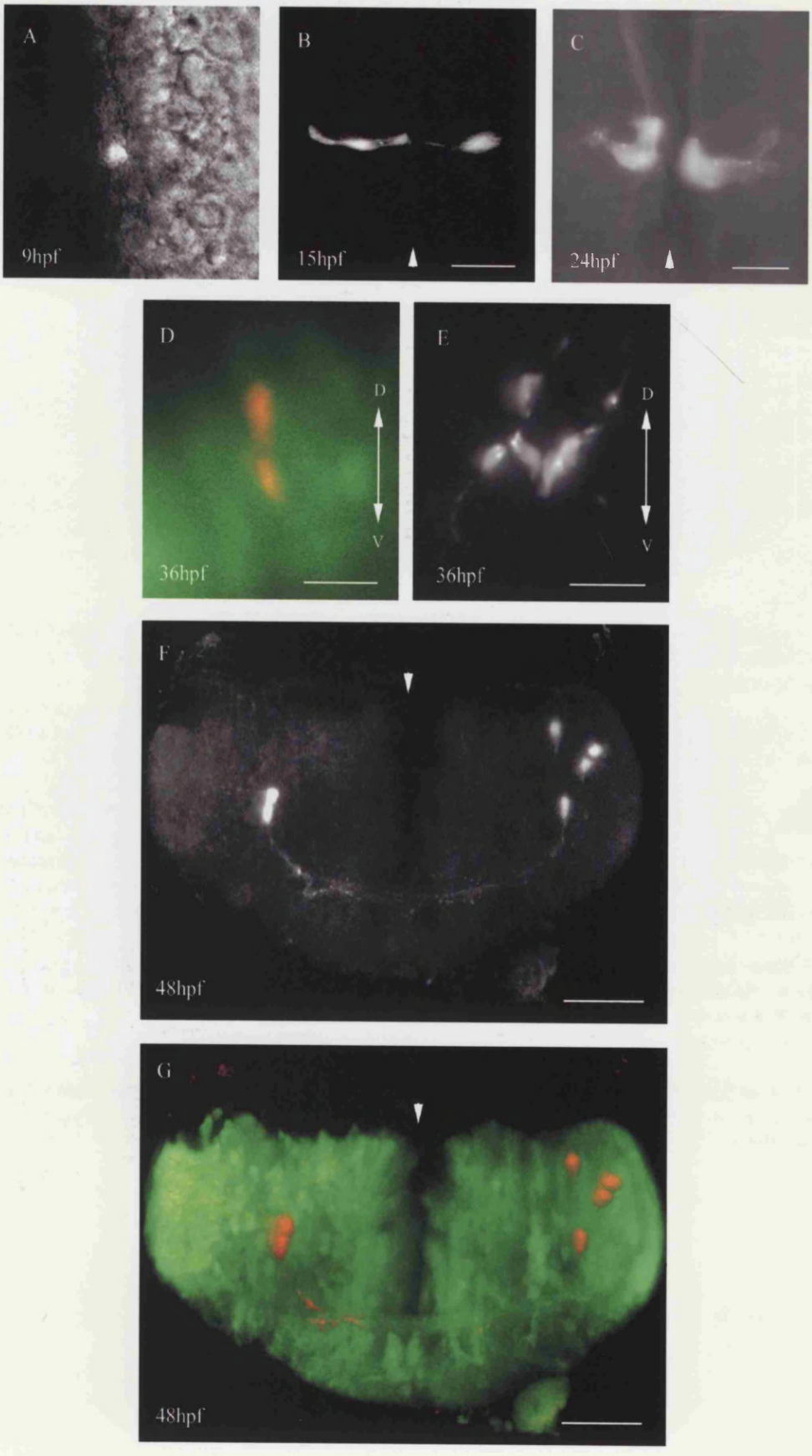
A
9hpf
B
15hpf
C
24hpf
D
D
V
36hpf
E
D
V
36hpf
F
48hpf
G
48hpf

Figure 5.4. Development of two more clones, one either side of the midline in the hindbrain.

A shows a horizontal view looking down on the hindbrain at 20hpf. Anterior is to the top and the embryonic midline is indicated by the arrowhead. The midline division has taken place and hence there is one progenitor on each side of the midline. The progeny of each of these two elongated progenitor cells will be considered as separate clones, as cells do not cross the midline after the midline seam has formed. Scale bar = 50μm.

B is also a horizontal view looking down on the hindbrain at 28hpf. Anterior is to the top and the midline is indicated by the arrowhead. There are two cells in the clone on the left hand side of the midline showing that the progenitor cell seen at 20hpf has divided. These cells are close to the ventricular surface and have long radial processes, indicating that they may still be progenitor cells. There are also two cells in the clone on the right hand side of the midline, showing that the progenitor cell seen on the right hand side of the midline at 20hpf has also divided. The position of these cell bodies is slightly further from the ventricular surface at the midline indicating the possibility that they are moving towards the mantle zone. Scale bar = 20μm.

C is a lateral view of the clone on the left hand side of the midline at 38hpf. This means that anterior is to the left and dorsal to the top. The ventricular surface is indicated by the dashed line. There are now four cells in this clone indicating that the two progenitors seen on the left hand side of the midline at 28hpf have divided again. The cell bodies of these cells have now moved a considerable distance away from the ventricular surface indicating that they may also be about to differentiate within the mantle zone. Scale bar = 10μm.

D is a lateral view of the clone on the right hand side of the midline at 38hpf. This means that anterior is to the right and dorsal to the top. The dashed line indicates the ventricular surface. The two cells have not divided since they were seen at 28hpf and have now migrated further away from the ventricular surface. Scale bar = 10μm.

E is a view of both clones at 48hpf in the fixed embryo. The dextran labelled cells have been revealed by staining the embryos with Texas Red avidin, which binds to the biotinylated dextran that was co-injected with the fluorescent dextran. The region of the hindbrain containing the two clones has been dissected and the clones viewed in transverse sections. This means that dorsal is to the top. The image is a confocal projection. There are still four cells in the clone on the left hand side of the midline and these cells have long processes that extend towards the pial surface. The arrowheads in the inset point out the two cell bodies that lie close together There are still two cells in the clone on the right hand side of the midline and these also extend processes towards the pial surface. Scale bar = 50μm.

F is a single confocal section through the two clones and is the same view as shown in E. Now the dextran labelled cells are shown in red and the HuC-GFP +ve mantle zone is shown in green. The edge of the dorsal ventricular zone is indicated by the dashed line and the midline indicated by the arrowhead. The cells of the two clones all co-express HuC-GFP indicating their neuronal phenotype. Scale bar = 50μm.

G and H are higher magnification views of the clone on the left side of the midline and is taken from the same section as F. It can be seen that all dextran labelled cells co-express with GFP in G and the GFP channel is shown alone in H to verify this.

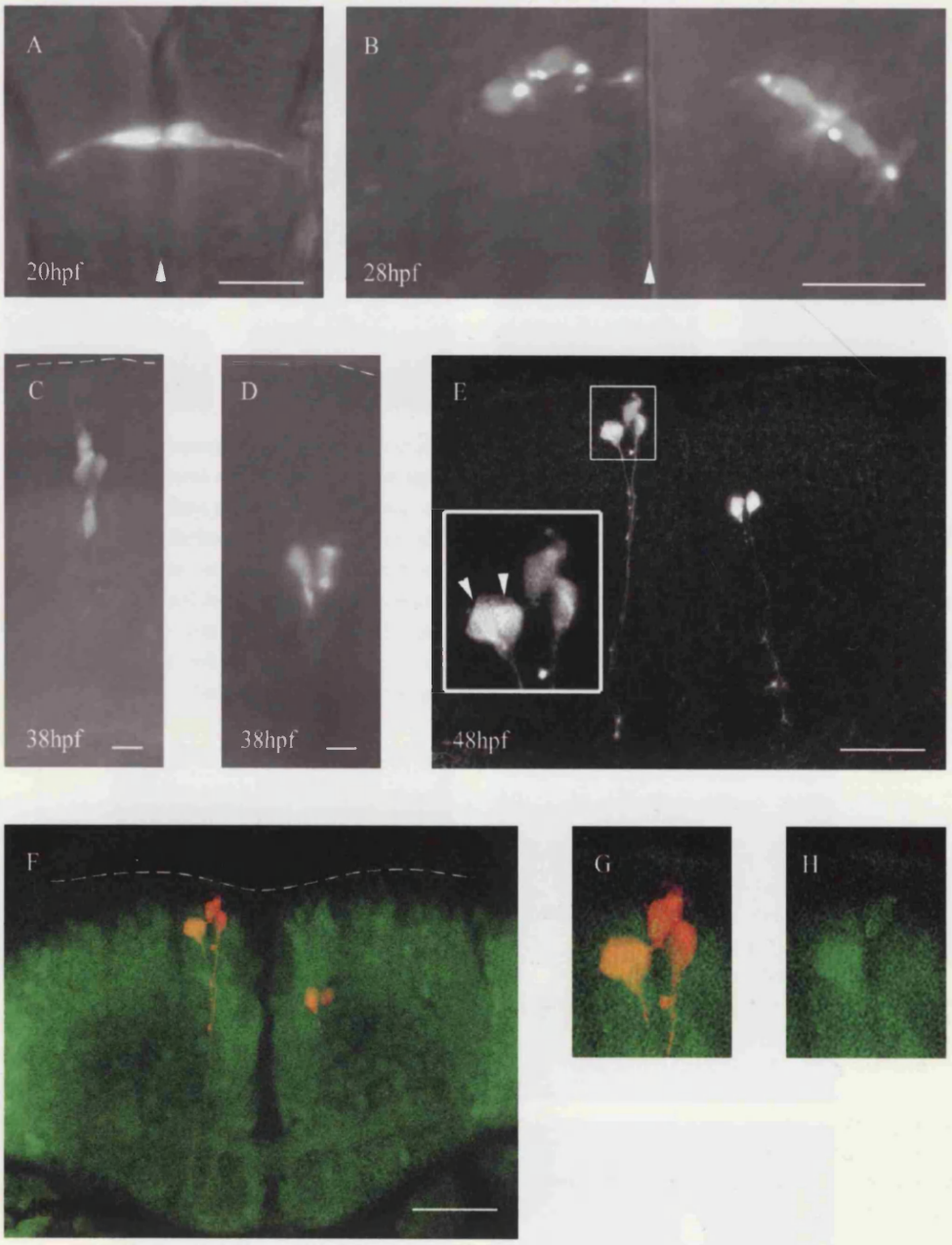
A
20hpf
B
28hpf
C
38hpf
D
38hpf
E
48hpf
F
G
H

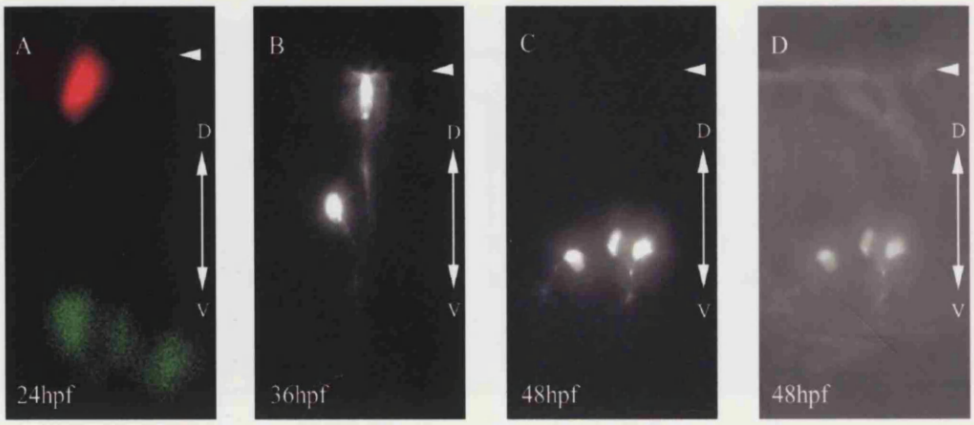

Figure 5.5. Development of a three neuron clone on one side of the midline.
All images are lateral views of a clone on the right hand side of the midline. Anterior is to the right and the arrowed lines indicate the direction of the dorso-ventral (D-V) axis.
A. One dextran labelled cell is seen at the ventricular surface (arrowhead). Three unrelated HuC-GFP +ve neurons (green) are seen near the ventral pial surface.
B. By 36hpf the cell has divided asymmetrically. One cell has moved away from the ventricular surface (arrowhead). The other cell has a typical elongate progenitor cell morphology.
C. The progenitor cell seen at 36hpf has divided again and three neurons with proceses are now visible.
D. Same view as C but with DIC background. Ventricular surface indicated by arrowhead.

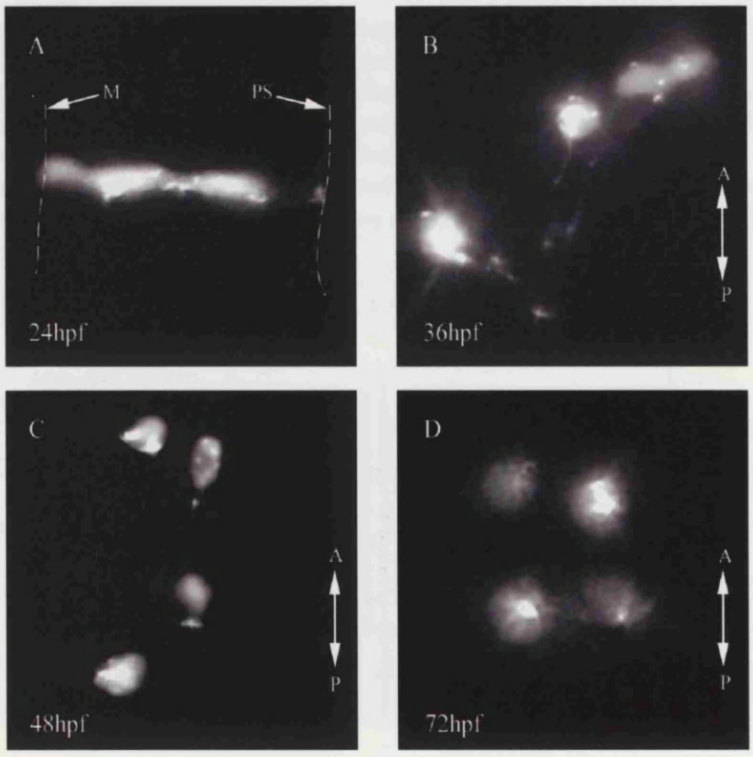

Figure 5.6. Development of a four neuron clone on one side of the midline.
A.Horizontal section through the hindbrain at 24hpf shows two elongated neuroepithelial cells that stretch from the midline (M) to the lateral pial surface (PS). This clone is on the right hand side of the midline and anterior is to the top.
B-D. Horizontal views of the hindbrain at 36 (B), 48 (C) and 72 hpf (D). The direction of the anterior-posterior (A-P) axis is indicated by the arrowed lines. All four cells are neruons whose processes can be seen in B. There is no further cell division up to 72hpf but some cell rearrangement occurs.

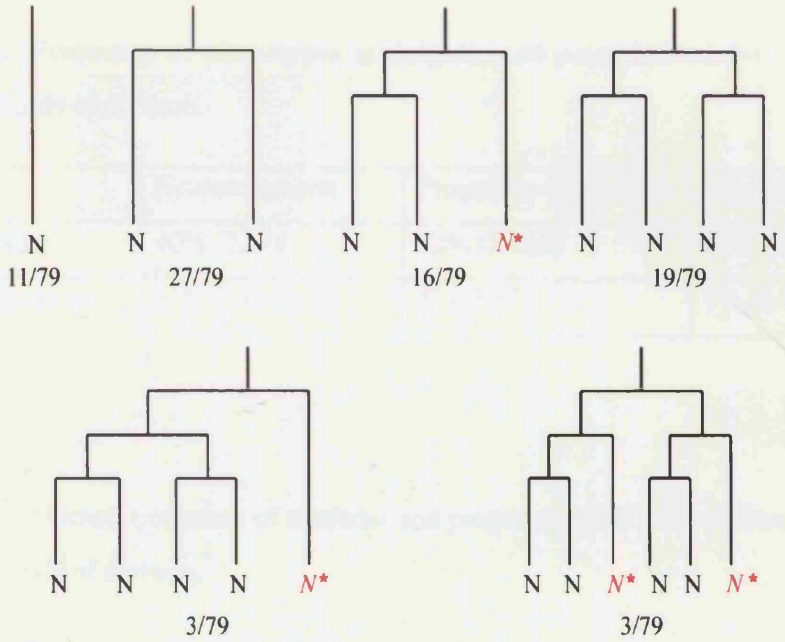

Figure 5.7. Summary of my 79 neuron only lineage trees.
The type and frequency of lineage trees observed are shown. For each tree schematically represented time runs from top to bottom and a branch in a line signifies a division. Divisions appear synchronised in these trees but this is not necessarily true as clones were not followed by high resolution time-lapse microscopy to determine this. The vast majority (73/79) clones I observed were one of the four depicted on the first row. The letter N signifies a neuron throughout and the *N* in red italics with the asterisks is one that is born following an asymmetric division that generated both this neuron and a progenitor cell that went on to divide again. These lineage trees show a dearth of such divisions and that the vast majority of neurons are generated by a division that produces two neurons. None of the reconstructed lineage trees contain repeated rounds of asymmetric division as might be expected of a classic stem cell.

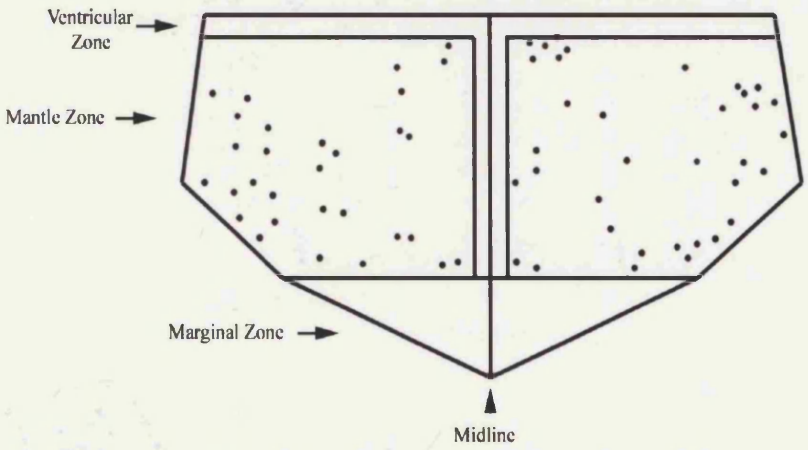

Figure 5.8. Distribution of neurons at 48hpf following random single cell injections in the neural plate. The position of 66 neurons taken from 19 clones at 48hpf is projected onto a schematic transverse section to determine if there was any bias in the distribution of cells analysed in the lineage study. It is clear that most areas of the mantle zone contain dextran labelled neurons and that there is no clear bias towards any one region of the mantle zone in particular.

Table 5.1. Frequency of phenotypes in daughter cell pairs derived from the first and second rounds of division.

	Neuron+neuron	Progenitor+progenitor	Neuron+progenitor
First division	40% (22/68)	32% (27/68)	28% (19/68)
Second division	86% (54/63)	5% (3/63)	9% (6/63)

Table 5. 2. Overall frequency of neuronal and progenitor cells derived from the first and second rounds of division.

	% Neurons (Q)	% Progenitors (P)
First division	54% (73/136)	46% (63/136)
Second division	90% (114/126)	10% (12/126)

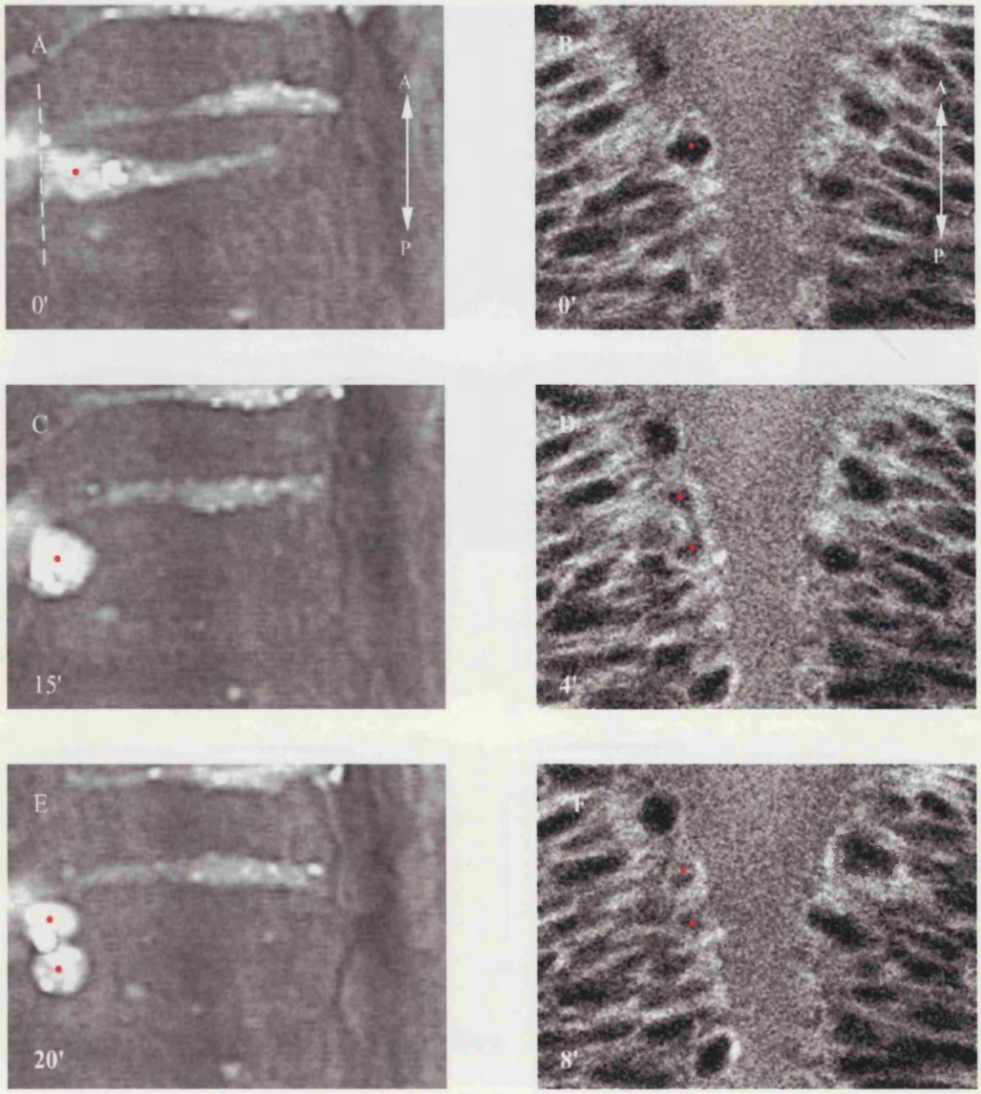

Figure 5.9. Orientation of division is almost always within the plane of the ventricular zone.
(A, C, E) Sequence from a time-lapse movie showing a dextran labeled cell divide along the plane of the ventricular zone. Horizontal view. The direction of the anterior-posterior (A-P) axis is indicated by the arrowed line in A and the ventricular surface is indicated by the dashed line in A.
The dividing cell and its daughters are indicated by red spots. It is clear that the dividing rounds up at the ventricular surface and that the two daughter cells lie along the ventricular surface immediately after cytokinesis.
(B, D, F) Sequence from a time-lapse movie of an embryo stained with Bodipy 505/515. This dye stains the cytoplasm and the nucleus is obvious as it is negaitvely stained. This is a horizontal confocal section and the direction of the anterior-posterior (A-P) axis is indicated by the arrowed line. A cell (with red spot) rounds up at the ventricular surface in B and just four minutes later we see a figure of eight shape where the cell is just undergoing cytokinesis and the cytoplasm is dividing and is about to be pinched apart. Four minutes later we can see that cytokinesis is complete and that the two daughter cells lie along the ventricular surface after division. See supplementary movies 5.1 and 5.2 to get a better feel for the dynamic nature of these cell divisions.

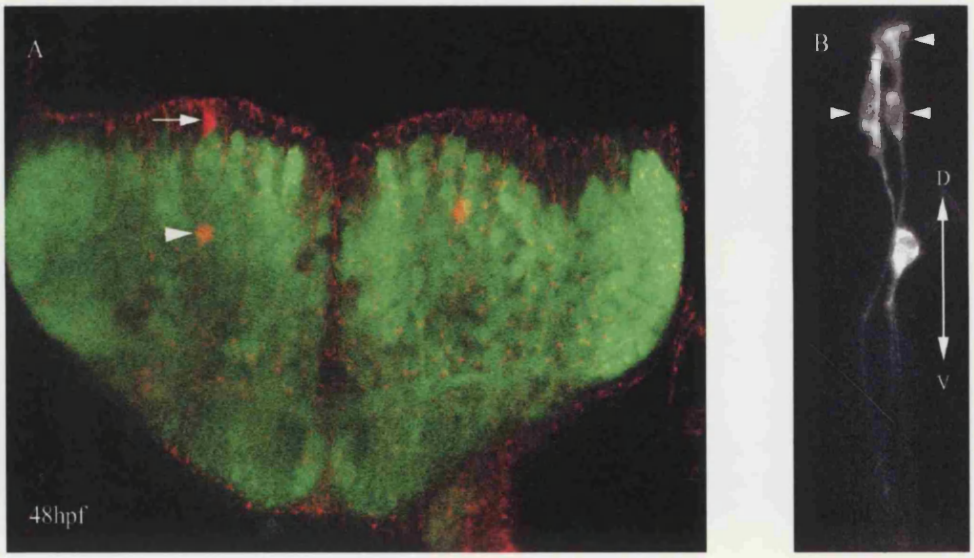

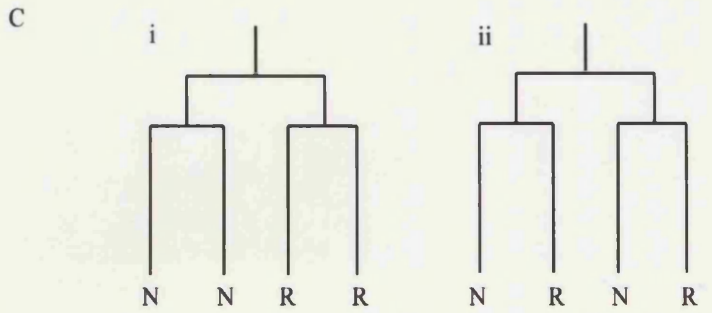

Figure 5.10. Non-neuronal cells in clones at 48hrs.
A. Transverse view of a single confocal section through two clones at 48h in a HuC-GFP +ve embryo. Dorsal is to the top. The clone on the left hand side of the midline actually contained two radial cells and two neurons but in this section only one radial cell and one neuron are seen. The cell body of the radial cell (arrow) lies in the ventricular zone outside of the HuC-GFP +ve area. A HuC-GFP +ve cell (arrowhead) that is also part of this clone can be seen in this section.
B. Lateral view of a clone on one side of the midline with 3 radial cells (arrowheads) and a neuron at 48hpf. The arrowed line shows the orientation of the dorso-ventral (D-V) axis.
C. Four out of seven clones that contained radial cells contained two radial cells and two neurons. These are the two most likely lineage trees that could generate a clone of two neurons and two radial cells. Time runs from top to bottom and a branch indicates a division. The start point is a cell on one side of the midline after the midline division. The lineage could have diverged at the next division such that the progenitors generated went on to produce two neurons or two radial cells (i). Alternatively the division after the midline division could have generated two progenitors that were still both capable of generating a neuron and a radial cell (ii).

Figure 5.11. Determining length of G2+M+G1

This figure shows examples of images that were used to calculate the duration between the end of one S phase of the cell cycle and the beginning of the next i.e. the duration of G2 + Mitosis + G1. BrdU is incorporated into cell nuclei when they are replicating DNA and thus is a marker of S phase of the cell cycle. When BrdU is administered by pulse labelling the embryo is only incubated in the drug for 20 minutes and hence many cells in the cell cycle will not incorporate BrdU if they are not in S phase during this 20 minutes. For instance some cells will have just left S-phase before BrdU was administered and wont re-enter S phase until they have passed through G2 + Mitosis + G1 of the cell cycle. The protocol illustrated in this figure calculates how long it takes for the cells that had just left S phase before BrdU administration to reach S phase again i.e. to measure the duration of G2 + Mitosis + G1. This can be calculated by giving embryos repeated pulses of BrdU at defined intervals after the initial pulse. There should then come a time when the cells that had just left S phase before the first BrdU administration will have reached S phase again and incorporate BrdU. In this case one would expect to see the maximal number of nuclei that are in the cell cycle labelled with BrdU as all cycling progenitors will have had time to enter S phase at least once. Some cells will receive multiple doses of BrdU if they were in the beginning of S phase at the initial time of incubation and still in S phase during a subsequent administration of BrdU. This accounts for the fact that some cells in these figures appear brighter than others.

A-D show single horizontal confocal sections through the hindbrain. The anterior- posterior (A-P) axis is indicated by the arrowed lines and the midline runs along the direction indicated by the arrowheads. Embryos were fixed 15 minutes after the final administration of BrdU i.e. at 36hpf (A), 38hpf (B), 40hpf (C) and 42hpf (D). Individual embryos were incubated in BrdU for 20 minutes at each the times indicated in the individual panels. It can be seen that the proportion of nuclei that incorporate BrdU (red) increases from A through to D. Almost all nuclei in the ventricular zone of embryos that labelled with BrdU at 36hpf, 39hpf and 42hpf are BrdU +ve. Embryos that were pulse labelled again after this point did not have more BrdU +ve nuclei indicating that the ventricular zone is saturated with BrdU +ve nuclei by repeated pulse labelling within 6 hours of initial pulse labelling. This indicates that all progenitors have passed into S-phase within 6 hours and that the duration of G2 + Mitosis + G1 is 6 hours.

E-H are single transverse confocal sections through the hindbrain. The dorso-ventral (D-V) axis is indicated by the arrowed lines and the midline runs along the direction indicated by the arrowheads.. BrdU +ve nuclei are shown in red and the mantle zone is shown by HuC-GFP expression in green. Performing this experiment in HuC-GFP +ve embryos allowed me to more accurately assess the domain of the ventricular zone and hence get an impression for when it was full of BrdU +ve nuclei. As with A-D embryos were fixed 15 minutes after the final administration of BrdU i.e. at 36hpf (E), 38hpf (F), 40hpf (G) and 42hpf (H). Individual embryos were incubated in BrdU for 20 minutes at each the times indicated in the individual panels. The same conclusion is reached as was from panels A-D i.e. that the ventricular zone is saturated with BrdU +ve nuclei after repeated pulses over 6 hours and that the duration of G2 + M +G1 is 6 hours. All scale bars = 50μm.

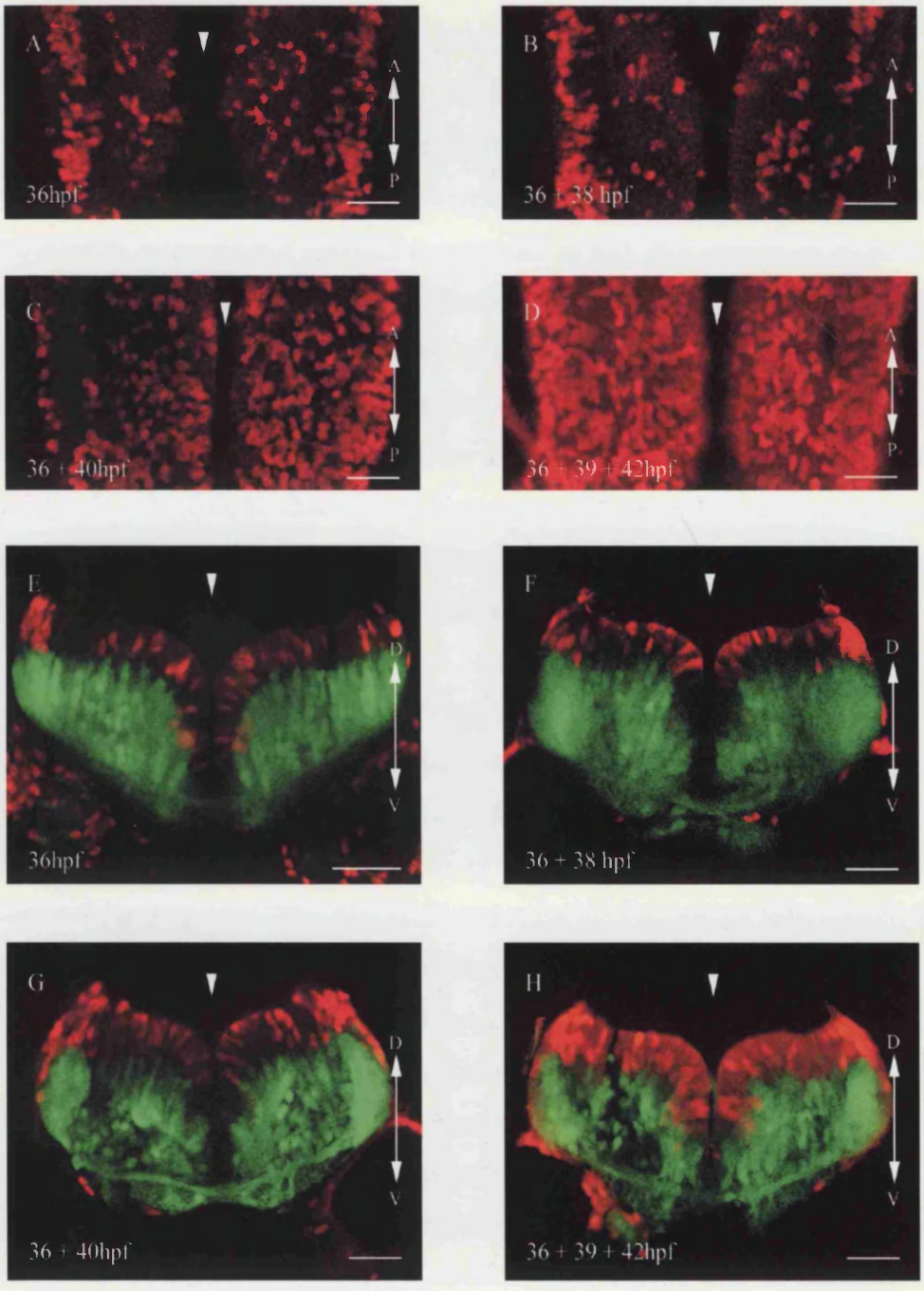
A
A
P
36hpf
B
A
P
36 + 38 hpf
C
A
P
36 + 40hpf
D
A
P
36 + 39 + 42hpf
E
D
V
36hpf
F
D
V
36 + 38 hpf
G
D
V
36 + 40hpf
H
D
V
36 + 39 + 42hpf

Discussion

By following the fate of fluorescently labelled neural progenitors through to their terminal divisions I have determined that the majority of neurons in the embryonic zebrafish hindbrain are born from progenitor divisions that generate two neurons. Asymmetric divisions that generate a progenitor as well as a neuron do occur but they represent only 17% of the progenitor divisions monitored and many of these divisions appear to be restricted to a particular generation within a family tree and hence a particular time during development. Over 90% of the progenitors monitored from the neural rod stage had their terminal mitoses prior to 48 hpf. These results show that in the embryonic zebrafish hindbrain most progenitors do not follow a stem cell mode of division. These results represent the first direct observations of multiple rounds of neurogenic divisions in an intact vertebrate nervous system.

Correlation between cell counting and lineage analysis

I wanted to be confident that the lineage tree analysis could account quantitatively for neurogenesis in the zebrafish hindbrain. The 86 original progenitors in the lineage analysis produce a total of 236 neurons by 48hpf. This gives a factor of 2.74 neurons produced per progenitor. This data predicts that the 1618 progenitor cells actually present at 15hpf should generate 2.74 x 1618 (4440) neurons by 48hpf. In fact the cell counts reveal that there are 4150 HuC-GFP +ve cells present at 48hpf (Chapter 3). This confirmed that the lineage data predicts actual neurogenesis with an error of only 7%. The lineage data also predicts that 319 non-neuronal cells should remain at 48hpf, but cell counts reveal 1217 HuC-GFP-negative cells. This discrepancy may be explained by the fact that the use of HuC-GFP expression to phenotype cells overestimates the non-neuronal population. Some of the HuC-GFP negative cells will be post-mitotic cells committed to a neuronal fate but not yet expressing HuC-GFP (Chapter 3). If the delay to differentiation is an average of 4 hours this predicts that there are 4636 neurons and 731 non-neurons at 48hpf (Chapter 4; Graph 4.6 +4.8 (orange line)). These numbers are closer to those predicted by the lineage study although there is still a dearth of non-neuronal cells at the end of the lineage analysis. When cells were randomly and mosaically labelled with α tubulin GFP and phenotyped based solely on morphological criteria only 9% of cells at 48hpf had a non-neuronal, radial glial morphology (Chapter

2). The relative number of non-neuronal cells from this mosaic analysis predicts that 483 non-neuronal cells are present at 48hpf, which is also closer to the number predicted by the lineage study. It is possible that the early neural plate is not homogeneous and that a particular area of the neural plate may be restricted to generating late non-neurons. If this were true then this would bias the relative number of neuron only clones against those containing radial glia in a random lineage analysis. It has been shown in the zebrafish spinal cord that there are regional differences in the composition of individual clones labelled in the medial neural plate relative to the lateral neural plate (Papan and Campos-Ortega, 1999) although the relationship with non-neuronal cells was ambiguous. There is some indirect evidence from some of my analysis that there may be regional differences in the fate of progenitor cells. The localisation of BrdU +ve cells at 48h is very restricted, to a ventral midline domain and to the dorsal rhombic lip (Chapter 3, Figure 3.12), which may correlate with a restricted position of non-neuronal progenitors during development. Despite the slight discrepancy in non-neuronal number at 48hpf there is a remarkable correlation between the numbers obtained in the stereological counts and those predicted following the lineage analysis. It is my belief that the stringency of this correlation could be increased further by increasing the number of lineage reconstructions performed and determining if there is a spatial bias in the progenitors that give rise to the late non-neuronal population.

Probabilities and implications for mechanisms

One major question in neurogenesis is how the intrinsic properties of a progenitor cell determine the eventual fate of daughter cells relative to the influence from the environment. Studies in the Xenopus retina, chick hindbrain and zebrafish spinal cord show that clone size is highly variable implying either that individual progenitors are highly variable with respect to the numbers of cells they can generate or that the decision to re-enter the cell cycle is made independently in individual cells after mitosis and is therefore stochastic (Wetts and Fraser, 1988; Lumsden et al., 1994; Papan and Campos-Ortega, 1997). Work from the McConnell lab on the other hand has shown that progenitors, at least during certain periods of development, have a restricted potential and are committed to generating daughters of a particular fate (Frantz and McConnell, 1996) and that this decision is made in late S-Phase or in the G2 phase before the terminal division (McConnell and Kaznowski, 1991).

Throughout this thesis I have described three types of division mode that progenitor cells can undergo during neurogenesis, a progenitor pair division, a terminal neuron pair division and an asymmetric division that generates a neuron and a progenitor and I have presented the relative frequency of these division modes observed in my lineage analysis (Table 5.1). I wished to compare the frequency of these division modes that I have observed during my lineage analysis to those predicted by chance. To do this I have used the model by Cai et al., 2002. This model is based on the assumption that the decision to re-enter the cell cycle or not is stochastic and is made independently in individual daughter cells. This model also allows for a combination of progenitor pair, neuron pair and asymmetric divisions to operate during neurogenesis. Over any one period a certain proportion of cells will leave the cell cycle. This is referred to as the Q fraction in the model of Cai et al., 2002 and a certain proportion will re-enter the cell cycle, referred to as the P fraction in this model. The proportion of each cell division mode that would operate given raw data about the Q and P fraction is given by the binomial expansion $(Q+P)^2 = 1$ or $Q^2+2PQ+P^2 = 1$ where Q^2 denotes the proportion of neuron pair division 2PQ the proportion of asymmetric divisions and P^2 the proportion of progenitor pair divisions. Table 5.2 shows the Q and P fraction for cells following the first round of division in my lineage study i.e. the proportion of daughter cells that left the cell cycle (Q fraction) and those that re entered the cell cycle (P fraction). By entering this data into the model proposed by Cai et al., 2002, I will get a prediction of the relative proportion of division modes that I should observe in my lineage analysis if the decision to re-enter the cell cycle is stochastic and made in individual daughter cells. I can then compare the predicted proportions of division mode from this model with the real numbers that I observed in my lineage analysis. If the predicted frequency of division mode is very similar to that which I have documented in my lineage analysis then it may suggest that the decision to re-enter the cell cycle or not is stochastic. However, if there is a considerable difference between the division modes predicted according to this model and those observed in my lineage analysis it may suggest that the decision to re-enter the cell cycle is biased by decisions made in the progenitor prior to terminal division.

Table 5.2 shows that over the course of the first cell cycle that the Q fraction of cells that differentiate is 0.54 and that the P fraction of cells that remain in the cell cycle is 0.46. By entering these values into the equation proposed by Cai et al., 2002 i.e. $Q^2 + 2PQ + P^2 = 1$ I find that I should observe 29% (0.54^2) neuron pair, 50% (2x0.54x0.46) asymmetric

and 21%(0.46^2) progenitor pair divisions in my lineage analysis at this stage if the decision to re enter the cell cycle is stochastic. Table 5.1 shows the actual frequency of division modes over this period and shows that there are more neuron pair and progenitor pair divisions during this period than predicted by the model and that there are many fewer asymmetric divisions in reality during neurogenesis than the model would predict. This leads to the conclusion that the decision of the daughter cell to re-enter the cell cycle is not random and that this decision may have been made prior to mitosis.

Where are the stem cells?

There is an increasing amount of circumstantial evidence that asymmetric divisions play a central role in neurogenesis of higher vertebrates. Retroviral studies in two systems have shown the co-existence of neurons with a single radial glial cell (Gray and Sanes, 1992; Noctor et al., 2001). The latter study showed that this was true after variable durations of retroviral infection. After short durations of infection a single radial glial cell was seen with one or two neurons and with increasing durations of infection a single radial glia was seen with increasing numbers of neurons. As there is evidence that radial glia are neural progenitors the implication is that radial glia divide by repeated rounds of asymmetric division to generate the increasing numbers of neurons seen in these clones (Noctor et al., 2001). I have presented data that appears to be in total contrast to such a model. I have seen no evidence of repeated rounds of asymmetric division and find a total dominance of progenitor pair and neuron pair divisions during neurogenesis. Despite the reported evidence that single radial glia are found in clones with multiple neurons (Gray and Sanes, 1992; Noctor et al., 2001) there is also evidence that neuron pair and progenitor pair divisions operate during neurogenesis (Mione et al., 1997; Reid et al., 1997).

My study has quantified the relative number of progenitor pair, neuron pair and asymmetric divisions during neurogenesis in a vertebrate. The zebrafish hindbrain is clearly a much simpler system than the mammalian forebrain so one might ask how the data and principles that I have uncovered could be scaled up to higher organisms?

There are an estimated 11 cell cycles during mouse neurogenesis (Takahashi et al., 1996). My analysis shows that the majority of zebrafish hindbrain neurons are made over 3 rounds of division after the appearance of the neural plate and occasionally four. In the mouse the first rounds of division are likely to be largely proliferative pair divisions and

the last rounds of division are likely to comprise terminal neuron pair divisions (Takahashi et al., 1996). I have actually shown this to be the case in my analysis. The midline division is largely a progenitor pair division and the final round largely terminal neuron pair divisions (Table 5.1). This leaves just 1 main round of division in the zebrafish to be correlated with the behaviour during 7-8 rounds of division in a mammalian system. I have documented that a mixture of the three modes of division, progenitor pair, neuron pair and asymmetric divisions exist during this period of cell division in hindbrain neurogenesis. A combination of all three modes of division was also deemed the most likely to exist during mammalian neurogenesis (Cai et al., 2002).

Therefore the strategies used in zebrafish may not differ in principle with those used in higher organisms during neurogenesis. The major difference that seems to exist between the systems is the existence of repeated rounds of asymmetric division. Their existence has been inferred from retro-viral studies in mammals (Gray and Sanes, 1992; Noctor et al., 2001) but has never been demonstrated directly. The existence of this pattern of division is very attractive due to its stem cell like nature but to my knowledge this has not even been observed in any system, vertebrate or otherwise. A modified variation on this division mode exists during Drosophila neurogenesis where the proliferating stem cell like neuroblast undergoes repeated rounds of asymmetric divisions but in fact the division itself generates two progenitors and not a progenitor and a neuron. There is further evidence to indicate that the search for repeated rounds of asymmetric divisions in the vertebrates might be a wild goose chase. This comes from data that suggests that the cells that are the real stem cells in the adult nervous system do not directly generate post-mitotic progeny but generate a sub-population of cells that divide themselves to generate differentiated cells (Johansson et al., 1999). Furthermore, in culture conditions where cortical progenitor cells have been isolated and followed by time-lapse microscopy no progenitors were seen to undergo repeated rounds of asymmetric divisions that generated a progenitor and a neuron (Qian et al., 1998; 2000)

The idea that repeated rounds of asymmetric division might operate in vertebrates is also attractive given that it provides a very nice link between embryonic neurogenesis and adult neurogenesis. This notion may also have been strengthened by the fact that many of the neuroblasts that generate the embryonic nervous system in Drosophila become quiescent and after larval hatching begin proliferating to generate the adult brain (Truman and Bate, 1988). The precise division modes that neuroblasts undergo during adult

neurogenesis are not known. My data would suggest that stem cell like modes of division are at best rare during embryonic neurogenesis and may not exist at all. Furthermore I have no evidence to suggest that those cells that are non-neuronal at the end of the major period of neurogenesis have descended from a lineage of repeated rounds of asymmetric division.

The relationship between non-neuronal cells at the end of embryogenesis and adult neurogenesis is very poorly understood. There is a period of renewed neurogenesis in the zebrafish after 2-3 weeks of development in the peripheral nervous system (PNS) (An et al., 2002). This study showed that the number of neurons in dorsal root ganglia (DRG) increased from 10-15 neurons per ganglion at 14 days post fertilisation (dpf) to over 100 at 28dfp. During this period the fish as a whole undergoes an exponential growth (Raible, pers comm.), which could mean that this renewed neurogenesis seen in the DRG might not be specific and that a similar process could take place throughout the entire organism. Studying the behaviour of cells from the end of embryogenesis to this period of potential renewed neurogenesis should be an achievable aim using a cell labelling strategy in the future, especially with the advent of higher resolution labelling techniques such as single cell electroporation (Haas et al., 2001).

Correlation between cell fate and plane of division

A pioneering initial report claimed that cortical progenitors dividing within the plane of the ventricular zone generated daughter cells that adopted similar fates, whereas progenitors dividing perpendicular to the plane of the ventricular zone generated daughters with different fates (Chenn and McConnell, 1995). This study reported that in divisions where daughter cells were separated perpendicular to the ventricular surface that the cell that moved further away from the ventricular surface expressed high levels of Notch 1 whilst its sister did not and that this reflected the fact that this cell was a neuron whilst its sister cell was still a progenitor. However the fate of such cells was never followed for a sufficiently long period of time or confirmed with additional molecular markers to determine their phenotype unequivocally. Recently others have readdressed the idea that the plane of a progenitor cell's division might correlate with fate but conflicting reports have been published, (Cayouette et al., 2001; Silva et al., 2002; Das et al., 2003; Cayouette and Raff, 2003). In one study the authors demonstrate that in the rat retina the proportion of cells dividing out of the plane of the ventricular zone peaks at P0

at 21%. The daughter cells of these divisions are shown to inherit numb asymmetrically. However these observations are made long after the bulk of retinal neurons are generated and do not address the fate of the daughter cells (Cayouette et al., 2001). However a more recent study from the same lab followed the fate of cells by time-lapse microscopy during this period, again in the rat retina. They showed that cells that divided out of the plane of the VZ generated daughters with distinct fates but those that divided within the plane of the VZ generated daughters with similar fates. However in this case the daughters with different fates were usually both differentiated cells and the authors showed no examples of a progenitor neuron type asymmetric division (Cayouette and Raff, 2003). In another study the orientation of division in the chick retina was compared between regions where neurons were being produced and regions where neurons were not being produced. In this study no difference in the orientation of division between these two regions is reported (Silva et al., 2001). This study just assumed that asymmetric divisions that would generate a progenitor and a neuron would take place in the neurogenic region without providing any evidence to that effect. Another, more recent study showed a correlation between the time of a change in division orientation and the onset of neurogenesis. This study was carried out in the zebrafish retina. No mitoses were ever seen to separate daughters perpendicular to the plane of the ventricular zone. Instead there is a shift in division orientation between divisions that separate daughters along the central to peripheral axis of the retina to divisions that separate daughters along the circumferential axis of the retina. This occurs at a time that correlates with the onset of neurogenesis. Interestingly this shift in division between the central/ peripheral axis and the circumferential axis is delayed in both the sonic you (shh) and lakritz (ath 5) mutants that have defects in retinal ganglion cell production (Das et al., 2003). However, no direct evidence is provided that asymmetric cell divisions that generate a progenitor and a neuron exists in this or indeed any of these studies so a direct correlation with division orientation and this type of asymmetric division cannot be made. My study addresses this issue more directly because analysis of division orientation is made during a period when there are a relatively high proportion of asymmetric divisions that generate a neuron and a progenitor. My findings strongly suggest there is no correlation between the orientation of division out of the plane of the ventricular zone and the fate of the daughter cells of asymmetric divisions as virtually all progenitors appear to divide within the plane of the ventricular zone irrespective of daughter cell fate. There is the possibility though that

relatively small differences in the angle of division orientation relative to the ventricular surface could be enough to allow the asymmetric inheritance of cell fate determinants (Huttner and Brand, 1997) but I think that carrying out an analysis of division orientation in a complicated 3-D tissue with such high resolution would be very difficult, especially in a system where the face of the ventricular surface is not perfectly flat.

The future

One of my initial goals when starting this project was to follow cell lineage by high resolution time-lapse microscopy. Despite considerable time and effort this did not prove technically feasible. Now, however, with the combination of multi-photon technology and GFP based lineage tracing protocols, for example single cell electroporation, such goals should be attainable. It is difficult to see how similar studies will feasible in more inaccessible and complex systems in the immediate future, which means that the zebrafish should lead the way in this field.

There are a number of questions that still need to be addressed with respect to the behaviour of progenitor cells. I have described divisions only at the level of whether they generate two progenitors, two neurons or one of each. I have defined an asymmetric division as one that generates a neuron and a progenitor but it is still possible that neuron pair divisions are also asymmetric in that they could generate sister neurons of a different phenotype, either in terms of their axonal trajectory or their gene expression profile. In the future it should be possible to address this possibility but not before a large-scale characterisation of neuronal sub-type is made in the zebrafish hindbrain. A classification of neuronal sub-type based on axonal trajectory exists for the early chick hindbrain (Clarke and Lumsden, 1993) and lineage studies in this system have shown that by and large individual progenitors generate neurons belonging to an individual sub-class of neuron (Lumsden et al., 1994; Clarke et al., 1998). This would suggest that neuron pair divisions might generate similar neurons. However this is far from clear in the zebrafish where many fewer neurons are generated but it would be interesting to investigate in the future. The question of neuronal identity could be addressed with respect to the phenotype of sister neurons but also with respect to lineages that include asymmetric divisions e.g. is a neuron produced following an asymmetric division of a similar sub-type to those produced by its sister cell later in development. We know that in the zebrafish that reticulospinal neurons (Mendelson, 1986) and Islet-1 +ve motor neurons

(Chapter 3) are born early relative to the rest of the population. This suggests either that neurons born at this time are likely to adopt these fates because the signals in the environment at that particular time instruct them to do so or that the progenitors that gave rise to these early born neurons are somehow different from progenitors that give rise to later born neurons. It would be interesting to see if an asymmetric division that generates a neuron would go on to generate two neurons of a similar or distinct class in its subsequent division. Such information would be interesting in the context of assessing the importance of lineage in determining neuronal phenotype. If neurons born at different times in development but from the same original progenitor were of the same phenotype then this may suggest that the phenotype of the original progenitor was important in determining the fate of the cells. However if neurons born at different times in development but from the same original progenitor were of differing phenotypes then this may suggest that the environment regulates the phenotype of the specific neurons. There is another school of thought that holds that individual progenitors can generate neurons of a different phenotype depending on what stage of development they are in and thus that the phenotype of the progenitor changes through time (e.g. Pattyn et al., 2003). One study has shown that a distinct pool of progenitor cells can generate both visceral motor neurons and serotonergic neurons but at different stages of development. This progenitor pool is defined by the spatio-temporal expression of a set of transcription factors and that the onset of expression of another transcription factor, Phox 2b, determines the switch in progenitor behaviour from generating visceral motor neurons to serotonergic neurons (Pattyn et al., 2003). This model is similar to one that proposes that a distinct pool of progenitors can generate somatic motor neurons and oligodendrocytes but at different times of development and that again this switch is determined by combinations of transcription factor expression (e.g. Zhou et al., 2000; Zhou and Anderson, 2002; Lu et al., 2000b; 2002). However in none of these studies is there any evidence that an individual progenitor can generate either a visceral motor neuron and a serotonergic neuron or a somatic motor neuron and an oligodendrocyte. Addressing this question in a system like the zebrafish hindbrain where such an analysis of cell lineage could be carried out would be fundamentally important in our understanding of neural progenitor behaviour.

Another open question relates to the behaviour of progenitor in the generation of neurons and glia at later stages of development than I have examined during this study. It would

be interesting to see if there is renewed neurogenesis in the CNS as there is in the PNS (An et al., 2002) during the larval growth phase where the animal grows dramatically and to document what cells contribute to this renewed neurogenesis. In the study of the renewed neurogenesis in the PNS the authors made the astounding claim that it was post-mitotic neurons that re-entered the cell cycle to generate new neurons (An et al., 2002). However this was based only on co-expression of a BrdU with a Hu antibody that recognises many different Hu epitopes some of which are expressed in progenitors (Marusich et al., 1994). A possible candidate to mediate any renewed neurogenesis in the CNS would be the radial glial like set of progenitors that I have shown remain at the end of embryogenesis and it would be interesting to try and follow the fate of these cells for as long as possible to asses any potential role they might play later in development. Such efforts are ongoing in the Clarke lab.

Chapter 6

Novel characterisation of the zebrafish neurogenic mutant, *mindbomb*

Introduction

The zebrafish is now established as a powerful genetic model organism as predicted over twenty years ago by George Streisinger. Its relatively small adult size, about 3-4 cm in length, means that many fish can be kept in a laboratory situation. It has a generation time of 3-4 months and a single female can produce several hundred eggs in one lay. Mutations can be chemically induced at a high frequency and recessive mutations can be recovered in two generations. Whilst work was previously carried out on several zebrafish mutants it wasn't until 1996, when the results of the first large scale forward genetic screens in any vertebrate were published, that the tiny tropical fish hit the headlines. Work in Janni Nusslein-Volhard's lab in Tübingen and Wolfgang Driever's lab in Boston generated a total of over 6000 mutants of which about 2000 were kept for further characterisation (Haffter et al., 1996; Driever et al., 1996). Since then many of these mutants have been cloned and characterised and resultant data has provided fundamental insights into many areas of development, including neurogenesis (e.g. Schier et al., 1996; Holley et al., 2000; Kay et al., 2001). The mutants in the first large scale screens were isolated following a simple screen for morphological defects. Mutants with subtle phenotypes were inevitably missed and so a large proportion of these mutants have been re-screened using different more specific assays. Concurrently other labs have initiated their own pilot screens motivated by the success of these early endeavours. A summary of the different types of genetic screens which can be designed and have been carried out on zebrafish is beyond the scope of this introduction but a good review by Patton and Zon, 2001, is available.

I was lucky enough to take part in a recent large scale mutagenesis screen in Tübingen which was a collaboration between Janni Nusslein-Volhard's lab and a young biotech company, Artemis Pharmaceuticals, but in this chapter I will just describe novel characterisation of a mutant isolated in the 1996 screens, the neurogenic mutant *mindbomb*.

The *mindbomb* mutant was isolated in the first large scale screens in both Boston and Tübingen by morphological defects. During somitogenesis the somite boundaries of *mindbomb* (*mib*) mutant embryos are indistinct and the neural keel has an irregular

morphology relative to wild type. Later on in development, there is a lack of neural crest derived melanophores and trunk crest from the lateral migratory pathway (Jiang et al., 1996). Rhombomere boundaries are also absent. Analysis of neurogenesis in this mutant showed an increase in the number of primary neurons including Mauthner neurons, Rohon Beard neurons, primary motor neurons, epiphyseal neurons, lateral line neurons and neurons of the trigeminal ganglion. Later differentiating neurons such as zn-5 +ve hindbrain commissural neurons and spinal cord secondary motor neurons were reduced in number. The zrf +ve glial curtain fibres were also reduced in number at 48hpf, which was interpreted as evidence for a reduction in the number of glia. The initial characterisation concludes with the remark that this phenotype is similar to neurogenic phenotypes in Drosophila, which are caused by mutations in the Delta Notch signalling pathway (Jiang et al., 1996). Another neurogenic mutant *white tail* (*wit*) was isolated in the Boston screen Schier et al., 1996) and was initially thought to be due to a mutation in a different gene but was later shown to be an allele of *mindbomb*.

Recently further characterisation and the cloning of *mindbomb* (*mib*) have been published (Itoh et al., 2003). The neurogenic phenotype of *mindbomb* was scrutinised further, but only in the spinal cord. An excess of HuC GFP +ve neurons was seen at 11hpf in the three longitudinal stripes that correspond to the domains of primary neurogenesis in the spinal cord. Compared to wild type, a greater proportion of cells expressing the proneural gene neurogenin went on to express Delta in *mib* mutant embryos, indicating a defect in lateral inhibition within the proneural domains. Indeed when ectopic proneural domains were generated in *mindbomb* embryos by injection of neurogenin-1 RNA the neurogenic phenotype was exacerbated and ectopic neurons were now found in positions outside the normal domains of early proneural gene expression (Figure 6.1 A; Itoh et al, 2003). Injection of constitutively active Notch abolished all neurogenesis in *mindbomb* embryos, as it also does in wild-type tissue, showing that the molecular machinery necessary to mediate inhibition of neurogenesis downstream of Notch was intact. Cloning of *mindbomb* showed that it encodes a RING ubiquitin ligase that interacts with the intracellular domain of Delta. In the wild type the *mindbomb* protein promotes endocytosis of Delta, which is consequently found primarily in cytoplasmic vesicles. In *mindbomb* mutant cells an excess of Delta is seen on the cell surface (Itoh et al., 2003).

Transplantation experiments were carried out to examine if the defect in lateral inhibition was due to the fact that mutant cells could not effectively inhibit their neighbours from

becoming neurons or if they were unable to receive inhibition from their neighbours. Cells were transplanted from HuC-GFP +ve donors into wild type hosts. Donor cells were of three classes, those injected with a control morpholino, those injected with a *mindbomb* morpholino and cells from the *mindbomb* mutant line that had been crossed into the HuC-GFP transgenic line. If more cells became neuronal following transplantation of *mindbomb* morpholino or mutant cells into wild type hosts than in wild-type to wild-type transplants then the defect would likely to reside in the mutant cells' ability to receive lateral inhibition as it would show that these cells could not be inhibited from correctly differentiating. However, if fewer *mib* transplanted cells became neuronal than in wild-type to wild type control transplants the defect would more than likely be in the mutant cells' ability to produce an inhibitory signal as they would have been clearly capable of being inhibited from differentiating themselves. On average 27% of control cells transplanted from wild type donors into wild type hosts differentiated into neurons by 24hpf, whereas only 17% of the *mindbomb* morpholino and 7% of the mutant transplanted cells did so by the same time in development. Fewer mutant cells became neuronal showing that they were effectively inhibited from differentiating by the surrounding wild type host tissue meaning that the defect in the mutant cells must lie in their ability to generate an effective inhibitory signal (Itoh et al., 2003).

Interestingly Drosophila *neuralized* mutants exhibit a neurogenic phenotype and encode a different ubiquitin ligase (Yeh et al., 2001). In *neuralized* mutants Delta protein also accumulates at the cell membrane. Furthermore, in both Drosophila and Xenopus, *neuralized* overexpression causes Delta to be removed from the cell surface more quickly than in wild type. In vitro, the *neuralized* ubiquitin ligase also interacts directly with Delta (Deblandre et al., 2001; Lai et al., 2001).

Previous studies in Drosophila have shown that transendocytosis of Notch into the Delta expressing cell is necessary for effective notch signalling. Briefly, Delta endocytosis facilitates the S2 proteolytic event that releases the extracellular Notch fragment. This Notch extracellular fragment undergoes transendocytosis into the Delta expressing cell. This leaves the remainder of the Notch protein susceptible to another cleavage, which releases the intracellular domain from the membrane, from where it goes into the nucleus to activate target genes (Parks et al., 2000). It has been shown that *neuralized* overexpression can increase endocytosis of Delta and consequently cause an increase in Notch signalling (Pavlopoulos et al., 2001).

This data from *neuralized* coupled with the observation that *mindbomb* primarily affects the signal sending cell suggests a model for how a mutation in these ubiquitin ligases can cause the neurogenic phenotype. *mindbomb* and *neuralized* mutant cells have an excess of Delta at the cell surface and hence no ability to transendocytose Notch which means that there is no effective Notch signalling and hence no cell can inhibit its neighbours. The phenotypic consequence is that every cell in a proneural cluster of cells that is competent to differentiate is free to so as there is no mechanism to inhibit this.

It has been suggested that the progenitor pool is entirely depleted in the *mindbomb* mutant spinal cord by 24hpf and that it is entirely composed of neurons (Itoh et al., 2003; Ajay Chitnis, pers. comm.). This is based on two observations. There is virtually no expression of Notch5 or DeltaA at 24hpf, which is taken as evidence for the absence of progenitors and newborn neurons respectively. Furthermore 3-D reconstruction of the HuC-GFP *mindbomb* spinal cord at this stage shows that the tissue uniformly expresses GFP (Itoh et al., 2003). If true this would suggest that between the neural plate stage and 24hpf every progenitor expressed proneural genes and thus became competent to generate neurons. Unfortunately the resolution of the 3-D reconstruction presented in the published study was poor (Figure 6.1B) and no other marker for progenitors was used in this study apart from Notch5. Given that only 25% of the total number of neurons predicted to exist in the spinal cord at 3.5 days post fertilisation have differentiated by 24hpf (Papan and Campos-Ortega, 1999) and that there are anti-neurogenic domains during early neurogenesis where neuronal differentiation is precluded (Brewster et al., 1998) it seemed unlikely to me that every cell in the neuroepithelium would have been competent to differentiate as a neuron up to this point.

It is for these reasons that I sought to re-examine the extent of the neurogenic phenotype in *mindbomb*. I was particularly keen to see if there were non-neuronal cells beyond the early stages of neurogenesis that are typically documented in analyses of neurogenic mutants or studies where neurogenic genes are altered in the vertebrate. The hindbrain was used as the system in which to address this question for several reasons. Primarily I could directly compare results obtained in analysis of *mindbomb* with those acquired elsewhere in this thesis. I have shown that in the wild type primary neurogenesis accounts for a small minority of total neurogenesis in the hindbrain and I thought it was very

unlikely that all cells of the early hindbrain neuroepithelium would be competent to differentiate as neurons and exhibit a neurogenic phenotype in *mindbomb* mutants. Overexpression of neurogenin 1 RNA in the *mindbomb* mutant hindbrain leads to an exacerbation of the neurogenic phenotype in the mutant (Itoh et al., 2003; Figure 6.1A). The effect of Neurogenin 1 overexpression is to generate cells that are now competent to differentiate as neurons in regions of the early neuroepithelium where they are not normally competent to do so. This accounts for the exacerbation of the neurogenic phenotype in the mutant. This also highlights that cells exist at least in the early hindbrain neural plate that are not competent to make neurons. I was interested to see how long into the development of the *mindbomb* hindbrain non-neuronal cells would exist as this might provide insights into the competence of progenitors to generate neurons during wild type neurogenesis.

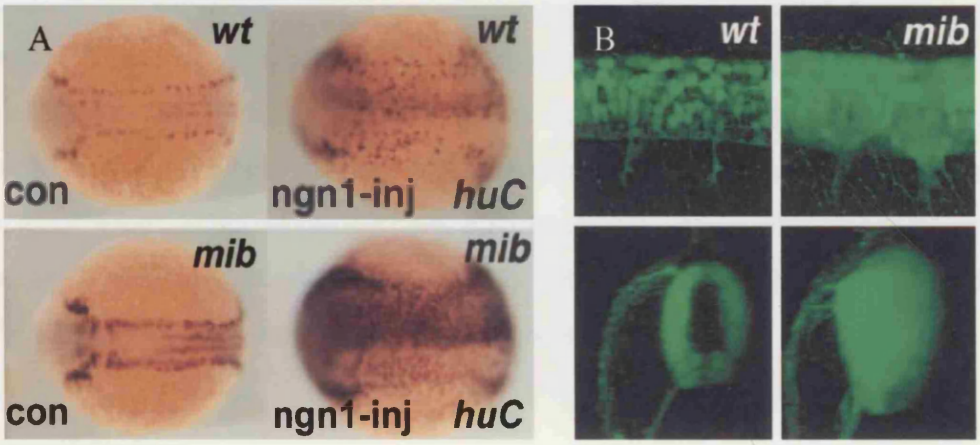

Figure 6.1. Images taken from Itoh et al., 2003.
A shows four panels that illustrate an experiment from Itoh et al., 2003. The top two panels are wild type embryos and the bottom two are mutants. Both left panels are control specimens and both right panels show embryos that were injected with neurogenin (ngn) 1 RNA at the one cell stage. All embryos are 12hpf and have been stained to reveal the GFP in neurons of the hindbrain diven by the HuC GFP transgenic line. We can see that there are very few post mitotic neurons in the wild type hindbrain (top left) and that this number is somewhat increased in the mindbomb mutant (bottom left) but only in positions where some neurons exist in the wild type. In wild type embryos injected with neurogenin 1 RNA there are an excess number of neurons and these are in regions of the hindbrain that don't normally produce neurons at this time. The actual concentration of neurons has not increased too dramatically. However, in mindbomb mutants injected with neurogenin 1 RNA it seems that the most of the hindbrain has become neuronal. The neurogenin overexpression has increased the domains of proneural gene expression and the lack of lateral inhibition within these domains means that all cells that are competent to make neurons differentiate. B shows four more panels that were used to illustrate that there are no non-neuronal cells in mindbomb at 24hpf. The top panels show single confocal lateral sections through wild type and mutant HuC-GFP +ve spinal cords respectively. The bottom panels show 3-D reconstructions made from stacks of such lateral sections. Unfortunately the resolution is poor in these 3-D reconstructions and much of the tissue is over exposed which in my opinion may occlude observation of non-neuronal cells that may exist in the mutant spinal cord (bottom right panel).

Methods

Generation of mib /HuC-GFP embryos

One tool that was used throughout this analysis was *mib* /HuC-GFP +ve embryos. To generate adults that carry both the *mindbomb (mib)* allele and the HuC-GFP transgene I crossed heterozygous *mindbomb* females with homozygote HuC-GFP males. Half of the progeny would be heterozygous for both the *mindbomb (mib)* allele and the HuC-GFP transgene and half would just carry a heterozygous copy of the transgene. This generation were grown up to sexual maturity and random sibling crosses were made to find adult carriers. Carriers were isolated by screening embryos by morphology for the *mindbomb* phenotype and by fluorescence for the presence of the transgene.

Cell counting

Cell counts were carried out using the Disector method (DC Sterio, 1984) described in chapter 4. Total cells were counted in specimens labelled with either Bodipy 505/515 or Texas Red Bodipy ceramide and neurons were counted from HuC-GFP +ve embryos co-stained with Texas Red Bodipy ceramide as described in chapter 4. However, it was not possible to determine the extent of rhombomeric compartments in *mib* /HuC-GFP embryos. When measuring the total volume of *mindbomb* tissue in which to perform cell counts the A-P length of wild type segments at each individual time-point was used also in the mutant. This seemed fair because the A-P length of the hindbrain was similar between wild type and mutant (Figure 6.2 C+D). Cell counting was performed on NIH image and volume estimation was calculated using Volocity (Improvision) as described in chapter 4.

Time-lapse analysis

mib/HuC-GFP embryos were imaged by time-lapse microscopy on a Leica confocal using a x40 water immersion lens. Bodipy 505/515 stained *mindbomb* embryos were also imaged by time-lapse microscopy on a Leica confocal microscope using a x 40 water immersion lens. Embryos were placed in PTU at 24hpf to prevent pigmentation and anaesthetised in 0.03% tricaine during imaging as described in chapter 2.

BrdU labelling

mindbomb embryos were pulse labelled with BrdU at 24, 36, 48 and 72hpf and fixed 15 minutes after the pulse as described in chapter 2.

Antibody labelling

Immunochemistry was carried out on *mindbomb* and *mib*/HuC-GFP embryos using anti GFAP, anti acetylated tubulin, anti BrdU and anti pH-3 s as described in chapter 2.

Preparation for transmission electron microscopy TEM

A PhD student in the lab of Dr. John Scholes, Tom Hawkins, helped me throughout the TEM protocol.

mib embryos and siblings were grown up at 28.5°C until 5 days post fertilisation (dpf) before being fixed for electron microscopy. The procedure thereafter was as follows.

1. Fix in Electron Microscopy fix for a minimum of 24 hours at 4°C (2% Paraformaldehyde and 2% gluteraldehyde in 0.1M Cacodylate buffer with 0.5% Calcium chloride ($CaCl_2$))
2. Wash 3x10 minutes in 0.1M Cacodylate with 0.5% $CaCl_2$ then put in glass vials.
3. Osmicate in 1% Osmium tetroxide (OsO_4), 8% sucrose in 0.1M cacodylate for 3 hours.
4. Wash 3x 10 minutes in 0.1M cacodylate with 8% sucrose.
5. Change to 0.1M Sodium Acetate with a couple of washes.
6. Stain in 2% Uranyl acetate 30 minutes-1 hour.
7. Rinse and wash 4x 10 minutes in 0.1M Sodium acetate.
8. Dehydrate through 25%, 50%, 75%, 90% ethanol for 5-10 minutes at each concentration then wash twice in 100% ethanol for 10 minutes per wash.
9. 2x propylene oxide 20 minutes
10. 1:1 resin: propylene oxide for 30 minutes
11. 3:1 resin: propylene oxide for 1-2 hours.
12. Pure resin 3-6 hours
13. Put in Mould and bake at 60°C at least over night or for up to 48 hours
14. Prepare suitable orientation of the moulded resin and cut ultrathin sections are on a LKB ultramicrotome

15. Mount sections on pioloform resin films (TAAB laboratories equipment ltd, Reading, Berks UK) on 1x2mm slot grids (Agar scientific, Essex UK).
16. Image specimens on a Jeol JEM-1010 transmission electron microscope.

Results

The mindbomb neurogenic phenotype is obvious in the hindbrain by 15 hpf

It was very difficult to distinguish between the wild type and mutant hindbrain until about 15hpf. At this point an enlarged ectopic bump could be seen in the middle of the hindbrain at the level of about rhombomere 4. When wild type/HuC-GFP and *mib*/HuC-GFP +ve embryos were analysed at this stage this bump in the mutant hindbrain was seen to be a cluster of early differentiating neurons in the region of rhombomere 4 (Figure 6.2 A+B). From this point on the mutant nervous system became progressively more easy to distinguish from the wild type. The mutant failed to undergo neurulation correctly and consequently a distinct neural tube was never obvious, nor was a defined midline seam that clearly separated the left and right hand side of the neuroepithelium (Figure 6.2 C-F). Consequently the stereotyped neuronal arrangement seen in wild type was very disrupted in the mutant (Figure 6.2 C+D) as was the stereotyped arrangement of white matter seen in the wild type (Figure 6.2 E+F). However, it was still clear that there were bundles of axonal tracts in the mutant that were often located in the ventral part of the neuroepithelium as seen in the wild type (Figure 6.2 E+F)

mindbomb embryos contain non- neuronal cells throughout embryogenesis

Having analysed *mib*/HuC-GFP +ve and acetylated tubulin stained *mindbomb* mutants it was unclear whether non-neuronal cells existed at later stages of embryogenesis i.e. from 24hpf onwards. To investigate this, *mib*/HuC-GFP +ve embryos were counterstained with Texas Red Bodipy Ceramide. Cells outlined by TR Bodipy ceramide that were not HuC-GFP +ve were seen throughout the development of *mindbomb* (Figure 6.3 A-D) up until 72hpf, which was the last stage examined using this technique. This suggested that some cells did not differentiate as neurons during this period. This result contradicted published data that suggested that the neuroepithelium of *mindbomb* embryos was entirely composed of neurons by 24hpf (Itoh et al., 2003; Ajay Chitnis, pers. comm.).

Cell quantification shows that most cells divide once in the neuroepithelium

In the light of this observation I wanted to compare the number of neuronal and non-neuronal cells throughout the first three days of *mindbomb* development to those in the wild type. It seemed likely that with such an excess of early born neurons in the mutant

that the progenitor population would be depleted early in development and that there would consequently be fewer neurons in the *mindbomb* brain than in wild type. However, in light of the observation of non-neuronal cells throughout the development of the mutant it was possible that these cells might be somehow capable of compensating for the initial loss of progenitor cells.

As described in chapter 4 total cells were counted from specimens stained with either Bodipy 505/515 or Texas Red Bodipy ceramide and neurons were counted by subtracting the number of non-neuronal cells seen in HuC-GFP +ve embryos co-stained with Texas red Bodipy ceramide from the total cell number in the same specimen. Unfortunately distinct rhombomeres were not recognisable in the *mindbomb* mutant so I estimated their A-P length as being the same as that of the wild type at each stage examined. This seemed reasonable as the overall A-P length of the hindbrain was similar in wild type and mutant embryos (Figure 6.2 C+D).

I found that the total number of cells in a domain corresponding to rhombomeres 4+5 in the mutant at 15hpf is very similar to that of wild type differing by only 7% (wt 1639 (n=3): *mib* 1770 (n=2)). Most cells in the wild type have undergone or are just about to undergo their first division in the hindbrain at 15 hpf. The fact that a similar number of cells exist in *mindbomb* as in the wild type indicates that most cells in the mutant hindbrain also undergo one round of division. At this stage there are clearly more differentiated neurons in the mutant than in the wild type but this only accounts for 10% (186/1770)(n=2) of the total cell number at this stage.

In order to see how the relative number of neurons and non-neurons developed between wild types and mutants over the next two days of development quantification was carried out at 24, 36, 48 and 60hpf (Graph 6.1). I saw that the total cell number increased by a factor of 1.8 from 1770 at 15hpf to 3203 at 60hpf in the mutant. This compares with an increase in total cell number by a factor of 3.8 over the same period in the wild type from 1639 to 6183 (Graph 6.2). This shows that the total cell number is in fact much smaller in the mutant than in the wild type by 60hpf, due to the early depletion of the progenitor pool and that this number is not restored later in development. The total neuronal number is much greater in the mutant at 24hpf than in the wild type but the depletion in the progenitor population also means that there are eventually many fewer neurons in the mutant tissue (Graph 6.3).

One interesting finding is that the number of non-neuronal cells at 60hpf is very similar in both the wild type and the mutant varying only by a factor of 1.4 (wt 576: *mib* 403) (Graph 6.4). This observation suggests that the non-neuronal cells seen in the mutant at 60hpf have arisen by a Notch Delta independent mechanism. The similarity in non-neuronal number between the mutant and wild type at this stage may indirectly imply that non-neuronal cells seen at 60hpf in the wild type may also arise by similar Notch Delta independent mechanisms.

A subset of mindbomb cells remain mitotically active

My cell counting indicated that the total number of cells in a region that corresponded to rhombomeres 4+5 increased by a factor of 1.8 between 15 and 60hpf. To get further evidence that cells in the *mindbomb* mutant were capable of proliferating throughout these stages of neurogenesis I stained *mindbomb* embryos with a number of cell cycle markers and analysed cell behaviour by time-lapse microscopy.

I pulse labelled *mindbomb* embryos at 24, 36, 48and 72 hpf with BrdU and checked other embryos for expression of the mitotic marker pH-3 at 24, 36 and 48hpf. Some cells in the *mindbomb* hindbrain did indeed incorporate BrdU at 24, 36 and 48hpf but none could be seen to do so at 72hpf. Cells also expressed the mitotic marker pH-3 at 24, 36 and 48hpf. In each case BrdU +ve cells and pH-3 +ve cells were localised to non-HuC-GFP +ve cells (Figure 6.4 A-F). I also examined the *mindbomb* spinal cord and could see clear examples of non-neuronal BrdU +ve cells at 24, 36 and 48hpf (e.g. Figure 6.4 G+H).

In time-lapse analysis of Bodipy 505/515 labelled *mindbomb* embryos I saw that cells in the hindbrain that did indeed round up and undergo cytokinesis as expected at periods between 15 and 48 hpf (Figure 6.5). Time-lapse analysis of *mib* /HuC-GFP +ve embryos GFP +ve neurons showed that HuC-GFP +ve cells never divided in the mutant verifying that they were post-mitotic.

In order to examine if cell death was influencing the interpretation of the cell quantification in the mutant, Acridine Orange labelling was carried out on *mindbomb* embryos at 24, 36, 48 and 60hpf. No difference was observable between *mindbomb* and sibling embryos (Figure 6.6). Both sets of embryos showed very little acridine orange labelling in the hindbrain at any of the stages examined.

These results, combined with the quantification data, show that *mindbomb* cells in the hindbrain are capable of dividing and generating new neurons up to at least 60hpf (Graph 6.2 + 6.3) and that a similar number of non-neuronal cells remain at 60hpf in the mutant as does in the wild-type tissue (Graph 6.4). Coupled with the fact that BrdU +ve cells were seen in the *mib* spinal cord these data strongly disagree with the assertion that the *mindbomb* neuroepithelium consists of only neurons at 24hpf (Itoh et al., 2003; Chitnis, pers. comm.).

Some non-neuronal cells have characteristics of radial glia

In the wild type hindbrain there are two distinct domains of progenitor cells from 36hpf. The most prominent region is the dorsal ventricular zone, which contains progenitors that express radial glial markers like GFAP and zrf-1. There is also a population of progenitors in a ventral midline domain dorsal to the floor plate (Chapter 3). However the morphogenesis of the hindbrain is disrupted in *mindbomb* mutants and it is impossible to recognise distinct analogous domains of proliferation by analysis of cell cycle markers.

In wild type embryos the expression of GFAP is largely co-incident with the extent of the dorsal ventricular zone at 36 and 48hpf and many GFAP +ve cells co-express markers of the cell cycle (Chapter 3). In order to see if there were cells with radial glial characteristics in *mindbomb* I stained cells with anti-GFAP although it had previously been reported that there was little or no expression of glial markers in the mutant's hindbrain (Jiang et al., 1996). At 36 and 48hpf I could see GFAP +ve cell bodies in the *mindbomb* hindbrain and in transverse sections cut through the hindbrain at both stages it could be seen that these congregated in the dorsal part of the tissue and projected long associated fibres towards the ventral midline (Figure 6.7). This suggested that these cells had a radial glial identity and that they accounted for at least some of the non-neuronal progenitor cells seen in the analysis of the cell cycle markers in the mutant.

Other non-neuronal in mindbomb cells may belong to an oligodendrocyte lineage

Some non-neuronal cells could be seen in *mib*/HuC-GFP +ve embryos co-stained with TR Bodipy ceramide in a domain above the notochord near the ventral midline of the neuroepithelium (Figure 6.8A). In the wild type non-neuronal cells in this region are a likely source of oligodendrocyte progenitors (Brosamle and Halpern, 2002). Furthermore individual cells were seen in *mib* embryos stained with Bodipy 505/515 in tissue that

looked like the white matter composed of axonal tracts (Figure 6.8 B) where oligodendrocytes are known to differentiate.

In order to further investigate whether there were oligodendrocytes in *mindbomb* mutants the embryos were grown up to 5 days post fertilisation (dpf) when oligodendrocytes are known to have started differentiating in the wild type (Brosamle and Halpern, 2002). Toludine blue sections were cut through the hindbrain at 5dpf in wild type and mutant embryos. In the wild type embryos at 5dpf many cell bodies were visible within the white matter (Figure 6.9 A) making them likely candidates to be oligodendrocytes. However, in the *mindbomb* mutant the distinction between the grey matter and the white matter is very ambiguous at this stage (Figure 6.9 B) meaning that it was impossible to judge whether cells might be oligodendrocytes or not by their position alone. To pursue this matter further I tested whether axons in the *mindbomb* hindbrain were myelinated.

Myelinating oligodendrocytes exist in the mindbomb hindbrain at 5 dpf

In the absence of a reliable and specific molecular marker of differentiated oligodendrocytes the most stringent assay for the presence of oligodendrocytes was a test for myelination, which has been observed in the wild type zebrafish hindbrain from 4 days post fertilisation (Brosamle and Halpern, 2002).

I grew up *mib* embryos to 5 days post fertilisation (dpf) and checked for evidence of myelination by transmission electron microscopy (TEM). At relatively low power magnification examples could be seen of axons in the white matter that seemed to be surrounded by a darkly stained band in both wild type (Figure 6.10 A) and mutant specimens (Figure 6.11 A). At higher power magnification of these specimens it could be seen that these black stained bands surrounding axons were composed of tightly packed concentric sheaths of myelin. Many examples of these were seen in both wild type (Figure 6.10 B-D) and mutant white matter (Figure 6.11 B-D). This demonstrates that not only do non-neuronal cells exist in *mindbomb* embryos but also that they are capable of generating differentiated glia as well as neurons.

Figure 6.2. Neurogenic phenotype of *mindbomb* in the hindbrain.

A + B show maximum intensity projections of the HuC-GFP +ve population in the hindbrain at 15hpf in the wild type (A) and *mindbomb* mutant (B). At this stage very few HuC-GFP +ve neurons have differentiated. In the mutant there are a clear excess of HuC-GFP +ve cells at this stage especially in the region that corresponds to rhombomere 4 (highlighted by the arrowed lines in B). The excess of neurons in this region give rise to a morphologically distinct bump in the hindbrain from this stage of development. Scale bars = 50μm.

C+D show maximum intensity projections of the HuC-GFP +ve population in the hindbrain at 36 hpf in the wild type (C) and *mindbomb* mutant (D). At this stage a very stereotyped arrangement of neurons is seen in each rhombomere in the wild type and the position of the midline (arrowhead) is obvious as a region devoid of neurons. However in the mutant the arrangement of neurons is totally disrupted and there is no clear midline seam in the tissue (position of arrowhead). Nonetheless the anterior posterior length of the hindbrain is very similar in the wild type and mutant as is indicated by the distance between the mid-hindbrain boundary and the lateral line ganglion indicated in each image by the arrowed lines. Scale bar = 100μm.

E+F show single confocal transverse sections through wild type (E) and *mindbomb* (F) hindbrains that have been stained with anti acetylated tubulin at 48hpf. In the wild type there is a very distinct arrangement of the axonal tracts that are strongly labelled with this antibody. Wild type hindbrain commissural neurons project into a tract (arrow) that crosses the embryonic midline ventral to the floor plate. Several tracts of axons (arrowheads) running along the anterior posterior axis i.e. through this section can be seen to lie just ventral to the commissural tract at several positions from the midline. In the mutant (F) the arrangement of axonal processes is very disrupted and the lack of a clear midline is obvious. No distinct commissural neuron tracts were ever obvious in the mutant. However, tracts of fibres (arrowheads) that run along the anterior posterior axis through the section can also be seen in the ventral part of the tissue. Scale bar = 50μm.


A
15hpf wt
B
15hpf *mib*
C
36hpf wt
D
36hpf *mib*
E
48hpf wt
F
48hpf *mib*

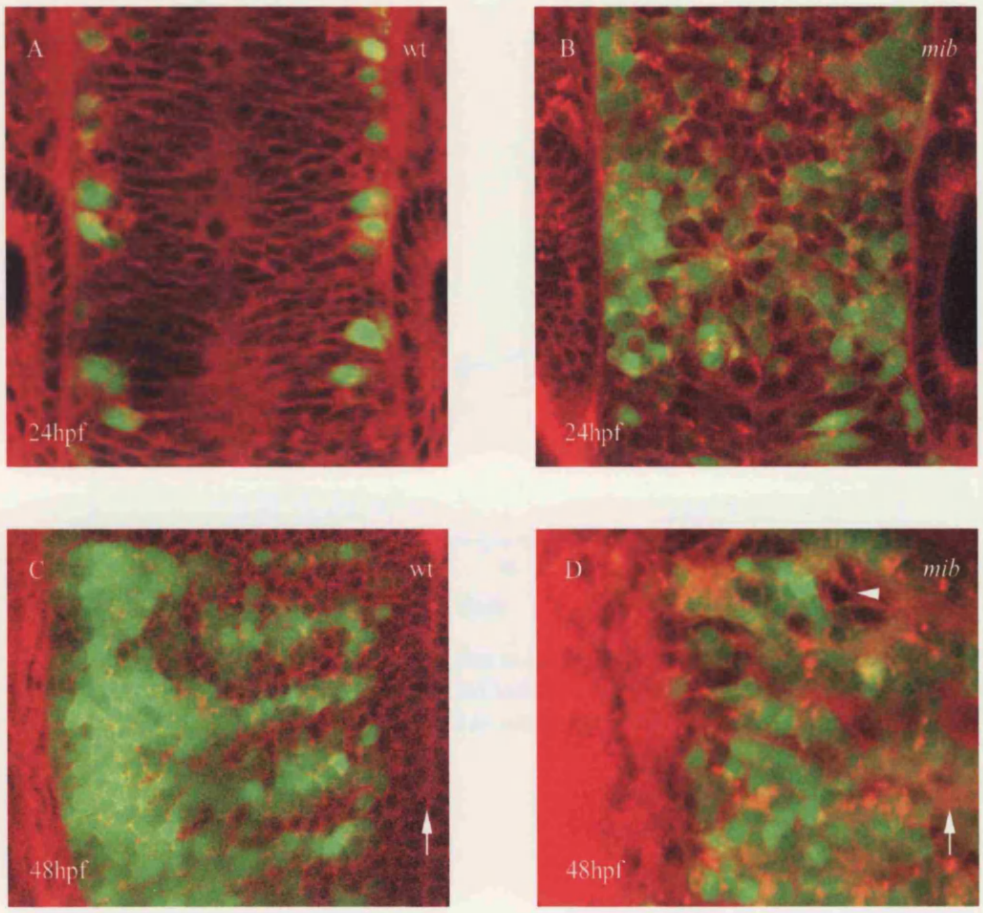

Figure 6.3. Non-neuronal cells exist in the *mindbomb* mutant.
A + B show single confocal sections through the living hindbrain at 24hpf of a wild type (A) and a *mindbomb* (B) embryo. The outline of all cells is show by Texas red bodipy ceramide (red) and the HuC-GFP +ve neurons are shown in green. Non HuC-GFP +ve cells exist in *mindbomb*.
C + D show single confocal sections through the living hindbrain at 48hpf of a wild type (C) and a *mindbomb* (D) embryo. Only one half of the midline (arrows) is shown and the figures show about two rhombomeres along the A-P axis. The outline of all cells is show by Texas red Bodipy ceramide (red) and the HuC-GFP +ve neurons are shown in green. Non HuC-GFP +ve cells exist in *mindbomb* (e.g. arrowhead) at this stage of development also.

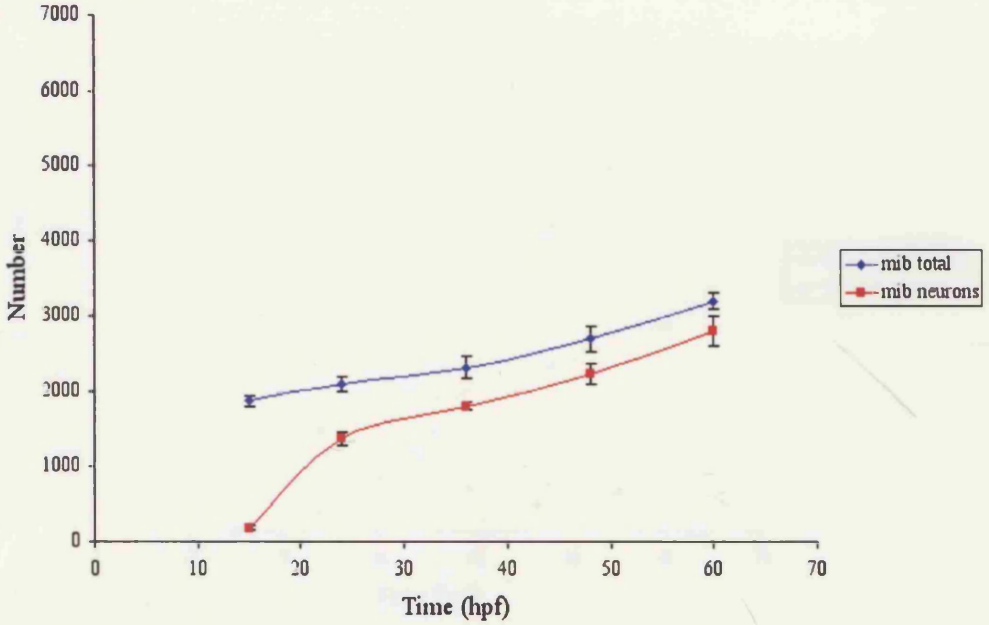

Graph 6.1. Total cell number and neuron number in *mindbomb*.
Graph shows the total cell number in (blue line) and the total HuC-GFP +ve neurons (red line) in the equivalent domain as rhombomeres 4+5 in *mindbomb* embryos. Error bars indicate the standard deviation either side of the mean.

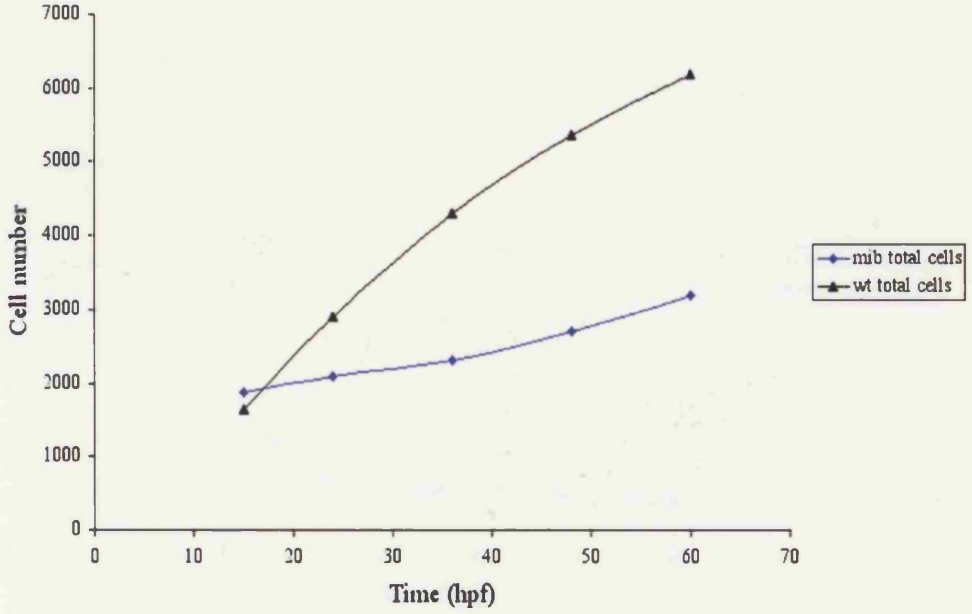

Graph 6.2. Comparison of total cell number in wild type and *mindbomb* embryos.
This graph shows that the total number of cells is similar in wild type (black line) and mutant (blue line) at 15hpf but that the by 60hpf there are about twice as many cells in rhombomeres 4+5 in wild type as in the mutant.

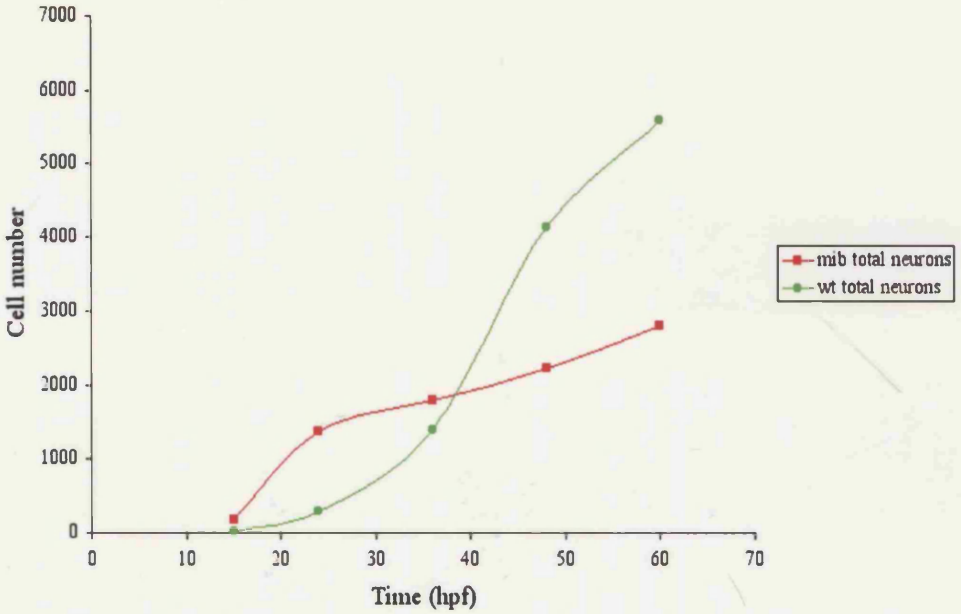

Graph 6.3. Comparison of HuC-GFP +ve neurons between wild type and *mindbomb* mutants. This graph shows that rhombomeres 4+5 in mindbomb (red line) have many more neurons at 24hpf than the wild type but that despite increasing in number until 60hpf eventually hab about half as many neurons as the wild type.

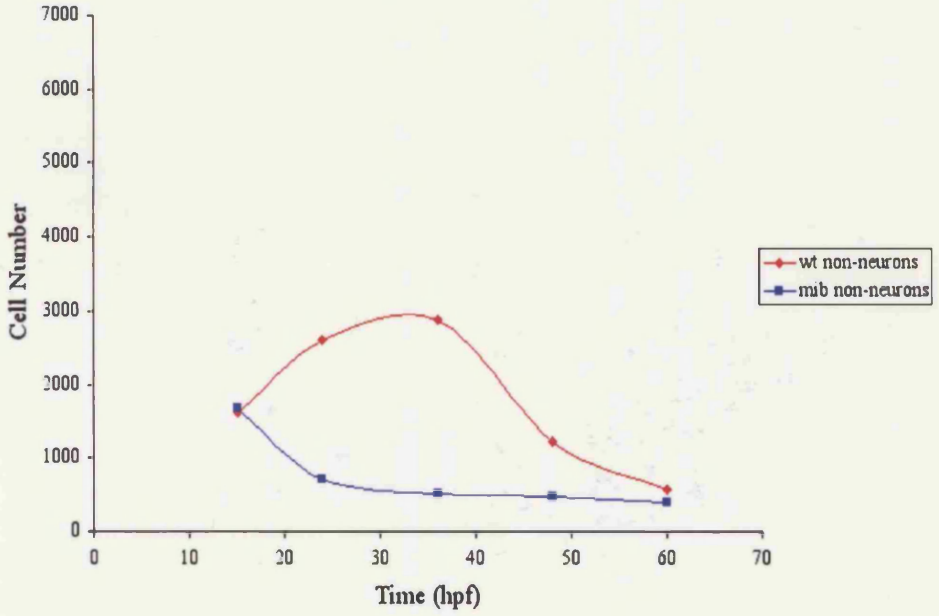

Graph 6.4. Comparison of non-neuronal number between wild type and *mindbomb* mutant embryos This graph highlights the fact that the number of progenitors in mindbomb (blue line) decrease dramatically after 15hpf whilst the number in wild type increase (red line). However as neurons are generated in the wild type the number of non-neurons decrease again so much so that by 60hpf the number of non neuronal cells between mutant and wild type varies little.

Figure 6.4. Non-neuronal cells express cell cycle markers in *mindbomb* mutants.

All images are single confocal sections. A-F are transverse views of the hindbrain. G+H are parasaggital sections through the spinal cord.

A shows a wild type HuC-GFP +ve embryo at 36 hpf that was pulse labelled with BrdU 15 minutes prior to fixation. The BrdU +ve cells (red) exist in a T shaped ventricular zone outside the HuC-GFP domain.

B shows a *mib*/ HuC-GFP +ve embryo at 36 hpf that was pulse labelled with BrdU 15 minutes prior to fixation. BrdU +ve cells (red) are seen in the neuroepithelium (e.g arrowheads) and are not also HuC-GFP +ve (green).

C+D show a *mib*/HuC-GFP +ve at 36hpf that have been stained with the mitotic marker pH-3. C shows two cells that express pH-3 (red) and D shows the same section but without the red channel and demonstrates that the two cells are clearly outside the HuC-GFP domain (green).

E shows a wild type HuC-GFP +ve embryo at 48 hpf that was pulse labelled with BrdU 15 minutes prior to fixation. A small number of BrdU +ve cells (red) are seen in the midline region of the tissue.

F.shows a *mib*/HuC-GFP+ve embryo at 48hpf that was pulse labelled with BrdU 15 minutes prior to fixation. BrdU +ve cells (red) are seen in the neuroepithelium (e.g. arrowheads) and are not also HuC-GFP +ve (green).

G shows a parasaggital view of the wild type HuC-GFP +ve spinal cord at 36 hpf. The arrowed line indicates the direction of the anterior- posterior (A-P) axis. BrdU +ve cells are shown in red (e.g. arrowheads) within the spinal cord at this stage.

H shows a parasaggital view of the *mib*/HuC-GFP +ve spinal cord at 36 hpf. The arrowed line indicates the direction of the anterior- posterior (A-P) axis. BrdU +ve cells are shown in red (e.g. arrowheads) within the mutant spinal cord. This is in contrast to the published account of this mutant that suggested that the entire spinal cord was composed of neurons by 24hpf.
All scale bars = 50 μm

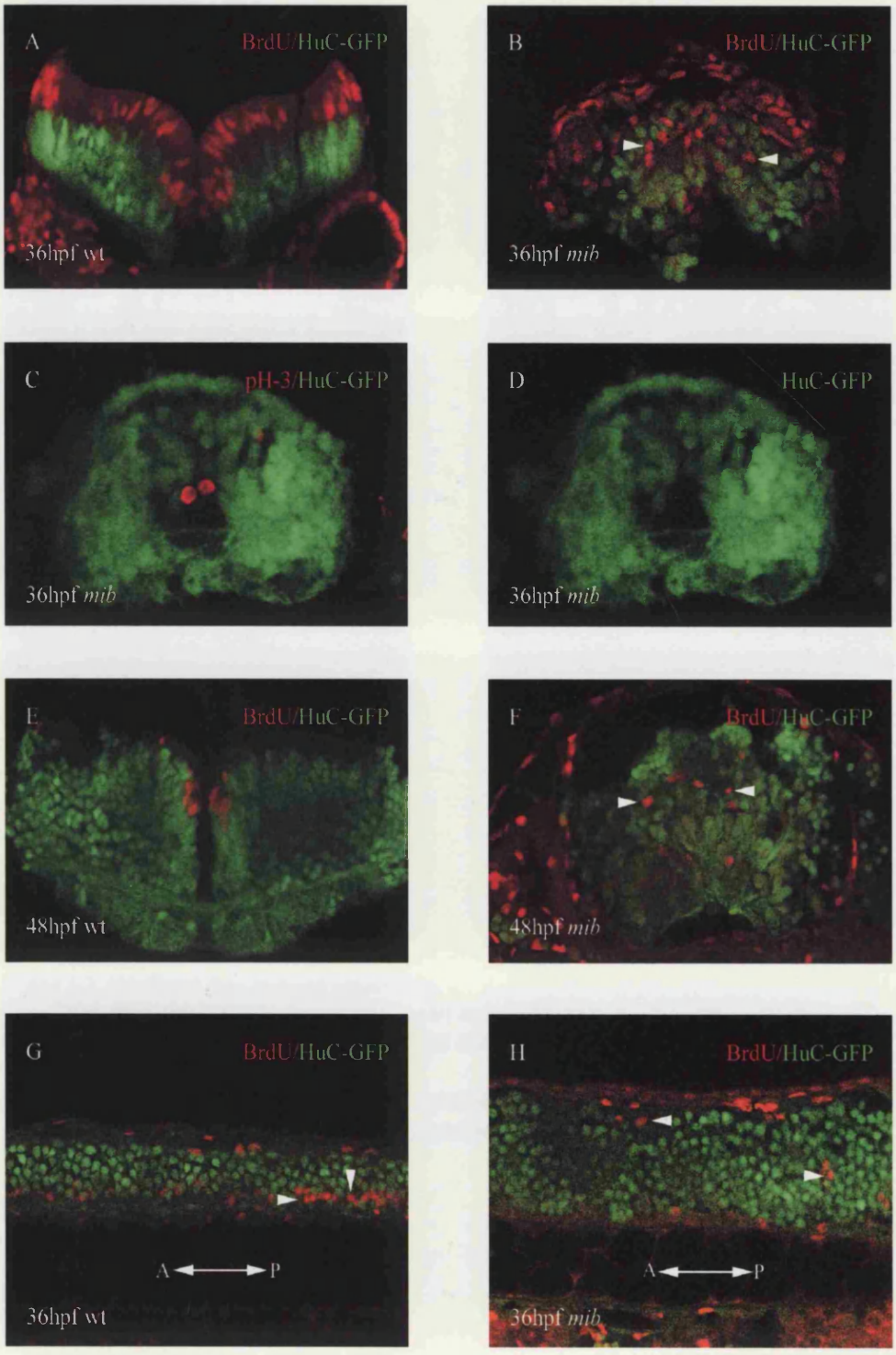
A
BrdU/HuC-GFP
36hpf wt
B
BrdU/HuC-GFP
36hpf mib
C
pH-3/HuC-GFP
36hpf mib
D
HuC-GFP
36hpf mib
E
BrdU/HuC-GFP
48hpf wt
F
BrdU/HuC-GFP
48hpf mib
G
BrdU/HuC-GFP
A
P
36hpf wt
H
BrdU/HuC-GFP
A
P
36hpf mib

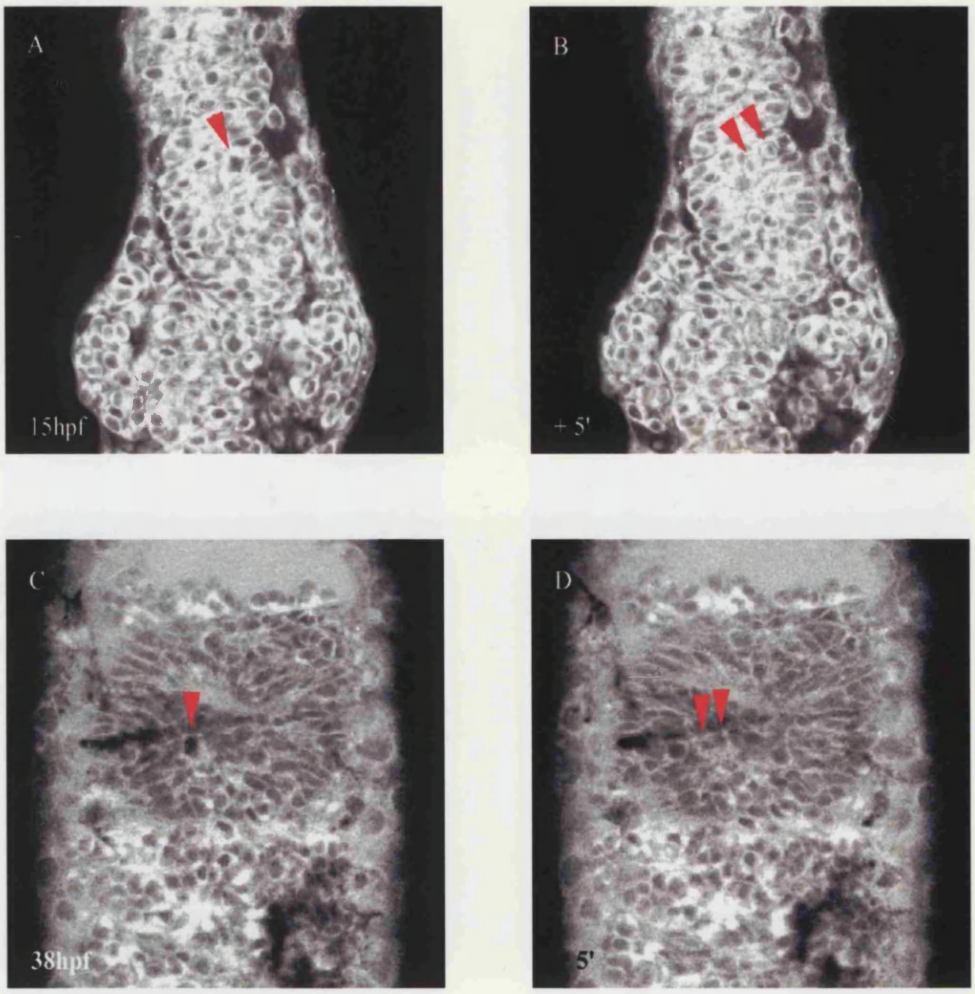

Figure 6.5. *mindbomb* cells undergo cytokinesis.
This figure shows consecutive time frames (A+B) and (C+D) from two time-lapse sequences of Bodipy 505/515 labelled mindbomb embryos. All images are single horizontal confocal sections with anterior to the top.
A+B shows a cell (red arrowhead) undegoing cytokinesis at 15hpf.
C+D shows a cell (red arrowhead) undergoing cytokinesis at 38hpf.

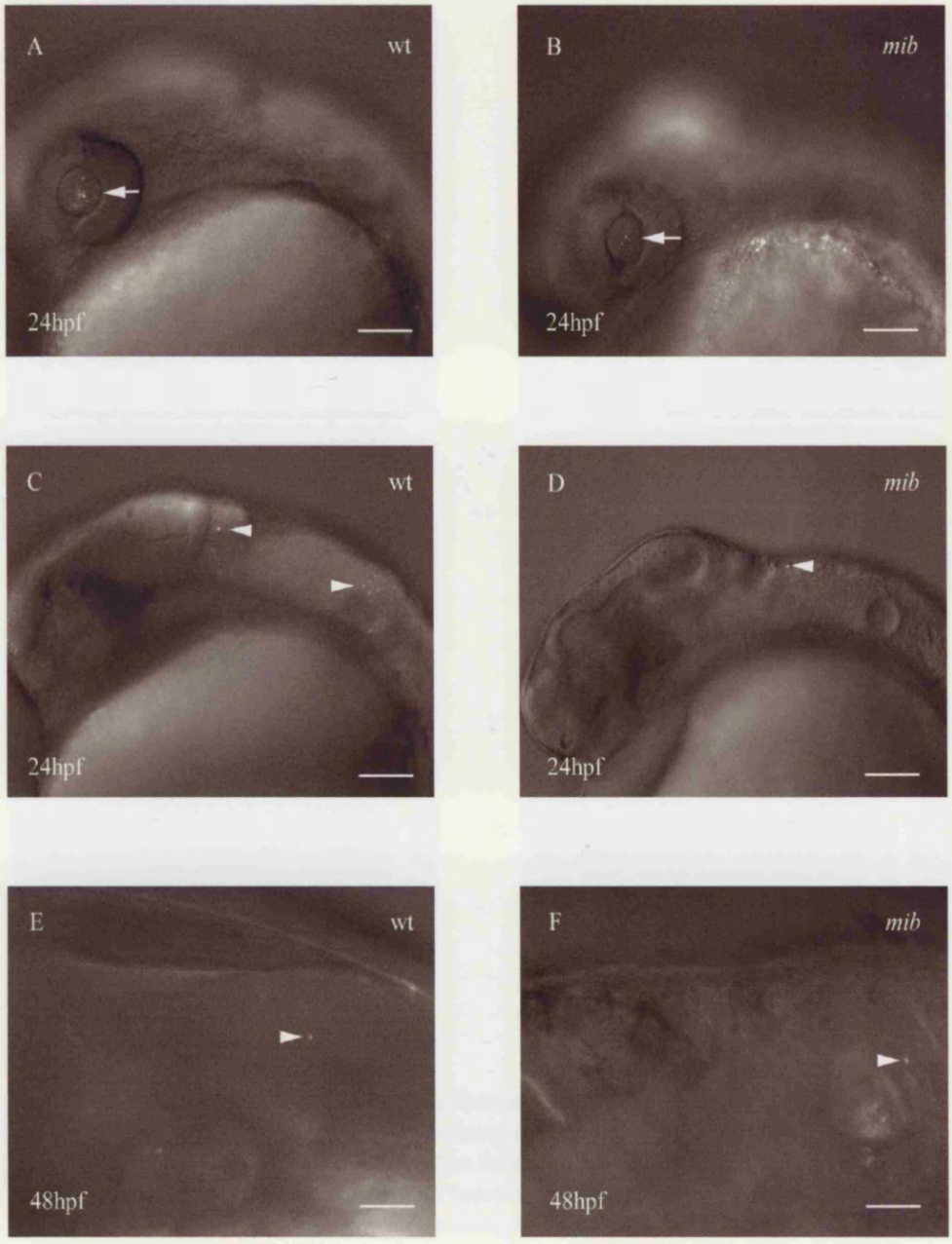

Figure 6.6. Cell death in the wild type and the *mindbomb* mutant.
Cell death was analysed in the living embryo by analysing acridine orange labelled apoptotic corpses.
A and B show that acridine orange labels corpses in the lens (arrow) where cell death is expected in both the wild type and mutant. Scale bars = 100μm
C and D show that very few apoptotic corpses (arrowheads) exist in either the wild type (C) or mutant (D) at 24hpf. Scale bars = 100μm
E and F show that there are even fewer apoptotic corpses (arrowheads) exist in the wild type at 48hpf than at 24hpf and still very few corpses in the mutant hindbrain (F arrowhead). Scale bars = 50μm

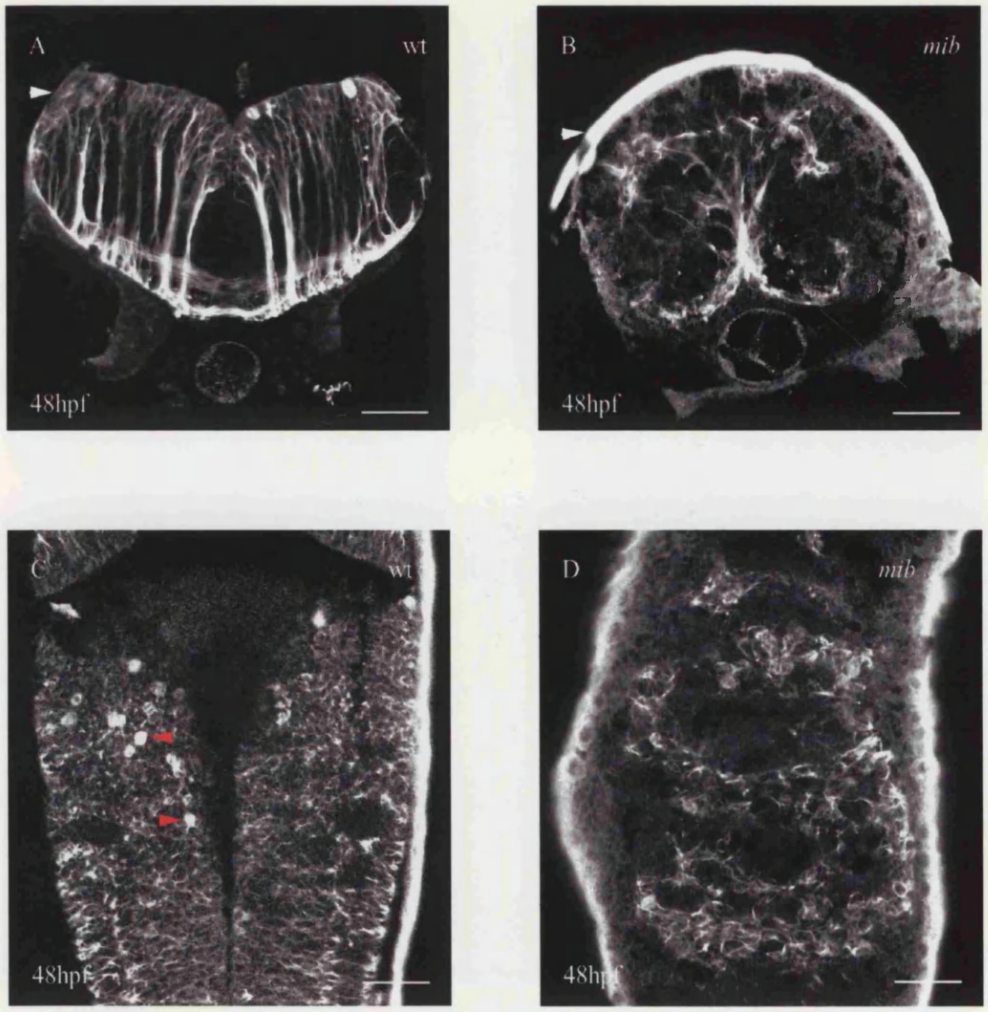

Figure 6.7. GFAP expression in the *mindbomb* mutant.
A+B show single confocal transverse sections through the hindbrain at 48hpf in the wild type and mutant respectively. In both cases the cell bodies lie towards the dorsal, top part of the tissue and extend long processes ventrally although their trajectory is disrupted in the *mindbomb* embryo. C+D show single confocal horizontal sections through the hindbrain at the level of where the GFAP +ve cell bodies lie. The approximate level of where the horizontal sections have imaged are shown by arrowheads in A and B respectively. In the wild type (C) GFAP +ve cell bodies cover the entire ventricular surface. Some cells (red arrowheads) are more storngly labelled relative to others. The significance of this was pursued by another student in the Clarke lab. In the mutant tissue the clustering of these cell bodies is discontinuous and disorganised. All scale bars = 50μm.

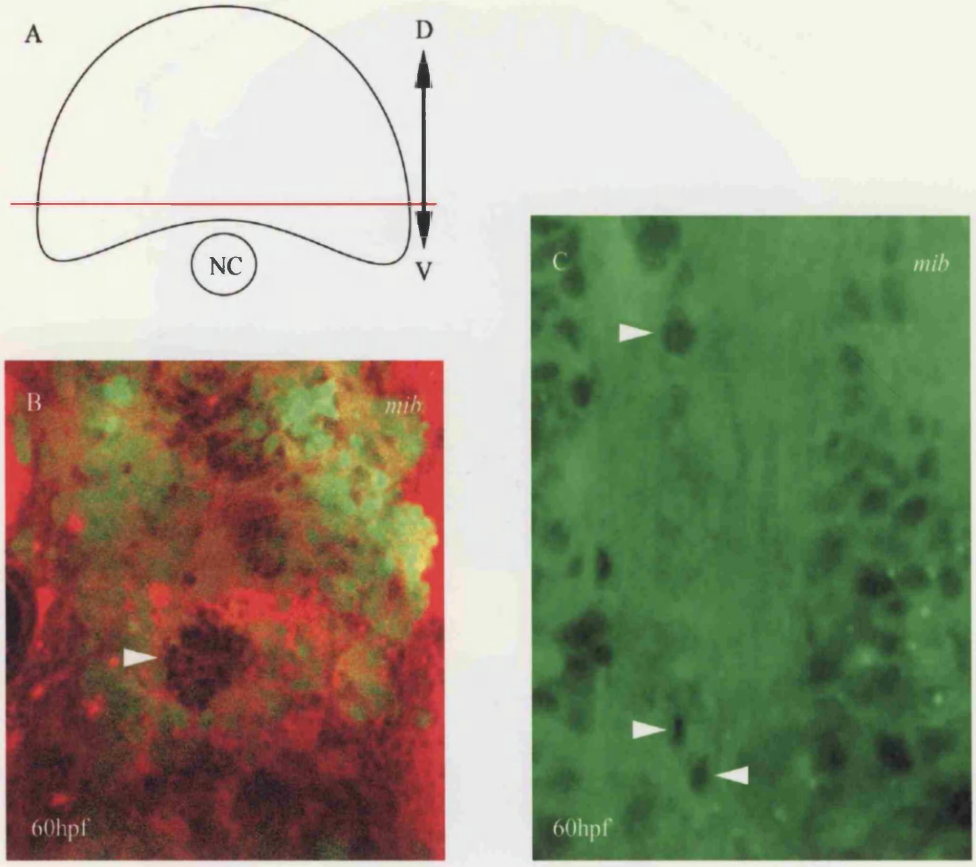

Figure 6.8. Non-neuronal cells in the ventral hindbrain and white matter of *mindbomb* mutants.
A is a schematic representation of a transverse section cut through the hindbrain of the *mindbomb* mutant at 60hpf. The orientation of the dorso-ventral (D-V) axis is shown by the arrowed line. The red line indicates the level at which the horizontal sections shown in B and C were taken. NC= Notochord.
B shows a confocal horizontal section through the living *mindbomb* hindbrain at 60hpf at the D-V level indicated in A. Cells that are stained with TR Bodipy ceramide (red) but are not HuC-GFP +ve (green) are found in the ventral hindbrain, often in clusters e.g. arrowhead. Anterior is to the top of this image.
C shows a confocal horizontal section through the living *mindbomb* hindbrain at 60 hpf at the D-V level indicated in A. Bodipy 505/515 negative nuclei (arrowheads) are shown within the ventral white matter. Anterior is to the top and the white matter can be seen to run primarily along the anterior posterior axis.

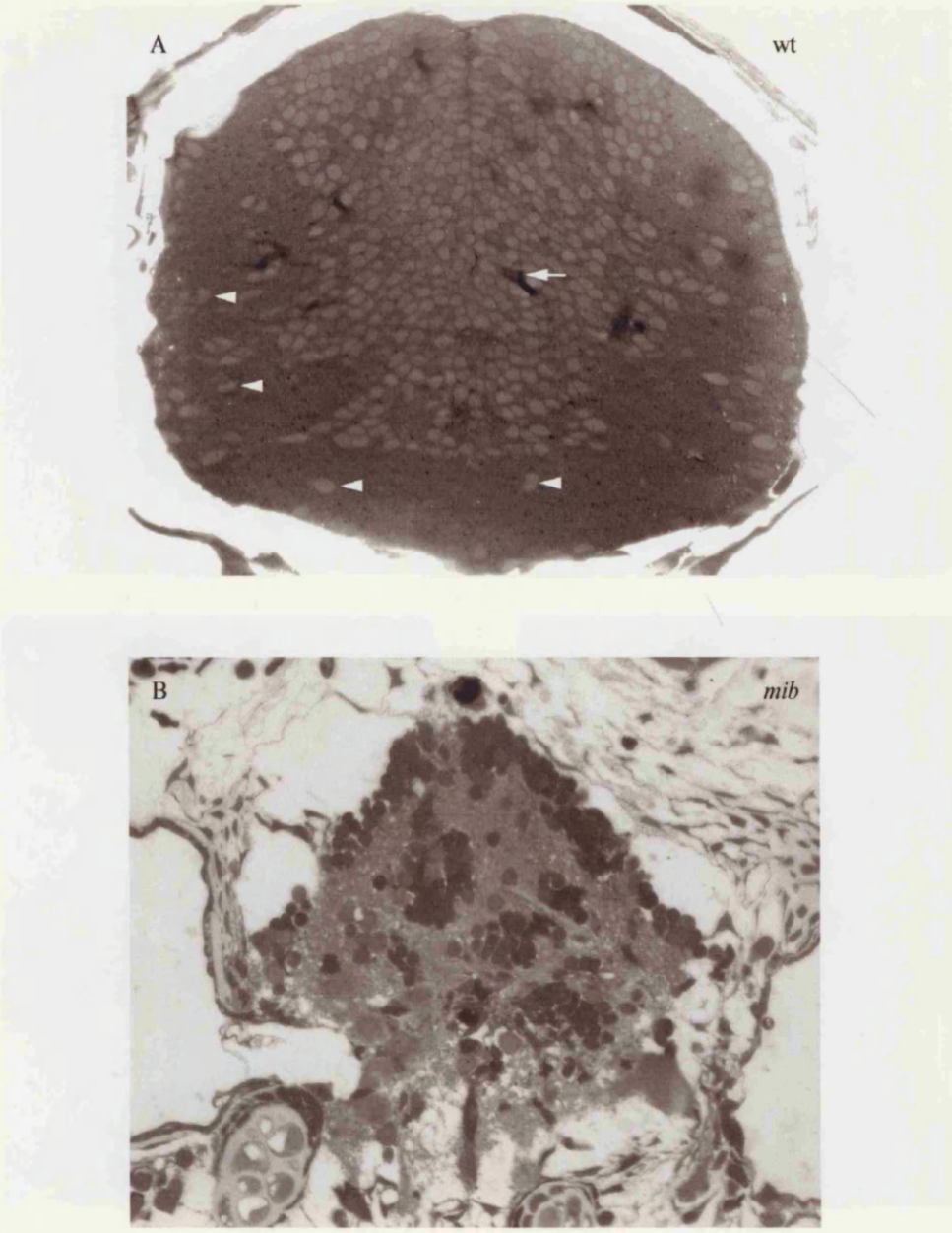

Figure 6.9. Organisation of grey and white matter in wild type and *mindbomb* embryos at 5 dpf.
A shows a Toludine Blue stained one micron thick transverse section through the hindbrain of a wild type embryo at 5 days post fertilisation. Dorsal is to the top. Cells (e.g. arrowheads) are visible within the darkly stained white matter. Darkly stained blood vessles (e.g arrow) run throughout the grey matter of cell bodies are also visible. There is a distinct separation between cell bodies and white matter in the wild type.
B shows a similar section through the *mindbomb* hindbrain at 5dpf, with dorsal to the top. In the mutant at this stage the integrity of the neuroepithelium is severely compromised. Cell bodies are darkly stained here and are interspersed in a disorganised fashion with more lightly stained white matter although there is an accumulation of cell bodies in the dorsal part of the neuroepithelium. There is no membrane or sheath surrounding the neuroepithelium in the mutant at this stage of development.

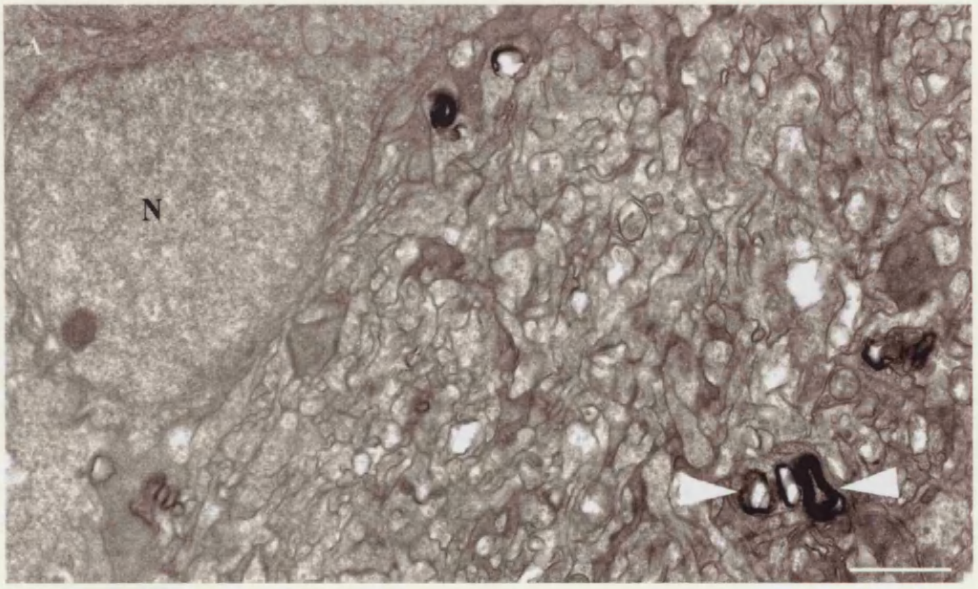

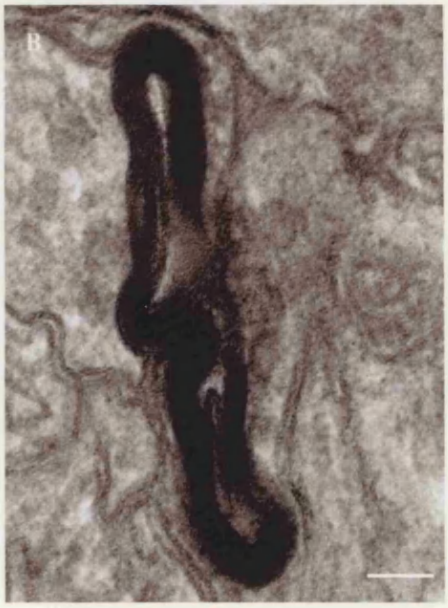

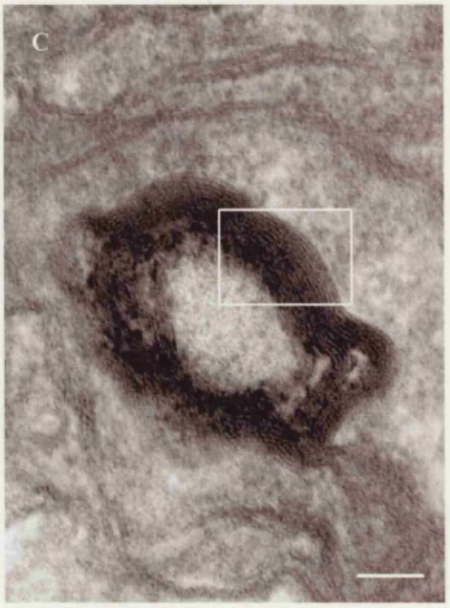

Figure 6.10. Myelination in wild type at 5dpf. A is a low power TEM section of the wild type white matter at 5 dpf. A nucleus is shown by the letter N and arrowheads point to myelinated axons. Scale bar = 1 micron. B+C are higher magnification views of myelinated axons. Scale bars = 50nm D is a higher magnification view of the box highlighted in C and shows multiple wraps of compact myelin. Scale bar = 20nm.

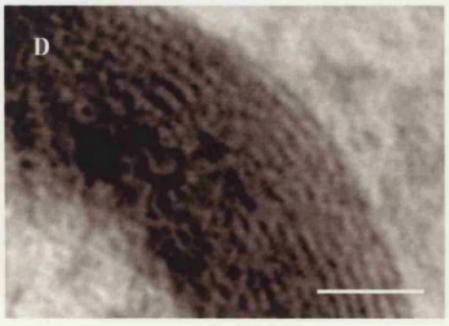

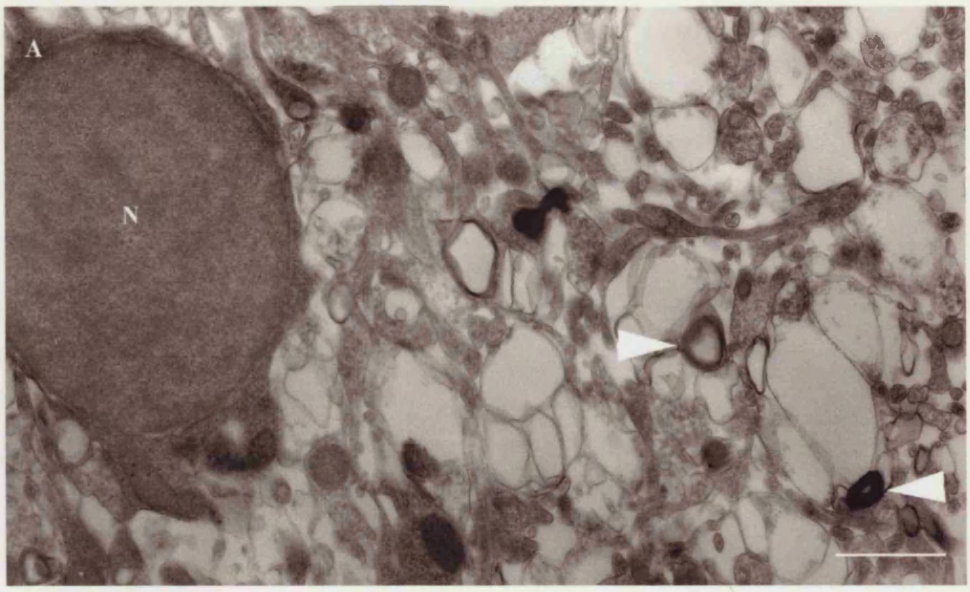

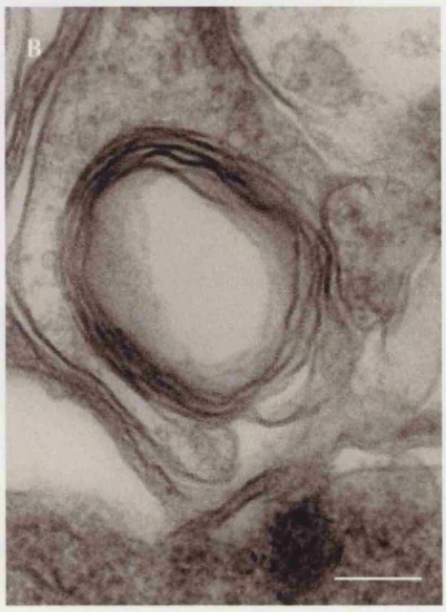

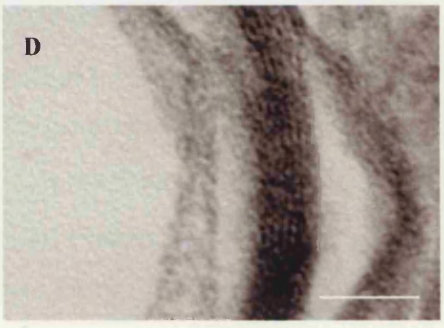

Figure 6.11. Myelination in *mind bomb* at 5dpf. A is a low power TEM section of the *mib* white matter at 5 dpf. A nucleus is shown by the letter N and arrowheads point to examples of myelinated axons. Scale bar = 1 micron. B+C are higher magnification views of myelinated axons. Scale bar = 100nm. D is a higher magnification view of the box highlighted in C and shows multiple wraps of compact myelin. Scale bar = 50nm.

Discussion

Previous studies have shown that *mindbomb* is a neurogenic mutant that is defective in Notch Delta mediated lateral inhibition. The phenotypic consequence of this mutation in the central nervous system is the appearance of a dramatic excess of early differentiating neurons. The theory to explain this phenomenon is that every cell that becomes competent to differentiate as a neuron during development does so because the mechanisms that normally inhibit them from doing so are defective in the mutant (Itoh et al., 2003). It was also suggested that all cells in the mutant spinal cord and perhaps the entire nervous system have differentiated as neurons by 24hpf (Itoh et al., 2003; Chitnis, pers. comm.). The results presented in this chapter strongly disagree with this latter assertion. I have shown that non-neuronal cells exist throughout the development of the *mindbomb* CNS and that mature glia are generated in this mutant. Although the vast majority of this work was carried out in the hindbrain I have also shown evidence that progenitor cells remain well after 24hpf in the *mindbomb* spinal cord which is a direct contradiction of published work (Itoh et al., 2003).

The non-neuronal cells in mindbomb may never be competent to make neurons

My observations about the phenotype of the *mindbomb* embryo raise important considerations about the competence of progenitor cells to make neurons and mature glia. Cell competence is defined as "the ability of a cell to respond to a cue or set of cues to produce a defined outcome," within the normal tissue environment of the cell's development (Livesey and Cepko, 2001). The assertion that all cells in the *mindbomb* CNS differentiate as neurons by 24hpf implies that all of these cells are competent to differentiate in the wild type but that are only inhibited from doing so by Notch Delta mediated lateral inhibition. My analysis has shown that non-neuronal cells exist in *mindbomb* and therefore conclude that these cells were never competent to make neurons because if they were competent to differentiate they would have done so in this mutant.

My results indicate a temporal difference in the competence of cells to differentiate between the hindbrain and the spinal cord. There is a profound excess of neurons visible in the spinal cord neural plate by 11hpf in the regions that normally correspond to the domains of primary neurogenesis in the wild type. However in the hindbrain the neurogenic phenotype is not obvious until 15 hpf and even then only accounts for 10% of

the total cell number (Graph 6.1). This more than likely reflects the difference in the time of onset of neurogenesis in the wild type embryo between the hindbrain and the spinal cord. A set of primary neurons leave the cell cycle soon after gastrulation in the spinal cord and account for a considerable proportion of neural plate cells (e.g. Hartenstein, 1989, Chitnis et al., 1995, Itoh et al., 2003). In contrast I have shown that the relative number of early differentiating cells in the hindbrain is small (Chapter 3). This difference is also reflected in the relative number of cells that seem to express proneural and neurogenic genes in the zebrafish spinal cord and hindbrain (e.g. Blader et al., 1997; Haddon et al., 1998). It is possible that this difference in cells' competence to differentiate as neurons between the early hindbrain and spinal cord neural plate correlates with an extra proliferative division in the hindbrain neural plate that might not take place in the spinal cord. I have seen in my quantitative analysis that the total cell number in the hindbrain does not vary much between wild type and mutant at 15hpf (Graph 6.2). Considering that most cells in the wild type hindbrain have undergone one round of division by this stage (Kimmel et al., 1994; Chapter 5) it is reasonable to assume that the same is also true in the mutant. On the other hand, the neurogenic phenotype in the mutant spinal cord is observed much earlier meaning that cells may not have had time to undergo any division in the neural plate, although this remains to be demonstrated. The fact that cells of the *mindbomb* hindbrain undergo a round of division before differentiating implies that most cells of the hindbrain are not competent to differentiate during early neurogenesis.

Neuronal and glial lineages may diverge early in development.

The fact that mature oligodendrocytes develop in a tissue that is defective in lateral inhibition raises the possibility that the progenitors that gave rise to them never passed through a state of competence to differentiate as neurons. If they had done so they would have differentiated into neurons, as there is no lateral inhibition mechanism in place in the mutant embryo to stop them from doing so. This suggests that these cells may descend from a restricted glial progenitor. It is likely that very few cells in the hindbrain are competent to differentiate during the first round of division in the neural plate. However, based on the number of neurons that differentiate in the mindbomb hindbrain by 24hpf it is clear that the majority of progenitor cells become competent to differentiate between 15 to 24 hpf i.e. during the second cell cycle in the neuroepithelium. If a glial

restricted progenitor exists it is likely to diverge from neural competent progenitors during this round of division at latest. A lineage analysis would be necessary to uncover if and when such a glial restricted progenitor might emerge. However, the number of oligodendrocyte progenitors is very small at the end of the main period of embryogenesis, with about 10-20 cells existing per rhombomere. This fact accounts for the reason that oligodendrocyte lineage was not analysed in detail in my lineage analysis. It is clear from work in other vertebrate systems that the oligodendrocyte progenitors that remain at the end of embryogenesis give rise to clones largely composed of oligodendrocytes (Parnavelas, 1999) but it is less clear when in development these progenitors diverged from a lineage that also generated neurons. Retro-viral clonal analysis in the chick has shown that mixed clones of oligodendrocytes and motor neurons are common when chick spinal cord progenitors are infected several rounds of division before the appearance of motor neurons (Leber et al., 1990). This point is important. It is possible that for the first few rounds of division in this clonal analysis progenitors were not competent to differentiate as neurons or oligodendrocytes and consequently that most divisions were simply multiplicative and that neuronal or glial restricted lineages did not emerge until later. It is still possible that restricted progenitors arose before motor neurons were generated but this would not be obvious in this study due to the time at which the first progenitor was infected. The period of multiplicative divisions in this system would correlate with the first round of division in the zebrafish hindbrain. It is my prediction that if a lineage study were carried out in the zebrafish hindbrain, cells labelled at the neural plate stage and analysed, for example at 5dpf, would generate mixed clones of motor neurons and oligodendrocytes as in the previous study. In contrast, I think that if cells were labelled during the second cell cycle in the neuroepithelium i.e. between 15 and 24hpf, when a majority of cells acquire the competence to generate neurons, that no mixed clones of oligodendrocytes and neurons would be observed.

The idea that oligodendrocytes and motor neurons are derived from a common progenitor, however, has recently been given support based on genetic analysis of a set of progenitor cells expressing a class of bHLH transcription factors. It is clear that oligodendrocytes and primary motor neurons both originate in the ventral spinal cord (e.g. Pringle et al., 1998; Park et al., 2002) and have now been shown to stem from a domain of progenitor cells that express the transcription factor, Olig 2 (Zhou et al., 2000; Zhou and Anderson, 2002; Park et al., 2002). In mammalian species an additional

transcription factor Olig 1 specifies a domain of oligodendrocyte and motor neuron progenitors in more rostral tissue (Lu et al., 2000b; 2002). Targeted knock down or knockout of Olig 2 in zebrafish and mouse give rise to animals with no oligodendrocyte progenitors or somatic motor neurons in the spinal cord (Park et al., 2002; Lu et al., 2002) and double knockout of Olig 1 and Olig 2 in the mouse results in a lack of oligodendrocyte progenitors and motor neurons throughout the whole embryo. However when Olig 2 is ectopically expressed by itself, for example in the dorsal spinal cord it does not give rise to ectopic motor neurons or oligodendrocytes. To give rise to ectopic motor neurons Olig 2 overexpression requires the ectopic co-expression of neurogenin 2 suggesting that these bHLH transcription factors act together to specify a motor neuron fate (Mizuguchi et al., 2001). Similarly overexpression of Olig 2 requires co-expression of Nkx 2.2 to generate ectopic oligodendrocytes (Sun et al., 2001; Zhou et al., 2001) again showing that the effect of Olig 2 gene expression requires additional factors to specify oligodendrocyte fate. These studies highlight that expression of the Olig transcription factors are necessary to determine a domain of progenitors with the competence to make either motor neurons or oligodendrocytes but that to actually adopt either specific cell fate these progenitors require the expression of additional and distinct transcription factors. There is no evidence from any of these studies that motor neurons and oligodendrocytes are necessarily derived from a single progenitor.

Retroviral clonal analysis in the chick spinal cord showed that oligodendrocytes and motor neurons are found in individual clones (Leber et al., 1990) but I have argued that restricted progenitors could have diverged early in the development of such clones before either cell type differentiated. To find out if neuronal and glial restricted progenitors diverged early or late in cell lineage isolated cortical progenitors were followed by time-lapse microscopy for up to seven days. It was found that glial restricted progenitors did not diverge from neural restricted progenitors until after the bulk of neurons were generated. In other words individual progenitors divided and made many progenitors that generated neurons and after several rounds of division then generated a progenitor that went on the produce only glia (Qian et al., 2000). How the behaviour of progenitor cells in culture reflects their behaviour in vivo is difficult to assess but it is interesting to note that in the aforementioned study that the temporal generation of neurons first and then glia observed in vivo was maintained in culture.

Tests of the theory

I have provided data and a model to explain it that is difficult to reconcile with the observations of progenitor cell behaviour in culture. I have suggested that cells that generate oligodendrocytes were never competent to make neurons and hence that neuronal and glial progenitors become restricted relatively early in neurogenesis before a majority of cells become competent to generate neurons, whereas the in vitro data suggests that they may be derived sequentially in the same lineage. It will be crucial in the future, therefore, to verify that all cells in the *mindbomb* neuroepithelium that are competent to make neurons really do so as predicted by the published reports of the *mindbomb* phenotype (Itoh et al., 2003). If some cells that are competent to become neurons can be inhibited from doing so by Notch Delta independent mechanisms then my conclusion that restricted neuronal and glial lineages must exist could be flawed. Overexpression of neurogenin in the hindbrain *mindbomb* embryos apparently generates tissue that is almost entirely composed of neurons (Itoh et al., 2003). It would be important to verify this finding, as a rigorous analysis of non-neuronal cells was not carried out in this initial study. In this overexpression study all cells should be forced to express neurogenin and should, in theory, then have the competence to generate neurons. This should mean that all of these cells would differentiate due to the lack of inhibition and that the entire neuroepithelium would become neuronal.

There is an additional experiment that may address the question of progenitor cell competence more directly. Zic genes are anti neurogenic transcription factors that are expressed in complementary regions to the proneural domains of the early frog spinal cord and thus are thought to limit the domains of early neurogenesis (Brewster et al., 1998). If the same is true in the zebrafish hindbrain then the following experiment could be attempted. Morpholinos (antisense oligonucleotides that block translation of mRNA) against the relevant zic genes should mean that all cells can express proneural genes and are thus competent to generate neurons. In a wild type this will likely generate extra neurons in a similar way to overexpression of neurogenin where the extent of the neurogenic phenotype is limited by the lateral inhibition mechanisms that still operate in the wild type tissue (Blader et al., 1997; Kim et al., 1997). However, if the relevant zic morpholino is injected into *mindbomb* embryos then all cells should differentiate as

neurons as there is no lateral inhibition to stop them from doing so. Again in this case one should not expect to see any evidence of non-neuronal cells or mature glia. If this result were obtained then this would provide compelling evidence that the mechanisms that generate glia in the wild type and indeed in *mindbomb* are related to a lineage that is separate from that that makes neurons.

It is possible of course that this scenario is an over simplification and that not all cells that express proneural genes in the *mindbomb* embryo necessarily differentiate as predicted. It is possible that additional Notch Delta independent mechanisms can prevent neural competent cells from differentiating. This would mean that my prediction that neuronal and oligodendroglial lineages must be separate could be incorrect. Therefore it will be essential to determine what modes of division underlie the generation of oligodendrocytes in the wild type and I believe that the zebrafish is ideally suited to such a study but that it would benefit hugely from the availability of a transgenic line that expressed GFP in oligodendrocytes and or their progenitors.

Chapter 7

General Discussion

The aim of thesis was to study neurogenesis in the zebrafish hindbrain (in case that wasn't clear up to now!).

In my first results chapter "Live imaging of progenitor cell behaviour and characterisation of zebrafish radial glia" I established the zebrafish hindbrain as a suitable system for the study of vertebrate neurogenesis and the imaging of dynamic cell behaviour in particular. In doing so I showed that cells of the early neural plate and neural keel is not a pseudostratified neuroepithelium as proposed by others (Schmitz et al., 1993). My observation shows that the structure of the early zebrafish neuroepithelium is more similar to that of the Xenopus neuroepithelium during neurulation where cells do not contact an apical and basal surface but exist in two distinct layers along the apico-basal axis that are in fact distinguishable on behavioural and molecular grounds (Hartenstein, 1989; Chalmers et al., 2002). However the zebrafish neural plate seems to be multi-layered as opposed to a simple bilayer.

I studied the morphology and dynamics of progenitor cell behaviour after neurulation and showed that once the neural rod and tube have formed that progenitor cells are always elongate and stretch right through the neuroepithelium from the ventricular surface to the pial surface. I found that progenitor morphology evolves through development such that progenitors eventually resemble radial glia. In addition I dispelled a myth that a morphologically distinct progenitor cell that is restricted within the ventricular zone exists during embryonic neurogenesis. My observation agrees with work published during the course of this thesis (Noctor et al., 2002) that showed that all progenitors in the mammalian cortex also stretch right throughout the neuroepithelium irrespective of the stage of development. In analysing the dynamics of progenitor cells during mitosis I noted that fluorescently labelled cells appear to withdraw all of their cytoplasm to the ventricular surface when undergoing cytokinesis. However I also presented data that for at least some cells a tiny membranous process may remain attached to the basal surface during cytokinesis in agreement with work also published during the course of this thesis (Miyata et al., 2001; Noctor et al., 2001; Das et al., 2003).

In this first results chapter I showed that progenitors undergo interkinetic nuclear migration until the ventricular zone is almost depleted of progenitors and that the position

of the progenitor's nucleus always remain within the ventricular zone. In addition I provided information about the development of the mantle zone and the localisation and morphology of progenitors late in neurogenesis and I also characterised zebrafish radial glia and showed that they are all located in a structure known as the glial curtain (Trevarrow et al., 1990) and that at least a subset of them have the properties of progenitor cells, in agreement with published data from mammalian systems (e.g. Hartfuss et al., 2000; Noctor et al., 2001).

In the second results chapter "Quantification of neurogenesis in the zebrafish hindbrain" I provided an in depth quantification of neurogenesis in two rhombomeres of the hindbrain as well as a concomitant description of the relative number of non-neuronal cells in these segments during the first three days of embryogenesis. I showed that very few neurons are produced in the hindbrain during the first day of development, which is in contrast to the spinal cord of fish and amphibians where a large number of primary neurons are born very early in development (Hartenstein, 1989, Gray et al., 2000). I calculated that the majority of neurons are born by the end of the second day of development. Furthermore I showed that by the end of the third day of development that the rate of neurogenesis has slowed down dramatically and that a relatively tiny number of non-neuronal cells are maintained for gliogenesis and further development. I used this analysis to make predictions of progenitor cell behaviour during neurogenesis and calculated that the majority of neurons ought to be generated from divisions that produce two neurons.

The third results chapter "In vivo analysis of cell lineage in the zebrafish hindbrain through multiple rounds of division" provided the main focus of this thesis where I documented the division modes of progenitor cells during neurogenesis. I showed that the vast majority of neurons arise following a division that generates two neurons and that asymmetric divisions that generate a neuron and a progenitor are comparatively rare. This further suggested that the decision to differentiate was made prior to terminal mitosis. I compared the results of my division mode analysis to a model (Cai et al., 2002) that was based on the fact that the decision to leave or re-enter the cell cycle was made after mitosis and found that my raw data was incompatible with this model indicating that the decision to re-enter the cell cycle was not made by chance and independently in daughter cells. This suggests that either the cell's lineage prior to mitosis plays a strong role in

determining the behaviour of cells after mitosis or that very strong environmental signals bias cells towards adopting similar fates. I showed that no progenitor underwent a stem cell like mode of division i.e. undergoing repeated rounds of asymmetric division. This was anathema to a popular model in mouse cortical development that predicts that such behaviour underlies cortical neurogenesis (e.g. Noctor et al., 2001). However it is possible that different strategies will be used during neurogenesis in different brain areas. In the mammalian cortex, a vast number of neurons have to be generated over a long period during which the embryo is protected inside the mother. In contrast a network of neurons that can underlie complex behaviour must be generated and functionally active by three days in the zebrafish when the animal becomes free living. Finally I showed that there was basically no correlation between the plane of progenitor cell division and the fate of daughter cells of an asymmetric division. Again this result contrasts one that has existed in the field for some time that absolutely linked plane of cell division with daughter cell fate (Chenn and McConnell, 1995).

In the final results chapter "Novel characterisation of the zebrafish neurogenic mutant, *mindbomb*" I attempted to provide just that and showed, in contrast to published data (Itoh et al., 2003), that non-neuronal cells exist throughout the development of the mutant. Upon characterisation of these non-neuronal cells over the first two days of development I observed that some had the properties of radial glial like progenitors, they expressed GFAP and cell cycle markers and were seen undergoing cytokinesis in time-lapse analyses. When non-neuronal cells were analysed at larval stages I saw that some cells in the mutant had characteristics of myelinating oligodendrocytes as axons in the white matter were surrounded by sheaths of myelin. I also observed that at 60hpf the overall number of non-neurons was very similar between mutant and wild type. These observations raised the possibility that cells that give rise to late non-neuronal cells and specifically mature glia descend from progenitors that were never competent to generate neurons. If such progenitors in the *mindbomb* embryo had ever been competent to make neurons they would have all differentiated because the mutant is defective in the lateral inhibition mechanism that prevents differentiation. This leads to a prediction that neuronal and glial restricted progenitors may diverge relatively early in neurogenesis and or that the mechanisms that generate mature glia do not rely on Notch Delta mediated lateral inhibition mechanisms.

In each results chapter I have provided discussion of the relevance of my observations in the field, therefore in this chapter I would just like to concentrate on discussing a few grey areas in the filed and speculate on the future of the zebrafish as a system for studying vertebrate neurogenesis.

The future

Despite a mammoth wealth of data existing in the field there are still massive gaps in our understanding of neural development. Some of the most prominent voids in our knowledge relate to the most basic descriptions of cell behaviour during neurogenesis and gliogenesis. These holes were hitherto unfilled due mainly to the limitations of the techniques being used and not the incompetence of those using them, despite the old adage about a bad worker always blaming his tools. Indeed many of the recent advances made in describing the behaviour of cells during neurogenesis have resulted almost directly from the development of new tools and techniques. Perhaps the single most important tool to emerge over the last decade or so, certainly in terms of cell imaging, has been the isolation and manipulation of the naturally fluorescent protein Green Fluorescent Protein (GFP) isolated from the jellyfish Aequorea Victoria. This protein and its variants have been modified to serve a multitude of functions and have been engineered to generate a plethora of transgenic reagents, the description of which is beyond the scope of this thesis (but for in depth reviews see Tsien, 1998 or Lippincott-Schwartz and Patterson, 2003).

The natural transparency of the zebrafish embryo makes it one of the most suitable platforms for utilising the imaging potential of transgenic GFP. Thus far the most striking use of transgenic zebrafish has been the creation of stable transgenic lines that express GFP in specific cells or tissues by driving its expression through the promoters of genes of interest. I had the advantage of being able to use the Islet 1-GFP line (Higashijima et al., 2000) and the HuC-GFP line (Park et al., 2001) for a variety of applications presented in this thesis. Without these tools I fear that this thesis would have looked a lot different. As more transgenic lines and constructs are generated, e.g. that express GFP in neuronal subclasses or that follow individual proteins, the chasm between our knowledge of the molecular and cellular bases of neruogenesis will be slowly be filled. The generation of multi-coloured reporters in transgenic lines will soon allow direct observation of cellular

and molecular interactions in the living embryo that could barely have been dreamed about even ten years ago.

It is in this uniting of the cellular and molecular basis of neurogenesis that I think the zebrafish may flourish most. I cannot honestly see how any of the other vertebrate systems are more suited to performing this wedding ceremony. The mouse will always be limited in terms of imaging potential by its inaccessibility, large size and opacity and despite its excellent reverse genetics I believe that the zebrafish will soon be an equally formidable genetic system. The zebrafish is more ideally suited to large scale forward genetic screens and the fruits of these are already clear and with the imminent completion of the zebrafish genome sequencing project reverse genetics will also become standard in zebrafish. Even now the development of Morpholino technology is forging great insights into many developmental processes. The accessibility and size of the zebrafish allows the development of many techniques for its manipulation including one particularly exciting one that has recently been applied to the zebrafish in the Clarke lab, focal electroporation. Using this technique charged molecules can be electroporated into single cells or small groups of cells at any time in the embryo or larva. This can include DNA and RNA constructs and morpholinos as well as simple fluorescent tracers and so on. This technique will allow unprecedented control over the genetic manipulation of cells in a vertebrate system and is only one of many that will help the zebrafish maintain its place amongst the elite vertebrate developmental systems.

In this thesis I have presented data that has begun to fill a lacuna in the field with respect to the behaviour of cells during neurogenesis. Despite uncovering a number of interesting phenomena there are many unanswered questions that still need to be addressed in the field.

Stealing from invertebrates

Much of what we have learned thus far about vertebrate neurogenesis has followed work pioneered in invertebrate systems. This has by and large been a fruitful exercise but in the analysis of cell lineage the transition of concepts from invertebrates to vertebrates has been very peculiar. Asymmetric divisions are an integral feature of much of invertebrate neurogenesis, most notably in Drosophila where the stem cell like neuroblast undergoes repeated rounds of asymmetric division in generating the nervous system. This strengthened unsubstantiated notions that asymmetric divisions must underlie vertebrate

neurogenesis as well. However, somewhere along the lines the definition and criteria for establishing a division as asymmetric became muddled. The standard definition of an asymmetric division in the vertebrate field has been to denote a division that generates a neuron and a progenitor (e.g. Mione et al., 1997; Noctor et al., 2001; Cai et al., 2002). Other divisions were labelled as symmetric, simply if they produced two neurons or two progenitors. Although it is clear that a division that produces a neuron and a progenitor is asymmetric I cannot think of any such division in the CNS neural lineages of the Drosophila. The irony of looking for repeated rounds of division that produce a progenitor and a neuron in the vertebrate cannot be overstated. For instance the archetypal asymmetric division, that of the Drosophila neuroblast, produces two progenitors and the divisions of the Sensory organ precursor, the other system from which much of our knowledge of the genetics of asymmetric division stems first produces two progenitors and then these two progenitors both produces two post mitotic cells. All of these divisions would be deemed symmetric by vertebrate definition.

I have found that most neurons in the zebrafish hindbrain are produced by divisions that generate two neurons. I have been careful not to label these divisions as symmetric because at present there is insufficient information about the molecular identity and indeed axonal trajectory of individual neurons in the zebrafish hindbrain to establish whether the sister neurons I have described are generally of a similar or distinct phenotype. Once such information is available it will be possible to assess the role of real asymmetric division in the vertebrate CNS.

Neurogenesis and the cell cycle

Another fundamental question that is unanswered in the field of neurogenesis is when the decision to leave the cell cycle is made with respect to the cell cycle itself. It is now accepted that the Delta-Notch signalling pathway acting through and regulating levels of proneural genes plays a role neuronal differentiation. The basic theory that explains this is called lateral inhibition with feedback and posits that in a field of cells expressing Delta and Notch, by chance a single cell expresses higher levels of Delta protein at one time and consequently activates the Notch pathway strongly in its neighbouring cells. This will reduce levels of proneural genes in these cells and inhibit them from becoming neurons, at least temporarily. These same cells also reduce their levels of Delta and hence there is less activation of Notch on the original cell and thus its levels of proneural genes

increase and this is thought to drive the differentiation programme (see review by Chitnis, 1999). It has always struck me that this model is too good to be true and a number of questions are still unanswered. For instance, when during the cell cycle can this apparently stochastic decision to differentiate be made and can a cell that has elevated levels of Delta and proneural genes go through a terminal division or does this trigger differentiation without further division?

It is generally assumed that once the decision to differentiate is made and a cell expresses high levels of Delta and proneural genes that it does not divide again. There are a number of reasons why this model is held in favour. Delta expressing cells don't incorporate BrdU and hence are thought to be post-mitotic (Henrique et al., 1995). The direction of Delta Notch signalling pathway is to inhibit differentiation in the cell that receives the signal and in neurogenic mutants where there is no inhibition of differentiation many more cells differentiate early in development relative to wild-type and do so perhaps too soon to have undergone a division (e.g. Itoh et al., 2003). Additionally, injection of a truncated form of Delta, that makes the protein inactive, into one cell of a two cell stage Xenopus embryo causes most cells on the injected side to differentiate as neurons very early in development because of a lack of lateral inhibition and does so perhaps too soon for cells to have undergone a terminal division (Chitnis et al., 1995).

In my opinion none of these arguments are particularly convincing by themselves. If embryos are left to develop for three hours after pulse labelling with BrdU then many BrdU +ve cells co-localise with Delta (Murciano et al., 2002). This shows that it is possible that Delta is expressed in cells before their terminal division. It is known that primary neurons in the wild type Xenopus are born following a single division within the neural plate soon after gastrulation (Hartenstein, 1989) and there is no evidence from the study of neurogenic mutants nor embryos injected with truncated Delta to rule out the possibility that these cells also undergo a division before differentiating. According to the model of lateral inhibition elevated levels of proneural genes drive neural differentiation (Chitnis, 1999). Again the assumption is that this precludes further cell division. However, in the proneural clusters in Drosophila ventral ectoderm the cell that is singled out by lateral inhibition, the neuroblast, does indeed express elevated levels of proneural genes but undergoes further division, thus elevated levels of these genes does not signal the end of cell division per se.

I believe that there is strong evidence that cells can in fact undergo a terminal division after the decision to differentiate has been made. Heterochronic transplantation of cortical cells that are in late G2 or the beginning of mitosis shows that they are largely resistant to environmental influence in that they migrate to the position that they would have adopted in their host tissue despite being placed into an environment that produces neurons fated for a different cortical layer (Mc Connell and Kaznowski, 1991). This shows clearly that cells undergoing mitosis already know what subtype of neuron they are going to be although it remains possible that this decision is made prior to the decision of whether to re-enter the cell cycle or not.

If the decision to differentiate is made independently and by chance in cells after division then one would expect to see many asymmetric divisions during neurogenesis. I have shown that this is not the case and that the relative dearth of asymmetric divisions suggests that the decision to re-enter the cell cycle or not is made prior to terminal mitosis (Chapter 5 discussion). Furthermore, since there is relatively little progenitor cell migration in the neuroepithelium during early neurogenesis in the hindbrain and spinal cord it is likely that sister cells would lie together within proneural clusters. If only one cell out of a proneural cluster differentiates then its sister cell that was in the same proneural cluster would re-enter the cell cycle giving rise to an asymmetric division. If this were generally the case then again a majority of asymmetric divisions would be expected during neurogenesis, which I have shown is not the case (Chapter 5).

It is clear that proneural genes and neurogenic genes play a role in a differentiation but the confusion arises in my mind because the relationship between the expression of these genes at the protein level is so unclear and hence there is no clue as to when or indeed where they are expressed relative to progenitors in various stages of the cell cycle. At present this information is absent due to the fact that antibodies are not available that recognise these proteins. Although in situ probes are available these do not necessarily provide insightful information. The activation of the Notch signalling pathway involves presentation of Delta at the cell surface, endocytosis of Delta along with transendocytosis of the extracellular domain of Notch. This releases the intracellular domain of Notch from the cell membrane and allows it to move to the nucleus where it activates target genes (Parks et al., 2000). Even if Delta or Notch RNA is detected in cells one cannot tell wherein the cell the protein lies and thus cannot get any clue as to whether the pathway is

active or not. If antibodies were available against different domains of Delta and the different domains of the Notch protein then one could tell for instance where Delta was in a cell, if it was at the cell surface or sequestered in vesicles or indeed if it was co-localised with the Notch extracellular domain protein within a vesicle, if the Notch ICD was at the cell surface or in the nucleus, so on and so forth. By correlating this information with data about stage of the cell cycle one could build up a picture of the dynamics of this signalling pathway. I believe that these tools or maybe even more so others that would allow the monitoring of these proteins in the living embryo throughout the cell cycle are necessary to further our understanding of this fundamental developmental pathway.

Another question that is still not absolutely and equivocally answered is whether there are specialised glial progenitors that do not make neurons. This question was first posed over 100 years ago and although it is clear that there is a lineage relationship between radial glia, neurons and astrocytes (e.g. Voigt et al., 1989; Gray and Sanes, 1992; Noctor et al., 2001) and possibly between neurons and oligodendrocytes (e.g. Leber et al., 1990; Park et al., 2002) the nature of the progenitor divisions that generate glia in vivo is largely unknown. I have made a prediction based on my analysis of the *mindbomb* mutant that neuronal and oligodendroglial lineage may diverge early in development but this prediction remains to be tested. I believe that this information could be easily acquired from the zebrafish using a similar approach as I have to monitoring the generation of the bulk of embryonic neurons. A transgenic zebrafish that expressed GFP in mature oligodendrocytes and or radial glia would be an indispensable tool in such a study as the HuC-GFP line was in my study.

There are a variety of other questions that remain to be answered in vertebrate neurogenesis and many more theses will be composed in the process of addressing them. I can only hope that this thesis has provided some useful insight into neurogenesis and that those souls who embark on such endeavours in the future enjoy their experience as much as I have.

References

Abdelilah, S., Mountcastle-Shah, E., Harvey, M., Solnica-Krezel, L., Schier, A. F., Stemple, D. L., Malicki, J., Neuhauss, S. C., Zwartkruis, F., Stainier, D. Y. et al. (1996). Mutations affecting neural survival in the zebrafish Danio rerio. *Development* 123, 217-27.

Alexiades, M. R. and Cepko, C. L. (1997). Subsets of retinal progenitors display temporally regulated and distinct biases in the fates of their progeny. *Development* 124, 1119-31.

Alvarez-Buylla, A., Garcia-Verdugo, J. M., Mateo, A. S. and Merchant-Larios, H. (1998). Primary neural precursors and intermitotic nuclear migration in the ventricular zone of adult canaries. *J Neurosci* 18, 1020-37.

An, M., Luo, R. and Henion, P. D. (2002). Differentiation and maturation of zebrafish dorsal root and sympathetic ganglion neurons. *J Comp Neurol* 446, 267-75.

Austin, C. P., Feldman, D. E., Ida, J. A., Jr. and Cepko, C. L. (1995). Vertebrate retinal ganglion cells are selected from competent progenitors by the action of Notch. *Development* 121, 3637-50.

Beattie, C. E., Hatta, K., Halpern, M. E., Liu, H., Eisen, J. S. and Kimmel, C. B. (1997). Temporal separation in the specification of primary and secondary motoneurons in zebrafish. *Dev Biol* 187, 171-82.

Belliveau, M. J. and Cepko, C. L. (1999). Extrinsic and intrinsic factors control the genesis of amacrine and cone cells in the rat retina. *Development* 126, 555-66.

Bentivoglio, M. and Mazzarello, P. (1999). The history of radial glia. *Brain Res Bull* 49, 305-15.

Bertrand, N., Castro, D. S. and Guillemot, F. (2002). Proneural genes and the specification of neural cell types. *Nat Rev Neurosci* 3, 517-30.

Birgbauer, E. and Fraser, S. E. (1994). Violation of cell lineage restriction compartments in the chick hindbrain. *Development* 120, 1347-56.

Blader, P., Fischer, N., Gradwohl, G., Guillemont, F. and Strahle, U. (1997). The activity of neurogenin1 is controlled by local cues in the zebrafish embryo. *Development* 124, 4557-69.

Bossing, T., Udolph, G., Doe, C. Q. and Technau, G. M. (1996). The embryonic central nervous system lineages of Drosophila melanogaster. I. Neuroblast lineages derived from the ventral half of the neuroectoderm. *Dev Biol* 179, 41-64.

Brewster, R. and Bodmer, R. (1996). Cell lineage analysis of the Drosophila peripheral nervous system. *Dev Genet* 18, 50-63.

Brewster, R., Lee, J. and Ruiz i Altaba, A. (1998). Gli/Zic factors pattern the neural plate by defining domains of cell differentiation. *Nature* 393, 579-83.

Brittis, P. A., Meiri, K., Dent, E. and Silver, J. (1995). The earliest patterns of neuronal differentiation and migration in the mammalian central nervous system. *Exp Neurol* 134, 1-12.

Broadus, J., Fuerstenberg, S. and Doe, C. Q. (1998). Staufen-dependent localization of prospero mRNA contributes to neuroblast daughter-cell fate. *Nature* 391, 792-5.

Brosamle, C. and Halpern, M. E. (2002). Characterization of myelination in the developing zebrafish. *Glia* 39, 47-57.

Cai, L., Hayes, N. L., Takahashi, T., Caviness, V. S., Jr. and Nowakowski, R. S. (2002). Size distribution of retrovirally marked lineages matches prediction from population measurements of cell cycle behavior. *J Neurosci Res* 69, 731-44.

Capela, A. and Temple, S. (2002). LeX/ssea-1 is expressed by adult mouse CNS stem cells, identifying them as nonependymal. *Neuron* 35, 865-75.

Cavalieri, B. (1635). Geometria Indivisibilibus Continuorum. Typis Clemetis Feronij, Bononi. Reprinted (1666) as Geometria degli Indivisibili. Unione Tipografico-editrice Torinese, Torino.

Caviness, V. S., Jr., Takahashi, T. and Nowakowski, R. S. (1995). Numbers, time and neocortical neuronogenesis: a general developmental and evolutionary model. *Trends Neurosci* 18, 379-83.

Cayouette, M. and Raff, M. (2003). The orientation of cell division influences cell-fate choice in the developing mammalian retina. *Development* 130, 2329-39.

Cayouette, M., Whitmore, A. V., Jeffery, G. and Raff, M. (2001). Asymmetric segregation of Numb in retinal development and the influence of the pigmented epithelium. *J Neurosci* 21, 5643-51.

Chalmers, A. D., Welchman, D. and Papalopulu, N. (2002). Intrinsic differences between the superficial and deep layers of the Xenopus ectoderm control primary neuronal differentiation. *Dev Cell* 2, 171-82.

Chenn, A. and McConnell, S. K. (1995). Cleavage orientation and the asymmetric inheritance of Notch1 immunoreactivity in mammalian neurogenesis. *Cell* 82, 631-41.

Chitnis, A., Henrique, D., Lewis, J., Ish-Horowicz, D. and Kintner, C. (1995). Primary neurogenesis in Xenopus embryos regulated by a homologue of the Drosophila neurogenic gene Delta. *Nature* 375, 761-6.

Chitnis, A. and Kintner, C. (1996). Sensitivity of proneural genes to lateral inhibition affects the pattern of primary neurons in Xenopus embryos. *Development* 122, 2295-301.

Chitnis, A. B. (1999). Control of neurogenesis--lessons from frogs, fish and flies. *Curr Opin Neurobiol* 9, 18-25.

Chu-Lagraff, Q., Wright, D. M., McNeil, L. K. and Doe, C. Q. (1991). The prospero gene encodes a divergent homeodomain protein that controls neuronal identity in Drosophila. *Development* Suppl, 79-85.

Clarke, J. D. (1999). Using fluorescent dyes for fate mapping, lineage analysis, and axon tracing in the chick embryo. *Methods Mol Biol* 97, 319-28.

Clarke, J. D., Erskine, L. and Lumsden, A. (1998). Differential progenitor dispersal and the spatial origin of early neurons can explain the predominance of single-phenotype clones in the chick hindbrain. *Dev Dyn* 212, 14-26.

Clarke, J. D. and Lumsden, A. (1993). Segmental repetition of neuronal phenotype sets in the chick embryo hindbrain. *Development* 118, 151-62.

Cole, L. K. and Ross, L. S. (2001). Apoptosis in the developing zebrafish embryo. *Dev Biol* 240, 123-42.

Concha, M. L. and Adams, R. J. (1998). Oriented cell divisions and cellular morphogenesis in the zebrafish gastrula and neurula: a time-lapse analysis. *Development* 125, 983-94.

Dahl, D., Crosby, C. J., Sethi, J. S. and Bignami, A. (1985). Glial fibrillary acidic (GFA) protein in vertebrates: immunofluorescence and immunoblotting study with monoclonal and polyclonal antibodies. *J Comp Neurol* 239, 75-88.

Das, T., Payer, B., Cayouette, M. and Harris, W. A. (2003). In Vivo Time-Lapse Imaging of Cell Divisions during Neurogenesis in the Developing Zebrafish Retina. *Neuron* 37, 597-609.

Datta, S. (1995). Control of proliferation activation in quiescent neuroblasts of the Drosophila central nervous system. *Development* 121, 1173-82.

Datta, S. and Kankel, D. R. (1992). l(1)trol and l(1)devl, loci affecting the development of the adult central nervous system in Drosophila melanogaster. *Genetics* 130, 523-37.

Deblandre, G. A., Lai, E. C. and Kintner, C. (2001). Xenopus neuralized is a ubiquitin ligase that interacts with XDelta1 and regulates Notch signaling. *Dev Cell* 1, 795-806.

Diez del Corral, R. and Storey, K. G. (2001). Markers in vertebrate neurogenesis. *Nat Rev Neurosci* 2, 835-9.

Doe, C. Q. (1992). Molecular markers for identified neuroblasts and ganglion mother cells in the Drosophila central nervous system. *Development* 116, 855-63.

Doe, C. Q., Chu-LaGraff, Q., Wright, D. M. and Scott, M. P. (1991). The prospero gene specifies cell fates in the Drosophila central nervous system. *Cell* 65, 451-64.

Doe, C. Q. and Technau, G. M. (1993). Identification and cell lineage of individual neural precursors in the Drosophila CNS. *Trends Neurosci* 16, 510-4.

Doetsch, F., Caille, I., Lim, D. A., Garcia-Verdugo, J. M. and Alvarez-Buylla, A. (1999). Subventricular zone astrocytes are neural stem cells in the adult mammalian brain. *Cell* 97, 703-16.

Doetsch, F., Garcia-Verdugo, J. M. and Alvarez-Buylla, A. (1997). Cellular composition and three-dimensional organization of the subventricular germinal zone in the adult mammalian brain. *J Neurosci* 17, 5046-61.

Driever, W., Solnica-Krezel, L., Schier, A. F., Neuhauss, S. C., Malicki, J., Stemple, D. L., Stainier, D. Y., Zwartkruis, F., Abdelilah, S., Rangini, Z. et al. (1996). A genetic screen for mutations affecting embryogenesis in zebrafish. *Development* 123, 37-46.

Ebens, A. J., Garren, H., Cheyette, B. N. and Zipursky, S. L. (1993). The Drosophila anachronism locus: a glycoprotein secreted by glia inhibits neuroblast proliferation. *Cell* 74, 15-27.

Eng LF., Vanderhaeghen JJ., Bignami A. and Gerstl B. (1971). An acidic protein isolated from fibrous astrocytes. *Brain Res* 28:2 351-4

Frantz, G. D. and McConnell, S. K. (1996). Restriction of late cerebral cortical progenitors to an upper-layer fate. *Neuron* 17, 55-61.

Fraser, S., Keynes, R. and Lumsden, A. (1990). Segmentation in the chick embryo hindbrain is defined by cell lineage restrictions. *Nature* 344, 431-5.

Fujita, S. (1962). Kinetics of cell proliferation. Exp. Cell. Res. 28, 52-60.

Furutani-Seiki, M., Jiang, Y. J., Brand, M., Heisenberg, C. P., Houart, C., Beuchle, D., van Eeden, F. J., Granato, M., Haffter, P., Hammerschmidt, M. et al. (1996). Neural degeneration mutants in the zebrafish, Danio rerio. *Development* 123, 229-39.

Garcia-Verdugo, J. M., Doetsch, F., Wichterle, H., Lim, D. A. and Alvarez-Buylla, A. (1998). Architecture and cell types of the adult subventricular zone: in search of the stem cells. *J Neurobiol* 36, 234-48.

Golgi, C. (1886). Sulla fina Anatomia degli organi centrali del sistema nervosa. Pavia.

Gowan, K., Helms, A. W., Hunsaker, T. L., Collisson, T., Ebert, P. J., Odom, R. and Johnson, J. E. (2001). Crossinhibitory activities of Ngn1 and Math1 allow specification of distinct dorsal interneurons. *Neuron* 31, 219-32.

Gray, G. E. and Sanes, J. R. (1992). Lineage of radial glia in the chicken optic tectum. *Development* 114, 271-83.

Gray, M., Moens, C. B., Amacher, S. L., Eisen, J. S. and Beattie, C. E. (2001). Zebrafish deadly seven functions in neurogenesis. *Dev Biol* 237, 306-23.

Haas, K., Sin, W. C., Javaherian, A., Li, Z. and Cline, H. T. (2001). Single-cell electroporation for gene transfer in vivo. *Neuron* 29, 583-91.

Haddon, C., Smithers, L., Schneider-Maunoury, S., Coche, T., Henrique, D. and Lewis, J. (1998). Multiple delta genes and lateral inhibition in zebrafish primary neurogenesis. *Development* 125, 359-70.

Haffter, P., Granato, M., Brand, M., Mullins, M. C., Hammerschmidt, M., Kane, D. A., Odenthal, J., van Eeden, F. J., Jiang, Y. J., Heisenberg, C. P. et al. (1996). The identification of genes with unique and essential functions in the development of the zebrafish, Danio rerio. *Development* 123, 1-36.

Hartenstein, A. Y., Rugendorff, A., Tepass, U. and Hartenstein, V. (1992). The function of the neurogenic genes during epithelial development in the Drosophila embryo. *Development* 116, 1203-20.

Hartenstein, V. (1989). Early neurogenesis in Xenopus: the spatio-temporal pattern of proliferation and cell lineages in the embryonic spinal cord. *Neuron* 3, 399-411.

Hartfuss, E., Galli, R., Heins, N. and Gotz, M. (2001). Characterization of CNS precursor subtypes and radial glia. *Dev Biol* 229, 15-30.

Hassan, B., Li, L., Bremer, K. A., Chang, W., Pinsonneault, J. and Vaessin, H. (1997). Prospero is a panneural transcription factor that modulates homeodomain protein activity. *Proc Natl Acad Sci U S A* 94, 10991-6.

Heins, N., Malatesta, P., Cecconi, F., Nakafuku, M., Tucker, K. L., Hack, M. A., Chapouton, P., Barde, Y. A. and Gotz, M. (2002). Glial cells generate neurons: the role of the transcription factor Pax6. *Nat Neurosci* 5, 308-15.

Heitzler, P., Bourouis, M., Ruel, L., Carteret, C. and Simpson, P. (1996). Genes of the Enhancer of split and achaete-scute complexes are required for a regulatory loop between Notch and Delta during lateral signalling in Drosophila. *Development* 122, 161-71.

Henrique, D., Adam, J., Myat, A., Chitnis, A., Lewis, J. and Ish-Horowicz, D. (1995). Expression of a Delta homologue in prospective neurons in the chick. *Nature* 375, 787-90.

Higashijima, S., Hotta, Y. and Okamoto, H. (2000). Visualization of cranial motor neurons in live transgenic zebrafish expressing green fluorescent protein under the control of the islet-1 promoter/enhancer. *J Neurosci* 20, 206-18.

Hirata, J., Nakagoshi, H., Nabeshima, Y. and Matsuzaki, F. (1995). Asymmetric segregation of the homeodomain protein Prospero during Drosophila development. *Nature* 377, 627-30.

Holder, N., Clarke, J. D., Kamalati, T. and Lane, E. B. (1990). Heterogeneity in spinal radial glia demonstrated by intermediate filament expression and HRP labelling. *J Neurocytol* 19, 915-28.

Holley, S. A., Julich, D., Rauch, G. J., Geisler, R. and Nusslein-Volhard, C. (2002). her1 and the notch pathway function within the oscillator mechanism that regulates zebrafish somitogenesis. *Development* 129, 1175-83.

Holley, S. A., Geisler, R. and Nusslein-Volhard, C. (2000). Control of her1 expression during zebrafish somitogenesis by a delta-dependent oscillator and an independent wave-front activity. *Genes Dev* 14, 1678-90.

Howard, C.V. and Reed, M.G. (1998). Unbiased Stereology

Huttner, W. B. and Brand, M. (1997). Asymmetric division and polarity of neuroepithelial cells. *Curr Opin Neurobiol* 7, 29-39.

Isshiki, T., Pearson, B., Holbrook, S. and Doe, C. Q. (2001). Drosophila neuroblasts sequentially express transcription factors which specify the temporal identity of their neuronal progeny. *Cell* 106, 511-21.

Itoh, M., Kim, C. H., Palardy, G., Oda, T., Jiang, Y. J., Maust, D., Yeo, S. Y., Lorick, K., Wright, G. J., Ariza-McNaughton, L. et al. (2003). Mind Bomb Is a Ubiquitin Ligase that Is Essential for Efficient Activation of Notch Signaling by Delta. *Dev Cell* 4, 67-82.

Jan, Y. N. and Jan, L. Y. (1998). Asymmetric cell division. *Nature* 392, 775-8.

Jiang, Y. J., Brand, M., Heisenberg, C. P., Beuchle, D., Furutani-Seiki, M., Kelsh, R. N., Warga, R. M., Granato, M., Haffter, P., Hammerschmidt, M. et al. (1996). Mutations affecting neurogenesis and brain morphology in the zebrafish, Danio rerio. *Development* 123, 205-16.

Johansson, C. B., Momma, S., Clarke, D. L., Risling, M., Lendahl, U. and Frisen, J. (1999). Identification of a neural stem cell in the adult mammalian central nervous system. *Cell* 96, 25-34.

Juan, G., Traganos, F., James, W. M., Ray, J. M., Roberge, M., Sauve, D. M., Anderson, H. and Darzynkiewicz, Z. (1998). Histone H3 phosphorylation and expression of cyclins A and B1 measured in individual cells during their progression through G2 and mitosis. *Cytometry* 32, 71-7.

Kawai, H., Arata, N. and Nakayasu, H. (2001). Three-dimensional distribution of astrocytes in zebrafish spinal cord. *Glia* 36, 406-13.

Kay, J. N., Finger-Baier, K. C., Roeser, T., Staub, W. and Baier, H. (2001). Retinal ganglion cell genesis requires lakritz, a Zebrafish atonal Homolog. *Neuron* 30, 725-36.

Kim, C. H., Bae, Y. K., Yamanaka, Y., Yamashita, S., Shimizu, T., Fujii, R., Park, H. C., Yeo, S. Y., Huh, T. L., Hibi, M. et al. (1997). Overexpression of neurogenin induces ectopic expression of HuC in zebrafish. *Neurosci Lett* 239, 113-6.

Kimmel, C. B., Ballard, W. W., Kimmel, S. R., Ullmann, B. and Schilling, T. F. (1995). Stages of embryonic development of the zebrafish. *Dev Dyn* 203, 253-310.

Kimmel, C. B., Warga, R. M. and Kane, D. A. (1994). Cell cycles and clonal strings during formation of the zebrafish central nervous system. *Development* 120, 265-76.

Knoblich, J. A., Jan, L. Y. and Jan, Y. N. (1995). Asymmetric segregation of Numb and Prospero during cell division. *Nature* 377, 624-7.

Koster, R. W. and Fraser, S. E. (2001). Tracing transgene expression in living zebrafish embryos. *Dev Biol* 233, 329-46.

Kraut, R., Chia, W., Jan, L. Y., Jan, Y. N. and Knoblich, J. A. (1996). Role of inscuteable in orienting asymmetric cell divisions in Drosophila. *Nature* 383, 50-5.

Lai, E. C., Deblandre, G. A., Kintner, C. and Rubin, G. M. (2001). Drosophila neuralized is a ubiquitin ligase that promotes the internalization and degradation of delta. *Dev Cell* 1, 783-94.

Lambert, J. D. and Nagy, L. M. (2002). Asymmetric inheritance of centrosomally localized mRNAs during embryonic cleavages. *Nature* 420, 682-6.

Leber, S. M., Breedlove, S. M. and Sanes, J. R. (1990). Lineage, arrangement, and death of clonally related motoneurons in chick spinal cord. *J Neurosci* 10, 2451-62.

Lehmann, R., Jimenez, F., Dietrich, U. and Campos-Ortega, J. A.(1983). On the phenotype and development of mutants of early neurogenesis in Drosophila melanogaster. Roux's Arch. Dev. Biol. 192, 62-74.

Lele, Z., Folchert, A., Concha, M., Rauch, G. J., Geisler, R., Rosa, F., Wilson, S. W., Hammerschmidt, M. and Bally-Cuif, L. (2002). parachute/n-cadherin is required for morphogenesis and maintained integrity of the zebrafish neural tube. *Development* 129, 3281-94.

Levitt, P., Cooper, M. L. and Rakic, P. (1981). Coexistence of neuronal and glial precursor cells in the cerebral ventricular zone of the fetal monkey: an ultrastructural immunoperoxidase analysis. *J Neurosci* 1, 27-39.

Levitt, P. and Rakic, P. (1980). Immunoperoxidase localization of glial fibrillary acidic protein in radial glial cells and astrocytes of the developing rhesus monkey brain. *J Comp Neurol* 193, 815-40.

Lippincott-Schwartz, J. and Patterson, G. H. (2003). Development and use of fluorescent protein markers in living cells. *Science* 300, 87-91.

Livesey, F. J. and Cepko, C. L. (2001). Vertebrate neural cell-fate determination: lessons from the retina. *Nat Rev Neurosci* 2, 109-18.

Lois, C. and Alvarez-Buylla, A. (1993). Proliferating subventricular zone cells in the adult mammalian forebrain can differentiate into neurons and glia. *Proc Natl Acad Sci U S A* 90, 2074-7.

Lu, B., Rothenberg, M., Jan, L. Y. and Jan, Y. N. (1998). Partner of Numb colocalizes with Numb during mitosis and directs Numb asymmetric localization in Drosophila neural and muscle progenitors. *Cell* 95, 225-35.

Lu, B., Jan, L. and Jan, Y. N. (2000a). Control of cell divisions in the nervous system: symmetry and asymmetry. *Annu Rev Neurosci* 23, 531-56.

Lu, Q. R., Yuk, D., Alberta, J. A., Zhu, Z., Pawlitzky, I., Chan, J., McMahon, A. P., Stiles, C. D. and Rowitch, D. H. (2000b). Sonic hedgehog--regulated oligodendrocyte lineage genes encoding bHLH proteins in the mammalian central nervous system. *Neuron* 25, 317-29.

Lu, Q. R., Sun, T., Zhu, Z., Ma, N., Garcia, M., Stiles, C. D. and Rowitch, D. H. (2002). Common developmental requirement for Olig function indicates a motor neuron/oligodendrocyte connection. *Cell* 109, 75-86.

Lumsden, A., Clarke, J. D., Keynes, R. and Fraser, S. (1994). Early phenotypic choices by neuronal precursors, revealed by clonal analysis of the chick embryo hindbrain. *Development* 120, 1581-9.

Luskin, M. B., Parnavelas, J. G. and Barfield, J. A. (1993). Neurons, astrocytes, and oligodendrocytes of the rat cerebral cortex originate from separate progenitor cells: an ultrastructural analysis of clonally related cells. *J Neurosci* 13, 1730-50.

Ma, Q., Fode, C., Guillemot, F. and Anderson, D. J. (1999). Neurogenin1 and neurogenin2 control two distinct waves of neurogenesis in developing dorsal root ganglia. *Genes Dev* 13, 1717-28.

Ma, Q., Kintner, C. and Anderson, D. J. (1996). Identification of neurogenin, a vertebrate neuronal determination gene. *Cell* 87, 43-52.

Maier, C. E. and Miller, R. H. (1995). Development of glial cytoarchitecture in the frog spinal cord. *Dev Neurosci* 17, 149-59.

Magini, G. (1888). Ulteriori ricerche istologiche sul cervello fetale. Rendiconti della R. Accademia dei Lincei. 4, 760-763.

Malatesta, P., Hartfuss, E. and Gotz, M. (2000). Isolation of radial glial cells by fluorescent-activated cell sorting reveals a neuronal lineage. *Development* 127, 5253-63.

Marcus, R. C. and Easter, S. S., Jr. (1995). Expression of glial fibrillary acidic protein and its relation to tract formation in embryonic zebrafish (Danio rerio). *J Comp Neurol* 359, 365-81.

Marin, F. and Puelles, L. (1995). Morphological fate of rhombomeres in quail/chick chimeras: a segmental analysis of hindbrain nuclei. *Eur J Neurosci* 7, 1714-38.

Marusich, M. F., Furneaux, H. M., Henion, P. D. and Weston, J. A. (1994). Hu neuronal proteins are expressed in proliferating neurogenic cells. *J Neurobiol* 25, 143-55.

Matsuzaki, F., Koizumi, K., Hama, C., Yoshioka, T. and Nabeshima, Y. (1992). Cloning of the Drosophila prospero gene and its expression in ganglion mother cells. *Biochem Biophys Res Commun* 182, 1326-32.

McConnell, S. K. and Kaznowski, C. E. (1991). Cell cycle dependence of laminar determination in developing neocortex. *Science* 254, 282-5.

Mendelson, B. (1986). Development of reticulospinal neurons of the zebrafish. I. Time of origin. *J Comp Neurol* 251, 160-71.

Miller, R. H. and Liuzzi, F. J. (1986). Regional specialization of the radial glial cells of the adult frog spinal cord. *J Neurocytol* 15, 187-96.

Mione, M. C., Cavanagh, J. F., Harris, B. and Parnavelas, J. G. (1997). Cell fate specification and symmetrical/asymmetrical divisions in the developing cerebral cortex. *J Neurosci* 17, 2018-29.

Miyata, T., Kawaguchi, A., Okano, H. and Ogawa, M. (2001). Asymmetric inheritance of radial glial fibers by cortical neurons. *Neuron* 31, 727-41.

Mizuguchi, R., Sugimori, M., Takebayashi, H., Kosako, H., Nagao, M., Yoshida, S., Nabeshima, Y., Shimamura, K. and Nakafuku, M. (2001). Combinatorial roles of olig2 and neurogenin2 in the coordinated induction of pan-neuronal and subtype-specific properties of motoneurons. *Neuron* 31, 757-71.

Mumm, J. S., Shou, J. and Calof, A. L. (1996). Colony-forming progenitors from mouse olfactory epithelium: evidence for feedback regulation of neuron production. *Proc Natl Acad Sci U S A* 93, 11167-72.

Murciano, A., Zamora, J., Lopez-Sanchez, J. and Frade, J. M. (2002). Interkinetic nuclear movement may provide spatial clues to the regulation of neurogenesis. *Mol Cell Neurosci* 21, 285-300.

Nadarajah, B. and Parnavelas, J. G. (2002). Modes of neuronal migration in the developing cerebral cortex. *Nat Rev Neurosci* 3, 423-32.

Nagele, R. G. and Lee, H. Y. (1979). Ultrastructural changes in cells associated with interkinetic nuclear migration in the developing chick neuroepithelium. *J Exp Zool* 210, 89-106.

Noctor, S. C., Flint, A. C., Weissman, T. A., Dammerman, R. S. and Kriegstein, A. R. (2001). Neurons derived from radial glial cells establish radial units in neocortex. *Nature* 409, 714-20.

Noctor, S. C., Flint, A. C., Weissman, T. A., Wong, W. S., Clinton, B. K. and Kriegstein, A. R. (2002). Dividing precursor cells of the embryonic cortical ventricular zone have morphological and molecular characteristics of radial glia. *J Neurosci* 22, 3161-73.

Nona, S. N., Shehab, S. A., Stafford, C. A. and Cronly-Dillon, J. R. (1989). Glial fibrillary acidic protein (GFAP) from goldfish: its localisation in visual pathway. *Glia* 2, 189-200.

O'Rourke, N. A., Dailey, M. E., Smith, S. J. and McConnell, S. K. (1992). Diverse migratory pathways in the developing cerebral cortex. *Science* 258, 299-302.

O'Rourke, N. A., Sullivan, D. P., Kaznowski, C. E., Jacobs, A. A. and McConnell, S. K. (1995). Tangential migration of neurons in the developing cerebral cortex. *Development* 121, 2165-76.

O'Rourke, N. A., Chenn, A. and McConnell, S. K. (1997). Postmitotic neurons migrate tangentially in the cortical ventricular zone. *Development* 124, 997-1005.

Papan C, Campos-Ortega JA (1994). On the formation of the neural keel and neural tube in the zebrafish Danio (Brachydanio) rerio. Roux's Arch Dev Biol 203: 178–186

Papan C, Campos-Ortega JA (1997). A clonal analysis of spinal cord development in the zebrafish. Dev Genes Evol 207, 71–81

Papan, C. and Campos-Ortega, J. A. (1999). Region-specific cell clones in the developing spinal cord of the zebrafish. *Dev Genes Evol* 209, 135-44.

Park, H. C., Hong, S. K., Kim, H. S., Kim, S. H., Yoon, E. J., Kim, C. H., Miki, N. and Huh, T. L. (2000a). Structural comparison of zebrafish Elav/Hu and their differential expressions during neurogenesis. *Neurosci Lett* 279, 81-4.

Park, H. C., Kim, C. H., Bae, Y. K., Yeo, S. Y., Kim, S. H., Hong, S. K., Shin, J., Yoo, K. W., Hibi, M., Hirano, T. et al. (2000b). Analysis of upstream elements in the HuC promoter leads to the establishment of transgenic zebrafish with fluorescent neurons. *Dev Biol* 227, 279-93.

Park, H. C., Mehta, A., Richardson, J. S. and Appel, B. (2002). olig2 is required for zebrafish primary motor neuron and oligodendrocyte development. *Dev Biol* 248, 356-68.

Parks, A. L., Klueg, K. M., Stout, J. R. and Muskavitch, M. A. (2000). Ligand endocytosis drives receptor dissociation and activation in the Notch pathway. *Development* 127, 1373-85.

Parnavelas, J. G., Barfield, J. A., Franke, E. and Luskin, M. B. (1991). Separate progenitor cells give rise to pyramidal and nonpyramidal neurons in the rat telencephalon. *Cereb Cortex* 1, 463-8.

Parnavelas, J. G., Mione, M. C. and Lavdas, A. (1995). The cell lineage of neuronal subtypes in the mammalian cerebral cortex. *Ciba Found Symp* 193, 41-58; discussion 59-70.

Parnavelas, J. G. (1999). Glial cell lineages in the rat cerebral cortex. *Exp Neurol* 156, 418-29.

Parnavelas, J. G. and Nadarajah, B. (2001). Radial glial cells. are they really glia? *Neuron* 31, 881-4.

Patton, E. E. and Zon, L. I. (2001). The art and design of genetic screens: zebrafish. *Nat Rev Genet* 2, 956-66.

Pattyn, A., Vallstedt, A., Dias, J. M., Samad, O. A., Krumlauf, R., Rijli, F. M., Brunet, J. F. and Ericson, J. (2003). Coordinated temporal and spatial control of motor neuron and serotonergic neuron generation from a common pool of CNS progenitors. *Genes Dev* 17, 729-37.

Pavlopoulos, E., Pitsouli, C., Klueg, K. M., Muskavitch, M. A., Moschonas, N. K. and Delidakis, C. (2001). neuralized Encodes a peripheral membrane protein involved in delta signaling and endocytosis. *Dev Cell* 1, 807-16.

Petersen, P. H., Zou, K., Hwang, J. K., Jan, Y. N. and Zhong, W. (2002). Progenitor cell maintenance requires numb and numblike during mouse neurogenesis. *Nature* 419, 929-34.

Price, J. and Thurlow, L. (1988). Cell lineage in the rat cerebral cortex: a study using retroviral- mediated gene transfer. *Development* 104, 473-82.

Pringle, N. P., Guthrie, S., Lumsden, A. and Richardson, W. D. (1998). Dorsal spinal cord neuroepithelium generates astrocytes but not oligodendrocytes. *Neuron* 20, 883-93.

Provis, J. M., van Driel, D., Billson, F. A. and Russell, P. (1985). Development of the human retina: patterns of cell distribution and redistribution in the ganglion cell layer. *J Comp Neurol* 233, 429-51.

Qian, X., Goderie, S. K., Shen, Q., Stern, J. H. and Temple, S. (1998). Intrinsic programs of patterned cell lineages in isolated vertebrate CNS ventricular zone cells. *Development* 125, 3143-52.

Qian, X., Shen, Q., Goderie, S. K., He, W., Capela, A., Davis, A. A. and Temple, S. (2000). Timing of CNS cell generation: a programmed sequence of neuron and glial cell production from isolated murine cortical stem cells. *Neuron* 28, 69-80.

Rakic, P. (1971a). Guidance of neurons migrating to the fetal monkey neocortex. *Brain Res* 33, 471-6.

Rakic, P. (1971b). Neuron-glia relationship during granule cell migration in developing cerebellar cortex. A Golgi and electronmicroscopic study in Macacus Rhesus. *J Comp Neurol* 141, 283-312.

Rakic, P. (1972). Mode of cell migration to the superficial layers of fetal monkey neocortex. *J Comp Neurol* 145, 61-83.

Ramon y Cajal, S. (1889). Coloracion por el metodo de Golgi de los centros nerviosos de los embriones de pollo. Gaceta Me´dica Catalana 12:6 –8

Ramon y Cajal, S. (1890). Sobre la existencia de celulas nerviosas especiales en la primera capa de las circunvoluciones cerebrales. Gaceta Me´dica Catalana 13:737–739

Ramon y Cajal, S. (1911). Histologie du syste`me nerveux de l'homme et des verte´bre´s. Paris: Maloine.

Ramon y Cajal, S. (1906) Relacion de meritos y trabajos cientificos del autor. Madrid: Universidad de Madrid

Ramon y Cajal, S. Recollections of my life (E. Horne Craigie, trans.). Cambridge, MA: MIT Press; 1996.

Reid, C. B., Tavazoie, S. F. and Walsh, C. A. (1997). Clonal dispersion and evidence for asymmetric cell division in ferret cortex. *Development* 124, 2441-50.

Reynolds, B. A. and Weiss, S. (1992). Generation of neurons and astrocytes from isolated cells of the adult mammalian central nervous system. *Science* 255, 1707-10.

Rhyu, M. S., Jan, L. Y. and Jan, Y. N. (1994). Asymmetric distribution of numb protein during division of the sensory organ precursor cell confers distinct fates to daughter cells. *Cell* 76, 477-91.

Samuelsen, G. B., Larsen, K. B., Bogdanovic, N., Laursen, H., Graem, N., Larsen, J. F. and Pakkenberg, B. (2003). The changing number of cells in the human fetal forebrain and its subdivisions: a stereological analysis. *Cereb Cortex* 13, 115-22.

Saper, C. B. (1996). Any way you cut it: a new journal policy for the use of unbiased counting methods. *J Comp Neurol* 364, 5.

Sauer, F.C. (1935a). Mitosis in the neural tube. J. Comp.Neurol. 62,377-405.

Sauer, F.C. (1935b). The cellular structure of the neural tube. J. Comp.Neurol. 63, 13-23.

Sauer, F.C. (1936). The interkinetic movement of embryonic epithelial nuclei. J. Comp. Neurol. 60, 1-11.

Sauer, F.C. (1937). Some factors in the morphogenesis of vertebrate embryonic neuroepithelium. J. Comp. Neurol. 61, 563-579.

Schier, A. F., Neuhauss, S. C., Harvey, M., Malicki, J., Solnica-Krezel, L., Stainier, D. Y., Zwartkruis, F., Abdelilah, S., Stemple, D. L., Rangini, Z. et al. (1996). Mutations affecting the development of the embryonic zebrafish brain. *Development* 123, 165-78.

Schmid, A., Chiba, A. and Doe, C. Q. (1999). Clonal analysis of Drosophila embryonic neuroblasts: neural cell types, axon projections and muscle targets. *Development* 126, 4653-89.

Schmitz B, Papan C, Campos-Ortega JA (1993) Neurulation in the anterior trunk region of the zebrafish, Brachydanio rerio. Roux's Arch Dev Biol 202: 250–259

Seymour, R. M. and Berry, M. (1975). Scanning and transmission electron microscope studies of interkinetic nuclear migration in the cerebral vesicles of the rat. *J Comp Neurol* 160, 105-25.

Shen, C. P., Jan, L. Y. and Jan, Y. N. (1997). Miranda is required for the asymmetric localization of Prospero during mitosis in Drosophila. *Cell* 90, 449-58.

Shen, C. P., Knoblich, J. A., Chan, Y. M., Jiang, M. M., Jan, L. Y. and Jan, Y. N. (1998). Miranda as a multidomain adapter linking apically localized Inscuteable and basally localized Staufen and Prospero during asymmetric cell division in Drosophila. *Genes Dev* 12, 1837-46.

Shen, Q., Zhong, W., Jan, Y. N. and Temple, S. (2002). Asymmetric Numb distribution is critical for asymmetric cell division of mouse cerebral cortical stem cells and neuroblasts. *Development* 129, 4843-53.

Sidman R.L., Miale, I.L. and Feder, N. (1959). Cell proliferation and migration in the primitive ependymal zone; an aoutoradiographic study of histogenesis in the nervous system. Exp. Neuol. 1, 322-333.

Silva, A. O., Ercole, C. E. and McLoon, S. C. (2002). Plane of cell cleavage and numb distribution during cell division relative to cell differentiation in the developing retina. *J Neurosci* 22, 7518-25.

Soula, C., Foulquier, F., Duprat, A. M. and Cochard, P. (1993). Lineage analysis of early neural plate cells: cells with purely neuronal fate coexist with bipotential neuroglial progenitors. *Dev Biol* 159, 196-207.

Spana, E. P. and Doe, C. Q. (1995). The prospero transcription factor is asymmetrically localized to the cell cortex during neuroblast mitosis in Drosophila. *Development* 121, 3187-95.

Spana, E. P. and Doe, C. Q. (1996). Numb antagonizes Notch signaling to specify sibling neuron cell fates. *Neuron* 17, 21-6.

Sterio, D. C. (1984). The unbiased estimation of number and sizes of arbitrary particles using the disector. *J Microsc* 134, 127-36.

Sulston, J. E., Schierenberg, E., White, J. G. and Thomson, J. N. (1983). The embryonic cell lineage of the nematode Caenorhabditis elegans. *Dev Biol* 100, 64-119.

Sun, T., Echelard, Y., Lu, R., Yuk, D. I., Kaing, S., Stiles, C. D. and Rowitch, D. H. (2001). Olig bHLH proteins interact with homeodomain proteins to regulate cell fate acquisition in progenitors of the ventral neural tube. *Curr Biol* 11, 1413-20.

Takahashi, T., Nowakowski, R. S. and Caviness, V. S., Jr. (1995). The cell cycle of the pseudostratified ventricular epithelium of the embryonic murine cerebral wall. *J Neurosci* 15, 6046-57.

Takahashi, T., Nowakowski, R. S. and Caviness, V. S., Jr. (1996). The leaving or Q fraction of the murine cerebral proliferative epithelium: a general model of neocortical neuronogenesis. *J Neurosci* 16, 6183-96.

Takahashi, T., Nowakowski, R. S. and Caviness, V. S., Jr. (1997). The mathematics of neocortical neuronogenesis. *Dev Neurosci* 19, 17-22.

Takizawa, P. A., Sil, A., Swedlow, J. R., Herskowitz, I. and Vale, R. D. (1997). Actin-dependent localization of an RNA encoding a cell-fate determinant in yeast. *Nature* 389, 90-3.

Temple, S. (2001). The development of neural stem cells. *Nature* 414, 112-7.

Thors, F., de Kort, E. J. and Nieuwenhuys, R. (1982). On the development of the spinal cord of the clawed frog, Xenopus laevis. I. Morphogenesis and histogenesis. *Anat Embryol (Berl)* 164, 427-41.

Tietjen, I., Rihel, J. M., Cao, Y., Koentges, G., Zakhary, L. and Dulac, C. (2003). Single-cell transcriptional analysis of neuronal progenitors. *Neuron* 38, 161-75.

Trevarrow, B., Marks, D. L. and Kimmel, C. B. (1990). Organization of hindbrain segments in the zebrafish embryo. *Neuron* 4, 669-79.

Truman, J. W. and Bate, M. (1988). Spatial and temporal patterns of neurogenesis in the central nervous system of Drosophila melanogaster. *Dev Biol* 125, 145-57.

Tsien, R. Y. (1998). The green fluorescent protein. *Annu Rev Biochem* 67, 509-44.

Turner, D. L. and Cepko, C. L. (1987). A common progenitor for neurons and glia persists in rat retina late in development. *Nature* 328, 131-6.

Udolph, G., Prokop, A., Bossing, T. and Technau, G. M. (1993). A common precursor for glia and neurons in the embryonic CNS of Drosophila gives rise to segment-specific lineage variants. *Development* 118, 765-75.

Uemura, T., Shepherd, S., Ackerman, L., Jan, L. Y. and Jan, Y. N. (1989). numb, a gene required in determination of cell fate during sensory organ formation in Drosophila embryos. *Cell* 58, 349-60.

Vaessin, H., Grell, E., Wolff, E., Bier, E., Jan, L. Y. and Jan, Y. N. (1991). prospero is expressed in neuronal precursors and encodes a nuclear protein that is involved in the control of axonal outgrowth in Drosophila. *Cell* 67, 941-53.

Voigt, A., Pflanz, R., Schafer, U. and Jackle, H. (2002). Perlecan participates in proliferation activation of quiescent Drosophila neuroblasts. *Dev Dyn* 224, 403-12.

Voigt, T. (1989). Development of glial cells in the cerebral wall of ferrets: direct tracing of their transformation from radial glia into astrocytes. *J Comp Neurol* 289, 74-88.

Waid, D. K. and McLoon, S. C. (1998). Ganglion cells influence the fate of dividing retinal cells in culture. *Development* 125, 1059-66.

Walsh, C. and Cepko, C. L. (1993). Clonal dispersion in proliferative layers of developing cerebral cortex. *Nature* 362, 632-5.

Weiss, S., Dunne, C., Hewson, J., Wohl, C., Wheatley, M., Peterson, A. C. and Reynolds, B. A. (1996). Multipotent CNS stem cells are present in the adult mammalian spinal cord and ventricular neuroaxis. *J Neurosci* 16, 7599-609.

Westerfield, M. (1995). The Zebrafish Book.

Wetts, R. and Fraser, S. E. (1988). Multipotent precursors can give rise to all major cell types of the frog retina. *Science* 239, 1142-5.

Wilkinson, H. A., Fitzgerald, K. and Greenwald, I. (1994). Reciprocal changes in expression of the receptor lin-12 and its ligand lag-2 prior to commitment in a C. elegans cell fate decision. *Cell* 79, 1187-98.

Wingate, R. J. and Lumsden, A. (1996). Persistence of rhombomeric organisation in the postsegmental hindbrain. *Development* 122, 2143-52.

Woo, K. and Fraser, S. E. (1995). Order and coherence in the fate map of the zebrafish nervous system. *Development* 121, 2595-609.

Wu, H. H., Ivkovic, S., Murray, R. C., Jaramillo, S., Lyons, K. M., Johnson, J. E. and Calof, A. L. (2003). Autoregulation of Neurogenesis by GDF11. *Neuron* 37, 197-207.

Wullimann, M. F. and Knipp, S. (2000). Proliferation pattern changes in the zebrafish brain from embryonic through early postembryonic stages. *Anat Embryol (Berl)* 202, 385-400.

Yeh, E., Dermer, M., Commisso, C., Zhou, L., McGlade, C. J. and Boulianne, G. L. (2001). Neuralized functions as an E3 ubiquitin ligase during Drosophila development. *Curr Biol* 11, 1675-9.

Zhong, W., Jiang, M. M., Weinmaster, G., Jan, L. Y. and Jan, Y. N. (1997). Differential expression of mammalian Numb, Numblike and Notch1 suggests distinct roles during mouse cortical neurogenesis. *Development* 124, 1887-97.

Zhou, Q., Wang, S. and Anderson, D. J. (2000). Identification of a novel family of oligodendrocyte lineage-specific basic helix-loop-helix transcription factors. *Neuron* 25, 331-43.

Zhou, Q., Choi, G. and Anderson, D. J. (2001). The bHLH transcription factor Olig2 promotes oligodendrocyte differentiation in collaboration with Nkx2.2. *Neuron* 31, 791-807.

Zhou, Q. and Anderson, D. J. (2002). The bHLH transcription factors OLIG2 and OLIG1 couple neuronal and glial subtype specification. *Cell* 109, 61-73.

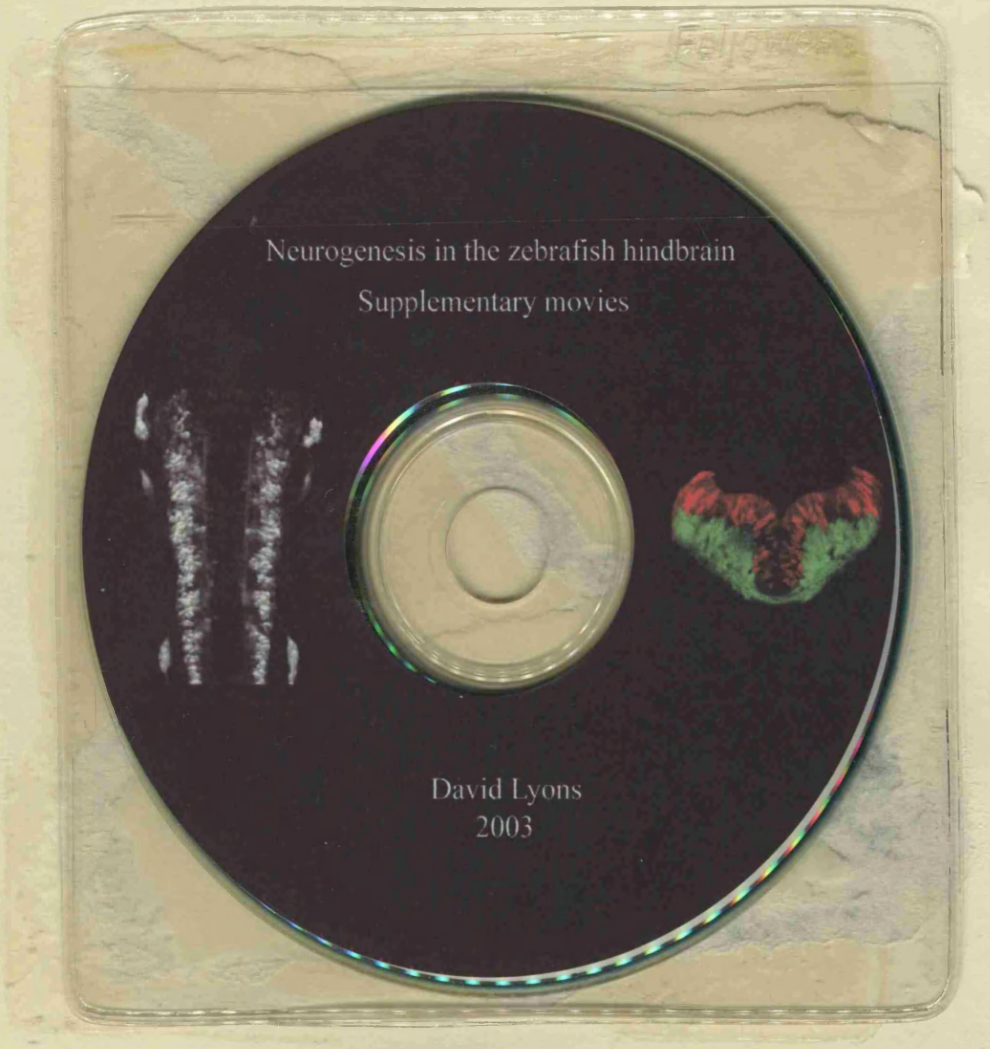
Neurogenesis in the zebrafish hindbrain
Supplementary movies
David Lyons
2003